Dynamics of tropical African climate and marine sedimentation during major climate transitions

Olubunmi Eniola

A thesis submitted to Newcastle University

In partial fulfillment of the requirements for the degree of

Doctor of Philosophy in the Faculty of Science and Agriculture

School of Civil Engineering and Geosciences,

Newcastle University, UK.

January 2011

Declaration

I hereby certify that the work described in this thesis is my own, except where otherwise acknowledged, and has not been submitted previously for a degree at this or any other university.

.....

Olubunmi Eniola

Table of Content

Abstract

This thesis presents the late Miocene/early Pliocene climate transition (7-5 Ma) as recorded in marine sediments from Ocean Drilling Programme (ODP) Site 959 in the equatorial Atlantic off tropical West Africa, and a reconstruction of changing Holocene environments of the Eastern Tropical Atlantic (CHEETA) based on surface and core sediments from a transect along the Portuguese and NW African margin.

The late Miocene to early Pliocene climate transition had irreversible consequences for atmospheric and ocean circulation leading to global cooling, northern hemisphere glaciations and modern climate conditions. In this study, continental climate, vegetation change and surface ocean dynamics at millennial time scale resolution is investigated from U^{K}_{37}' alkenone derived SST, leaf wax lipids and organic carbon records (TOC). Despite low TOC (<1%) which was highly variable at cm-scale (~2.5-5 kyr) resolution, ubiquitous evidence from alkenones ($C_{37:2}$ and $C_{37:3}$) and leaf wax lipids indicate that the primary climate signal was preserved. The U^{K}_{37}' based SST estimates (24.8-29°C) showed pronounced warm and cool cycles in the magnitude of 4°C. Elevated leaf wax lipids *n*–alkanes (C_{27}, C_{29}, and C_{31}) correspond with cool SSTs and indicate a coupled relationship between upwelling and atmospheric ocean circulation patterns which intensified around 5.6 Ma arguing for wind driven deposition from terrestrial sources related to the position and strength of the ITCZ. The high amplitude cyclic patterns in the ODP Site 959 records were investigated by time frequency analyses. The common 41 kyr in all records supports a response to high latitude climate forcing. The 75 kyr variations and lead/lag observed in the leaf waxes and SST records during the late Miocene to early Pliocene are probably related to continental ice volume variations.

The study on surface sediments from the Portuguese and NW African margins, confirm the presence of two soil-specific biomarkers, branched GDGTs (expressed as the BIT index) and bacteriohopanepolyols (BHPs), in this region of almost exclusive aeolian export. TOC exceeding 2% and $\delta^{13}C_{org}$ gradients from -22.5‰ off Portugal to -19‰ off W Africa identify areas of upwelling off Cape Blanc and the transition from C_3 to C_4 vegetation habitats in Northern Africa, respectively. Despite low signals of the molecular records, slightly stronger response of soil-marker BHPs in the sediments is attributed to preferential erosion of the upper, (oxic) part of the soil column in central African source areas, the proposed source for soil BHPs. An alternative explanation is that in situ production of the branched GDGTs may be responsible for the low BIT index. As yet there is no evidence of the soil BHPs, adenosylhopane produced in situ in marine systems and aeolian transport of GDGTs is yet to been proven. More studies on dust samples from continental margins needs to be carried out to validate this transport mechanism of branched GDGTs and BHPs.

A compilation of first bulk geochemical and molecular results from a selection of cores from the Portuguese and NW African margin within an integrated chronological framework document the variations in marine sedimentation and constrain regional variations in continental climate and terrigenous supply since the last glacial period. TOC accumulation records document millennial scale variability in response to the African Humid Period. Carbon isotope trends pronounced during the last glacial maximum support organic matter input from C_4 type vegetation during colder glacial periods. Preliminary molecular isotopic records of *n*-alkanes identify gaps in this study that will need further investigation to assess and confirm vegetation sources and continental climatic conditions over Northwest Africa.

Acknowledgements

I thank my family and friends who have been very supportive throughout the entire PhD. Without you all, it would not have been possible to juggle the extensive work which this PhD entailed. I especially thank my husband and my young son for their unfailing support throughout the duration of this PhD.

I would like to express my appreciation and gratitude to my supervisor, Professor Tom Wagner, for his guidance, during the entire PhD. I would also like to thank Dr Helen Talbot for her input and advice on certain aspects of the project specifically on BHPs, and the use and applications of the HPLC-MS. Also, thanks to Dr. Erin McClymont for her painstaking patience throughout this PhD especially her contribution to the ODP 959 project. I am undoubtedly grateful to the Dorothy Hodgkin's Postgraduate Award for funding this research which has been invaluable to ensuring the completion of this PhD. I thank the Ocean Drilling programme (ODP) and the CHEETA Cruise staff who ensured there were samples for me to work on in the laboratory. At Newcastle University, I would like to thank Mr. (s) Phil Green; Paul Donohoe; Bernie Bowler and Ian Harrison for technical advice and assistance throughout this PhD. Thank you to Yvonne Hall for all her help with administrative issues.

1 Chapter One

1.1 *Introduction*

Until now, the tropics have been presented by global models as a relatively passive component of the Earth's climate system because observations of large scale variations have been mainly documented from the high latitudes (Chiang, 2009). Emerging evidence however suggest that SST variability, a critical parameter of climate conditions, occurred in the late Quarternary and the Pleistocene climate period in the tropics (e.g. Schefuß *et al.,* 2005; McClymont and Rosell Mele, 2005). Apart from SST variability, terrestrial vegetation response is another aspect of the tropics that needs further development as it reflects the climate of the region. Many sedimentary records have shown that the origin and subsequent expansion of terrestrial vegetation is linked to climate change (e.g Cerling *et al.,* 1993; 1997; Tipple and Pagani, 2007).

Further, terrestrial vegetation dynamics have also been previously linked to SST cooling events associated with millennial scale shifts which occurred at higher latitudes during the Holocene (de Menocal *et al.,* 2000b). Despite this, there is a need to better understand the teleconnections and causal relationships between the tropics and high latitudes. The mechanisms driving such changes and what the consequences are on the tropical African climate is a focus in this thesis in order to understand tropical African climate within major climate transitions, particularly the late Miocene to early Pliocene and the glacial to Holocene climate transitions.

The late Miocene to early Pliocene climate transition (7-5 Ma) has been largely ignored because this transition showed no dramatic long time scale changes (See Zachos *et al.,* 2001). Hence, studies particularly to show the influence of high latitude climate forcing on records from this transition in the eastern equatorial Atlantic have been minimal. Previous studies in the eastern equatorial Atlantic with regards to the Pleistocene, for example, have shown that Pleistocene African climate responded to both high and low latitude forcing (de Menocal et al., 1993). Initial spectral analyses on eastern equatorial Atlantic records (TOC content and carbonates) from the late Miocene to early Pliocene suggested that African climate variability suggested high latitude climate forcing (Wagner *et al.,* 1998). Although this initial observation strengthened the influence of high latitude forcing on eastern equatorial Atlantic sedimentation, this was at high resolution. These records also do not provide a complete view on past atmospheric and ocean circulation patterns in the eastern equatorial Atlantic, a key mechanism for driving teleconnections between the ocean and land, particularly, the evolution of African trade winds, upwelling and vegetation response and supply to the eastern equatorial Atlantic.

A working hypothesis of this thesis is to test if higher latitude climate forcing contributed to or was directly linked to the late Miocene to early Pliocene climate (7-5 Ma) in the equatorial Atlantic which forced flunctuations in continental upwelling and terrestrial vegetation supply and preservation. Higher resolution records (SST; higher plant leaf waxes and TOC content) for the late Miocene to early Pliocene interval coupled with detailed time-series analyses

from the equatorial Atlantic and off the NW African region will be a primary focus of this thesis. It is expected that testing these can document atmospheric ocean circulation patterns and orbital driven insolation changes associated with the late Miocene to early Pliocene African climate.

The last glacial to Holocene climate transition (35 ka) documents three climatic states : the glacial, deglacial and the Holocene that experienced several global environmental conditions which shifted rapidly between extreme, but stable states on a millennial scale (Johnsen *et al.,* 1992; Jennings *et al.,* 2002; de Vernal *et al*., 2000). This time period documents rapid shifts between warm and cold conditions (Alley *et al.,* 1993; Severinghaus and Brook, 1999).

Glacial periods have shown enhanced atmospheric circulation patterns interpreted to indicate higher productivity in combination with increased dust input and higher sedimentation rates in glacial continental margins sediments from NW Africa (Kulhman *et al.,* 2004 and references therein). Despite these advances in Holocene climate research, high resolution transect study records covering the Medittereanean and North West African climate from this time are still rare. Earlier tropical Atlantic records (e.g. de Menocal *et al.,* 2000a; Haug *et al.,* 2001) and terrigenous sediments from NW Africa (Holz *et al.,* 2007) suggest that this region did experience characteristic century-millennial scale variability. The records from these studies however were determined from individual core sites and not a continental transect of multiple high accumulations rate core sites which may be able to strategically monitor changes in the NW African

climate. This thesis will contribute to part of a larger international project of the eastern tropical Atlantic (CHEETA programme), which provides sediment core material from high accumulation rate sites along the NW African transect (40°N-15°N) to define tropical modes and mechanisms associated with the last 35 kyrs covering the glacial to the Holocene. The transect approach used in this programme and this thesis will provide new sedimentation and terrestrial organic carbon burial records for the eastern Atlantic from the mid-latitudes to the tropics.

1.2 *Study regions*

In this thesis, two regions have been identified as strategic locations to reconstruct tropical African climate and marine sedimentation dynamics under major climate transitions. They are

1. The Deep Ivorian Basin (ODP Site 959) in the tropical equatorial Atlantic when the Late Miocene to early Pliocene climate transition is exceptionally preserved. High resolution (every 2.5 kyr) alkenone derived SST record combined with higher plant leaf waxes and organic carbon records from marine sediments from the tropical equatorial Atlantic will be a significant part of this study.
2. The NW African margin where Holocene to deglacial variations in climate are known to be well preserved. New datasets from surface sediments to track soil organic matter export to the ocean are provided from evidence of a paired novel biomarker approach. Further, from the NW African margin, an integrated chronological framework developed in this thesis

defines tropical mechanisms associated with glacial to Holocene climate variability.

1.3 *Aims and Objectives*

The overall aim of this thesis is to investigate the dynamics of tropical African climate and marine sedimentation during periods of major climate transitions. Two main research studies have been identified to address the aims of this thesis.

The first study investigates the climate and organic carbon dynamics in the tropical equatorial Atlantic using high resolution sediments recovered from the **O**cean **D**rilling **P**rogram (ODP 959) across the late Miocene to early Pliocene climate transition.

The second main research focus is the CHEETA transect, which investigates surface and gravity core sediments in order to test the sensitivity of biomarkers for tracking SOM and exploring glacial to Holocene climate variability respectively.

This thesis identifies the following objectives.

1.3.1 *The Miocene/Pliocene climate transition (7-5 Ma) at ODP site 959*

1. To infer variations in sea surface temperature (SST) in the tropical eastern equatorial Atlantic using the $U^{k'}_{37}$ index from unsaturated long chain alkenones ($C_{37:2}$ and $C_{37:3}$).
2. To explore organic carbon supply and preservation and burial from North West Africa transported to the equatorial Atlantic by quantifying long

chain *n*-alkanes and organic carbon burial records from organic carbon (TOC) and $CaCO_3$ along eastern equatorial tropical Atlantic.

3. To investigate the nature of TOC cycles, their relationship to orbital forcing, continental climate, and vegetation change, and surface ocean dynamics at millennial time scale resolution using time series analyses.

1.3.2 *The glacial to Holocene transect- CHEETA Transect*

1. To carry out an independent study to trace soil organic matter (SOM) (surface sediments only) along the NW African transect by combining traditional organic geochemical bulk parameters with SOM tracers i.e. branched glycerol dialkyl glycerol tetraether (GDGTs) the branched vs. isoprenoid tetraether (BIT index) and hopanoid lipids, bacteriohopanepolyols (BHPs).
2. To develop an integrated chronological framework for all cores from the NW African margin using ^{14}C AMS and bulk $^{13}C_{org}$ data. It is important to note that the ^{14}C AMS data used for this framework was kindly provided by and owned by Professor P.de Menocal.
3. To utilize multiple organic multiple organic geochemical proxies from gravity core sediments including elemental data (TOC, Carbonates, Bulk accumulation rates); abundance and isotopic composition of bulk organic matter ($\delta^{13}C_{org}$) and higher plant leafwaxes (*n*-alkanes) to constrain regional variations in continental climate and terrigenous supply.
4. To identify the timing and regional extent of specific time intervals: the glacial; deglacial and Holocene (African Humid Period) over NW Africa as represented by organic carbon burial and bulk $\delta^{13}C_{org}$ records.

1.4 *Scope and arrangement of thesis*

Chapter 1 introduces this thesis and its aims and objectives. In **Chapter 2** the two climate transitions in this thesis: the late Miocene to early Pliocene climate transition and the glacial to Holocene climate transition are described. Modern conditions of the tropical eastern equatorial Atlantic and its potential to better understand regional and large scale connections between the atmosphere and ocean system in climate development is also described. Further, the biomarker approaches applied in this thesis are presented. In **Chapter 3**, the analytical approach to achieve the aims and objectives of this thesis are detailed. The results and discussion are detailed in **Chapters 4-6**. **Chapter 4** couples the high resolution records during the late Miocene to early Pliocene climate transition with detailed time-series analyses and suggest that high latitude climate forcing influenced the tropical African climate during the late Miocene to early Pliocene climate. **Chapters 5 and 6** concern the CHEETA project. In **Chapter 5**, biomarkers to track soil organic matter dynamics and surface deposition from surface sediments along the North West African margin show the presence of branched GDGTs (BIT index) and BHPs for the first time in open marine environments supporting soil organic matter input at least off NW Africa. **Chapter 6** presents the development of an integrated chronological framework from the ^{14}C AMS (P.de Menocal *et al,* in prep) and $^{13}C_{org}$ records and sedimentation profiles of the North West African margin and investigate terrestrial vegetation and climate change from the glacial to the Holocene. In addition, a biomarker pilot study from few cores from the NW African margin

which identifies areas of further research. Finally, the major results of this thesis are concluded and suggestions made for future research outlined in **Chapter 7.**

2 Chapter Two

2.1 *The Miocene/Pliocene climate variabilty*

The Miocene/Pliocene interval placed within the Cenozoic (Fig. 2.1) (Zachos 2001) covered short and longer-term climate transitions that document accumulative perturbations of the Earth system. Deep sea stable isotope oxygen (δ^{18} O) and carbon (^{13}C) isotopic records showed episodes of global cooling, ice sheet growth and decay and global vegetation change. Gradual reestablishment of a major ice-sheet on Antarctica was around 10 Ma. Between 7 and 5 Ma, mean (δ^{18}O) continued to rise gently indicating additional cooling on a small-scale with ice sheet expansion on West Antarctica and in the Arctic.

In contrast, the Pliocene period (Fig 2.1) shows warming trends until about 3.2 Ma with the onset of the Northern Hemisphere glaciation (NHG) (Shackleton *et al.,* 1988; Maslin *et al.,* 1998). The Pliocene climate has been linked to the modern conditions of today, cooler and drier, and seasonal, similar to modern conditions. Mid Pliocene average temperature was however 2-3°C higher, suggesting increased CO_2 levels, (van der Burgh et al., 1993; Raymo et al., 1996) warm sea surface temperature in upwelling regions and at high latitudes (e.g Dowsett *et al.,* 1992; Herbert and Schuffert, 1998; Wara *et al.,* 2005; Lawrence *et al.,* 2006). These changes caused ice sea melt and increased temperatures during the early Pliocene. There has been increased interest in assessing climate sensitivity during the early Pliocene due to its implications for modern climate conditions, with changes in green house gas levels and oceanic heat transport during an interval of global warmth (Raymo *et al.,* 1996; Billups *et*

al., 1998; Ravelo and Andreasen, 2000) with an impact on atmospheric ocean circulation patterns. Despite much evidence from the high latitudes for increased high latitude warmth during the Pliocene climate transition (Billups *et al.,* 1998 and references therein) and global cooling during the late Miocene (Shackleton and Kennet, 1975a) studies in the tropical eastern Atlantic are still rare. These previous studies have been from the South Atlantic (e.g. Billups *et al.,* 2002); the North Atlantic (Dowsett *et al.,* 1992) and the Western equatorial Atlantic (Billups *et al.,* 1998). This thesis investigates records from the low latitudes- the eastern tropical equatorial Atlantic, where high resolution data coverage have been rare to add to knowledge and specifically address the interaction between ocean system/ climate through time. Previous studies which have at least shown interest in this interval and region (e.g Norris, 1998; Wagner; 1998) have been at lower resolution which is not sufficient to understanding the complex processes and feedbacks associated with the transition.

Towards this end, this thesis will help to identify key mechanisms and eventually contribute to better constrain possible consequences on future climate. Specifically, this thesis uses coupled signatures of plant leaf waxes preserved in marine sediments along with the reconstruction of alkenone sea surface temperature (SST) from the Deep Ivorian Basin (DIB) off Equatorial West-Africa (ODP Site 959) and organic carbon burial (TOC and carbonate) in order to develop novel high resolution records (every 2.5 cm corresponding to

2.5 Kyr) of tropical African hydrology and vegetation change for the time interval of about 7-5 Ma.

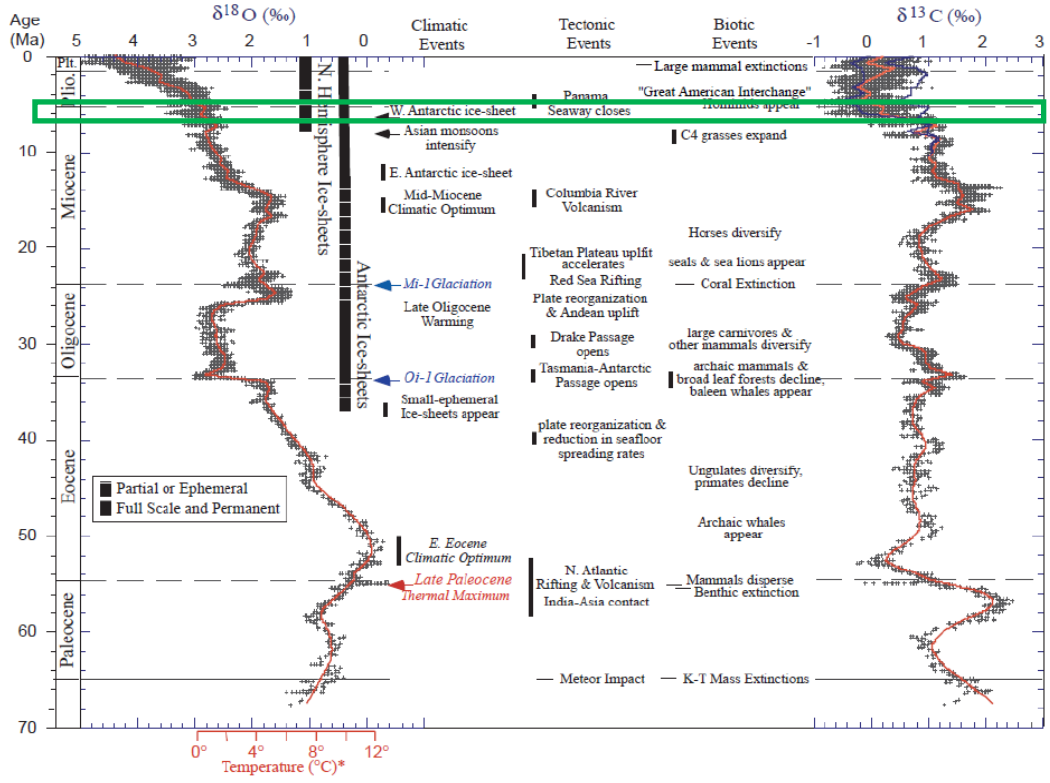

Figure 2.1 Global deep –sea oxygen and carbon isotope records from > 40 ODP and DSDP sites (Zachos, 2001). Green bar, this study, the late Miocene to early Pliocene climate transition (~7-5 Ma)

The evidence for global vegetion change from $\delta^{13}C$ values during the late Miocene have been recorded in the tropics when rapid expansion of C_4 biomass occurred (Cerling *et al.,* 1993; 1997). This expansion was linked to lower atmospheric CO_2 levels which favoured C_4 photosynthesis rather than C_3 photosynthesis (Cerling *et al.,* 1993) and found to occur at lower latitudes with warmer temperatures (Cerling et al., 1997). More recently, expansion of C_4 during the late Miocene to early Pliocene in the Gulf of Mexico have been linked to substantial changes in global climate (Tipple and Pagani, 2010).

With regards to changes in SST, the tropics have been shown to influence global climate under different past climate transitions and under different timescales (e.g. Schefuß *et al.,* 2005; McClymont and Rosell Melé, 2005; Lea *et al.,* 2003). Studies carried out on records from the mid-Pleistocene climate transition using alkenone derived $U^{k'}_{37}$ index for SST proxy showed that global climate was associated with the tropical circulation in the Pacific similar to those caused by the modern El Niño mechanisms and not simply a development within the Northern Hemisphere ice sheets and high-latitude climates (McClymont and Rosell Melé 2005). Alkenone derived $U^{k'}_{37}$ index for SST during the Late Miocene to early Pliocene will provide key information on ocean circulation dynamics in the tropics at this time. Further, previous studies have revealed that rapid shifts in SST occurred on centennial timescales or less as the earth warmed up at the end of the last ice age (between 14,600 and 11,400 years) from sediments recovered from the Cariaco Basin, off tropical Africa (Lea *et al.,* 2003). On shorter time scales associated with the Holocene, large scale hydrological changes in equatorial Africa during the past 20,000 years have been linked to changes in SST between the tropics and subtropics of the South Atlantic which modulated the moisture transport onto the central African continent (Schefuß *et al.,* 2005).

These studies on surface ocean variability and vegetation change have indeed provided an insight into the climate dynamics at different regions and of different timescales. However, challenges remain and there is a need to understand

what the lead /lag relationships are between surface ocean dynamics and terrestrial vegetation change during this climate transiton which will determine drivers and spatial coverage to reconstruct temporal migration or documentation of climate change. Specifically, key questions still remain on how large temperature changes may have influenced the precipitation patterns near the equator especially because of the complex wind systems and rainfall patterns associated with the Intertropical convergence zones. Further, the amplitude of change on different time scales which is controlled by the sensitivity and response time of the region and dominant drivers and/or mechanisms translating such changes to the equatorial tropical Atlantic and NW Africa must be explored.

There are still gaps in knowledge due to the limited marine records from the low latitude tropical regions which can monitor temporal and spatial sensitivities of the continent to climate change. Generation and assessment of high resolution paleoclimate records using bulk geochemical and novel biomarker approaches that specifically target and provide climate information from marine sediments from tropical and subtropical Africa are therefore needed to accurately delineate and track parts of the global climate system that responded on different time scales (See Fig 2.2)

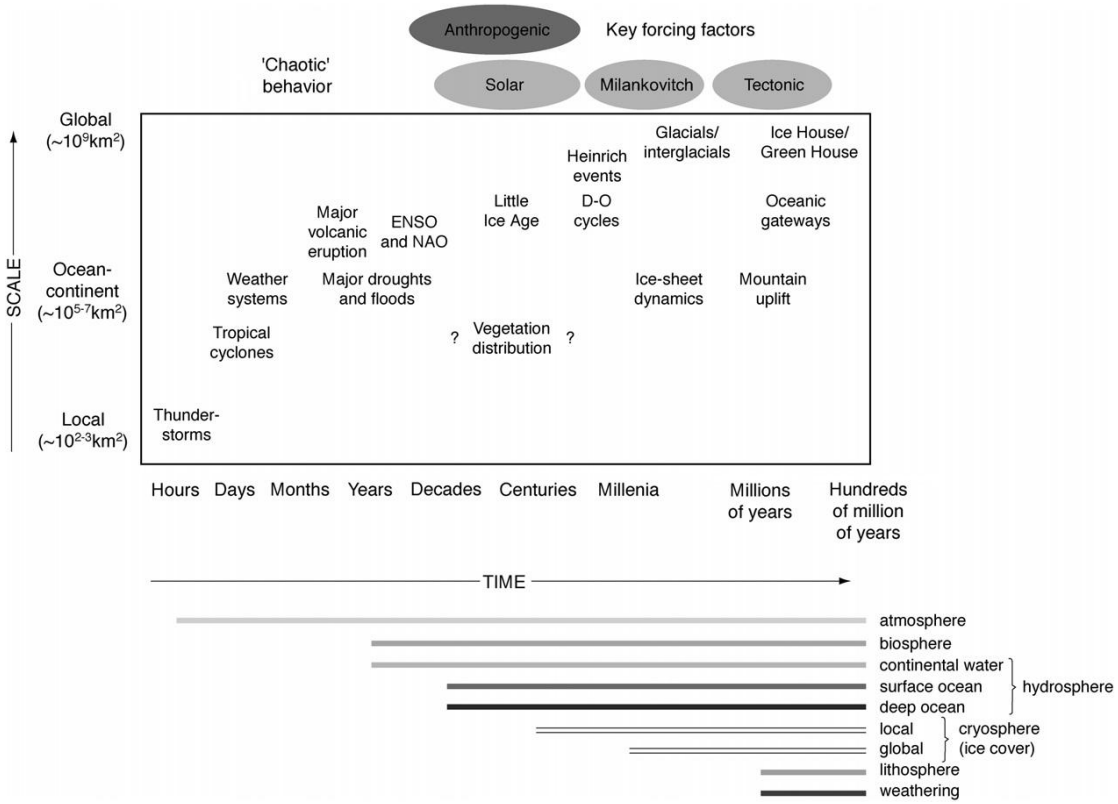

Figure 2.2 The spatial and temporal dimensions of the earth's climate system (plotted on logarithmic scales). The key forcing functions and response time of different sections of the global climate systems (Adapted from Maslin and Christensen, 2007

The late Miocene to early Pliocene transition therefore provides an ideal backdrop to investigate the effect of global ocean and land-atmosphere circulation for tropical African climate with progressive move towards more warmer and humid environments on the continent and subsequent changes in ocean current and marine carbon burial.

2.1.1 *Orbital Forcing*

It is well documented that the Earth climate experienced major continuous shifts from extreme expansive warmth (ice free poles) to extreme cooling (continental ice sheets and polar caps) during the last 65 million years and beyond

(summary in Zachos *et al.,* 2006). Such long term trends in climate have been linked to Earth's orbital geometry and plate tectonics which are in constant motion. Variations in the earth's orbit and axial parameters in the region of 10^4 - 10^5 years are linked to the intensity of the solar energy that hit the atmosphere (insolation) that oscillate with the Earth's orbital parameters of eccentricity, obliquity and precession (Fig .2.3).

The eccentricity frequency cycles of 400 and 100 ky refers to the shapes of the Earth's orbit around the sun, varying from near circular to elliptical (Hays *et al*. ., 1976). Although this has an effect on insolation, the effect has been regarded as relatively small, and in most cases will not account independently for the changes in the Earth's climate during the past. The obliquity orbital frequency is 41 kyr which reflects the tilt of the Earth's axis relative to the plane of the ecliptic varying between 22.1° and 24.5°. A high angle of tilt indicates seasonal contrasts, predominantly and more effective at high latitudes (e.g. winters in both hemispheres will be colder and summers hotter as obliquity increases) while a low angle of tilt indicates seasonal contrast which may be more effective at low latitudes. Precession consists of frequencies of 23 kyr and 19 kyr and refers to the wobble of the axis of rotation describing a circle in space with a period of 26 kyr. Precession is modulated by orbital eccentricity frequencies and determines where the seasonal variations in the hemispheres occur. Precession determines overall seasonal contrast in one hemisphere and relationship in another. Consequently, the effect of precession has been documented to be largest at the equator and decreases with increasing latitude. These distinct

frequencies in the orbital bands, affects climate either by modulating the amplitude in the other frequency (e.g. eccentricity and precession), thereby changing annual and or seasonal energy budget or changes the latitudinal distribution of insolation. Therefore the stability of these changes over long periods of time allow for predictable pacing of climate (Laskar, 1993).

The orbital frequencies have also been linked to changes in response to the Earth's climate dependent on gradual changes in geological boundary conditions such as continental distribution/ topography (Fig.4.2),opening and closure of oceanic gateways and changes in atmospheric greenhouse gases (Crowley, 1998). Perturbations to these boundary conditions affect the amplitude of changes induced by orbital frequencies (e.g. Raymo and Ruddiman, 1992; Kutzbach *et al.,* 1993; Mikolajewicz *et al.,* 1993).

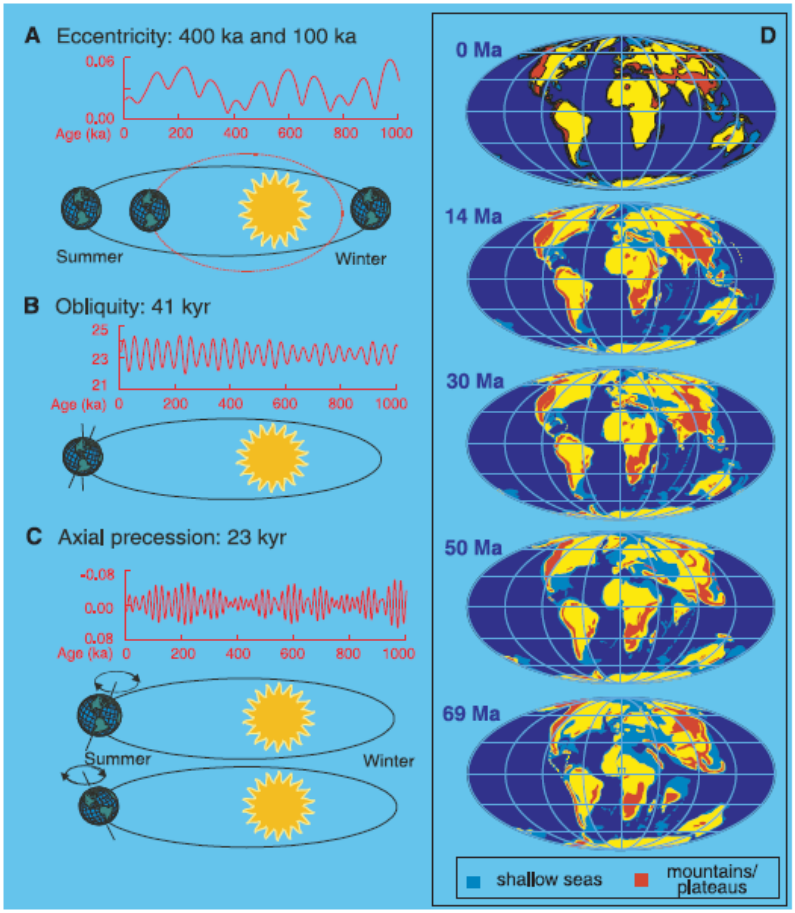

Figure 2.3 Primary orbital components of the earth displayed from (A-C). Gravitational forces exerted by other celestial bodies affect the earth's orbit, resulting in the variations in the intensity of the sun. Orbital perturbations have five periods: eccentricity (at 400 and 100 ky), obliquity (41 ky), and precession (23 and 19 ky) Adapted from Hays et al., 1976. (D) Continental geography reconstructed for five intervals of the last 70 My (Zachos et al., 2006).

2.1.2 *High and Low latitude influence on tropical African climate:*

Understanding processes that drive tropical African climate has been a major issue for debate, the main controversy being the sensitivity of the low latitude regions to high latitude climate forcing (de Menocal *et al.*, 1993). Previous studies have proposed that the establishment of the early African monsoon/trade system during the late Miocene – early Pliocene may have been

directly linked to eustatic sea level dynamics and hence higher latitude climate dynamics (Kennett, 1982; Zhang and Scott, 1996).

One main driver for high latitude climate processes is ice sheet response to earth's orbital variations (Hays, 1976; Imbrie *et al.,* 1984). Previous studies on the climate sensitivity to orbital forcing based on proxy-based and modeling studies have been shown in the Pliocene (e.g Raymo *et al.,* 1992); the late Miocene (Hilgen, 1991; Krijgsman *et al.,* 1994; 1995; Hilgen *et al.,* 1995), Pliocene (Shackleton *et al.,* 1995; Tiedemann and Franz, 1997), but to date, no studies have explored the late Miocene to early Pliocene time period in a tropical setting. One central aspect of this thesis is to gain insight into the proposed African climate response to high latitude forcing during the late Miocene to early Pliocene climate transition. Time series analyses of high resolution (2.5-5 kyr) records from ODP Site 959 including records of TOC; alkenone –derived SST and biomarkers of higher plants (leafwax lipids) will be investigated to explore the influence of high latitude influences.

2.2 *The Eastern equatorial Atlantic - Modern Conditions*

In many ways the tropical eastern equatorial Atlantic and the North West African region is ideally suited for investigative studies on climatic development, dynamics fluctuations as a result of this, and the biogeochemical interactions between the land and oceans. In this thesis, the core of the late Miocene to early Pliocene climate transition is to couple SST records with higher plant leafwaxes preserved in marine sediments from the equatorial Atlantic in order to reconstruct the history of tropical African marine sedimentation and African climate. It is expected that study wil give an integrated view on the processes, feedbacks and time relationships of the tropical climate ocean system.

The equatorial Atlantic acts as a corridor for the transfer of major deep and surface water in and out of the ocean, providing a driving process for interhemisphere and latitudinal heat transfer (Zabel *et al.,* 2004). Equally important, the relationships between the equatorial Atlantic and the North West African region is influenced by the complex wind systems and interchange of seasonal cycles between the Northern and Southern Hemisphere at the Intertropical Convergence Zone (ITCZ; Fig 2.4); the low altitude north east Trade Winds (NETW); the middle altitude Saharan Air Layer (SAL); the highly productive upwelling areas of the Congo area and the Canary current (Zhao *et al.,* 2000 and references therein).

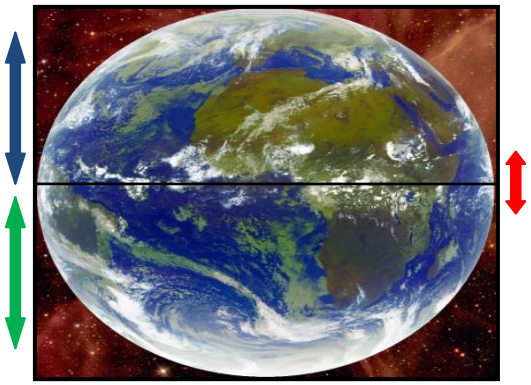

Figure 2.4 The position of the ITCZ across the African continent and the eastern equatorial Atlantic (red arrow), black line separates the Northern Hemisphere (blue arrow) from the Southern Hemisphere (green arrow, (source, http://earthobservatory.nasa.gov).

Under modern conditions, over the coast of North West Africa, atmospheric circulation is driven by the easterly SAL and the northeasterly NETW (Fig 2.5) generating an upwelling zone and high productivity areas. The interactions of these wind systems contribute terrigenous material to the marine environment (Tetzlaf and Wolter, 1980; Sarnthein *et al.,* 1981, Sarnthein 1982; Ruddiman *et al.,* 1989; Adegbie *et al.,* 2003)

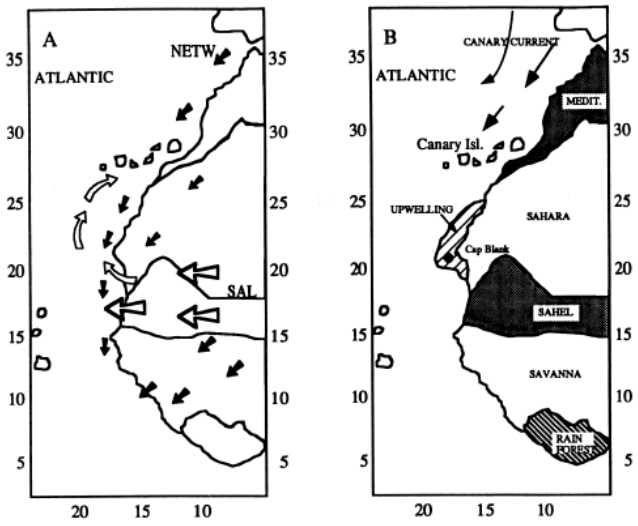

Figure 2.5 Present day major wind belts (A) and vegetation zones,(B) surface ocean currents and upwelling region in the North West African region (modified from Zhao et al., 2000 from Hooghiemstra, 1989)

Surface water circulation in the equatorial Atlantic is largely a product of the strength and position of the (ITCZ) which will drive the complex wind systems, seasonal variations and upwelling in the equatorial region. The temperature changes between the land and the ocean on either a global or regional scale combined with air pressure gradients is responsible for atmospheric circulation, driving climate conditions and marine sedimentation in the equatorial Atlantic (Zabel *et al.,* 2004; Wagner *et al.,* 2000).

These complex interchanges between climate and sediments in the equatorial Atlantic have led to understanding the sub-processes that alter sedimentation, or control African climate and terrestrial vegetation (e.g. Parkin and Shackleton, 1973; Street and Grove 1976; Pokras and Mix., 1985; Zabel *et al.,* 1999; Wagner *et al.,* 2004; Schefuß *et al.,* 2005). However, past efforts to monitor these changes, such as the evolution of sea surface temperature in the past, have been hampered by laborious techniques (e.g faunal analysis) (Dowsett *et al.,* 1996 Nikolaev *et al.,* 1998; Dowsett *et al.,* 2005); discontinuous records of sedimentation (Thompson and Flemming 1996), or by the use of proxies with multiple climate sensitivities (e.g. planktonic $\delta^{18}O$, Shackleton and Opdyke 1973; Chappell and Shackleton 1986).

Other gaps in knowledge with regards to climate change in the equatorial Atlantic refer to the relationship between high –and low- latitude climate drivers or controls. The high latitudes are dominated by temperature climate signals while low latitudes can often be characterised by terrestrial response (de

Menocal *et al.,* 1993) primarily controlled by precipitation onto the West African continent (e.g. Street and Grove, 1976; Pastouret *et al.,* 1978; Kutzbach 1981; Pokras and Mix, 1985; Prell and Kutzbach, 1987; McIntyre *et al.,* 1989; Molfino *et al.,* 1990; Griffin, 2002; Schefuß *et al.,* 2003).

Today, NW Africa is one of the regions with large equatorial land mass, and its vegetation and climate zones differ significantly from tropical to extratropical. These vast differences have led some studies to show that tropical climate variability such as past aridity during glaciations was directly linked to expansions of terrestrial vegetation for example the savannah belt in glacial boundary conditions emanating from higher latitudes (Gasse *et al.,* 1990).

The eastern equatorial Atlantic off North West Africa region provides critical sediment archives that contain detailed paleoenvironmental information on production, burial and dilution of organic matter. Previously, extensive work from marine and lacustrine sediments in the equatorial Atlantic region has improved our knowledge on the biogeochemical causes and effects on climate change (Zabel *et al.,* 1999; Mulitza and Ruhlemann 2000; Schefuß *et al.,* 2003; Schefuß *et al.,* 2005). Further, other studies from the equatorial Atlantic using inorganic terrigenous material support the conclusion that both high-latitude and low-latitude forcing influence tropical climate and marine sedimentation (Zabel *et al.,* 1999) and that changes in ocean circulation, and hence sea surface temperature patterns, were important in modulating atmospheric moisture transport onto the central African continent (Schefuß *et al.,* 2005).

However, the link and amplitude of change between African climate and terrestrial vegetation response in the eastern equatorial Atlantic region remains unclear. Terrestrial vegetation change from inputs of terrestrial source material to equatorial Atlantic sediments (See Fig 2.6) reflects continental climate conditions at the time of deposition. Changes in wind intensity, direction and seasonality as well as vegetation cover, and the balance between aeolian and fluvial transport (Cole *et al.,* 2009) can indeed affect the amount of terrestrial material deposited in deep sea sediments off equatorial West Africa. Therefore, critically investigating marine sediments in from this sector from organic carbon records (TOC and carbonates) can provide key information on terrestrial organic supply and preservation and how African climate evolved in the past.

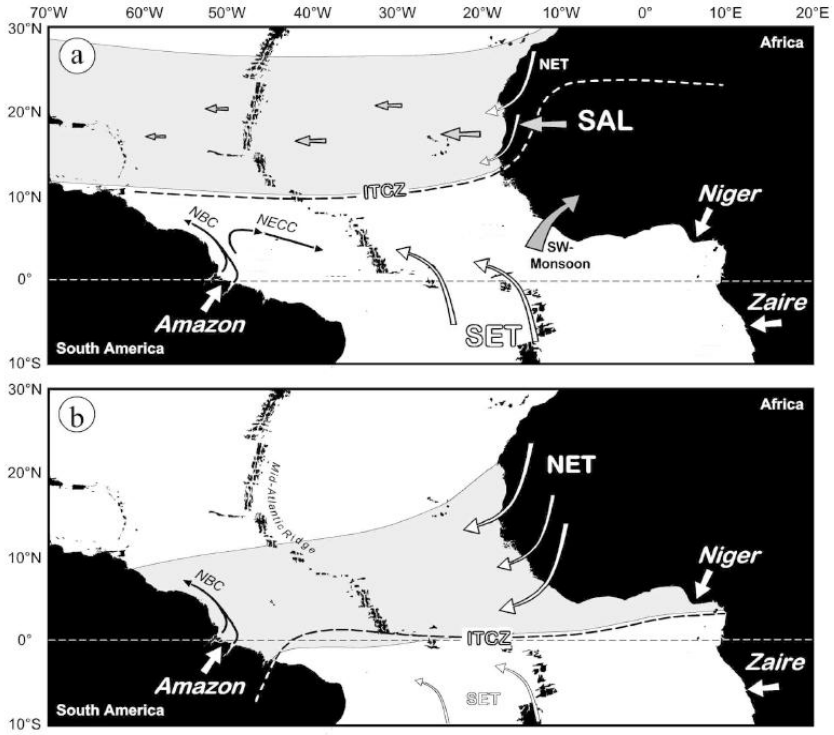

Figure 2.6 The equatorial Atlantic and source areas for terrigenous input showing the current low, mid –tropospheric and underlying wind systems and river (Niger, Amazon and Zaire). a) Summer, when the SE trade winds are strongest, moving the ITCZ to ~10°N b) winter, NE trade winds are strongest, with ITCZ located close to the equator. Grey shaded areas show the seasonal migration of dust plumes and the movement of the ITCZ during the seasons (Modified after Zabel et al., 2004).

2.2.1 *The Intertropical Convergence zone (ITCZ)*

Today, the movement of the ITCZ (Fig 2.7) marks the longitudinal area where the trade winds of the Northern and Southern Hemispheres converge. It is well documented that the convergence of the trade winds, the rising of the buoyant air in the ITCZ, which expands and cools, are linked to the precipitation changes in the African continent and the intensity of the summer insolation (Kutzbach and Liu 1997; Partridge *et al.,* 1997) as well as the northward movement of the ITCZ and associated precipitation belt (Street-Perrott, 1990).

The mechanisms and seasonal shifts in the location of the ITCZ drastically affects rainfall in many equatorial regions, resulting in the wet and dry seasons of the tropics rather than the cold and warm seasons of higher latitudes. The present day ITCZ migrates seasonally between 0° to 15°N over the eastern Atlantic due to the westward North Equatorial Current (NEC) and its counterpart current the South Equatorial current (SEC) (Peterson and Stramma 1991; Richardson and Philander 1987; Richardson and McKee 1984). In the summer, when the ITCZ is well north of the equator (Philander and Pacanowsi, 1986) wind stress fields from the SEC trade winds are strongest and reach its maximum velocity (Höll, 2000) depositing aeolian transported matter materials from land to the ocean. The summer monsoonal circulation sets in and transports dust westward as far as the Caribbean (Carlson and Prospero, 1972; Prospero and Lamb, 2003) and possibly beyond. During the winter, the African continent cools relative to the adjacent ocean and the regional atmospheric circulation patterns reverses; the ITCZ is pushed to its southward position and dry but variable NE winds predominate. A separate dust plume is associated with the SE winds, (the Harmattan), which transports large volumes of dust ocean wards. Thus during cooler periods, when the ITCZ is in its SW position, persistent and coastal upwelling is established along the North West and tropical African margin (Muller and Fischer, 2001).

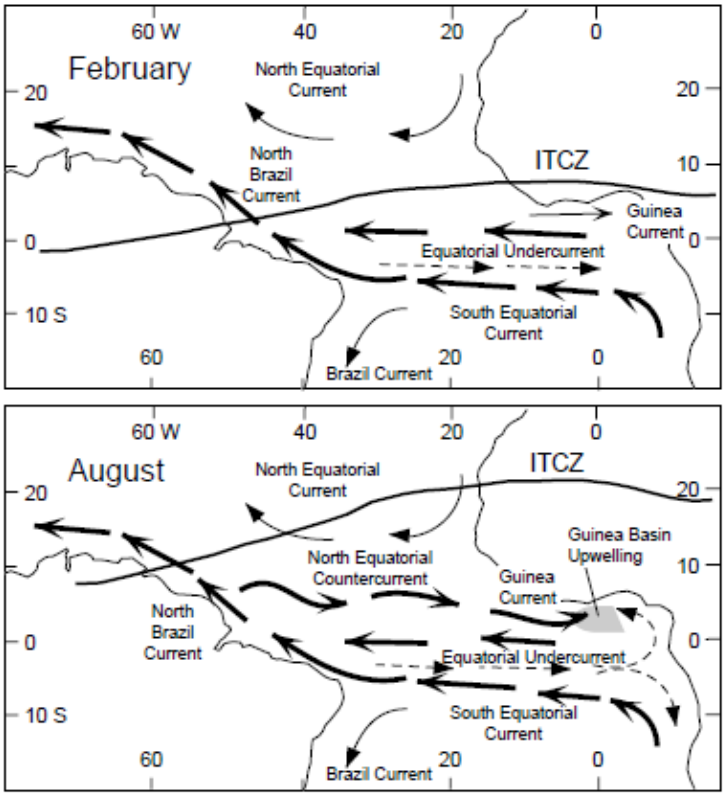

Figure 2.7 The movement of the ITCZ during boreal winter (February) and summer (August) in the equatorial Atlantic.Major currents are shown (adapted from Norris, 1998)

To establish source regions of dust and consequent terrestrial vegetation supply, satellite imaging of atmospheric aerosols showed the dust producing areas of North West Africa to be from the Chad area, the Mauritania and Western Sahara (Prospero *et al.,* 2002). The Western Sahara influenced by the SAL (See Fig 2.5) occurs due to the stronger influence of the NE trade winds (Chiapello *et al.,* 1995; Chiapello *et al.,* 1997). The deposition of terrestrial input from dust to the eastern equatorial Atlantic will therefore be stronger influenced by the North Easterly trade winds. In this thesis, the role of the ITCZ is investigated by obtaining higher plant leafwax record in combination with TOC and SST records. It is expected that increased wind energy inferred from dust

transported terrigenous organic matter will translate to cooler temperatures and enhanced upwelling in the study area.

2.2.2 *Upwelling and the modern depositional enivironment*

Sediment redistribution occurs as a result of upwelling due to the interactions of the currents i.e. the Canary Current (Mittlestaedt, 1991), Guinea Current, which remains constant all year round, deep water masses (North Atlantic deep water below 2000m) and north-flowing Antarctic bottom water below ~3600m (Sarnthein *et al.,* 1982). Upwelling from the Ivory coast/Ghana current is related to the Guinea current which comes from two sources, the North Equatorial Countercurrent (NECC) and the Canary Current (Fig 2.7). The seasonal instability of these two currents can affect the seasonal variability of the Guinea Current (Longhurst 1962, Ingham 1970). The Guinea Current, (Fig 2.7) like other eastern ocean boundary currents, is characterized by areas of upwelling (Bakun 1978) and increased biological productivity (Binet 1997). However, the Guinea Current is unusual among upwelling regions in that there seems to be no correlation between sea surface temperature and wind patterns on a seasonal time scale (Longhurst 1962, Bakun 1978) and can remain constant all year round.(Sarnthein *et al.,* 1982).

Under modern conditions, along West Africa margin, deposition of marine organic matter is linked to high plankton productivity due to fluvial input and influence of upwelled nutrient rich waters from the south Atlantic central water (SACW) (Voitureiz and Herbland, 1978). Oceanic upwelling occurs in the eastern equatorial Atlantic along the equatorial divergence zone as a result of

lateral advection of nutrient rich cold waters from the westward flowing south equatorial current (SEC) combined with trade wind divergence (Peterson and Stramma; 1991, Voituriez and Herbland, 1982; van Leeuwen, 1989). All year round wind induced coastal upwelling occurs off the coastal areas off NW (Schemainda *et al.,* 1975) and SW Africa (Lutjeharms and Meewis, 1987; Hart and Currie, 1960), with regionally upwelling cells being developed off the Ivory Coast and Ghana (Verstraete, 1992; Voiteruz and Herbland, 1982) and southern Senegal during the winter and spring (Westerhausen *et al*., 1993). Upwelling processes control the organic carbon supply and preservation in the equatorial Atlantic (Huang *et al.,* 2000; Wagner and Dupont, 1999; Westerhausen *et al.,* 1993) but is diluted by both fluvial and aeolian terrigenous organic matter controlled by the Trade–Harmattan and monsoon wind systems (Wagner, 1998; Westerhausen *et al.,* 1993).

The release of aeolian material across a broad area of the eastern equatorial Atlantic (Wagner, 1998) in particular have been attributed to the arid to semi arid zones of central Africa (Pokras and Mix, 1985; Sarnthein *et al.,* 1982, Bonifay and Giresse, 1992) which generally constitute of terrestrial organic matter from savannah vegetation and lake deposits indicative of terrestrial higher plants. Total organic carbon and carbonate sedimentary records from the eastern equatorial Atlantic have been influenced by low sedimentation rates linked to climatic cycles and evolution (Wagner *et al.,* 1998). Carbonate patterns are mainly driven by Atlantic type carbonate dissolution patterns that are driven by productivity along the African continental margin (Wagner *et al.,* 1998)

Hedges *et al*. (1997) and Calvert and Pedersen (1992) found that several processes affect the rate of deposition of terrestrial and marine organic carbon in marine environments such as oxic or anoxic conditions.

2.3 *The Glacial to Holocene climate (35 Ka)*

On glacial to interglacial timescales, continental climate of northern Africa fluctuated between arid and hyperarid conditions since the last glacial period with much wetter conditions during the Holocene, known as the African Humid period (Gillespie *et al.,* 1983; Ritchie *et al.,* 1985; Gasse, 2000; Swezey, 2001; de Menocal *et al.,* 2000a, 2000b). These dynamic shifts in African climate have been documented from several studies, e.g. in terrestrial records of fossil mammals (McIntosh and McIntosh, 1983); in ancient lake highstands (Street and Grove, 1979); and marine records of fossil pollen (Hooghiemstra *et al.,* 1998), terrigenous matter (de Menocal *et al.,* 2000a; 2002b) and more recently from marine sediments (GeoB 7920) in the North West African region (Tjallingii *et al.,* 2008).

Previously, the climate of the Holocene has been known to be fairly stable (Dansgaard *et al.,* 1993). However, there is now abundant evidence from the high latitude regions, in particular the sub polar North Atlantic, that abrupt millennial scale climate changes comparable in timing, duration and abruptness to glacial events also occurred during the Holocene warm climate (Bond *et al.,* 1997; 2001; Jennings *et al.,* 2002; O'Brien *et al.,* 1995; Dahl–Jensen *et al.,* 1998). The last glacial maximum (LGM), terminated with the onset of the Northern Hemisphere deglaciation, apparently induced by an increase in northern summer insolation. This caused an abrupt increase in sea level, evident also in the southern hemisphere (Clark *et al.,* 2009).

The increase in humid conditions e.g. in subtropical Africa led to long term variations in humidity which were influenced by the African monsoon, related to precessional changes in low latitude summer insolation (Schefuß *et al.,* 2003; Weldab *et al.,* 2007; Claussen *et al.,* 1999). The most prominent period, the African Humid Period (AHP), occurred between 9 to 6 ka (Ritchie *et al.,* 1985), with wettest conditions around 12.3 to 5.5 ka (Adkins *et al.,* 2006; de Menocal *et al.,* 2000b), and caused dramatic changes in North West African climate and marine sedimentation.

Unlike the high latitudes, less knowledge exists on the mechanisms by which subtropical Africa was influenced and/or responded to global climate variability during this climate transition. Some studies have suggested that the perturbations in the high latitude North Atlantic regions may have been initiated in the tropics and propagated from there into high latitudes (Cane, 1998; Stocker, 1998; Schmittner and Clement, 2002; Chiang and Bitz, 2005). Irrespective, high resolution records of Holocene tropical Atlantic climate variability are still rare despite the long knowledge of existence of high accumulation rate regions off subtropical regions (e.g. Kuhlmann *et al.,* 2004). Previous studies of tropical Atlantic paleoclimate have indeed demonstrated that this region experienced centinnial–millennial scale variability during the Holocene (de Menocal *et al.,* 2000a; Huag *et al.,* 2001; Holz *et al.,* 2007; Holzwarth *et al.,* 2010) but the data from these studies have been limited in resolution and areal coverage to give consistent indications of the amplitudes and relationships across the different climate zones characterising NW Africa.

There is a need for additional continuous high-resolution records from identified high accumulation rate sites that cover the LGM to Holocene period to fill the gap of how Northern Africa changed, and in particular if the changes differed between the tropical and Mediterranean latitudes. This thesis will contribute to filling this gap by providing new geochemical and isotopic and molecular records from sediments recovered during the CHEETA (Changing Holocene Environments of the Eastern Tropical Atlantic) cruise in order to understand NW Africa climate variability (Chapter 6).

2.3.1 *Modern vegetation zones from the tropical to Medditerenean*

Under modern conditions, the vegetation in North and Central Africa consist of tropical rain forest, trees, grasses, savannah and semi-deserts in the Sahel zone (Fig 2.8) which are directly linked to the intensity of the North African monsoon (de Menocal, 2000a). Research on terrestrial vegetation change using bulk carbon isotopic and molecular records along the North West African margin, covering Europe and North West Africa during the Holocene is a relatively new area of research but has been shown to provide some relevant information (Niedermeyer et al., 2010) There are many methods for reconstructing vegetation changes from marine sediments including direct information from pollen and spores (palynology) and molecular proxy data from sporopollenin and lignin which comprise the protective coating of plant stems and pollen (de Leew *et al.,* 2006). Generation of these palynological and

molecular proxy data however is often not being favourable for high resolution temporal studies, especially when TOC concentrations are low.

Vegetation classes can reflect the type of CO_2 fixation mechanisms adopted by the originating plant, namely the Calvin Benson cycle (C_3); the Hatch–Slack (or dicarboxylic acid) (C_4) and Crassulacean Acid Metabolism (CAM) plants type (Collister *et al.,* 1994; O'Leary *et al.,* 1981; Rieley *et al.,* 1993). C_3 plant–derived $\delta^{13}C$ values are typically -36‰ (-31 to -39‰ vs. Pee Dee Belemnite), whereas C_4 plants are characterised by a distinct heavy average *n*-alkane $\delta^{13}C$ value of around -21.5‰ (-18 to -25‰) (Schefuß *et al.* 2003 and references therein). The C_4 pathway is utilised by plants in arid environments to limit the amount of water loss from their leaves and stomata, which results in less fractionation and consequently heavier $\delta^{13}C$ values than the C_3 plants. CAM plants are intermediate and can use both pathways with *n*-alkane $\delta^{13}C$ values of (-25 to -27‰). Virtually all trees, shrubs, and cool season grasses and sedges use the C_3 plant pathway while C_4 plants consist of warm season grasses and sedges. CAM plants on the other hand are cacti plants and succulent in nature (Cerling *et al.,* 1993; Spicer, 1989). C_4 plants are found predominantly in tropical savannas, temperate grasslands and semi deserts (Cerling *et al.,* 1993). Most African grasslands in the subtropical belt are dominated today by C_4 plant vegetation (Collatz *et al.,* 1998) due to the hot and arid climate conditions. CAM plants have not been found to be significantly dominant in the North West African region (Farquhar *et al.,* 1989; Collister *et al.,* 1994; Winter and Smith, 1996).

The techniques used for determining the isotopic signals (See Chapter 3) can differentiate the dry grassland dominated C_4 type vegetation from the more humid forest C_3 type vegetation, as well as algal organic matter both marine and lacustrine. In North West Africa, this information is particularly useful to reconstruct the development of continental climate dynamics in the past.

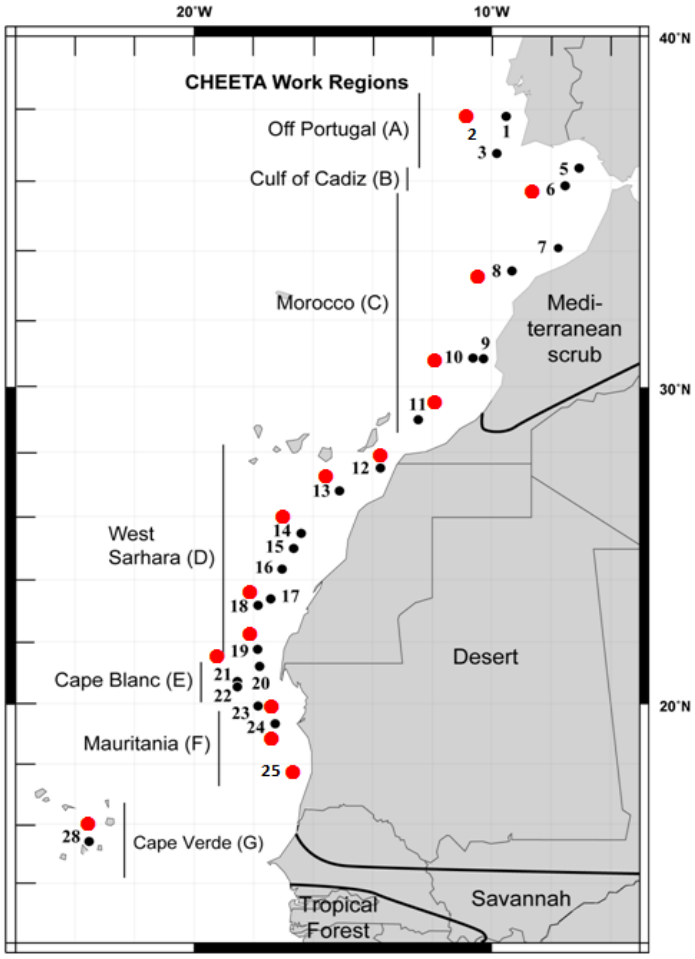

Figure 2.8 CHEETA cores and vegetation zones along the NW African margin. Red dots, gravity cores investigated in this study. Station list, water depth and work regions are detailed in the Appendix B and C

Carbon isotopic compositions to determine C_3 vs. C_4 vegetation type organic material from North West African sediments (Bird *et al.,* 1995; Huang *et al.,* 2000; Kuypers *et al.,* 1999; Zhao *et al.,* 2003) have confirmed aridification cycles of the North West African region linked to past glacial periods. Other studies exploring glacial aridification cycles in North West Africa have used the supply and composition of lithogenic dust (de Menocal, 1995); latitudinal changes in vegetation biome boundaries (Dupont *et al.,* 1989), changes in river or wind borne organic matter to the equatorial Atlantic (Zabel *et al.,* 2001; Holtvoeth *et al.,* 2001); dust–borne radiogenic isotope records during the Holocene (Jung *et al.,* 2004); and phytoliths (Alexandre *et al.,* 1997). Compound specific carbon isotopic signatures from terrestrial lipid biomarkers are an additional and particularly strong, analytical technique to accurately separate between supply from C_4 and C_3 type vegetation (Schefuß *et al.,* 2003; Zhao *et al.,* 2000) and will be presented as a pilot in this thesis.

2.3.2 *Climate History of North West Africa*

The climate history of the North West African hinterland has been documented from freshwater diatom (*Melosira*) records and through various terrigenous sediment components preserved in the North West African marine sediments (Pokras and Mix, 1985). Arid and cooler conditions in North West Africa have been linked to glacial periods but conditions started to change around 15 ka in the deglacial period and around 9 ka with the onset of the African Humid Period (AHP) which markedly changed central African climate for a few thousand years (9-6 Ka) until the present day with widespread dry and arid conditions (Gasse,

2000; Zhao *et al.,* 2003). In this regard, studying the variability in NW African climate across the entire length from tropical to Mediterranean climate zones is particularly interesting as it can detail changes in continental supply of terrigenous organic matter within a spatiotemporal context, as well as vegetation change and climate change during past glacial – interglacial periods.

The AHP occurred between about 9-6 ka cal. BP (Ritchie *et al.,* 1985) and is linked to a period of enhanced monsoonal activity due to earth orbital changes which increased summer season insolation forcing of the African monsoon (de Menocal, 2000a). Consequences were, amongst others, increased C_3 type terrestrial vegetation cover and the presence of large permanent lakes, both of which supported human life in the modern day hyper arid desert of the Sahel Zone (Ritchie *et al.,* 1985; Roberts 1988). It is not well known, however, how abrupt or gradual the climate shifts occurred during the beginning and termination of the AHP and if the onset and duration of the AHP migrated across latitudes. Previous studies to address these climate shifts indicate that abrupt shifts from West African pollen and lake records were linked to much wetter conditions than today (Gasse and Van Campo, 1994). Other evidence for changes and climate shifts associated with the onset and termination of the AHP have included a fall in lake levels in the Ziway–Shala lake basin in Ethiopia (Street and Grove, 1979), a rapid retreat of habitats from lake sediments in central Africa (Lamb *et al.,* 1995; Lezine *et al.,* 1991), and rapid migration of human populations from central and southern Saharan to be replaced by more mobile, pastoralist–traditional cultures (McIntosh and McIntosh, 1983).

Several paleorecords from ODP Site 658, off Cape Blanc which identified climate variability and vegetation changes since the last glacial period have been obtained (Zhao *et al* .,2000; deMenocal *et al*., 2000). However, these studies were carried out at one site which does not constrain regional variations in continental climate and terrigenous supply.

This thesis develops the first integrated chronological framework for the CHEETA core transect and obtains a set of paleoclimate records with consistent bulk and elemental data in order to assess the sensitivities of the records to continental climate and vegetation since the last glacial period.

2.4 ***Biomarkers: origin, application and limitations***

Biomarkers originate from biological species that contain information in their chemical structures which provide information on the nature of the biological species synthesising them, the environment in which they thrived and the climate conditions in which they existed. Proxy data by means of analyses of biomarkers is commonly used for the reconstruction of past climatic parameters.

The diverse applications of biomarkers as proxies in paleoclimate studies have gained enormous ground. For example, the use of compound specific stable isotopic composition of carbon ($\delta^{13}C$) and hydrogen (D) of long chain *n*-alkanes have been used to identify vegetation sources and climate (e.g. Chikaraishi *et al.,* 2004a; Schefuß *et al.,* 2005) while $U^{k'}_{37}$ alkenone derived SST variations is a well established proxy for reconstruction of surface ocean temperature (Prahl *et al.,*1988). Unlike the paleotemperature curve based on $\delta^{18}O$ (Emiliani, 1955; Shackleton and Opdyke 1973; Shackleton and Kennett, 1975a, 1975b) alkenone derived SST have no high dependency on the abundance and preservation of the well preserved foraminifera or *coccolithophores* species and other marine invertebrates producing or synthesising these compounds (Korte *et al.,* 2005). The determination of $\delta^{18}O$ records from the skeletal and non-skeletal carbonates such as the planktonic $\delta^{18}O$ depends heavily on the secondary or pristine nature of the carbonates, and is sensitive to multiple climate conditions (Shackleton and Opdyke 1973) making it difficult to assess independent and accurate temperatures.

Other SST proxies have been developed in recent times. The glycerol dialkyl glycerol tetraether lipids (GDGTs) and it's derived TEX_{86} (Schouten *et al.,* 2000) are now used extensively in reconstruction of ocean SST variations in marine environments. The applications of GDGT biomarkers have been successful due to the robustness in its diagenetically stable structure and prolonged residence time in the environment (Schouten *et al.,* 2002; 2003; Wuchter *et al.,* 2004; Kim *et al.,* 2006; Kim *et al*., 2007).

Although it is generally agreed that biomarkers are useful in understanding and reconstructing past climate change and environmental conditions, caution still needs to be applied during interpretation. There are, as with any other paleo proxies, challenges surrounding the use of biomarkers. Some of these challenges start with the accurate sediment recovery and assessment of continuous high resolution proxy records which may be due to cost and or dating inaccuracy (e.g. Herbert and Schuffert, 1998; Schefuß *et al.,* 2004).

Biomarkers carry detailed information about their source organisms, which differentiates them into different types; therefore, it is crucial to understand the extent to which biomarkers can provide information from sedimentary organic matter. To date, the exact origin, source and distribution of some biomarkers have not been elucidated. For example, the exact origin of the branched GDGTs remains enigmatic and is subject of ongoing research (Weijers *et al.,* 2006). In this study, the source of organic matter is traced using a paired

biomarker approach which will give a less biased view on the source origin of the biomarkers.

There remain key questions on the preservation potentials of biomarkers and how far back in time they can be applied to record past climate change accurately and continue to be subject of further research (Review by Eglinton and Eglinton, 2008). Despite these limitations, biomarkers are powerful tools as molecular proxies for paleoclimate studies. Today, it has become a very important tool in reconstructing past climate dynamics because it has proven to be very valid especially when linked to other traditional methods of organic geochemistry, inorganic geochemistry (e.g. clay minerals, mineral isotopes) sedimentology or geomorphology, microfossil analysis (e.g. foraminifera or pollen analyses) or climate models. To ensure further development and robustness of biomarkers, continuous research in several applicable natural environments, development of novel analytical techniques integrated with traditional methods is necessary. New ground in biomarkers, especially in regions where limited high resolution studies have been carried out or extreme environmental conditions must involve the use of a multiproxy approach in combination with already established traditional organic and inorganic geochemistry tools to reconstruct paleoclimate parameters as not one biomarker can accurately determine the amplitude or extent of climate variability.

2.4.1 *Selected biomarkers for the tropical Eastern Equatorial Atlantic and North West African margin.*

The following section gives a detailed view of the biomarkers used in this thesis. From a broad spectrum of biomarkers, this thesis identifies specific biomarkers which can accurately identify and estimate past climatic parameters suitable for the region of study and time interval.

- Leafwax lipids (*n*-alkanes) concentrations and its isotopic signature from core sediments along the NW transect will be used to source terrestrial organic matter and explore terrestrial vegetation change reflecting large scale patterns of atmospheric circulation (Rieley *et al.,* 1991; Ohkouchi *et al.,* 1997; Huang *et al.,* 1999). These are long-chain, odd-numbered C_{25} to C_{35} *n*-alkanes and are major lipid constituents of the epicuticular wax layer of terrestrial plants (Eglinton, 1967). Leafwax lipds have been shown to be most useful in low latitude Atlantic climate reconstructions and have generally excellent preservation potential (Meyers, 1997). They are removed from leaf surfaces preferentially during dust storms, and thus are common organic compounds of aeolian dust (Eglinton *et al.,* 2002; Schefuß *et al.,* 2003) that can be transported via long distances by aeolian processes (Gagosian and Peltzer, 1986; Ohkouchi *et al.,* 1997).

- $U^{k'}_{37}$ alkenones will be used for the reconstruction of sea surface temperature (SST). This molecular approach, commonly applied to carbonate-rich marine sediments, uses long-chain (C_{37}-C_{39}) unsaturated ketones (alkenones) from haptophytes, e.g. the marine coccolithophore

Emiliania huxleyi, (Volkman *et al*., 1980) as a proxy for past ocean SST. In this thesis, standard SST reconstructions will be used to constrain eastern equatorial Atlantic surface ocean temperature dynamics at high time resolution.

- Branched GDGTs (glycerol dialkyl glycerol tetraethers) based BIT (branched vs. isoprenoid tetraether) index (Hopmans *et al.,* 2004; Weijers *et al.,* 2007a) and soil specific biohopanoids-bacteriohopanepolyols (BHPs) (Cooke *et al.,* 2008a) will be applied to surface sediments from the NW African margin to trace soil organic matter (SOM) input. GDGTs are common in peat bogs and soils (Sinninghe Damsté *et al.,* 2000; Weijers *et al.,* 2006) and marine environments which are largely influenced by riverine input (Weijers et al., 2007a). This thesis pairs the soil specific BHPs and the BIT index to test its applicability in tracing SOM in regions not largely influenced by river input.

2.4.2 *Terrestrial Biomarkers*

2.4.2.1 *Long chain n-alkanes (Leafwax lipids): Abundance and source types*

The odd numbered homologues of the long chain *n*-alkanes, $C_{27\text{-}33}$ are specific to higher land plant leaf waxes (Eglinton and Hamilton, 1967; Kolattukudy, 1976; Marty and Saliot, 1982) and represent terrigenous input into marine sediments. They have been found in aeolian dust (Simoneit *et al.,* 1977; Gagosian *et al.,* 1981; Huang *et al.,* 1993, Huang *et al.,* 2000) and fluvial particulates (Bird *et al.,* 1995) and in sediments (Zhao *et al.,* 2006). The C_{29} homologue, nonacosane, has been used in several marine studies as a proxy for leafwax input to indicate variations in the extent of terrigenous input related to wind strength (Poynter *et al.,* 1989a, b; Madureira *et al.,* 1997). These long chain odd numbered *n*–alkanes are relatively stable and resistant to degradation making them ideal biomarkers to trace input in the past (Cranwell, 1981). In addition long chain *n*-alkanes have been found in lacustrine sediments (Ellesmere Lake) and have maximised at C_{27}–C_{29} indicating input of terrestrial organic matter into this lake (Rieley *et al.,* 1991) and showing their applicability in such sediments. Other distribution proxies for leaf wax lipids are described by the abundances or concentration normalised against sediment weight (e.g. µg/g) or total organic carbon content (TOC) (e.g. Zhang *et al.,* 2006).

Leafwax lipids distributions are also expressed in terms of carbon preference index (CPI) (e.g. Boot *et al* 2006); average chain length (ACL) (e.g. Jeng, 2006) or alkane index (A.I) (e.g. Schefuß *et al.,* 2003). The CPI is a numerical representation of how much the original biological chain length specificity is

preserved in sediments. CPI measures the odd over even predominance (OEP) of the *n*-alkanes in an extract sample and is an indication of the *n*-alkane source. The calculation of the CPI (Bray and Evans 1961; Cooper and Bray 1963) is routinely used to suggest predominance of odd numbered over even carbon chain lengths in sediments from natural environments.

$$CPI = 0.5 \times \frac{n(C25 + C27 + C29 + C31 + C33)}{n(C24 + C26 + C28 + C30 + C32)} + \frac{(C25 + C27 + C29 + C31 + C33)}{(C26 + C28 + C30 + C32 + C33)}$$

High CPI values indicate that the *n*-alkanes originate from higher plants while low CPI values are attributed to marine components (Eglinton and Hamilton, 1967; Kollatukudy, 1976) and degradation microbial and algal inputs (Clark and Blumer, 1967). Natural vegetation waxes have high CPI (>5) (Eglinton and Hamilton, 1963; Mazurek and Simoneit; 1984), whereas marine –derived *n*-alkanes > C_{23} have CPIs lower than that of natural vegetation.

There are considerations in this thesis for the limitations associated with using the CPI as a sole indicator of *n*-alkane source. Limitations highlighted by Marzi *et al* (1993) addressed a mathematical problem in the CPI calculations and suggested using the CPI in conjunction with other indices. Some of the other concerns highlighted in the literature are the potential contamination of the sediments from petrogenic sources or input of marine and algal biological origin which may result in lower CPI values (Jeng *et al.,* 2006). In addition, lower CPI values from Pliocene oil shale have argued for an algal input (Lichtfouse *et al.,* 1994) while in relatively recent sediments lower CPI values were also attributed

to the weathering of soil or shales (Eglinton *et al.,* 1997). This thesis combines the CPI as determined by Bray and Evans (1961) with other indices of leafwax lipids including average chain length (ACL), the alkane index (A.I.) and the concentration of the leaf wax lipids to provide a comprehensive assessment of the source of *n*-alkanes and its distribution patterns in the sediments.

$$ACL = \frac{27 \times nC27 + 29 \times nC29 + 31 \times nC31 + 33 \times nC33}{nC27 + nC29 + nC31 + nC33}$$

$$A.I = \frac{nC31}{nC29 + nC31}$$

The ACL describes the average number of carbon atoms per molecule based on the abundance of the odd-carbon-numbered higher plant *n*-alkanes (Poynter and Eglinton, 1991). Vegetation types from several temperate and/ or tropical regions have been studied and it has been suggested that they are the main influence on the chain length of terrigenous leaf lipids (Jeng *et al*., 2006). Leaf wax lipids derived from grasslands may on average have longer chain lengths than the leaf lipids from plants in forests as it has been shown that plants produce longer-chain compounds in warmer climates and shorter longer chain lengths in temperate regions (Poynter *et al.,* 1989a). Other studies consistent with these results have attributed the ACL to arid and humid vegetation sources (Huang *et al.,* 2000; Schefuß *et al.,* 2003).

These studies revealed that changes in the chain length distributions of *n*-alkanes from atmospheric dust samples collected in transects along the West African coast was linked to arid conditions. In contrast, studies from conifers in Oregon showed decreased chain lengths with increasing distance away from

shore suggesting an adaptation by conifers to humid climate conditions (Oros *et al.,* 1999). Further application of the ACL has been shown to differentiate between low latitude climates and higher latitude climates (e.g. Poynter, 1989 and Poynter and Eglinton 1991). The distribution of ACL has also been linked to the geographical distribution of fluvial and aeolian inputs and source regions (Poynter and Eglinton, 1991).

Another approach to differentiate the contributions of lipids from different vegetation types is the A.I. that provides information on the relative shares of e.g. trees versus grasses (e.g. Zhang *et al.,* 2006; Schefuß *et al.,* 2003; Pancost and Boot, 2004). The A.I is defined as the ratio of C_{31} versus C_{29}+C_{31} (Schefuß *et al.,* 2003; Rommerskirchen *et al.,* 2003) with higher ratios indicating a dominant input from grassland and savannahs. This ratio has been applied to late Quarternary sediments from the southern African continent (Schefuß *et al.,* 2003; Rommerskirchen *et al.,* 2003) and in central Europe (Schwark *et al.,* 2002). Values indicative of grass type vegetation greater than 0.5 were determined, for example, from dust in the lower atmosphere of the equatorial Atlantic (Schefuß *et al.,* 2003), while lower values in European pollen lake records were interpreted to measure vegetation input. Other studies have focused on the application of this proxy to Holocene environments (Zhang *et al.,* 2006; Xie *et al.,* 2002; Xie *et al*., 2003) on the Chinese loess plateau.

In this thesis, a combination of the CPI, ACL and A.I and abundance of leafwaxes give an integrated view on continental climate along the equatorial

Atlantic and North West African region to constrain climate variability and terrestrial vegetation change.

2.4.2.2 *Bulk and compound specific carbon isotopic signatures*

Bulk carbon isotopic signatures of sedimentary organic matter ($\delta^{13}C_{org}$) and compound specific ($\delta^{13}C$) signatures of *n*-alkanes are commonly used in paleoclimate research to evaluate organic matter input and trace the source of vegetation respectively. Typically vegetation sources in the North West and tropical Africa are of C_3 or C_4 vegetation plants (Cerling et al., 1995; 1997). C_3 plants are exclusively dominated by the C_3 photosynthetic pathway and are usually found in temperate regions and consist of shrubs and closed forest plants with ($\delta^{13}C_{org}$) between (-25 to -29‰) (Bird *et al.,* 1995). C_4 plants instead uses the C_4 photosynthetic pathway and consist of plants typically found in arid tropical regions (e.g. grasses) leading to bulk $\delta^{13}C_{org}$ values (-8 to -19‰) of approximately -12‰ (Fry and Sherr, 1984; Tyson, 1995). Although several studies (e.g. Collister *et al.,* 1994; Zhang *et al.,* 2003; Zhang *et al.,* 2006; Schefuß *et al.,* 2003; Zhao *et al.,* 2003; Schefuß *et al.,* 2005; Zhang *et al.,* 2009; Bird *et al.,* 1995; Cerling *et al.,* 1997) have now found the application of carbon isotopic compositions of *n*-alkanes invaluable in differentiating the source of *n*-alkanes to types of vegetation, caution must be used when applying the end member values because of the potential for admixture of C_4 with C_3 plants or marine organic matter (MOM) which may lead to an underestimation of the input of terrestrial organic matter in marine sediments (See Schefuß *et al*. 2005; Weijers *et al.,* 2009). A multi proxy approach is therefore necessary to monitor

vegetation changes and related climate variability under major climate transitions.

2.4.2.3 *Bacteriohopanepolyols (BHPs) as tracers of soil organic matter.*

The application of BHPs is a relatively novel approach in tracing terrestrial organic matter. BHPs are pentacyclic triterpenoids (Fig.2.9) with a high degree of structural variability biosynthesised by many prokaryotic organisms (e.g. Rohmer *et al.,* 1984; Rohmer, 1993; Talbot *et al.,* 2008). BHP structures have hexafunctionalised structures with functional groups at C-32 to C-35, C-31 to C-35, or C-30 to C-35 (Rohmer, 1993).

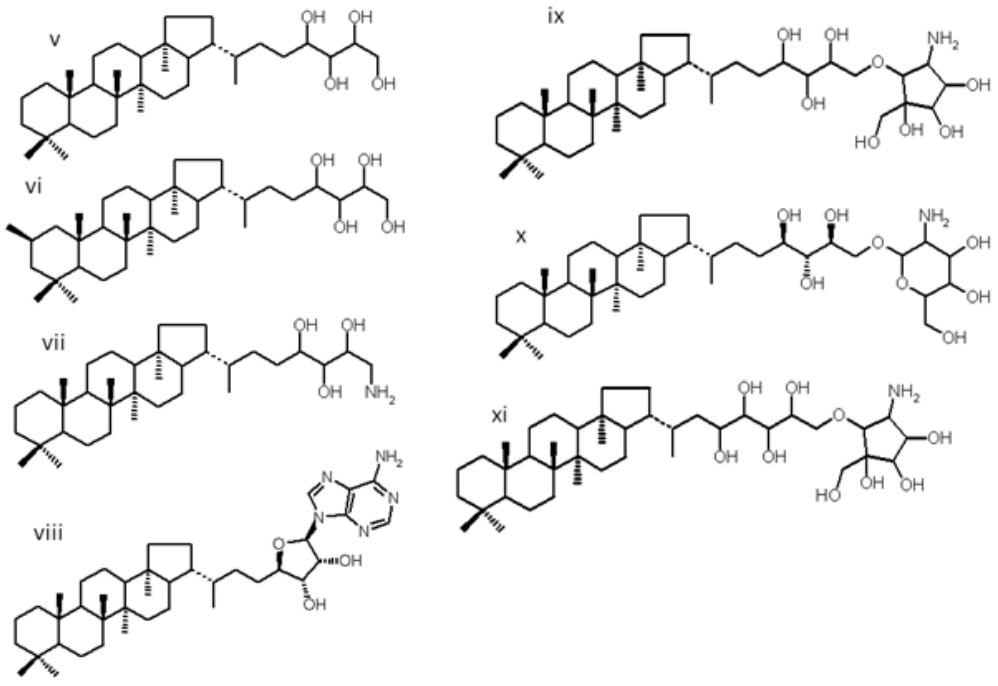

Figure 2.9 Some typical bacteriohopanepolyols (BHPs) shown as triterpenoids with an extended polyfunctionalised side chain.

BHPs are biosynthesised by many prokaryotes and have been suggested to add stability to their cell membranes (Kannenberg and Poralla, 1999). BHPs are

also precursors of the ubiquitous geohopanoids (e.g. hopanoic acids, hopenes, hopanes; Ourisson and Albrecht, 1992). The origins of BHPs are attributed to a wide variety of bacteria known to be producing them. For instance, Rohmer *et al* (1984) and Farrimond *et al* (1998) showed that some bacteria, specifically the proteobacteria, cyanobacteria and planctomycetes were the most prolific sources of BHPs. BHPs have been found in both recent and ancient sediments although they are suggested to be more abundant in recent sediments (Cooke *et al.,* 2009 and references therein).

In ancient sediments, BHPs in sediments from the Kilwa area Tanzania covering the Paleogene and the Cretaceous have been found (van Dongen *et al.,* 2006 and Cooke *et al.,* 2008a). Cooke *et al* (2008a) showed that BHPs were found in late Quaternary sediments from the Congo Deep Fan ODP site 1075 supporting its case for tracking soil organic carbon via riverine input. BHPs have been known to be present in soils as either intact structures (Ries-Kautt and Albrecht, 1989; Cooke *et al.,* 2008b; Redshaw *et al* ., 2008; Xu *et al.,* 2009) or degraded compounds with the side chains in the BHPs cleaved to produce hopanoids (Crossman *et al.,* 2001; Winkler *et al.,*2001; Shunthirasingham and Simpson, 2006). Few studies exist on the inputs of soil organic matter and the strength of the molecular signals in low TOC sediments distal from any fluvial influence.The identification and quantification of BHPs biosynthesised from bacteria and found predominantly in soils is key as a biomarker for tracing terrestrial organic matter input. In Chapter 5, the BHPs will be determined from surface sediments from the North West African margin to trace soil organic

matter input in a region of exclusive aeolian transport, distal from river influences. This will contribute to knowledge of how soil organic matter input, a previously disregarded component of terrestrial organic matter was exported from soils to the tropical continental margin of North West Africa. Previous studies both on river influenced cores (Schefuß *et al.,* 2005; Holtvoeth *et al.,* 2005); and sediments record from deep central equatorial Atlantic (Wagner *et al.,* 2004) document that export of terrestrial organic matter, in particular from soils, has been impacted by cyclic fluctuations in climate.

2.4.2.4 *Branched Glycerol diakyl glycerol tetraether (GDGTs) and isoprenoid GDGT-crenarchaeol*

In recent years, various branched GDGTs (**I-III)** a group of membrane lipids which differ both in the amount of methyl groups attached to their alkyl chains and in the amount of cyclopentyl moieties (Sinninghe Damsté *et al.,* 2000; Weijers *et al.,* 2006) (Fig. 2.8) have been discovered in peat bog deposits and identified using nuclear magnetic resonance (NMR) spectroscopy (Schouten *et al.,* 2000; Sinninghe Damsté *et al.,* 2000). They were later found in coastal marine and lake sediments, and suggested to be derived from river-transported terrestrial soil organic matter (Hopmans *et al.,* 2004;Weijers *et al.,* 2006; Kim *et al.,* 2006; Bechtel., 2010; Blaga *et al.,* 2009; Powers *et al.,* 2004).

Although the branched GDGT is thought to originate from bacteria thriving in the anoxic parts of peat bogs and soils fluvially transported to the marine environment (Hopmans *et al.,* 2004; Weijers *et al* 2006), their exact origin and

distribution is still subject of study. Crenarchaeol (**IV**) (Fig 2.10) on the other hand is a biomarker for mesophillic pelagic *Creanarchaeota* (Schouten *et al.,* 2000; Sinninghe Damsté 2002a) which is structurally related to the branched GDGT but isoprenoid in its structure and commonly found in large lakes (Keough *et al.,* 2003) and the world's large oceans (Karner *et al.,* 2001).

Crenarchaeol can be found in peat and soils but with lower concentrations in comparison to the branched GDGTs (Weijers *et al.,* 2004; Kim *et al.,* 2006). Studies have shown that branched GDGTs were found to be ubiquitous in soils worldwide (Weijers *et al.,* 2006b), but have also been found to be transported into coastal marine sediments by rivers from land (Schouten *et al.,* 2000; Hopmans *et al.,* 2004; Weijers *et al.,* 2006b; Kim *et al.,* 2006; Rueda *et al.,* 2009). Due to the relative distributions of the branched GDGTs and Isoprenoid GDGTs, the branched vs. Isoprenoid tetraether index (BIT) was proposed to trace fluvial transported SOM in marine sediments (Hopmans *et al.,* 2004).

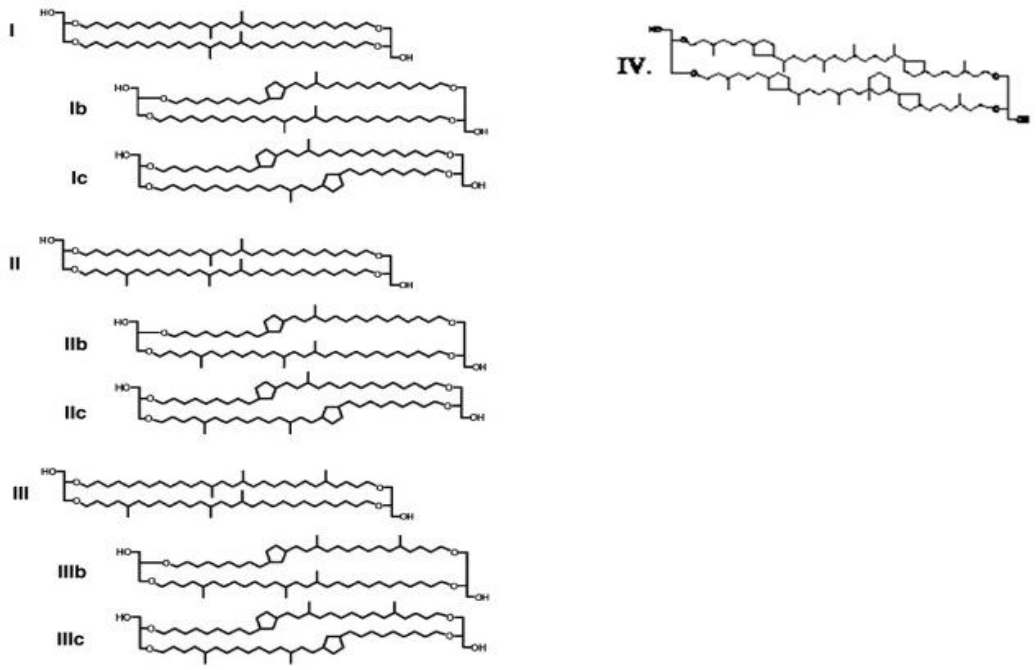

Figure 2.10 Chemical structure of the glycerol dialkyl glycerol tetraethers (GDGTs) used in this thesis. I, II, III are the branched GDGTs, b, C: methyl branches and cyclopentyl moieties of the branched GDGTs. IV refers to the Isoprenoid GDGT-crenarchaeol.

2.4.2.5 *The BIT index*

The ratio between the two groups of GDGTs (I-III vs. IV) was the basis of the BIT (Branched versus Isoprenoid Tetraether) index which refers to the proportion of fluvial derived SOM in marine sediment (Hopmans *et al.,* 2004).

$$BIT = \frac{[I + II + III]}{[I + II + III + IV]}$$

The applicability of this index was tested on soils from all over the world, (Weijers *et al.,* 2007) including the NW Mediterranean (Kim *et al.,* 2007) and in peat bogs (Sinninghe Damsté *et al.,* 2000; Weijers *et al.,* 2006a, Weijers *et al.,* 2006b). The BIT index can reach values ranging from 0, representing no branched GDGTs, to 1, representing no crenarchaeol. The BIT index has been found to be applicable in marine settings highly influenced by rivers. For example, Hopmans *et al* (2004) showed that when the BIT index was applied to

core top sediment from the Angola Basin near the mouth of the Congo River, there was a higher BIT (0.91) near the mouth of the river compared to that from open marine sediments which was closer to 0. In testing this BIT index in areas far removed from the rivers with a highly productive zone, such as the Peru margin, Hopmans *et al* (2004) also revealed that the extremely low values suggested that the component to building the BIT index may not be transported via the atmosphere. There is also increasing evidence that branched GDGTs may be produced in situ in lake sediments (e.g Sinninghe Damsté *et al.,* 2009; Tierney and Russel, 2009; Blaga *et al.,* 2009; Powers *et al.,* 2004) and marine sediments (Peterse *et al.,* 2009) but this has yet to be proven in marine sediments.

2.4.2.6 *MBT/CBT index*

The relative distribution of the soil derived GDGT membrane lipids have been suggested to be controlled by mean annual air temperature (MAT) and soil pH determined by the so called MBT/CBT index (Weijers *et al.,* 2007a). The detailed characteristics and definitions of the methylation index of branched tetraethers (MBT) and cyclisation ration of the branched tetraethers (CBT) have been described (Weijers *et al.,* 2007a).This thesis applies the MBT/CBT index to surface sediments from the North West African margin to evaluate in situ production and confirm soil organic matter transport to the continental margin.

2.4.3 *Marine Biomarkers*

2.4.3.1 *Alkenones : origin , occurrence and the $U^{k'}_{37}$, index*

Several proxies for paleotemperatures have been developed including the alkenone –based $U^{k'}_{37}$, index (Brassell *et al* 1986; Prahl and Wakeham, 1987; Prahl *et al.,* 1988), Mg/Ca ratios from foraminifera (Nurnberg *et al.,* 2000; Rosenthal *et al.,* 1997; Lea *et al.,* 1999; Rosenthal *et al.,* 2000) and the TEX_{86} (Schouten *et al.,* 2002, 2003), each distinctively offering new insights into reconstructing past near surface ocean temperatures. In this thesis, the focus is on the use of $U^{k'}_{37}$ alkenones for reconstruction of past SST in the tropical eastern equatorial Atlantic because analysis of the proxy is rapid and robust for the generation of reliable SST estimates.

Alkenones have been found in both ancient and recent sediments. Their first discovery was in the sediments from Southwest Africa of Miocene to Pleistocene age (Boon *et al.,* 1978). They have been found in sediments dated to the Cretaceous age (Farrimond *et al.,* 1986; Brassell and Dumitrescu, 2004). Long chain (C_{37} to C_{39}) alkenones are biosynthesised by few species of the haptophyte algae *Prymnesiophycaea* class of algae including coccolithophores, (Volkman *et al.,* 1980; Marlowe *et al.,* 1984; Conte *et al.,* 1994; Volkman *et al.,* 1995; Versteegh *et al.,* 2001). The alkenones differ in their lipid content and are distinguished into several types of alkenones by the number of carbon atoms (C_{37}, C_{38} or C_{39}) (Brassell et al., 1986) their degree of unsaturation (di, tri and tetra unsaturation) and the structure in their terminal group (i.e either the methyl or ethyl terminal group) (Volkman *et al.,* 1980; Marlowe *et al.,* 1984; 1990).

The identification and characterisation of the structures of the alkenones were done by de Leeuw *et al* (1980) and Volkman *et al* (1980) with full chemical characterisations by Rechka and Maxwell (1988). These studies established the alkenones as compounds synthesized from *E.huxleyi* (Okada and Honjo , 1973; Okada and McIntyre, 1977) and *Geophyrocapsa oceanica,* two geographically wide spread species known to be surface dwelling, *coccollith* producing, haptophyte algae of the order of *Isochrysidales* in the modern ocean (Conte *et al.,* 1994; Volkman *et al.,* 1995). Field data in combination with the *E huxleyi* culture, proposed that the relative abundances of the C_{37} corelated with growth temperatures as confirmed from surface ocean $U^{k'}_{37}$ temperatures (Marlowe, 1984; Prahl and Wakeham, 1987; Prahl *et al.,* 1988). The temperature dependency of the $C_{37:3}$ and $C_{37:2}$ alkenones is attribuited to the relative number of unsaturations (the number of carbon-carbon double bonds) within the molecules. This unsaturation has been expressed mathematically as a calibration curve (Muller *et al.,* 1998) providing an estimate of the annual SST at the ocean surface.

$$UK'37 = 0.033SST + 0.044\ (r2 = 0.958)\ (Muller\ et\ al., 1998)$$

Recently, the $U^{k'}_{37}$ was modified to include core top sites that covered the entire range of temperatures and widely distributed geographic alkenone producing species from major biogeographical zones in the global ocean (Conte *et al.,* 2006). Here, $U^{k'}_{37}$ -SST relationship was found to be independent of *E.huxleyi*, the dominant species in many modern marine environments (Okada and Honjo,

1973; Okada and McIntyre, 1977), making it a particularly useful proxy in determination of SSTs for sites where *E.huxleyi* is not dominant, and in sediments that pre-date the emergence of *E.huxleyi* ca. 260 ka (McIntyre, 1970).

Previous applications of the alkenone proxy for reconstruction of SST have been from core top sediments from the Atlantic Ocean (Rosell Melé *et al.,* 1995); the Indian Ocean (Sonzogni *et al.,* 1997), the Californian margin (Herbert *et al*., 1998) and in lakes, (Sun *et al.,* 2004; Chu *et al.,* 2005; D'Andrea and Huang, 2005).

2.4.3.2 *Paleoapplications of the alkenone derived* $U^{k'}_{37}$

The development of the alkenone derived $U^{k'}_{37}$ index for ocean SST reconstruction on a global or temporal/spatial scale over the years has been extensively reviewed (Eglinton *et al.,* 2000; Eglinton *et al.,* 2001). However, the application of the alkenone derived $U^{k'}_{37}$ index for SST reconstruction to time intervals preceeding the late Pleistocene is limited. This thesis presents detailed records from marine sediments that date back to the late Miocene to early Pliocene climate transition. Its application during major climate transitions such as the Holocene and the Pleistocene have been described (e.g. Farrington *et al.,* 1988; McCaffrey *et al.,* 1990; Herbert *et al.,* 1998 and Zhao *et al.,* 2000). During the late Pleistocene, response of surface ocean temperatures to the ice age cycles have been explored (e.g. Lyle *et al.,* 1992; Villanueva and Grimalt, 1996; Kirst *et al.,* 1999 and Herbert *et al.,* 2001). More recently, the proxy has been used to show cooling in the eastern equatorial Pacific ODP sites 806 and

849 which provided a history of the strength of the Walker circulation during the mid Pleistocene climate transition (McClymont and Rosell-Melé, 2005). In the Western Mediterranean, the alkenone derived $U^{k'}_{37}$ index from ocean sediments revealed rapid changes in the SST reconstruction indicative of many abrupt and cooling episodes during the last glacial (Martrat *et al.,* 2004; 2007). Further studies using this proxy in the south east Atlantic; (Sachs *et al* 2001); sub Antarctic ocean (Sachs and Anderson, 2005); North Pacific (Haug *et al.,* 2005); East Pacific and Atlantic ocean during the last deglaciation (Kienast *et al.,* 2006) have shown evidence of ocean climate change variations.

2.4.3.3 *Limitations of the $U^{k'}_{37}$ alkenone proxy*

Comparative studies of the $U^{k'}_{37}$ index with other known proxies for SST reconstruction such as the Mg/Ca, planktonic $\delta^{18}O$ and fauna assemblages have found differences in the SST estimates (Nürnberg *et al.,* 2000; Calvo *et al.,* 2001; Steinke *et al.,* 2001 and Seki *et al.,* 2002). These differences however have been attributed to changes ecology, physical factors and the genetics of the organisms producing the biomarkers (Castañeda *et al.,* 2010). Therefore, the alkenone derived proxy may also be useful in combination with these other proxies to confirm and validate ocean change dynamics and response to climate change. Some of the uncertainties of using this SST proxy relates to whether the $U^{k'}_{37}$ acts as a true representative past ocean SST. Growth temperature may indeed differ from SSTs (reviews by Prahl *et al* 2000; Bijma *et al.,* 2001; Herbert, 2001) while there may be a bias in the temperature estimates from locations with significant production of alkenones in the marine

environment (Prahl *et al.,* 1993; Ternois *et al.,* 1997; Bentaleb *et al.,* 1999; Ohkouchi *et al.,* 1999). These studies suggested that alkenone production may be dominant below the surface mixed layer, in which case sub-surface temperatures which are cooler than surface temperatures may bias the SST estimates. In addition, physiological factors such as light, ecology, preservation potential, and genetics may limit the application of the use of the alkenone proxy (Prahl *et al.,* 2000). Therefore these factors must be put into consideration when interpreting past SST records.

During geochemical analysis, limitations of the proxy also relate to co-elution and or low concentrations/non-detection of the alkenones. In some ODP 959 samples, for example, this limitation was considered and values where co-elution occurred were not included in the result section. Grimalt *et al (*2001) and Pelejero and Calvo (2003) have reviewed errors in SST estimation that may be associated with compounds of as low as 0 °C or as high as 28°C (in which case the $U^{k'}_{37}$ ratio reaches 1) and as with most geochemical and molecular techniques, caution and accuracy of records must be examined when interpreting SST estimates. Despite these uncertainties, alkenones are still useful and have been fundamentally tested and found to be robust in measuring past SST when compared to other biomarkers for past SST reconstructions.

2.5 ***Summary***

The tropical eastern equatorial Atlantic and the North West African margin offers immense potential in studying tropical African climate and marine sedimentation under past climate conditions.To understand how these mechanisms changed and how far different modes of climate triggered or influenced the African climate, a host of proxies using new and traditional analytical methods will be applied.

3 Chapter Three

3.1 *Methodology*

3.1.1 *The Ocean Drilling Programme (ODP) Site 959*

ODP Site 959 samples (133) analysed and reported in this thesis were recovered off the Deep Ivorian Basin in the equatorial Atlantic. The samples were taken on board at 2.5 cm resolution, freeze dried and subsequently stored until further processing in the laboratory. Prior to analyses, all samples were homogenized and weighed out in the laboratory.

3.1.2 *CHEETA Surface sediments*

All surface sediments samples (28) were collected from multi cores from the Portuguese and NW African margin, sampled at 0-1 cm, taken on board and kept frozen until further processing in the laboratory.

3.1.3 *CHEETA Gravity core*

All gravity core sediments from R/V Oceanus (OC-437-7) were obtained from the Portuguese and NW African margins as part of the CHEETA Cruise program. Cores were sampled at Lamont Doherty University and stored and cooled in the freezer. Freeze dried core material was homogenized and analysed for geochemical and molecular work at Newcastle University. The other splits of homogenized material were sent from Lamont Doherty University. Additional ^{14}C AMS datings, generated and owned by the Lamont-Doherty Earth Observatory of Columbia University, are kindly made available for this study by Prof. Peter DeMenocal. The ^{14}C AMS calendar dates were calculated from raw

^{14}C AMS (deMenocal *et al.,* in prep) and, together with additional age tie points derived from $\delta^{13}C_{org}$ provide the basis for an integrated chronological age framework detailed in Chapter 6.

3.2 ***Bulk Geochemistry***

3.2.1 *TOC and Carbonates (%)*

Total organic carbon content (TOC) was measured on the homogenised sediments using a LECO CS 244 Carbon-Sulphur -elemental analyser according to the method by Kröm and Berner (1983) at Newcastle University.

For determination of organic carbon, calcium carbonate was removed by repetitive addition of 0.50 N HCL, dried and combusted at a temperature over 1000°C in porous crucibles. Carbonate content data was provided by Lamont Doherty University and was calculated from the difference in value between total and organic carbon expressed as calcite.

$$CaCO3 = Ctot - Corg\ x\ 8.33.$$

TOC on a carbonate free basis was calculated as:

$$TOC\ carbonate\ free = 100/[100 - CaCO3]\ x\ TOC$$

The relative accuracy of the instrument was ± 0.05%. To evaluate reproducibility of the carbon data 0.01 TOC (%) reproducibility was achieved for duplicated samples. Geochemical parameters including TOC AR based on sedimentation rates (SR) and dry bulk densities (DBD) were calculated using the following equation:

$$Bulk\ AR\ (g/cm^2ka^{-1}) = Bulk\ SR\ (cm/ka) \times DBD\ (g/cm^{-3}).$$

$$TOC\ AR\ (g/cm^{-2}/\ ka^{-1}) = Bulk\ AR \times TOC\ (\%)/100.$$

3.2.2 *Bulk carbon isotopes (‰) analyses*

All bulk carbon isotope analyses (for CHEETA core sediments only) were carried out by Iso-Analytical using the elemental analyser isotope ratio mass spectrometry (EA-IRMS) method. Prior to carbon-13 analysis, the sediment samples were treated with hydrochloric acid to remove inorganic carbon. Initially, ca. a 400 mg sub-sample was weighed into a Universal tubes and 1 M HCl added. The sample and acid were mixed and left for 24 hours to allow the carbonate content of samples to be liberated as CO_2. The acid was further decanted and the sediment was washed with distilled water. The samples were completely dried at 60 °C and ground to a powder prior to weighing. An appropriate size of sub-sample was weighed into a tin capsule (8 x 5 mm) and sealed ready for analysis.

3.2.2.1 *Carbon-13 Analysis*

The samples and references were weighed into tin capsules, sealed, and loaded into an auto-sampler on a Europa Scientific elemental analyser and dropped in sequence into a furnace held at 1000 °C and combusted in the presence of oxygen. The tin capsules flash combust, raising the temperature in the region of the sample to ~1700 °C. The combusted gases are swept in a helium stream over combustion catalyst (Cr_2O_3), copper oxide wires (to oxidize hydrocarbons), and silver wool to remove sulfur and halides. The resultant gases, N_2, NO_x, H_2O, O_2, and CO_2 were swept through a reduction stage of pure copper wires held at 600 °C. This removes any oxygen and converts NO_x species to N_2. A magnesium perchlorate chemical trap is used to remove water.

Nitrogen and carbon dioxide are separated using a packed column gas chromatograph held at a constant temperature of 100 °C. The resultant carbon dioxide peak enters the ion source of the Europa Scientific 20-20 IRMS where it is ionised and accelerated. Gas species of different mass are separated in a magnetic field then simultaneously measured using a Faraday cup collector array to measure the isotopomers of CO_2 at m/z 44, 45, and 46. Both references and samples are converted to CO_2 and analysed using this method. The analysis proceeds in a batch process by which a reference is analysed followed by a number of samples and then another reference.

The reference material used during analysis of the samples was IA-R001 (Iso-Analytical working standard Flour, 40.2% Carbon), with a $\delta^{13}C$ value of -26.43 ‰ vs. V-PDB. IA-R001 is traceable to IAEA-CH-6 (sucrose, $\delta^{13}C$= -10.43 ‰ vs. V-PDB). IA-R001 was chosen as a reference material as it most closely matches the organic matrix of the samples. Reference standards IA-R001, IA-R005 (Iso-Analytical working standard Beet Sugar, $\delta^{13}C$ = -26.03 ‰ vs. V-PDB, traceable to IAEA-CH-6) and IA-R006 (Iso-Analytical working standard Cane Sugar, $\delta^{13}C$ = -11.64 ‰ vs. V-PDB, traceable to IAEA-CH-6) were measured as quality control check samples during analysis.

3.3 ***Biomarker extraction and analyses***

3.3.1 *Extraction of n-alkanes and alkenones*

Approximately 10g of each sediment sample (for both ODP Site 959 and CHEETA samples) was ground and weighed prior to extraction. Extraction of

sediments commenced with a mixture of 9:1 (v/v) dichloromethane (DCM) and methanol (MeOH) via accelerated soxhlet extraction using the Dionex ASE 200. Settings were at 100°C and a pressure of 7.6 x 10 6 Pa for 5 minutes. Lipid extracts were collected in a 40ml ASE vial and reduced to 1ml using a turbo evaporator, Turbo Vap® II workstation. The total lipid extract (TLE) was then dried under a gentle stream of nitrogen to near dryness for separation into compound fractions by silica gel chromatography. A known amount of internal standard, *heptadecycyclohexane* (HDCH) was added to the total lipid extracts prior to analyses. The aliphatic hydrocarbon fraction containing the leaf wax lipids (long chain *n*-alkanes) was eluted with 100% hexane while the polar fraction containing the alkenones was eluted with 100% DCM. Compound identification and distributions of the *n*-alkane and alkenone fractions were analysed using a gas chromatography mass spectrometer (GC-MS) and gas chromatography-flame ionisation detector (GC-FID) respectively.

3.4 ***Instrumental conditions***

Agilent 5890 gas chromatograph (GC) was fitted with an Agilent HP-5 fused silica capillary column (30m x 0.25mm i.d. x 0.25µm film thickness), a split/splitless inlet with tapered glass liner, and a flame ionisation detector (FID). Samples were injected in split/splitless mode (1 min. splitless, then 30 ml/min split) using an Agilent HP 7673 automatic injector. The inlet temperature was 300ºC and the detector temperature was 310°C. Hydrogen was used as the carrier gas at constant pressure (50 kPa) and an initial flow-rate of 1.5 ml/min.

The GC oven was heated from 70°C to 130°C at 20ºC/min and then to 320ºC at 4°C/min (final hold time 20 min).

Data were acquired and processed using *Thermo Atlas* software. In order to increase sensitivity and reproducibility, samples were run in duplicates and in some cases triplicates. Quantification of compounds was performed by peak area integration in the FID chromatograms relative to the internal standard.
For structural identification, samples were analysed using an Agilent 7890A gas chromatograph (GC) fitted with an HP-5MS fused silica capillary column (30m x 0.25mm i.d. x 0.25µm film thickness) and interfaced to an Agilent 5975C Mass Selective Detector (MSD).

The GC inlet was fitted with a tapered glass liner and the inlet temperature was 280°C. Samples were injected on to the GC column in pulsed splitless mode (1 min. splitless at inlet pressure 150kPa, then 30ml/min split) using an Agilent 7683B automatic injector. Helium was used as carrier gas at a constant flow-rate of 1ml/min.The GC oven was heated from 50°C (initial hold time 0 min) to 310°C (final hold time 13 min) at either 4ºC/min or 5°C/min. The GCMS interface temperature was 310°C.The MSD was operated in electron impact mode (electron voltage 70eV, source temperature 230°C, quad temperature 150°C, multiplier voltage ca. 1800V). Data were acquired with the MSD operating in full scan mode (range 50-600 amu/sec) after a solvent delay of 5 min. Data were acquired and processed using *Chemstation* software. Component mass spectra of the *n*-alkanes and C_{37} alkenones were identified by

comparison of mass spectra with those in the NIST05 mass spectra library or in the published literature.

3.4.1 *Quantification of biomarkers (n-alkanes and alkenones)*

Analyses of the *n*-alkanes from the GC-FID enabled quantification from the peak integrations. Concentrations of the *n*-alkanes were calculated in µg/g and normalised against TOC.The distribution of the *n*-alkanes was calculated using the carbon preference index (CPI) according to Bray and Evans (1961), Average chain length (ACL) and Alkane index (A.I).

The alkenones were quantified by the peak integration of the two C_{37} alkenones: $C_{37:3}$ and $C_{37:2}$ alkenones relative to the internal standard. The equations for SST estimation from $U^{k'}_{37}$ index have been described in detail in Chapter 2. The relative distribution of marine over terrestrial input the *n*-alkane/alkenone index according to Marret *et al* (2001) was applied as:

$$n-alkane/\ alkenone\ index = \frac{[odd\ numbered\ n-\ alkanes]}{[odd\ numbered\ n-\ alkanes]+3\ x\ [C37\ alkenones]}$$

Odd numbered *n*-alkanes comprise 6 compounds (C_{25}-$_{35}$) and the C_{37} alkenones comprise of two compounds $C_{37:3}$ and $C_{37:2}$. The alkenone concentration was multiplied by three, and an index approaching 1 indicates terrestrial input while that approaching 0 indicates marine input.

3.4.2 *GC-Isotope Ratio Monitoring-MS (GC-irms-MS)*

Compound specific carbon isotope composition for the preliminary work on the leaf wax *n*- alkanes (for the CHEETA cores only) was performed on a Thermo Trace Ultra GC using a split less injector (280°C) via a Combustion III Interface linked to a Thermo Delta V+ IR-MS (HT voltage 3-5kV, Trap current 0.75mA, Box current 0.7mA). The acquisition was controlled by a Dell computer using the Thermo Isodat software in Carbon mode monitoring the CO_2 $^{44/45}$ $\delta C^{12/13}$ ratio. (1µl) of the sample in hexane was injected by a CTC auto sampler and the split opened after 1 minute. The temperature programme was from 50-320°C at 5°C min and held at final temperature for 6 minutes with Helium as the carrier gas (flow 1ml/min, initial pressure of 50kPa, split at 20 mls/min).

The solvent peak was diverted to the FID and CO_2 reference gas was pulsed into the Mass Spectrometer and after 7 minutes, the back flush valve directed the split sample via the combustion furnace (940°C) and reduction furnace (650°C) into the Mass Spectrometer and the isotope ratio was measured. Chromatographic separation was performed on a fused silica capillary column (30m x 0.25mm i.d) coated with 0.25µm Di-methyl Poly-siloxane (HP-5) phase. The acquired data were processed using the Isodat dynamic background integration of mass 44, 45 and 46 ion currents (Merrit *et al.,* 1994). Analyses were done in duplicate or triplicate with standard deviation better than (1‰) $\delta^{13}C$ values are expressed vs. Vienna Pee Dee belemnite.

3.4.3 *Bacteriohopanepolyols (BHPs)*

Extraction and derivatisation of BHPs was carried out using the Bligh and Dyer Method as described by (Talbot *et al.,* 2008 and references therein). After addition of the internal standard (5α-pregnane-3β, 20β-diol) to the total extract an aliquot was acetylated by heating with acetic anhydride and pyridine (4 ml; 1:1 v/v) at 50 C for 1h and then leaving at room temperature overnight. The samples were rotary evaporated and diluted in MeOH: propan-2-ol (60:40 v/v). The samples were analysed by high performance liquid chromatography atmospheric pressure chemical ionisation mass spectrometry (HPLC-APCI-MS^n).

3.4.3.1 *Instrumental conditions for BHPs*

The instrumental conditions for the HPLC-APCI-MS are described in detail by Cooke *et al*. (2008, a, b). Reversed-phase HPLC was determined using a Surveyor HPLC system (ThermoFinnigan, Hemel Hempstead, UK) fitted with a Phenominex (Macclesfield, UK) Gemini C_{18} 5 m HPLC column (150 mm × 3.0 mm I.D.) and a security guard column cartridge of the same material. Separation of compounds in question was achieved at 30 °C with a flow rate of 0.5 ml min^{-1} and the following gradient profile: 90% A, 10% B (0 min); 59% A, 1% B, 40% C (at 25 min) then isocratic to 70 min (where A = MeOH, B = water and C = propan-2-ol; all HPLC grade, from Fisher [Loughborough, UK]) returning to the starting conditions in 5 min and stabilising for 15 min.LC-MS^n was performed using a ThermoFinnigan LCQ ion trap mass spectrometer equipped with an APCI source operated in positive ion mode.

The settings of the LCMS were a capillary temperature of 155°C, APCI vaporiser temperature of 400 C, corona discharge current 8 μA, sheath gas flow 40 and auxiliary gas 10 (arbitrary units). The instrument was tuned as described previously (Talbot *et al.,* 2003c). To detect the BHPs, an isolation width of *m/z* 5.0 and fragmentation with normalised collisional dissociation energy of 35% and an activation *Q* value (parameter determining the *m/z* range of the observed fragment ions) of 0.15 was employed. LC-MS^n was carried out in data-dependent mode with three scan events: SCAN 1 – full mass spectrum, range *m/z* 300–1300; SCAN 2: data-dependent MS^2 spectrum of the most intense ion from SCAN 1; SCAN 3: data-dependent MS^3 spectrum of the most intense ion from SCAN 2. Structures were assigned from comparison with published spectra where possible such as that published in (Talbot *et al.,* 2003b; Talbot *et al.,* 2003c, Talbot *et al.,* 2007)Structural characterisation of unsaturated bacterial hopanoids was by atmospheric pressure chemical ionisation liquid chromatography/ion trap mass spectrometry or by comparison of APCI MS^2 and MS^3 spectra with those of known compounds.

BHP abundance was calculated from the characteristic base peak ion peak areas of individual BHPs in mass chromatograms (from SCAN 1) relative to the *m/z* 345 ($[M + H\text{-}CH_3COOH]^+$) base peak area response of the acetylated 5*α*-pregnane-3β,20β-diol internal standard. Averaged relative response factors (from a suite of five acetylated BHP standards) were used to adjust the BHP peak areas relative to that of the internal standard where BHPs containing one or more N atoms give an averaged response approximately 12 times that of the

standard and compounds with no N atoms give a response approximately 8 times that of the standard.

3.4.4 *GDGT analyses*

Glycerol diakyl glycerol Tetraether lipids (GDGTs) were extracted as described by (Weijers *et al.,* 2007a). Using an ASE 200; Dionex accelerated solvent extractor. The resulting extract was blown down by a Turbo Vap II evaporator to 1ml, evaporated to dryness and separated over an activated Al_2O_3 column, using hexane :DCM 1:1 (v/v) and DCM: MeOH 1:1(v/v) solvent mixtures. The polar fraction containing the GDGT mixture was dried and ultrasonically dissolved in a hexane: propanol 99:1 (v/v) solvent mixture and passed through a 0.45μm filter prior to analysis.

3.4.4.1 *Instrumental conditions for GDGTs*

The extract containing the GDGTs were analysed on a normal-phase HPLC using a Surveyor HPLC system (ThermoFinnigan, Hemel Hempstead, UK) fitted with a Grace Prevail Cyano HPLC column (3μm, 150 mm x 2.1 mm i.d.) and a guard column of the same material. Separation was achieved at 30°C with a flow-rate of 0.2 mL min^{-1} and the following gradient profile: 50% A, 50 % B (0-5 min); 10% A, 90% B (at 25 min); 100% C at 30 min (hold 10 min) then return to starting conditions and allow to equilibrate for 20 min (where A = Hexane, B = 2% propan-2-ol in Hexane, C = 10% propan-2-ol in Hexane; all HPLC grade purchased from Fisher [Loughborough, UK]). LC-MS^n was performed using a ThermoFinnigan LCQ ion trap mass spectrometer equipped with an atmospheric pressure chemical ionisation interface (APCI) source operated in

positive ion mode. LC-MS settings were as follows: Vaporiser 400°C, capillary temperature 200°C, discharge current 5 µA, sheath gas flow 40 and auxiliary gas 6 (arbitrary units). Detection was achieved using two mass ranges m/z 1280-1310 (for Isoprenoid GDGTs) and m/z 1015-1055 for branched tetraethers.

3.4.4.2 *The GDGT indices*

GDGT concentrations unfortunately could not be obtained for the purpose of this thesis due to the unavailability of the standard. However, the LCMS yielded reliable GDGT peaks which were used to calculate the BIT index from the peak integration of the GDGTs (Chapter 5). The Branched vs. Isoprenoid Tetraether Index (BIT) is based on the relative abundance of branched GDGTs (**I-III**) representing terrestrial organic matter to crenarchaeol (IV) representing aquatic organic matter. The BIT index according to Hopmans *et al.,* 2004 has been described in Chapter 2. Chemical structures of the GDGTs representative of the roman numerals and the application of this index have been described in Chapter 2. To identify in situ production of the GDGTs the Methylation/ Cyclisation Branched Tetraether/ (MBT/CBT) index (Weijers *et al.,* 2007) is used in this thesis and defined as:

$$MBT = \frac{[I + Ib + Ic]}{[I + Ib + Ic] + [II + IIb + IIC] + [III + IIIb + IIIc]}$$

$$Cylisation\ ratio = \frac{[Ib] + [IIb]}{[I] + [II]}$$

3.5 *Time series analyses (ODP Site 959)*

Complementary time series analyses using SPECTRUM and MATLAB were carried out on ODP 959 geochemical data to determine the orbital frequencies controlling bulk organic and molecular proxies. The SPECTRUM programme (Schulz and Stategger, 1997) is a menu driven PC program that allows the analysis of unevenly spaced time series in the frequency domain. Specific settings for SPECTRUM include the univariate and harmonic analysis to determine the dominant periodicities above background noise (Schulz and Stattegger, 1997). Siegel's test was used to identify the dominant periodic variations in the proxy records. The level of significance was 0.05 for statistical tests; oversampling factor (OFAC) was set to 4, and the high frequency factor (HIFAC) to 1. Cross spectral analyses between signals sharing the same variance in similar frequencies were performed to explore the coherency and phasing of their cycles. Phase angles for lead /lag relationships was carried out with cross spectral significance as 0.1. Harmonic analysis refers to time series in terms of precisely specified wavelength components (Percival and Walden 1993) where the periodogram power values exceed those of background noise. Cross spectral analysis is used to compare the time series of different variables measured at the same time on the same samples (Weedon, 2003).

MATLAB based code (Pisias *et al.,* 1995) uses evolutionary spectra as a tool for studying changing data through time. To obtain the frequencies the periodicities was calculated in time relative to the depth records (cmbsf) using the existing LSR (cm/kyr). MATLAB based code developed by (Pisias *et al.,* 1995) was used

to obtain the evolutionary spectrum of the records. It needs interpolation onto an evenly spaced time step and linear trends removed before it can work with long series of data. MATLAB was used for the evolutive spectral analysis of the high resolution ODP Site 959 TOC records by depth (cmbsf) rather than mbsf for easier interpretation of the data and to identify changes in periodic components over time (Pisias, 1995).

Two sets of series analysis were performed on the TOC carbonate free record using Matlab, the generation of a Blackman-Tukey periodogram and a Blackman-Tukey evolutionary powerspectrum, the latter showing the evolution of the dominant frequency signals with depth which could be directly compared to our analysis with SPECTRUM. For both sets of analysis by MATLAB, the data were first linearly interpolated into 4 cm intervals and the linear trend was removed. The periodogram was calculated using the "periodogram" function in Matlab, applying a rectangular window and a Fast Fourier Transform. The evolutionary power spectrum was calculated using the "spectrogram" function in Matlab, with a moving window of 75 data points and an 85% overlap.

4 Chapter Four

4.1 *Coupling of Miocene-Pliocene (7-5 Ma) African climate: high-resolution, multi-proxy records from the eastern equatorial Atlantic (ODP Site 959).*

This study couples molecular signatures from alkenones and *n*-alkanes with organic carbon preservation in marine sediments from the Deep Ivorian Basin (DIB) off the Equatorial Atlantic (ODP Site 959) in order to develop novel, high resolution records (up to every 2.5 cm, corresponding to ~2.5-5 kyr based on the age model by Norris, 1998) of tropical African response and climate change during the late Miocene to early Pliocene climate transition (7-5 Ma). The combination of these proxies will allow me to test if during the late Miocene to early Pliocene, upwelling processes and terrestrial vegetation change were linked to the migration history of the ITCZ. In addition, the records will be investigated by time series analyses to test if high and low latitude climate influenced the late Miocene to early Pliocene records at ODP Site 959.

The late Miocene early Pliocene climate transition introduced in chapter 2, and reviewed by Zachos *et al.,* 2001 (See Chapter 2) was a period of major climate transition with events that impacted on large scale ocean and atmospheric circulation and consequently global climate. Previous studies which have investigated this climate transition are discussed in this chapter to identify gaps and take the discussion further.

Norris (1998) used low time resolution $\delta^{18}O$ records from planktonic and benthic foraminifera from ODP Site 959 sediments to reconstruct surface ocean and deep ocean responses in the equatorial Atlantic (Fig 4.1). Decreasing oxygen isotope gradients in the upper ocean between 4.9-4.3 Ma was observed and attributed to the first appearance of the Guinea current. From this observation, Norris (1998) suggested that the east-west African coastline had drifted far north to allow the North equatorial counter current (NECC) to flow into the gulf of Guinea and that the ITCZ had migrated south from a position in central Northern African at this time to its present day position at 0° to 15°N over the eastern Atlantic. The timing deduced from the eastern Equatorial Atlantic is in general agreement with reconstructions from the West and eastern Pacific and Atlantic oceans where the emplacement of the ITCZ to its modern position has been placed between 4.4-4.3 Ma (Billups *et al.,* 1999).

Further, studies by Wagner (2002) on ODP 959 showed that the late Miocene to early Pliocene was modulated by cyclic high amplitude swings in organic carbon concentrations (Fig 4.1). To understand the processes driving the nature of these TOC cycles, Wagner (2002) linked the TOC records to carbonate, $\delta^{18}O$ (Norris, 1998) and glacio- eustatic sea level drops (Zhang and Scott, 1996) (Fig 4.1). Wagner (2002) suggested that peaks in TOC records were typically associated with minimum carbonate concentrations and increased oxygen isotopic signatures, which imply warm surface waters and drastic sea level drops. These observations implied that the organic carbon deposition was closely linked to the evolution of African trade winds, continental upwelling in

the eastern equatorial Atlantic and eustatic sea level fluctuations during the late Miocene –early Pliocene. With regard to fluctuations and levels of SST, Norris (1998) inferred a surface ocean cooling of SST by ~ 2 to 3°C during the late Miocene (6.7-5.9 Ma) and proposed that the onset of modern type climate ocean dynamics around 4.4 Ma. However, no quantitative SST estimates were recorded at this site which is necessary to truly unravel the processes and feedback mechanisms of surface ocean response and document the extent of ocean response to upwelling intensity or atmospheric ocean circulation at that time.

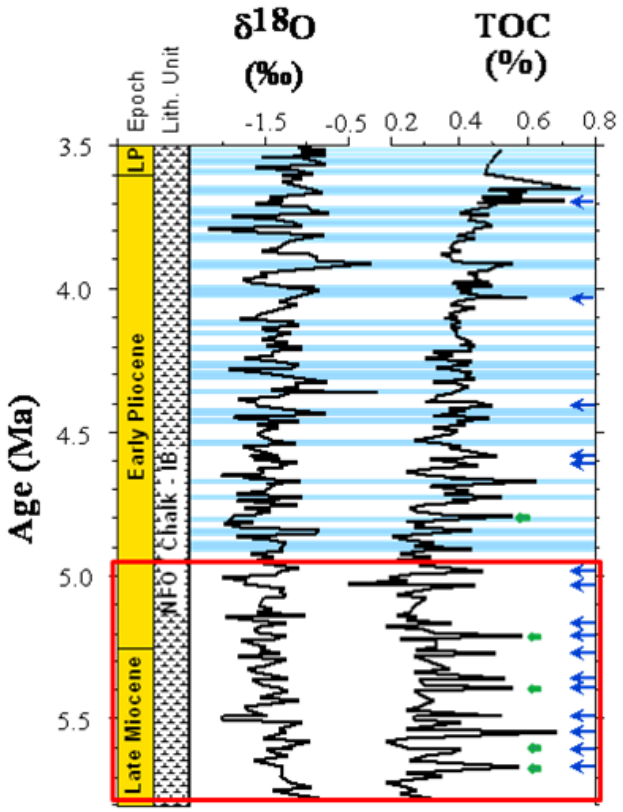

Figure 4.1 Published $\delta^{18}O$ isotopic (Norris, 1998) and TOC records (Wagner, 2002) from the upper Miocene–lower Pliocene section of ODP Site 959. Blue bars; upwelling as proposed by Norris (1998); blue arrows; additional upwelling proposed from organic carbon maxima records, green arrows; TOC peaks correlated with sea level drops (Zhang and Scott, 1996), red box includes this study.

Other relevant studies (e.g. Billups *et al.,* 2002; 1998; Zhiseng *et al.,* 2001; Prell and Kutzbach, 1992; Molnar *et al.,* 1993; Jiménez-Moreno *et al.,* 2010) have explored the mechanisms and impacts of the major global climatic and ocean circulation changes that occurred during the late Miocene to early Pliocene using a wide range of micropaleontological, paleobotanical, geochemical and isotopic tools to reconstruct surface water paleohydrographical changes.

None of these studies, however, were carried out at high (millennial and shorter) resolution which prevents the identification of short term drivers , feedbacks and time relationships between the ocean, land surface and atmosphere. Tectonic events such as the uplift of the Tibetan Plateau and Himalayas at about 8 Ma (Prell and Kutzbach, 1992; Raymo and Ruddiman, 1992); the early Pliocene closing of the Indonesian Seaway at 5.4 Ma (Srinivasan *et al.,* 1998) and the closure of the Isthmus of Panama at ~3.5 Ma (Coates *et al.,* 1992) are thought to have caused a long term cooling trend and a principal change in vegetation in low latitude ,with a general shift from C_3 vegetation to C_4 vegetation around 8 to 6 Ma ago (Cerling *et al.,* 1997; Retallack *et al.,* 2002; Strömberg, 2005).

More recently, the geographical distribution of C_4 plants has been shown to have steadily increased during the late Miocene into the Pleistocene (e.g.Tipple and Pagani, 2010) and large scale hydrological changes, as recorded by carbon isotopic ratios in carbonates and soil organic matter, were interpreted to control the relative abundances of C_3 and C_4 plants in the Himalayan foreland and

Arabian Peninsula (Huang *et al.,* 2007; Quade *et al.,* 1995; Pagani *et al.,* 1999). Global events such as the Messinian desiccation from about 6 to 5 Ma (Brewster, 1980; Cita and McKenzie, 1986; Hodell *et al.,* 1986), the marine biogenic bloom between 8 to 5 Ma (Diester-Hass *et al.,* 2005), and the establishment of modern type atmospheric and ocean circulation in tropical Africa about 4.4 to 4.3 Ma (Norris, 1998; Billups, 1999) are also proposed as having irreversible impacts on the climate trend since the late Miocene to early Pliocene.

Upwelling is described by the intimate ocean–atmospheric relationships, with stronger winds driving the cooling of the oceans via upwelling, and potentially increasing organic carbon supply and preservation via higher biological production and flux to the sea floor. Plant leafwax lipids (long chain *n*-alkanes C_{27} to C_{33}) are common organic compounds of aeolian dust (Eglinton *et al.,* 1967) which are well preserved in marine sediments and can detail both wind intensity and climatic conditions in the dust source area. Enrichment of leafwax lipids in near continental marine settings therefore can be used to infer dry climate conditions in continental dust source areas (grass type vegetation in subtropical Africa) combined with enforced wind strength. Such records from higher plant leaf waxes were not available from previous studies on ODP Site 959 which would have strengthened the proposed migration history of the ITCZ around Miocene-Pliocene transition.

4.1.1 *Aims and objectives*

The overarching aim of this chapter is to investigate the relationships between sea surface ocean dynamics, terrigenous supply and organic carbon preservation at millennial time scales at ODP Site 959 across the late Miocene /early Pliocene climate transition.

4.1.2 *Objectives*

1. To explore sea surface ocean dynamics using the unsaturation index $U^{k'}_{37}$ alkenones ($C_{37:3}$ and $C_{37:2}$) and its relationship to terrestrial vegetation and trade wind intensity in the eastern equatorial Atlantic. Higher plant leaf waxes are known components of dust transported organic matter and can reflect atmospheric circulation patterns. Therefore the combination of the SST with higher plant leaf waxes records will reflect the relationship between upwelling and terrestrial organic supply.
2. A second objective is to document the distribution and transport of higher plant leaf wax lipids using *n*-alkane distribution proxies including the CPI, ACL, A.I, and the *n*-alkane/alkenone index. These parameters will enable the assessment of the distribution patterns of terrestrial vegetation, broadly classify the source of vegetation and examine the contribution of terrestrial organic matter relative to marine organic matter in the case of the alkane/alkenone index.
3. To explore high resolution bulk records of organic carbon content (TOC) and carbonate ($CaCO_3$) concentration in order to evaluate organic carbon burial beneath the eastern equatorial Atlantic. TOC and

carbonate from marine sediments can be used to reconstruct the history of productivity and the depositional environment respectively. High productivity is expected to correspond to cooler SST temperatures and drier continental climate as inferred from TOC records.

4. To present time series data on all records (TOC, SST and leaf waxes) using SPECTRUM and MATLAB in order to identify periodic components; examine phase and coherent relationships, and to understand influence of high and /or low latitude climate drivers and mechanisms during the late Miocene to early Pliocene.

4.2 ***Site location and sample strategy***

ODP Site 959 (Fig.4.2), was drilled at a water depth of 2100m, and is situated on the southern margin of the Deep Ivorian Basin (DIB) on the edge of the Cote d'Ivoire Ghana transform Margin (CITGM) (Mascle *et al.,* 1996). The CITGM is located at the intersection of the Romanche Fracture Zone and the Ghanaian shelf, with the CITGM recording lateral plate movements that started when the South America and Africa separated to create the Equatorial Atlantic Gateway (Mascle *et al.,* 1996).

ODP Site 959 was drilled close to the mixing zone between North Atlantic Deep water and intermediate water and is sensitive to water mass fluxes and intensity of trade winds (Mascle *et al.,* 1996). Site 959 offers a rare opportunity for high resolution analyses in the equatorial Atlantic because of complete recovery (Mascle *et al.,* 1996). Generalised stratigraphy, chronology and lithography are detailed in (Wagner, 1998; 2002; Giresse *et al*, 1998). Seasonal upwelling (Voiturez and Herbland 1982; Verstraete, 1992) and the continuous deep water circulation along the margin (Mascle *et al.,* 1996) makes this site ideal for exploring the ocean atmospheric processes and continental climate change off the equatorial Atlantic. Sediments from ODP 959 have been shown in Fig 4.3 with 6 main sedimentary units (A-F) thinned in the upper crust by dip –slip faults trending north-south to north east- south west. These faults bound tilted blocks and half grabens, which are infilled by thick syn-tectonic sediments (Unit A, Fig 4.3). Geophysical and geological features of ODP Site 959 have been described in (Basile *et al.,* 1993; Mascle *et al.,* 1996). Sediments used in this

study taken every 2.5 cm from Hole 959C from the top of Core 159-959C-9H to the base of the Core 159 -959C-11H 9 (~77- 97 mbssf) is used to produce a record from~ 5 Ma to 7 Ma based on planktonic and benthic foraminifers biostratigraphy (Norris, 1998). Methods of extraction and analyses of ODP Site 959 sediments are detailed in Chapter 3.

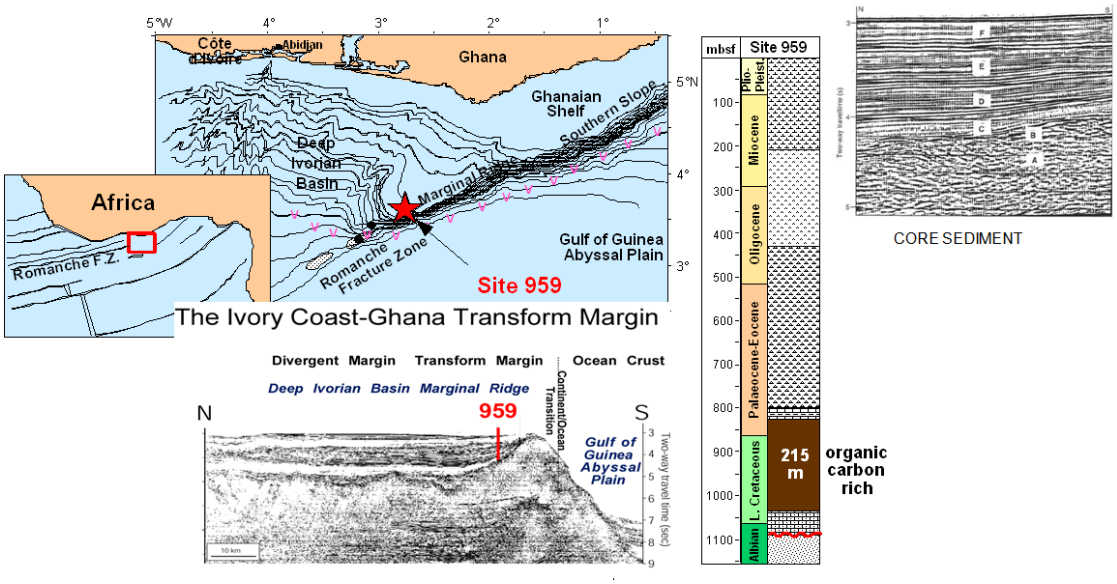

Figure 4.2 ODP Site 959 drilled along the Cote d'Ivoire–Ghana transform margin (CIGTM) (Pletsch et al., 2001) and the Deep Ivorian Basin (Mascle et al., 1999).A representative core image of ODP Site 959 sediments is shown to the right (Mascle et al., 1999).

4.3 ***Age Model ODP Site 959***

All age model data including LSR (cm/ka), biozones and planktonic $\delta^{18}O$ records from Norris (1998) are shown in the Appendix A. The age model of Site 959 based on planktonic foraminifers biostratigraphy is from Norris (1998).

In this thesis, LSR data was extrapolated between 90-89 mbsf to reduce minor inconsistencies in the Norris age assignment. A 50% drop in the LSR (cm/ka) from about 2 to 1cm/ka marks the early Pliocene boundary (Fig 4.3). Sedimentation rate then step up 1cm/ka to 1.2cm/ka, followed by another step u to 2cm/ka. An age/depth plot indicates the approximate late Miocene to early Pliocene climate boundary relative to the depth (mbsf) at ODP Site 959 (Fig.4.3).

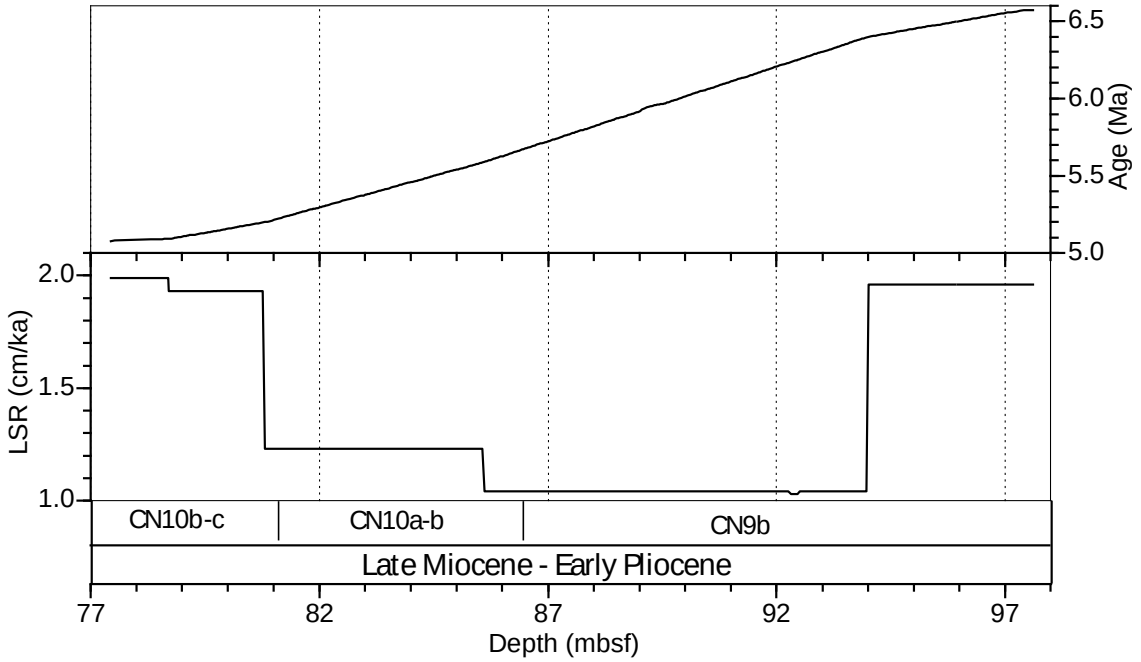

Figure 4.3 Age model (Norris, 1998) versus depth plot of sediment core ODP site 959 showing a ~50% drop in linear sedimentation rate(LSR).Age/depth plot for ODP Site 959 Hole according to linear interpolation between the biostratigraphy age points in Norris (1998), nannofossil biozones indicated by the straight lines, EP; Early Pliocene, LM; Late Miocene.

4.4 ***Results***

All raw data from ODP Site 959 are presented in Appendix A. The total number of ODP samples run for organic geochemical and molecular analyses were 136.

4.4.1 *Organic carbon and carbonate burial records*

High resolution bulk organic and carbonate records are presented in Fig 4.4. ODP 959 bulk TOC composition and TOC carbonate free (TOC_{cf}) was plotted against carbonate records to determine any corresponding relationship between the data and identify carbonate influence on the TOC records. The scatter plots (not shown) reveal no relationship between the TOC records and carbonates (bulk TOC and TOCcf) with both R^2=~ 0.02.

The late Miocene to Pliocene organic carbon record shows distinct high amplitude variability patterns that can be subdivided into four intervals. The first interval lasts for about 400 kyrs and shows organic carbon records commenced to increase from pelagic level of <0.2% to about 0.4% at 6.2 Ma. From here, this time, TOC records increase up to 0.8% at ~6.4 Ma. The second interval lasting about 500 ka from 6.2 Ma – 5.7 Ma shows organic carbon records from baseline levels to about 0.6%.The third interval, of a shorter time ~300 kyrs, shows highly variable records which range from 0.1% to 0.7% between 5.7 Ma and 5.3 Ma. A decreasing trend in the TOC records (0.5% to 0.1%) is observed in the late Pliocene with a spacing of about 250 kyrs between 5.35 to 5.1 Ma.

The marine baseline values in the TOC record are consistent with lower time resolution TOC values presented by Wagner (2002) which suggested intense

early diagenesis alteration of organic carbon burial with full oxic / redox conditions. The nature of the cycles observed in the records suggests a response to the main frequency bands of orbital forcing which is investigated in this chapter.

The carbonate carbon record in the ODP Site 959 sediments range from 20 to 60% and is presented in Fig 4.4. The records show highly variable patterns across the climate transition. Between 6.8 Ma to 6.2 Ma, carbonate burial decreased by 20% interrupted by two peaks in carbonates (60%) at 6.5 Ma and 6.3 Ma respectively. Between 6.2 Ma and 5.95 Ma, a 25% increase is when carbonate reach values as high as 65%. From here, there is a long term decrease in carbonate burial until 5.4 Ma when values reach below 30% followed by higher records and fluctuations in the early Pliocene between 5.2 Ma and 5.1 Ma.

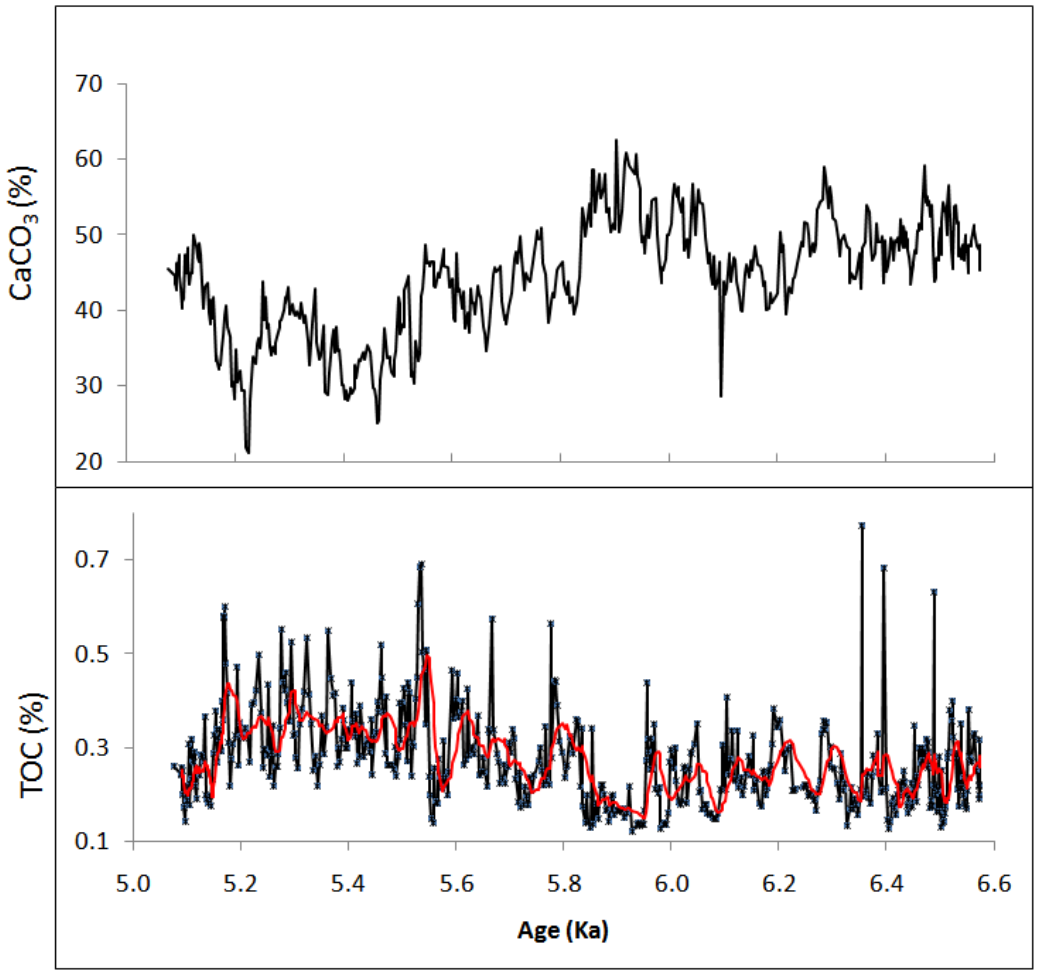

Figure 4.4 ODP Site 959 Organic carbon and carbonate records showing highly variable patterns across the late Miocene to early Pliocene climate transition. Red line denotes the 10 pt. moving average.

4.4.2 *Alkenones and $U^{k'}_{37}$ based SST records*

C_{37} di- ($C_{37:3}$) and tri- ($C_{37:2}$) methyl unsaturated ketones were detected in over 98% (133 out of 136) of the ODP 959 samples. Representative chromatograms are shown in (Fig.4.5). Integration of the $C_{37:3}$ and $C_{37:2}$ peaks were used for determination of $U^{K}_{37}{}'$ derived SST reconstruction (Prahl and Wakeham, 1987). The C_{38} di- and tri-unsaturated ethyl ($C_{38:2et}$; $C_{38:3et}$) ketones detected in the samples (Fig. 4.5.) are shown for illustration purposes only. They are of lower concentrations than the C_{37} alkenones and are not used to calculate SSTs due to the co-elution of the C_{38} alkenones (Lawrence *et al.*, 2007). Both the detection and good separation of the C_{37} alkenones in ODP Site 959 samples enabled accurate quantification of alkenone concentrations and the $U^{K}_{37}{}'$ index.

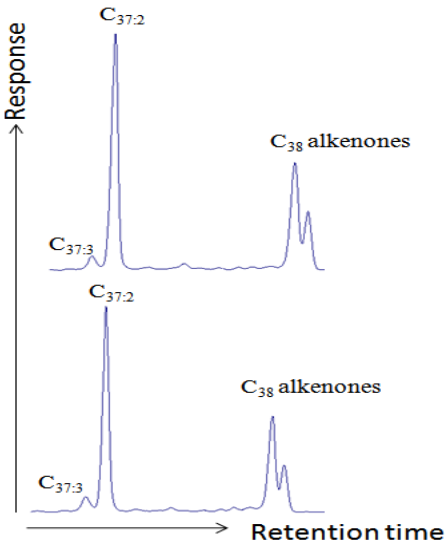

Figure 4.5.Representative chromatograms of detected alkenones at ODP Site 959 (Holes 959C-10H6, 40-50m and 959C-11H3, 120-130m) showing the ($C_{37:3}$; $C_{37:2}$ and C_{38}) alkenone used in calculation of SST

In Fig 4.6 total concentrations of C_{37} alkenones from the ODP 959 sediments vary from near absence to 250µg/TOC across the late Miocene to early Pliocene interval. The maximum and low concentrations have been found in previous studies (Westerhausen *et al.,* 1993). They found maximum concentrations of about 250-300µg/TOC in surface sediments from the continental margin offshore Guinea, Ivory Coast Ghana and Gabon while low concentrations (<30µg/TOC) were found in marine sediments from the equatorial region. The alkenone concentrations show high amplitude variable patterns with a spacing of ~ every 200 kyrs in the upper part of the record across the late Miocene to early Pliocene. The first interval covering 3 cycles of 200 kyrs do not exceed 50µg/TOC between 6.6 Ma to 6 Ma. From this time, a peak in the record is shown every 200 kyrs with alkenone concentrations of 100µg/TOC at 5.9 Ma, 250µg/TOC 5.65 Ma, and 60µg/TOC at 5.35 Ma. The early Pliocene also shows high amplitude cyclic patterns with a spacing up to 60µg/TOC. Similar to the organic carbon records, the cyclicity of the alkenone records suggests a link to orbital frequencies.

4.4.3 *Alkenone derived SST*

The clear separation of the alkenones allows precise determination of the unsaturation indices and thus robust SST data (standard deviation based on duplicate or triplicate analysis of the SST estimates is 0.3°C or 0.01 $U^{k'}_{37}$ units). Similar to the patterns in the alkenone concentrations, the SST record derived from the unsaturation index range from 24.8 °C to 29°C (Fig.4.6) with high amplitude fluctuations. No long term trend is observed in the SST record but instead pronounced warming and cooling across the climate transition are revealed with a large magnitude of up to~4°C across the climate transition. At the start of the record, SST (26°C) is within the modern temperatures for the equatorial Atlantic (Conte *et al*., 2006). From 6.6 Ma to 6.4 Ma, cooling and warming of up to a magnitude of 2°C are revealed. Between 6.4 and 6.2 Ma, warming/cooling cycles of up to 2.5°C in magnitude continues until 5.6 Ma. This magnitude is nearly doubled when lowest SST records of 24.8°C is shown at 5.6 Ma and maximum SST of 29°C at 5.5 Ma. Here, another cooling by 4°C is evident at 5.4 Ma. In the early Pliocene, SST records show also show variations in SST as it increases from 25°C-28°C and back down again to 27°C.

Warm SSTs (26-29°C) are within the range of modern temperatures in the equatorial Atlantic (Conte *et al.,* 2006). Opposite from that, cool SSTs below~26°C site fall within the temperature change from low latitude regions during the LGM (Webb *et al.,* 1997). The cool SSTs are consistent with the various estimates of surface ocean cooling during the last glacial in the tropical and subtropical Atlantic ocean which ranged from <2 to 10°C (Nurnberg *et al.,*

2000; Niebler *et al.,* 2003). To validate the alkenone based SST data, I compare the record to the oxygen isotope data from Norris (1998) (Fig 4.6). Warm SSTs are expected to correspond to heavier $\delta^{18}O$, which indicate warmer temperatures. The alkenone based warm SST estimates from ODP 959 however align with lighter oxygen isotope records. Norris (1998) proposed that the modest trend in *G. sacculifer* $\delta^{18}O$ between 6.7 Ma and 5.9 Ma in the same core reflected cooling of SST suggesting a long term 2 to 3°C decline across the late Miocene to early Pliocene interval. This new alkenone based SST records do not support this trend but identifies a series of high amplitude cooling across the late Miocene to early Pliocene climate transition, which clearly occurred earlier than the proposed 4.4 Ma for the onset of modern type climate-ocean dynamics (Norris, 1998).

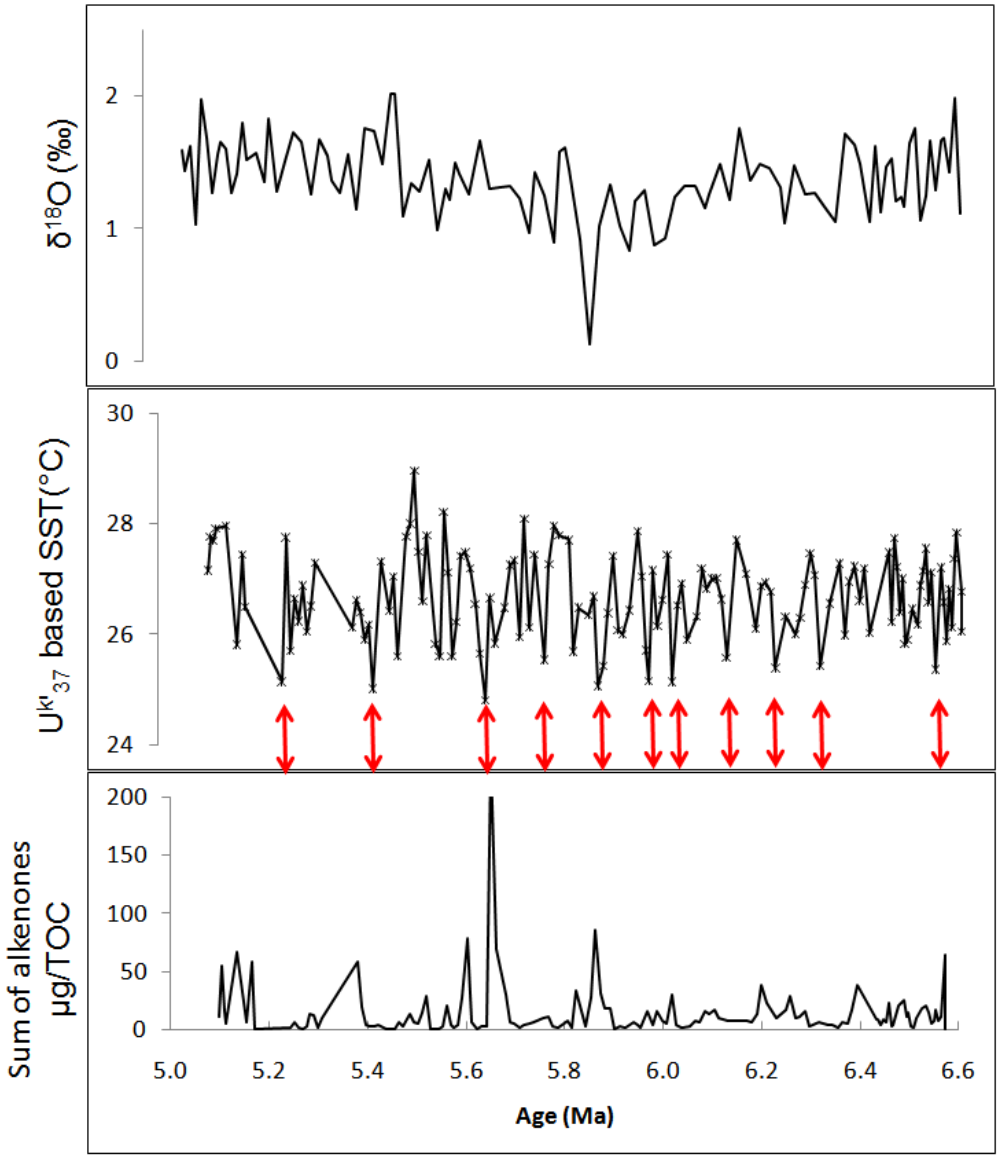

Figure 4.6 $\delta^{18}O$ records from the eastern equatorial Atlantic (Norris, 1998) plotted with the $U^{k'}37$ based SST and alkenone concentrations from ODP Site 959 (this study), red arrows denote cool SSTs at ODP Site 959.

4.4.4 *Leafwax lipids*

ODP Site 959 sediment apolar extract fractions are dominated by homologous series of long chain *n*-alkanes (Fig.4.7). The *n*-alkanes in the studied sediments range from C_{24} to C_{35} with a predominance of the odd over even-carbon-numbered homologues.

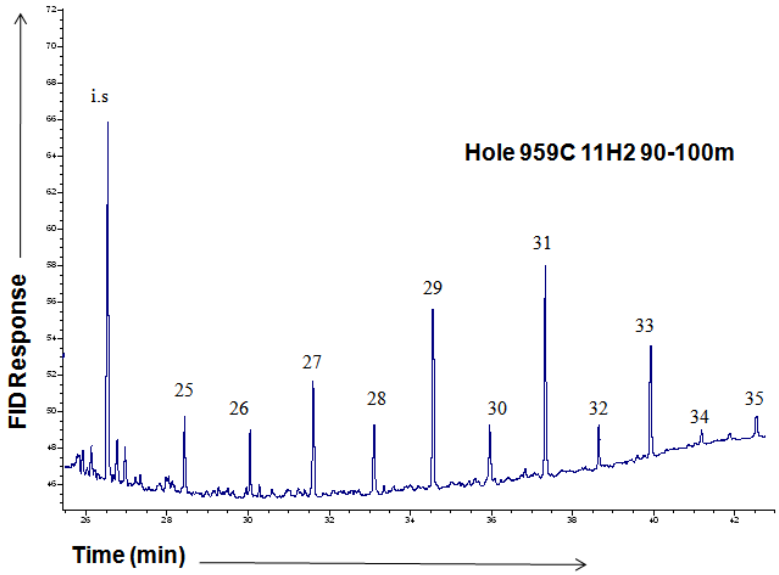

Figure 4.7 Representative gas chromatogram of the n-alkanes detected in ODP Site 959 sediments (sample from Hole 959C-11H2 90-100m) showing odd over even carbon number predominance. Numbers represent the carbon number of n-alkane, i.s, internal standard.

The concentration of HMW *n*-alkanes is presented in Fig 4.8 and varies from 0.1 to 35µg/TOC with high amplitude patterns similar to the SST record. Baseline records remain low throughout the climate transition but peaks tend to increase between 6.3-5.85 Ma, before the start to decrease again. From 5.7 Ma, the concentration of leafwaxes decrease from 35µg/TOC to minimum values at 5.45 Ma. Above 5.45 Ma, consistently low concentrations of the leaf waxes are evident in the early Pliocene.

Similarly, CPI values which range from 2 to 16 (Fig. 4.8) show high amplitude variations across the climate transition. Baseline values remain low across the climate transition, but show peaks which tend to increase between 6.3 Ma to 6.2 Ma, before they start to decrease. The decrease in CPI values from 15 at 6.2 Ma to 2 at 5.8 Ma reflects the distribution patterns of the leaf wax lipids at this time. From 5.7 Ma, there is an increase to maximum values which then decrease again gradually until 5.4 Ma. From here, values tend to increase until the early Pliocene apart from at 5.2 Ma, when minimum values are observed. The contents of the *n*-alkanes and CPI in this study are comparable with studies in the equatorial Atlantic and NW Africa (Westerhausen *et al*., 1993; Zhao *et al.,* 2000; Zhao *et al.,* 2003). The ACL record presented in Fig 4.8 shows moderate amplitude variations with an average value of 29.9 (29.2-30.4) during the late Miocene to early Pliocene climate transition. ACL tend to increase from between 6.6 Ma and 6.3 Ma before they start to decrease, first for a short time at 6.2 Ma and then increase again from this time till 6.1 Ma for ~100 kyrs. Further variation in the records is shown between 5.6 Ma and 5.2 Ma with large shifts in the record observed at 5.2 Ma.

Previous studies (for example Schefuβ *et al.,* 2003; Hinrichs, 1998; Rinna *et al.,* 1999; Pancost and Boot, 2006) have shown the applicability of the ACL in marine sediments and suggested it varied with nature and source vegetation, temperature and or humidity. The nature of variability in the records from this study reflects that the type of vegetation supplied to the African continent may have been in response to alternating climate conditions during this climate

transition. Similarly, moderate variations in the A.I (Fig 4.8) are shown across the climate transition with values that range from ~0.4 to 0.7 with an average of 0.5. Between 6.6 Ma and 6.5 Ma, variable patterns are shown in the records with values that oscillate from 0.3 and 0.6. An increasing trend in the record between 6.4 Ma and 5.9 Ma reflects an increase in or prominent grass type source supply. Following on from this, a drop in A.I is shown at 5.7 Ma and increases again at 5.6 Ma. From this time on, moderate variation at the top of the record is shown with values not exceeding 0.6, followed by a drop to 0.4 at 5.1 Ma in the early Pliocene. Peaks in the A.I. are observed at 5.61 Ma during the late Miocene while minimum values are observed during the early Pliocene at about 5.10 Ma. The A.I. record has over 50% of its values above 0.5 indicating supply from similar sources of vegetation type throughout the recorded section.

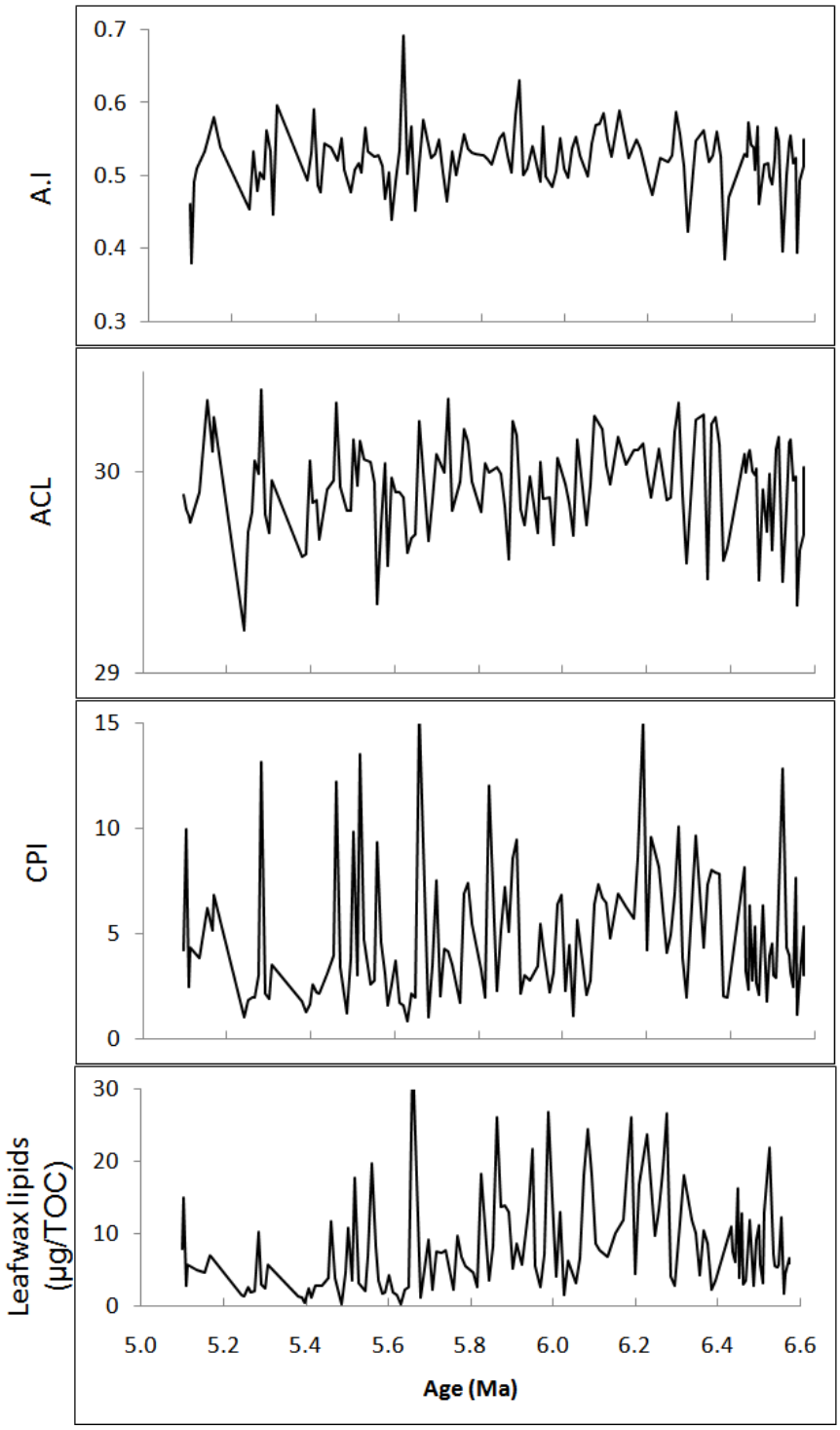

Figure 4.8 ODP Site 959 leaf wax concentration, CPI; ACL; A.I across the late Miocene to early Pliocene climate transition.

4.5 ***Time Series Analyses***

4.5.1 *Frequency Analyses of the TOC record*

The SPECTRUM and MATLAB analyses were run by depth. All settings have been described in the Methods, Chapter 3. The purpose of the spectrum harmonic analyses is to detect periodic signal components in the Milankovitch frequencies. Milanovitch frequencies were calculated based on the LSR/age model (Norris, 1998). All three spectral analyses for TOC identified strongest power at 0.01 (1/89cm) and significant power at 0.02 (1/48 to 1/50cm) (Fig 4.9) These results confirm consistent dominant cycle frequencies in the TOC record for which the age model (Norris, 1998) provides dominant time frequencies of 110kyr (for 1/89cm); 41kyr (1/50cm) and 42.5 kyr (1/48cm). These readings are well aligned to the 100 kyr eccentricity and 41 kyr obliquity bands.

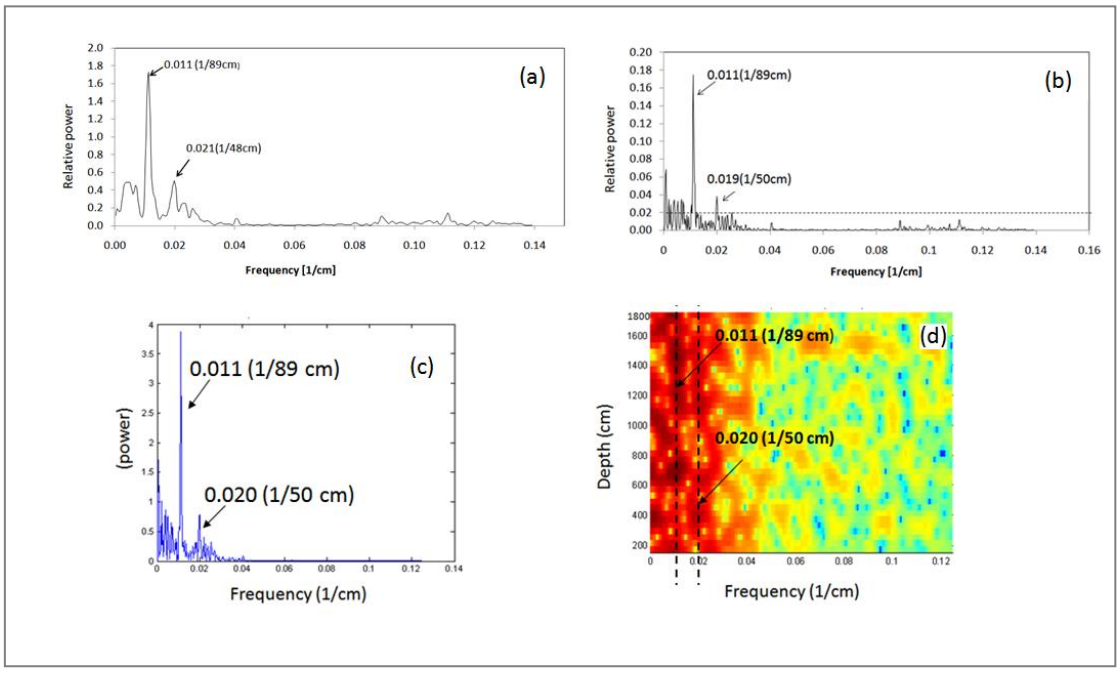

Figure 4.9 Spectral analyses of TOC records from ODP 959 as a function of depth (cmbsf); dashed line 95% significance level , dominant peaks annotated (a) univariate spectral analysis (b) harmonic analysis (c) blackman tukey periodogram (d) evolutionary spectrum.

4.5.2 *Frequency analyses of leaf waxes and SST*

Different main frequencies are observed for SSTs and leafwaxes. The harmonic analyses for both SST and leaf waxes (Fig 4.10) reveal a very strong peak at 0.0075 (1/133cm) and significant peak at 0.0129 (1/77.52cm).These results confirm consistent dominant cycles at time frequencies with periods of 75kyr (for 1/133cm) and ~42 kyr (1/77cm). Due to the similarity in frequency peaks observed in the SST and leaf wax lipids harmonic analyses, we compared both records using bivariate analyses. Autospectra plotted on a decibel scale, with 90% confidence levels independent of frequency (Schulz and Stattegger, 1997) confirm the two periodic components found in the SST and leaf wax harmonic records at 0.0075 (1/133cm) and at 0.00128 (1/77.25cm) respectively (Fig. 4.10).

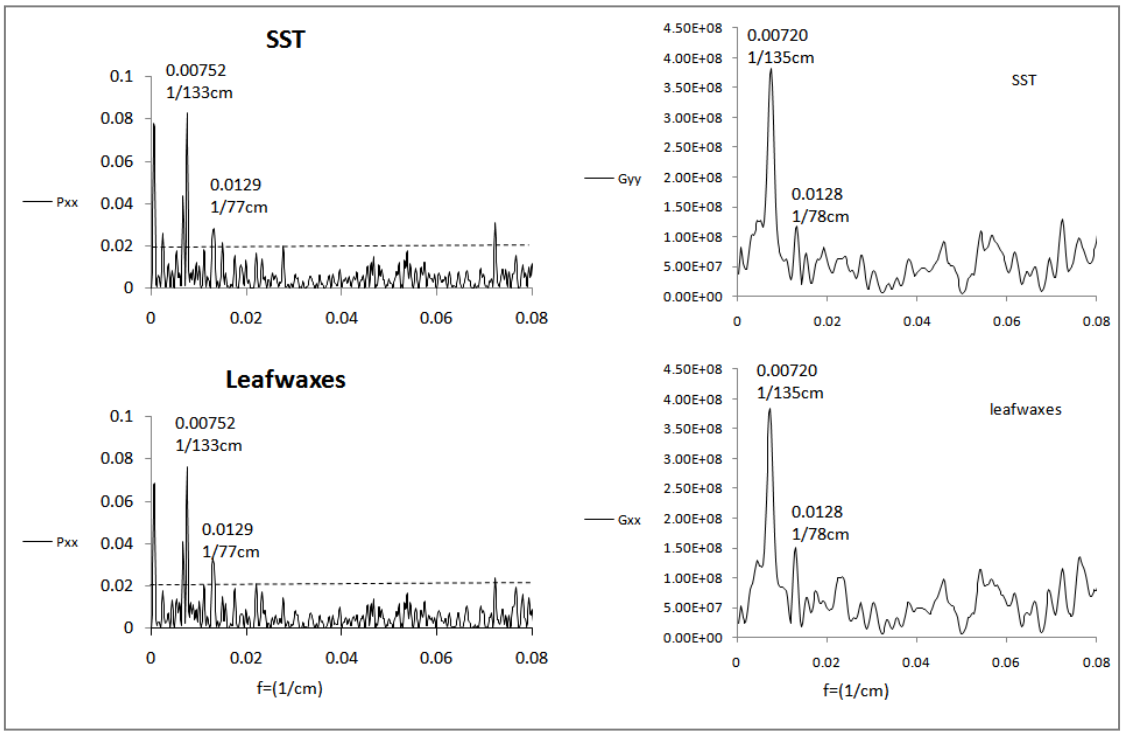

Figure 4.10 Harmonic analyses of ODP Site 959 SSTs and leaf wax lipids. Dashed line: 95% confidence level. Autospectra of SSTs and leaf wax lipids: Dominant frequencies are annotated.

The coherency spectra at 90% confidence level exhibit significant coherencies at 0.0072 and at 0.013 corresponding to ~72 kyrs and ~41 kyrs, respectively (Fig.4.11). The phase spectrum describes the average difference in phase between two time series at different frequencies (Bloomfield, 1976; Priestley, 1988). A zero phase difference indicates that oscillations are in phase while other values indicate that the oscillations are out of phase (Weedon, 2003). Phase relationships are expressed as time delay that equal cycle period x phase (°)/360°). The phase spectrum for leaf waxes and SST records show that leaf waxes lead the SST records by 2kyrs at 72 kyrs (+10°) and lag SST by 5kyrs at 41 kyrs (-40°). This observation is significant and has implications for the drivers and mechanisms of climate change during the late Miocene to early Pliocene climate transition.

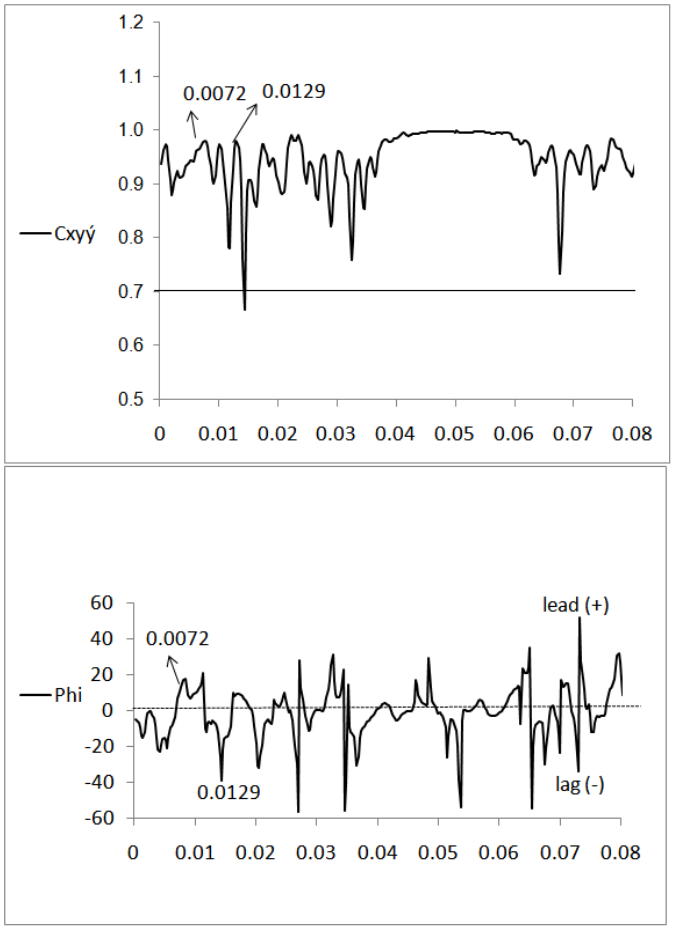

Figure 4.11 Coherency spectrum exhibit significant coherencies at the frequencies at which the harmonic analysis suggested the presence of periodic components. Black line indicates false alarm level at (α=0.1) 90% confidence intervals are plotted only for coherencies exceeding this level. Phase spectrum show that leaf waxes lead SST at positive angles and lag SST at negative angles.

4.6 ***Discussion***

4.6.1 *Organic carbon burial, SST and leafwaxes*

The highly variable nature in the ODP Site 959 records suggests large contrast in the equatorial Atlantic during the late Miocene to early Pliocene climate transition. High amplitude fluctuations in SST records from ODP 959 marine sediment indicates cooling and warming cycles that may reflect periods of intense and low upwelling in the tropical eastern equatorial Atlantic. In general, when SSTs are low, leafwaxes tend to be higher (Fig 4.12) reflecting higher winds and or more arid conditions in Africa supporting the interpretation of upwelling.

Interestingly, increases in TOC are not reflected when SST is low or high leaf wax lipids apparent (Fig 4.12) not likely supporting the interpretation of marine productivity in the tropical eastern equatorial Atlantic. Arguably, the low TOC values observed strongly suggest low productivity and that a significant proportion of the primary organic carbon signal has been lost due to diagenetic processes, leaving only a relict signal in the sediments. Therefore as organic carbon maxima do not generally correspond with low SST across the study interval, it is suggested that upwelling may not be the main driver for the nature of the observed TOC cycles at ODP Site 959 during the late Miocene to early Pliocene. This suggestion has been confirmed by the time series analyses which revealed no phasing and coherent relationship between the TOC and SST, but rather a persistent 100 kyr and 41kyr cycles in the TOC records

suggesting strong response of the organic carbon in the equatorial Atlantic to high latitude climate

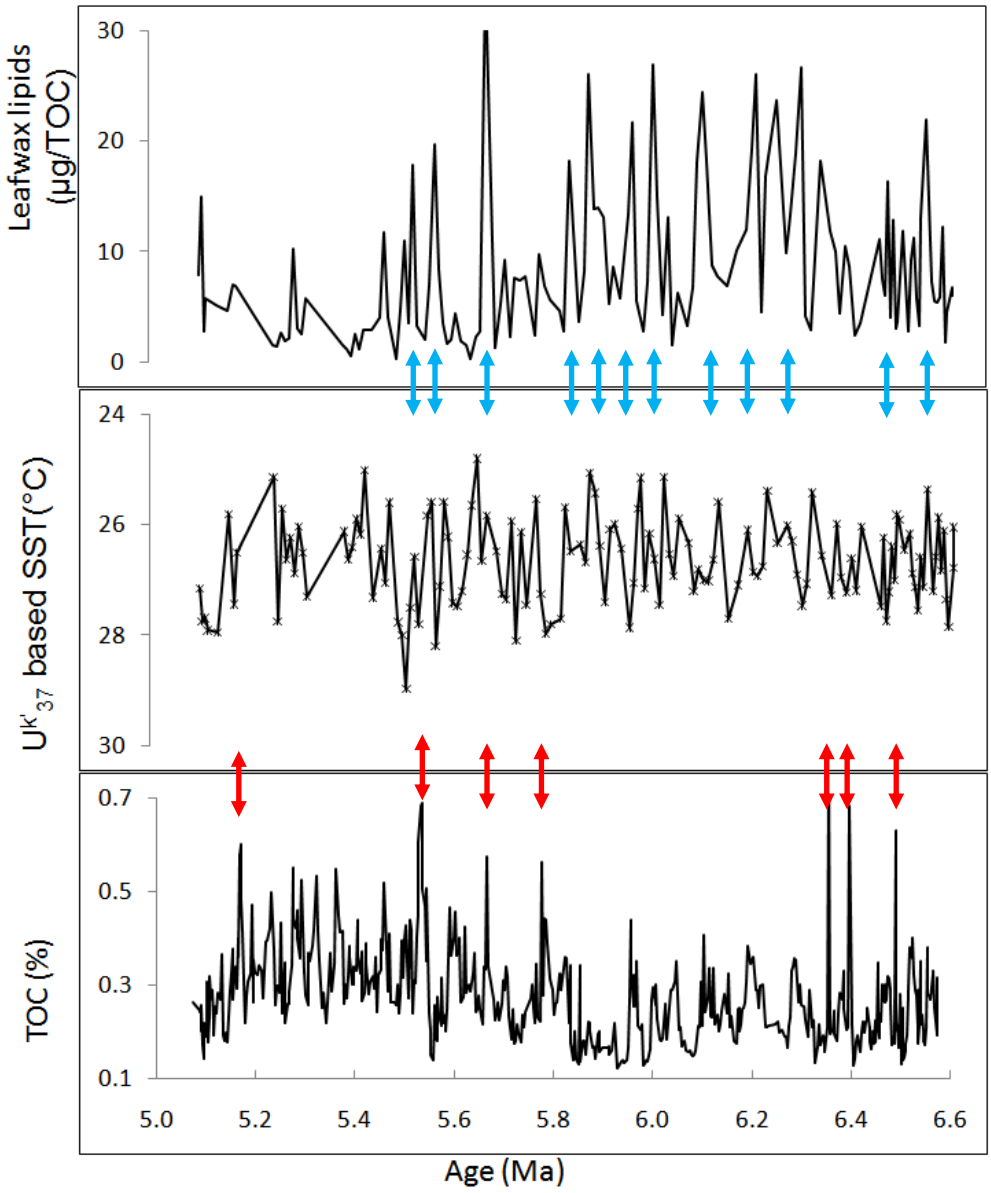

Figure 4.12 Relationship between TOC, SST and leaf wax lipids. Blue arrows show instances when cooler SST (<26°C) generally correspond with higher leaf wax concentrations.Red arrows indicate peaks in TOC, proposed to correspond with warmer SST.

The TOC records generally show contrasting cyclic patterns to carbonate records indicating fluctuations in organic carbon burial and productivity cycles during this climate transition. There are instances when carbonate reduction

coincides with the documented Messinian desiccation event (6.2 Ma to 5 Ma, Cita and McKenzie, 1986; Hodell *et al.,* 1986), an event when lowered sea levels and enhanced organic matter deposition occurred at sites across the North Atlantic Basin (Ciesielski *et al.,* 1982). Previous studies from ODP /DSDP cores have also shown that Messinian sections are barely preserved in the deep ocean and incomplete due to bottom water erosion and severe carbonate dissolution in the ocean (e.g. ODP Site 608, Iberian basin; Zhang and Scott, 1996 in Wagner, 1998). Despite the high carbonate content and low TOC content during the late Miocene to early Pliocene, evidence of alkenones for reliable SST and leaf wax lipid reconstruction provide evidence that the dissolution patterns and depositional environments of the equatorial Atlantic did not alter part of the primary climate signal. These biomarker responses shed light on the climate pattern, specifically sea surface ocean dynamics and atmospheric circulation patterns in the equatorial Atlantic.

SST cooling-warming cycles in the magnitude of ~ 4°C and the enhanced *n*-alkane concentrations off equatorial West Africa strongly support wind driven upwelling paired with enhanced aeolian supply or terrigenous organic matter from a relatively dry hinterland, both being directly linked through the position and dynamics of the ITCZ. Time series analyses on the SST and leaf wax lipid reveal that both records are intimately linked with evidence of 41 kyr and strong 75 kyr cycles. Distinct peaks in SST clearly mirrors intense upwelling of cooler waters which is highly influenced by the strength of the trade winds and indicates that the migration of the ITCZ and a change in thermocline structure

across the equatorial Atlantic was already in place much earlier than 4.4 Ma (Norris, 1998).

The SST record in this study argues for cooling of the equatorial Atlantic with greater amplitude at a much earlier time which intensified around 5.6 Ma. At this time, surface water movement of cold and nutrient rich surface waters in the tropical Atlantic was effectively influenced by the position and strength of the ITCZ. The timing of the positioning of the ITCZ intimately linked to trade wind strength and upwelling ITCZ must have moved seasonally to its northerly position establishing the seasonal migration cycles of the ITCZ today. Previous reconstructions of the ITCZ from stable isotopic and carbonate accumulation data in the late Miocene and early Pliocene in the Pacific (Hay and Brock, 1992) and the Atlantic (Pisias *et al.,* 1995) placed the position of the ITCZ in a relatively northern position, as it is today.

Other studies using paleoclimate evidence such as aeolian grain size in the eastern equatorial pacific (Hovan, 1995); foraminifera fauna assemblages in the western equatorial Atlantic place the ITCZ in a northerly position during the early Pliocene (Chaisson and Ravelo, 1997); and eastern and western Pacific (Chaisson, 1995) have also suggested that the ITCZ was located further north during the late Miocene but prior to 4 Ma. These studies (e.g. Pisias *et al.,* 1995; Hay and Brock, 1992) speculated that the northern position of the ITCZ during the late Miocene and early Pliocene was partly as a result of expansion of glaciers on the Antarctica.

Apart from cooling and arid conditions interlinked with regional upwelling, this new study proposes an associated link of the SST cycles with global cooling events documented during the late Miocene (reviewed by Zachos *et al.,* 2001). Late Miocene cooling was associated with an increase in Northern Hemisphere (NH) ice sheets and build up from ice from the Antarctica. Northern Hemisphere cooling in particular during the late Miocene to early Pliocene led to an increase meridonial wind strength and heat transport (Chaisson and Ravelo, 2000; Vellinga and Wood, 2002) as indicated by increased dust flux and inferred wind strength in the Northern Hemisphere Deep Sea (Rea, 1994). Therefore, cooling in the equatorial Atlantic may have been potentially influenced by these factors, consequently influencing the position of the ITCZ.

Repetitive variations in African climate with arid periods are represented by the clear evidence of leafwax lipid records during the late Miocene to early Pliocene transition. Leafwax lipids transported by aeolian dust to marine sediment have also been recorded by in several studies from the African region (Schefuß *et al.,* 2003; Tiedemann *et al.,* 1994; Hovan *et al.,* 1995; Ruddiman *et al.,* 1989). The comparison of the leaf waxes with the other proxies such as the the alkane/alkenone index (Fig 4.13) determined in this study indicate that the preservation and supply of organic matter at least terrestrial input related to regional upwelling. The delivery of *n*-alkanes will have been enhanced when conditions were cooler and wind intensity greater. Therefore changes in the variation of leaf wax lipids are related to changes in wind strength, cooler but

drier conditions related to the position of the ITCZ reflects the atmospheric circulation patterns over central Africa.

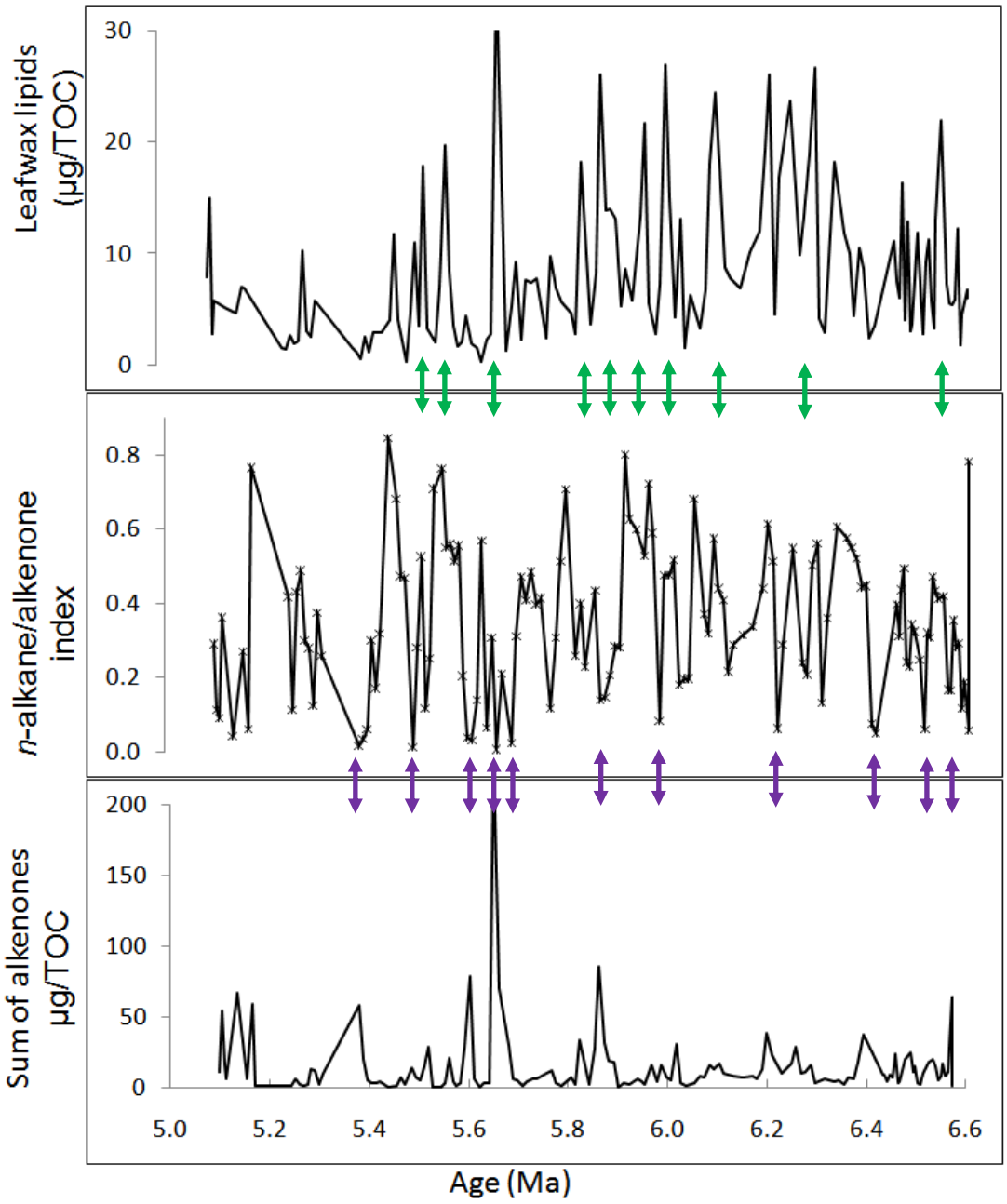

Figure 4.13 Comparison of the ODP Site 959 leafwaxes and alkenone concentrations (µg/TOC) to the n-alkane/alkenone index. An n-alkane/alkenone index approaching 1 (green arrow) indicate a predominant terrestrial source, whereas an index approaching 0 (purple) would indicate a predominant marine input. There are instances when maximum alkenone concentrations correspond with an index approaching 0 and vice versa for n-alkanes.

The CPI values confirm the dominance of leafwaxes from higher terrestrial plants. These records are comparable to what is expected for modern higher plant *n*-alkanes (Bi *et al.,* 2005; Chikaraishi and Naraoka, 2003; Chikaraishi *et al.,* 2004; Collister *et al.,* 1994) and modern soils and dust (Huang *et al.,* 1997; Schefuß *et al.,* 2003). The ACL record at ODP 959 with moderate variations with cyclic patterns suggests that the type of vegetation supplied to the African continent may vary depending on alternating climate conditions. The controls on the average chain lengths (ACL) of *n*-alkanes in higher plants remain relatively unclear. To date, published evidence suggests that changes in the ACL can be interpreted as a change in the nature of the source vegetation (Pancost and Boot, 2006). Certain studies have found the ACL to vary with temperature and humidity (Schefuß *et al.,* 2003; Hinrichs, 1998; Rinna *et al.,* 1999) while other studies have found the ACL to coincide directly with changes in the pollen-inferred input of grasses vs. trees and shrubs (Fisher *et al.,* 2003). The A.I. records measures the type of vegetation source and this record at least indicate there are different vegetation sources but predominantly of African grassland, Sahel and savannah.

4.6.2 *Time series analyses*

4.6.2.1 *Pacing of organic carbon burial*

Spectral analyses of the TOC records from ODP Site 959 show that the organic carbon equatorial Atlantic responded strongly to the obliquity and eccentricity bands of orbital periodicities during the late Miocene to early Pliocene. This observation strongly suggests that high latitude climate considerably influenced the region at that time consistent with initial results from Wagner *et al. (*2002) from the same site which revealed strong power at the obliquity and eccentricity bands. High latitude climate processes are typically dominated by 100 kyr and 41 kyr cycles (Ruddiman and McIntyre, 1984; Boyle and Keigwin, 1982; Raymo *et al.,* 1990) and there are several mechanisms that may have linked the tropics to high latitude climate forcing during the late Miocene to early Pliocene.

Firstly, the establishment of the Early African monsoon /trade system linked to drops in sea level may have influenced organic carbon burial off tropical West Africa at the Miocene Pliocene climate transition in response to the Miocene cooling events and the Messinian salinity crisis (Zhang *et al.,* 2006). However, as the intensity of the African monsoon is typically linked to precessional control of monsoons varying at periods of 19 kyrs to 23 kyrs, (Prell and Kutzbach, 1987), no detection precessional cycles from the ODP Site 959 spectral records suggests that the African monsoon trade system was not the main driver for the nature of the observed TOC cycles.

Secondly, the migration of the ITCZ and the complex lateral displacement of ocean currents may have enhanced upwelling and marine productivity and deposition of organic carbon off equatorial Africa at that time. It is speculated that the TOC variability reflects changes in preservation in the deep ocean, which would be driven by large scale deep ocean currents and maybe this is where the high latitude signal originate from. Past studies have shown that oceanic currents during the late Miocene may have been linked to the response of the migration of the ITCZ (Mix and Morey, 1996; Schneider *et al.,* 1996) suggesting that northward cold and nutrient rich deep waters from southern sources may have been transported to the Gulf of Guinea during the Miocene to early Pliocene (Wagner *et al.,* 2002). However, a direct link to this mechanism proves elusive and it is not yet clear what the exact mechanisms for driving the nature of the observed TOC cycles are. What is imminently clear however is that the dominance of the 100 kyr and 41 kyr cycles in the organic carbon records is the proposed high latitude climate processes associated with the climate evolution of the Miocene/Pliocene transition.

The late Miocene to Pliocene climate between (7-5 Ma) as recorded from $\delta^{18}O$ of foraminifera was a period of relatively stable climate during the Cenozoic, which did not indicate any dramatic climate events (Zachos, 2001) but, the establishment of Antarctic ice sheets, increased ice volume, and build up of ice from the Northern Hemisphere (e.g Mercer, 1976; Shackleton and Kennett, 1975; Brewster, 1980; Ciessielski et al.,1982; Kennett and Barker,1990) during

the Miocene through the Pliocene may provide a case for associated linkages with the records at ODP Site 959.

The TOC cycles may have responded to these events at least periodically as reflected in the time series records, with increased deposition of organic matter due to displacement of higher productivity areas towards the open ocean. Higher TOC records were expected to correspond with cooler SST records to validate interrelationships between organic carbon burial and upwelling, however this was not the case and upwelling does not seem to be the likely driver for the TOC spectral observations. This conclusion, confirmed by comparison of the spectral results of the TOC and molecular records which show no apparent correlation during the late Miocene to early Pliocene climate transition proposes a different mechanism for the nature of the observed TOC cycles.

4.6.2.2 *Pacing and phasing relationships of SST and leaf wax lipids*

Unlike the TOC records, the spectral records performed on the SST and leaf wax lipids do not show a very strong eccentricity signal, but rather different time frequencies dominated by 75 kyr and significant obliquity 42 kyr cycles. It should be noted however that these molecular records were of much lower depth resolution than the TOC records which may to some extent have impacted on the frequency patterns. The amplitude of warm/cold cycles of ~ 4°C has been proposed to be associated with variations in upwelling along the tropical West African continental margin. Accordingly, cool SST intervals would have corresponded generally to more arid conditions in central Africa.

Significant and persistent coherency between the SST and leafwax lipids further suggests that upwelling and atmospheric and ocean circulation patterns were intimately coupled. For African aridity and terrestrial climate, the tropics have been linked to 100kyr and 41 kyr glacial/interglacial ice volume signals emanating from higher latitudes for the last glacial maximum (e.g. Parkin and Schackleton, 1973; Pokras and Mix, 1985), when conditions were much drier and arid and for the Pleistocene (de Menocal *et al.,* 1993) when ice sheet evolutions predominated.

The curious finding of the ~75 kyr cycles in the ODP 959 molecular records makes it difficult to solely attribute the SST and leaf wax records from the equatorial Atlantic to high latitude climate influences. One of the explanations for the 75 kyr cycle could be a sub frequency associated with the 100 kyr cycle due to a bias by limitations in the age model which may have reduced the amplitude of the 100 kyr orbital periods. Alternatively, the 75 kyr cycle may be related to ice volume changes as it transitions from 41 kyr to 100 kyr, producing a shorter cycle of 75 kyr. Such cycles of similar frequencies have been reported from Mid Pleistocene tropical SST records (Schefuß *et al.,* 2004) and $\delta^{18}O$ records (Mudelsee and Schulz, 1997) and interpreted in a similar way. 76-80 kyr cycles from benthic $\delta^{18}O$ and SST records in the tropical Angola basin (Site 1077) were linked to transitional continental ice volume variations in the mid Pleistocene (Schefuß *et al.,* 2004). Mudelsee and Schulz (1997) found 77 kyr cycles in global $\delta^{18}O$ from several sites and linked this to pseudo regular ice calving cycles with periods between ~76 and 100 kyrs. Approximately 80 kyr

variations were detected in sediments from the Congo fan and linked to the doubling of the 41 kyr cycles (Berger *et al.,* 1998).

During the late Miocene to early Pliocene, the buildup of ice and consequent changes in temperature, expansion of ice sheets on the West Antarctica and the Northern Hemisphere influenced global environmental conditions. These processes may have driven the nature of the cycles observed in the equatorial Atlantic SST and terrestrial response. Therefore it is likely that the equatorial Atlantic was linked to glacial/colder and arid conditions associated with the late Miocne to the late Pleistocene (Lawrence *et al.,* 2009).

The lead/lag relationship between leafwaxes and SST show that leafwaxes lead the SSTs at the 75 kyrs band by 2kyrs and lag at ~41 kyrs by 5 kyrs. A lead in terrigenous supply at the obliquity frequency indicates that African arid conditions preceeded changes in SST. Hence when Central Africa cooled, wind intensity became higher, increasing dust supply to the ocean and at the same time fostering upwelling along the continental margin. Consequently, the African continent seemed preconditioned for aridity during ice growth or transition to ice growth in high latitudes, similar to the late Quaternary. A lag in leaf waxes at the obliquity frequency indicates that upwelling processes may have been responsible for regulating the supply of terrestrial organic matter to the equatorial Atlantic. Cooler SSTs would have transported less moisture to Central Africa, stimulating aridity. General circulation models have demonstrated that cold glacial North Atlantic SSTs result in annually cooler and

drier conditions over North Africa, increasing trade winds and aeolian export. Consistent with that, other global climate models have shown that driest model years in the Sahel were related to cool North Atlantic SST anomalies (Druyan, 1989). Given the strong dominance of the 75 kyr, it is likely that maximum wind intensity had driven upwelling but that the equatorial Atlantic SST responded at least remotely to Northern hemisphere high latitude climate during the late Miocene to early Pliocene climate transition.

4.7 ***Conclusions***

The high resolution records from ODP Site 959 show that despite low organic carbon burial content, molecular proxies were well preserved in the sediments revealed by $U^{k'}_{37}$ alkenone SST and higher plant leafwaxes. Upwelling and atmospheric circulation patterns in the equatorial Atlantic between 7-5 Ma were intimately linked to high amplitude changes in SST and corresponding fluctuations in wind intensity and African aridity/humidity. Generally, when SSTs were low evidence there is evidence for high *n*-alkane supply supporting wind driven upwelling in the equatorial West Atlantic. The nature of the records at ODP Site 959 in the equatorial Atlantic investigated by spectral analyses show that 41 kyr cycles is a common frequency in all records.

Organic carbon records show an additional persistent and strong cycle of eccentricity ~100 kyr during the late Miocene to early Pliocene which strongly suggests the influence of high latitude climate forcing typically dominated by 100 and 41 kyr cycles. SST and leaf wax spectral records show dominance of 75 kyr and 42 kyr cycles during the late Miocene and early Pliocene, and the nature of these cycles may be linked to the global cooling proposed during the late Miocene. The lead and lag relationships between the leaf waxes and SST show the coupled relationships and mechanisms driving the processes of upwelling and regulation of supply of terrestrial organic matter to the equatorial Atlantic.

5 Chapter 5

5.1 *General Introduction to the International CHEETA project*

The international **Changing Holocene Environments of the tropical Eastern Tropical Atlantic** (CHEETA) project is a collaboration of work by three different groups: Professor P. deMenocal, Woods Hole Oceanographic Institution (WHOI); Lamont Doherty Observatory of Columbia University; Professor Tim Eglinton, Eidgenössische Technische Hochschule (ETH), Zurich; and Professor Thomas Wagner at Newcastle University. The overall purpose of the programme is to develop new records of NW African climate and tropical Atlantic ocean variability utilizing a transect study from the Portuguese to NW African margin (40°N-15°N). As part of Newcastle University, this thesis contributes to the larger CHEETA project in two ways:

1. A standalone independent study to test the transport of soil organic matter (SOM) along the transect is investigated from surface sediments using a combined novel biomarker approach. (Chapter 5)
2. Sediment core material that generate datasets within a newly developed integrated chronological framework that document variations in organic carbon burial and terrestrial vegetation supply associated with the glacial to Holocene climate variability (Chapter 6). Although most molecular work was designated to the other collaborating bodies, the preliminary biomarker work on higher leaf wax lipids acts as a pilot study which identifies the need for further research in this regard.

5.2 ***Testing the applicability of novel soil biomarkers on surface sediments.***

This chapter introduces the first part of the CHEETA project which tracks soil organic matter in North West African surface sediments using traditional bulk geochemical and novel biomarkers. Large amounts of terrestrial organic matter (approximately 400 x 10^{12} gCyear^{-1}) are transported from the continent into the open ocean by rivers through fluvial input (Schlünz and Schneider, 2000) and aeolian processes (Romankevich, 1984). Its distribution and fate remains poorly constrained (Hedges and Keil, 1995; Hedges *et al.,* 1997; Wagner and Dupont, 1999; Eglinton and Repeta, 2003: Wagner *et al.,* 2004; Burdige, 2005). This is particularly so with respect to aeolian inputs which may be as large as 320 x 10^{12} gC year^{-1} and may be important at open ocean environments (Romankevich, 1984).

Much of our understanding of terrestrial organic matter inputs stems from studies of vascular plant-derived biomarkers, such as those derived from epicuticular wax lipids and lignin (Eglinton and Hamilton, 1963; de Leeuw and Largeau, 1993). However, the transport and fate of soil-derived organic matter (SOM) is still the subject of debate and large uncertainty, in particular beyond the influence of large river plumes. Increasing evidence from a wide range of marine settings, using other molecular proxies (e.g. Gough *et al.,* 1993; Wagner *et al.,* 2004) and bulk geochemical information (Holtvoeth *et al.,* 2005) support the notion that preservation of SOM is likely important in deep sea sediments.

The significance of SOM delivered via atmospheric deposition however is unclear, and this study explores the use of novel biomarkers to trace SOM export and burial in marine sediments underlying an area that is recognised for its prominent eolian transport and minimal influence from large rivers - the continental margin off NW Africa. Soil organic carbon accounts for 66% of the total terrestrial carbon budgets (Batjes, 1996). The fate and turnover of SOM, as well as its interactions with nutrients and (clay) minerals, are intimately linked to changes in climate, catchment hydrology, and runoff.

To understand the export and transport pathways of terrigenous organic matter into the open marine setting, previous studies have focused on the use of bulk elemental and isotopic parameters including C/N ratios, plant wax and lignin content and composition, and bulk sediment $^{13}C_{org}$ values (Westerhausen *et al.,* 1993; Goni *et al.,* 1998; Huang *et al.,* 2000; Wagner *et al.,* 2004). Other studies (Madureira *et al.,* 1997; Schefuβ *et al.,* 2003) have used concentrations and molecular isotopic compositions of terrestrial biomarkers to assess C_3 versus C_4 vegetation inputs, reconstruct past variations in higher plant habitats, and to relate these variations to changes in continental climate. Such measurements have been applied to the organic fraction within the dust emanating from NW Africa (Eglinton *et al.,* 2002). Plant wax carbon isotopic signatures in atmospheric dust samples collected in the eastern subtropical N Atlantic reflect the latitudinal gradients in C_3 and C_4 vegetation present on the adjacent continent (Schefuβ *et al.,* 2003).

Molecular isotopic measurements of continental margin surface sediments from the same region show similar spatial trends (Huang *et al.,* 2000), implying that the terrestrial inputs are dominated by eolian transport (Schefuβ *et al.,* 2003; Huang *et al.,* 2000). Down-core plant wax biomarker carbon isotopic measurements also imply past climate-driven shifts in the distribution of C_3 and C_4 vegetation (Zhao *et al.,* 2000, 2003).

Recently, two new molecular markers have been proposed as tracers of soil-derived organic matter in the marine and aquatic environment – The branched glycerol dialkyl glycerol tetraethers lipids (GDGTs; **I-III** and crenarchaeol **IV**) and certain bacteriohopanepolyols (BHPs) specifically adenosylhopane (**VIII**). Branched GDGTs (structure, chapter 2) are a group of tetraether membrane lipids found in peat bogs and soils worldwide (Sinninghe Damsté *et al.,* 2000a,b; Weijers *et al.,* 2006) that form the basis of the BIT (branched and isoprenoid tetraether) index (equation, chapter 2; Hopmans *et al.,* 2004; Weijers *et al.,* 2006; Tierney *et al.,* 2009). BHPs (structure, chapter 2) are pentacyclic triterpenoids biosynthesised by many prokaryotes (Talbot and Farrimond, 2007; Cooke *et al.,* 2008a,b, 2009). The measurements of these biomarkers can highlight the potential importance of SOM for the marine organic carbon budget. Thus far, studies employing the GDGT-derived BIT index and BHPs have focused mostly on marine (Hopmans *et al.,* 2004; Weijers *et al.,* 2006; Kim *et al.,* 2006, 2007; Cooke *et al.,* 2008a, 2009) and lake sediments (Powers *et al.,* 2004; Blaga *et al.,* 2009) influenced by fluvial inputs.

BHPs exhibit a high degree of structural variability (e.g. Rohmer *et al.,* 1984; Rohmer, 1993; Talbot *et al.,* 2008) and are precursors of the ubiquitous geohopanoids (hopanoic acids, hopenes, hopanes; (Ourisson and Albrecht, 1992) in the geologic record. Four BHPs have recently been suggested to be highly characteristic of SOM input (Talbot and Farrimond, 2007; Cooke *et al.,* 2008a) including adenosylhopane (**VIII**), 2-methyladenosylhopane and two structurally related compounds. Adenosylhopane is one of the four most common BHPs in soils (Cooke *et al.,* 2008a) making it a useful biomarker for tracing SOM in lacustrine and marine sediments (Talbot and Farrimond, 2007; Cooke *et al.,* 2008b). Up to now, soil BHPs have been found in lakes with large soil organic carbon supply (Talbot and Farrimond, 2007), a transect from the River Rhone (Cooke *et al.,* 2008b), The Congo deep-sea fan (Cooke *et al.,* 2008a) as well as river and estuary sediments from seven major Arctic Rivers (Cooke *et al.,* 2009). This study presents data to assess the transport and deposition of these marker compounds into the continental transect off the North West African continental margin.

5.3 *Aims and Objectives*

The overall aim of this chapter is to couple measurements of the BIT index and a SOM derived BHP with bulk geochemical measurements on surface sediments in order to assess inputs of SOM, and the strength of the molecular signals in low total organic carbon (TOC) continental margin sediments distal from any fluvial influence.

The objectives are:

1. To obtain bulk organic carbon and isotopic records including TOC, $CaCO_3$; C_{org}/N_{tot} and $\delta^{13}C_{org}$.
2. To detect GDGTs for calculation of the BIT index to trace soil organic matter along the North West African margin.
3. To detect and quantify BHPs, to trace soil organic matter along the North West African margin.
4. To compare the two tracers of SOM in order to explore and assess the inputs of SOM and strength of these molecular signals.

5.4 ***Study interval and sampling strategy***

All methods for analyses of the surface sediments have been detailed in Chapter 3. The sample set comprises 23 new surface sediments along a latitude transect (40°N-15°N) extending from southern Portugal to the NW Africa (Fig.5.1) that were recovered during the CHEETA (Changing Holocene Environment Eastern Tropical Atlantic) cruise (OC437-7) in July 2007. The sediments were recovered using a multicorer device. Each sub core was sectioned in 1 cm increments, frozen immediately after sampling onboard, and kept frozen until further processing in the laboratory. All station list and depth have been provided in Appendix B

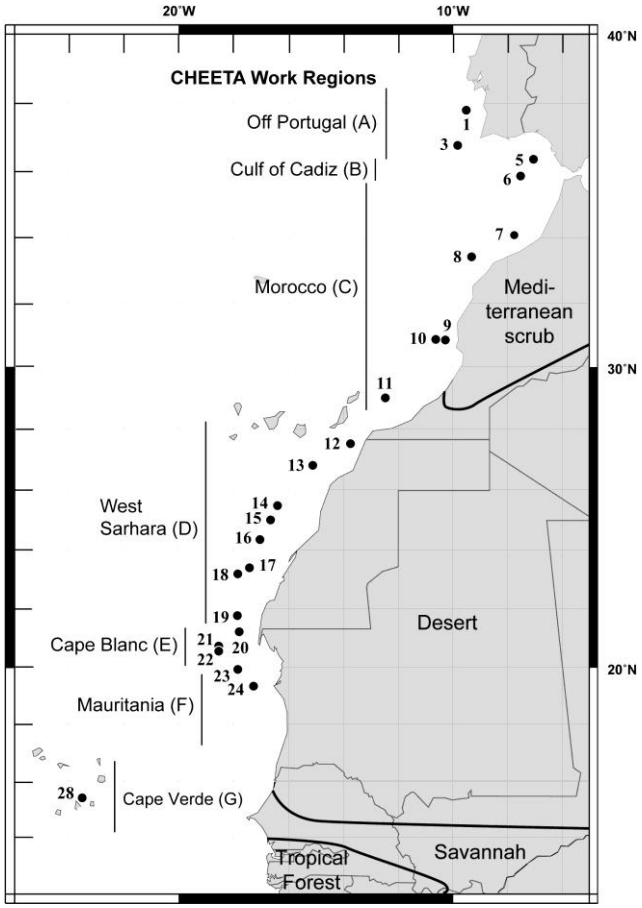

Figure 5.1. CHEETA work regions showing the modern vegetation zones along the North West African margin. The black dots indicate the surface sediments investigated for this study. Regions are annotated along the transect.

5.5 ***Results***

All raw data and stations identification are compiled in the Appendix B.

5.5.1 *TOC contents*

TOC content from the North West African margin vary from 0.4 to 2.2 %. (Fig.5.2). Highest TOC values are confined to Stations 20-28, the Cape Blanc and Cape Verde regions, with a clear maximum linked to the Cape Blanc upwelling region. Higher TOC values reflect productivity and conditions favourable for the preservation of organic matter. Lowest TOC values are observed in the Morocco regions and remain stable below 1% in the Portuguese regions.

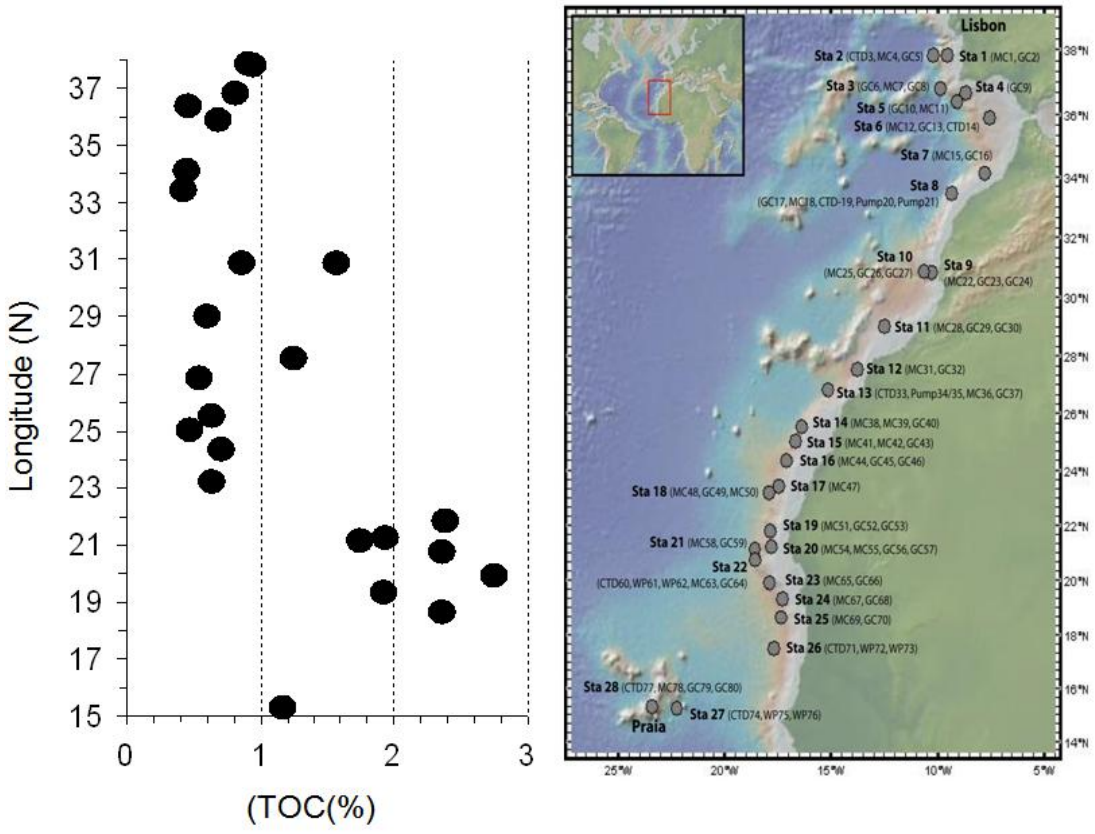

Figure 5.2 TOC records from the North West African margin showing longitudinal and latitudinal trends

5.5.2 *$CaCO_3$*

The carbonates from the North West African margin surface sediments vary from 12% to 60 % (Fig 5.3). At Station 24, further south of the transect, surface sediments show that minimum carbonates correspond with high TOC values which then generally increase to Station 16 followed by a pronounced decrease at Station 13 and a further elevation at Station 12 in the West Sahara, indicating slight variations in the carbonate records. Station 9 shows the maximum carbonate content followed by another pronounced decrease towards the Cape Blanc regions. Although there is no clear trend in carbonates, the decrease towards the Cape Blanc region probably reflects changes in the primary producers of organic carbon, possibly from carbonaceous in non upwelling regions to biosilicious in upwelling regions.

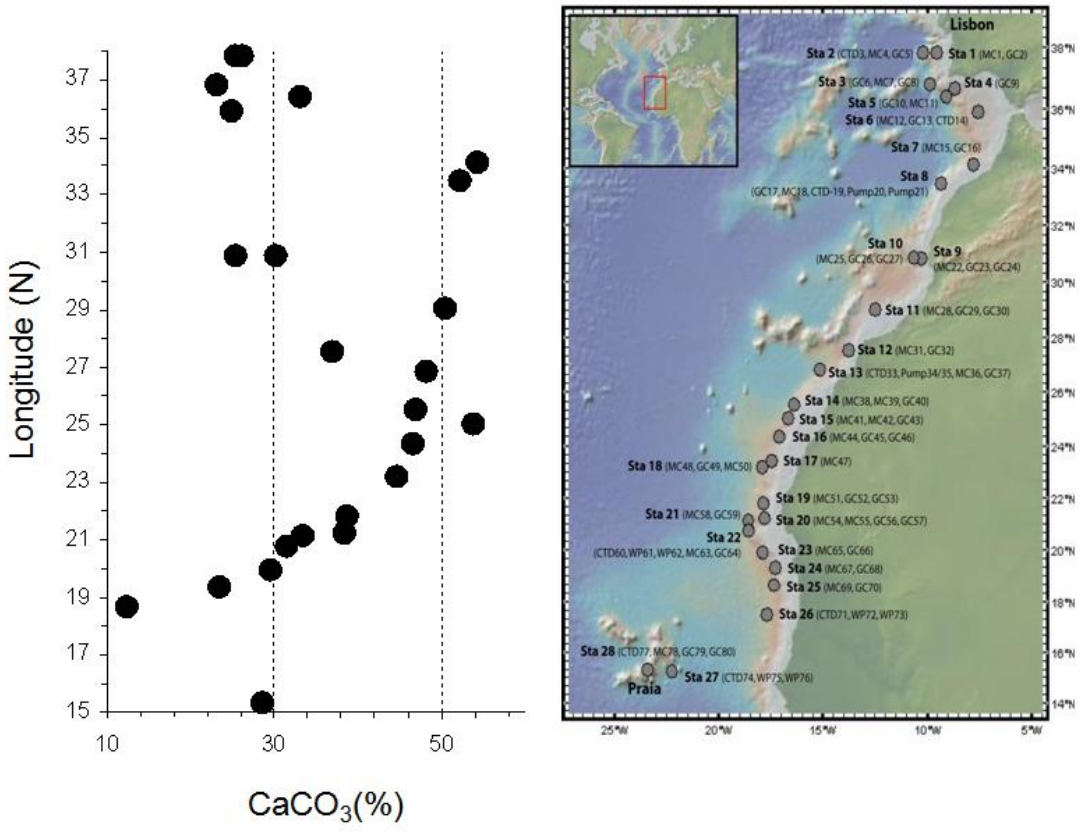

Figure 5.3 Calcium carbonate records from the NW African margin

5.5.3 C_{org}/N_{tot}

The C/N ratio range from 7 to 9 (Fig. 5.4) and indicates the relative composition of organic carbon to nitrogen which can reflect the nature of the sedimentary organic matter along the continental margin. There appears to be no clear trend in this ratio across the North West African margin. However, maximum values are shown twice in the south of the transect at Stations 19 and 13 in the West Sahara, and in the North at Station 9 in the Mediterranean region distinguishing the origin of sedimentary organic matter.

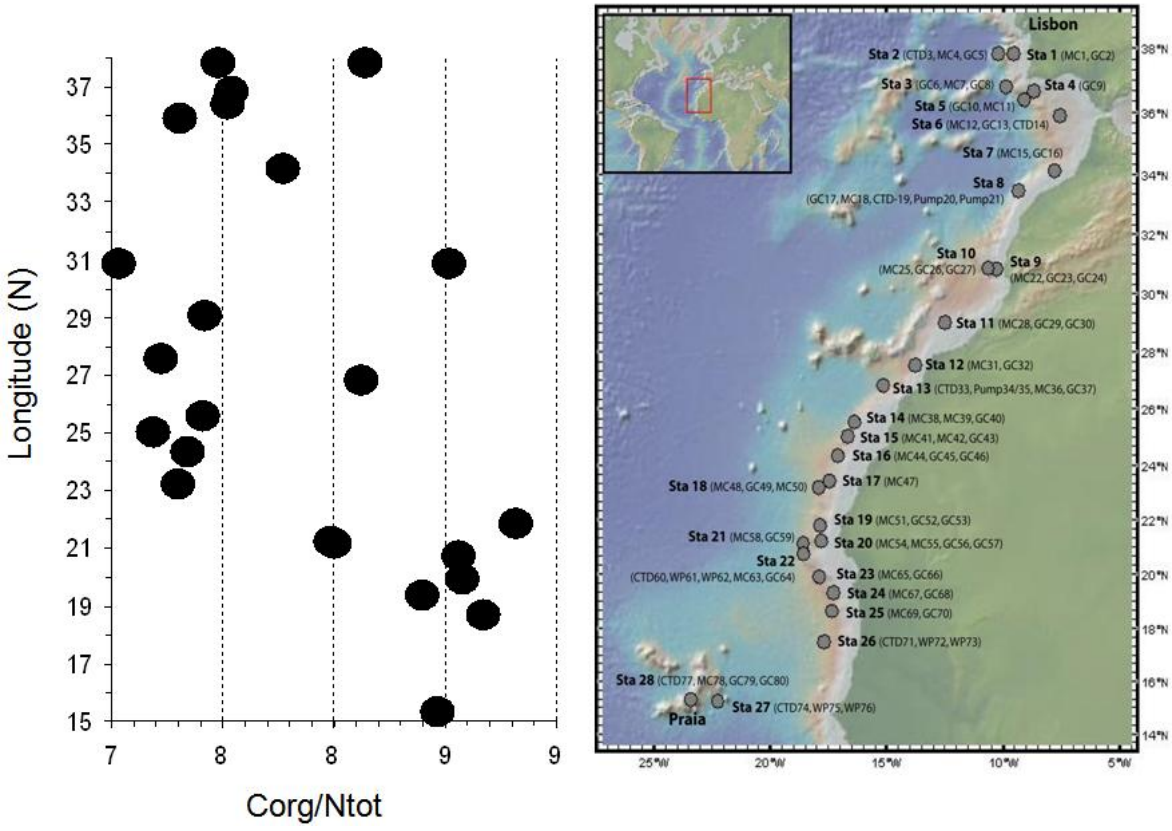

Figure 5.4 C_{org} /N_{tot} values from the NW African margin

5.5.4 $\delta^{13}C_{org}$

The $\delta^{13}C_{org}$ values for sedimentary organic matter range from (-19‰ to -23‰) with a distinct negative 3.5-4 ‰ shift between Morocco and the northern part of the W African sector (35-25°N; South of 25°N) (Fig.5.5). The $\delta^{13}C_{org}$ values remain stable at around -19‰ as compared to more depleted but equally constant values around -22.5‰ in the Gulf of Cadiz and off Portugal.

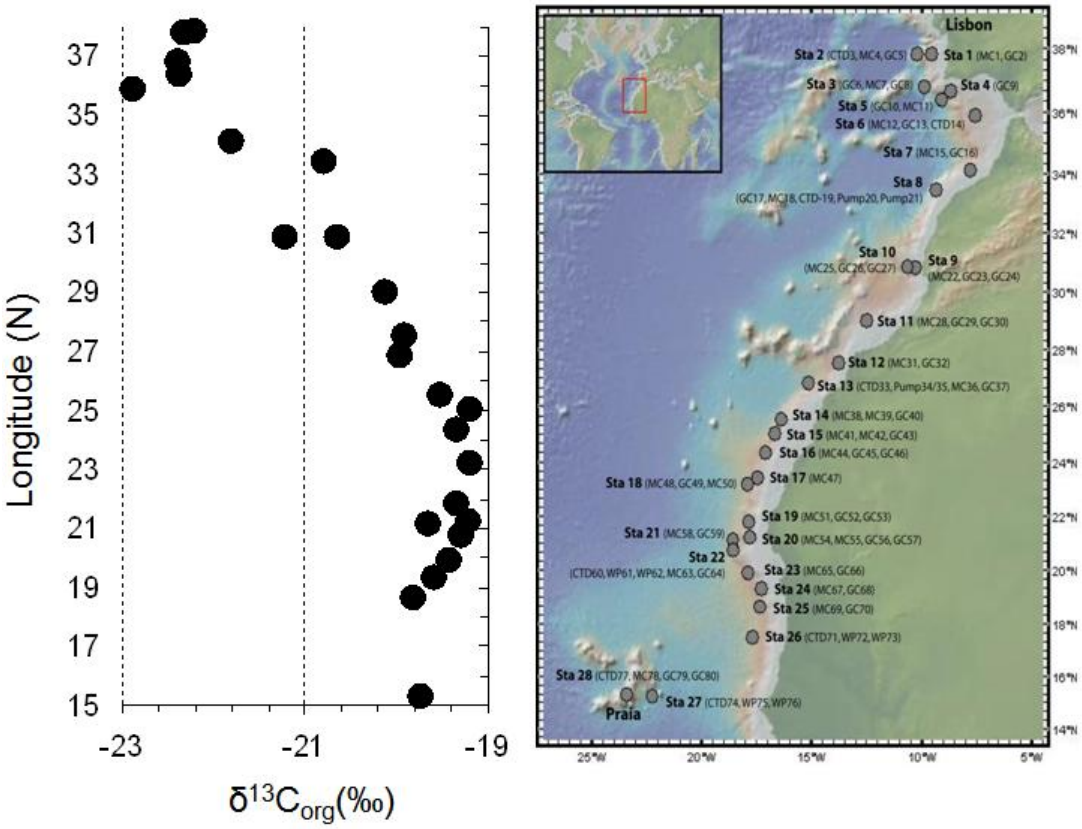

Figure 5.5 $\delta^{13}C_{org}$ from the NW African margin

5.5.5 *Molecular Markers- GDGTs and BHPs*

Branched tetraethers (**I-IV)** (structure, Chapter 2) are observed in measurable quantities in most but not all surface sediments (Table, appendix). Chromatograms from the Gulf of Cadiz and Off Mauritania confirm the presence and clear chromatographic separation of the target compounds; (Fig.5.6 a, b).These compounds yield very low BIT indices across the transect (Fig 5.7; Table 5.1) ranging from 0 to 0.05 .The highest BIT value is observed at 15° N off Cape Verde (Station 28). No branched tetraethers were detected in surface sediments at Stations 14, 16 and 18 within the sector of the most depleted $^{13}C_{org}$ signatures.

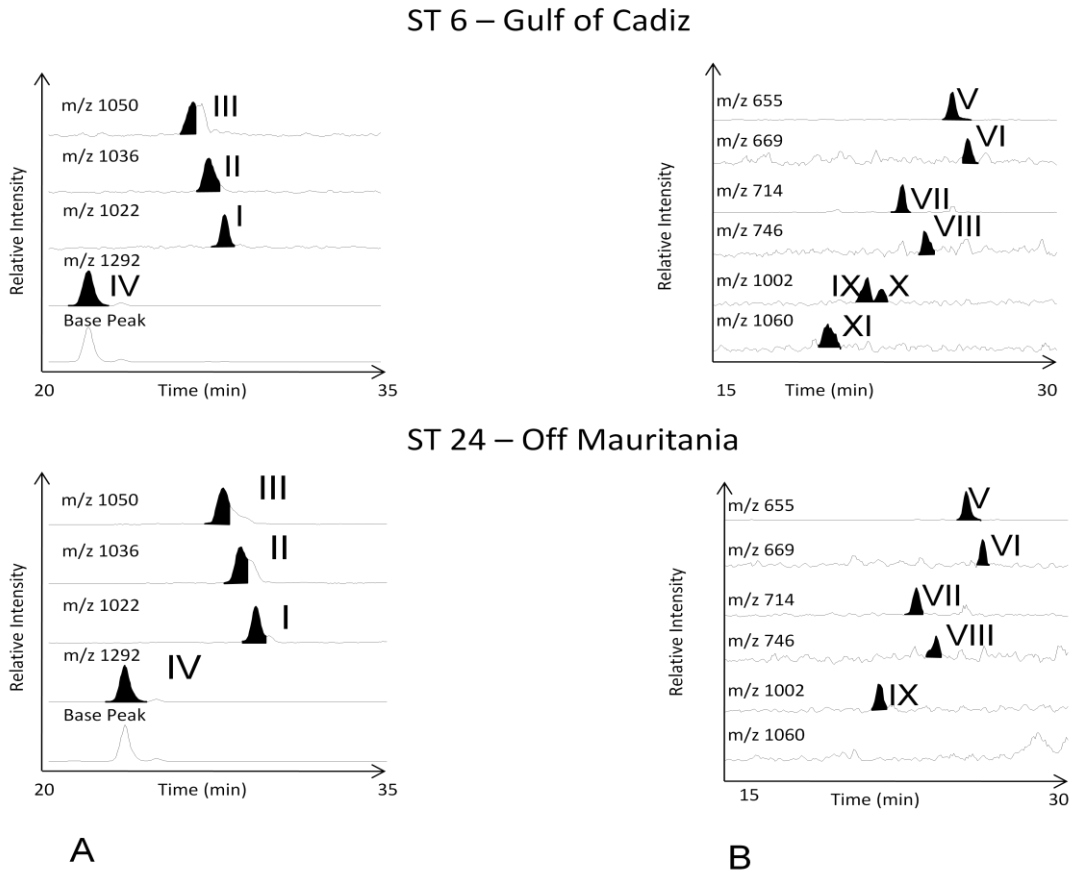

Figure 5.6 Representative chromatograms of GDGTs (a) and BHPs (b) detected in surface sediments from the NW African margin

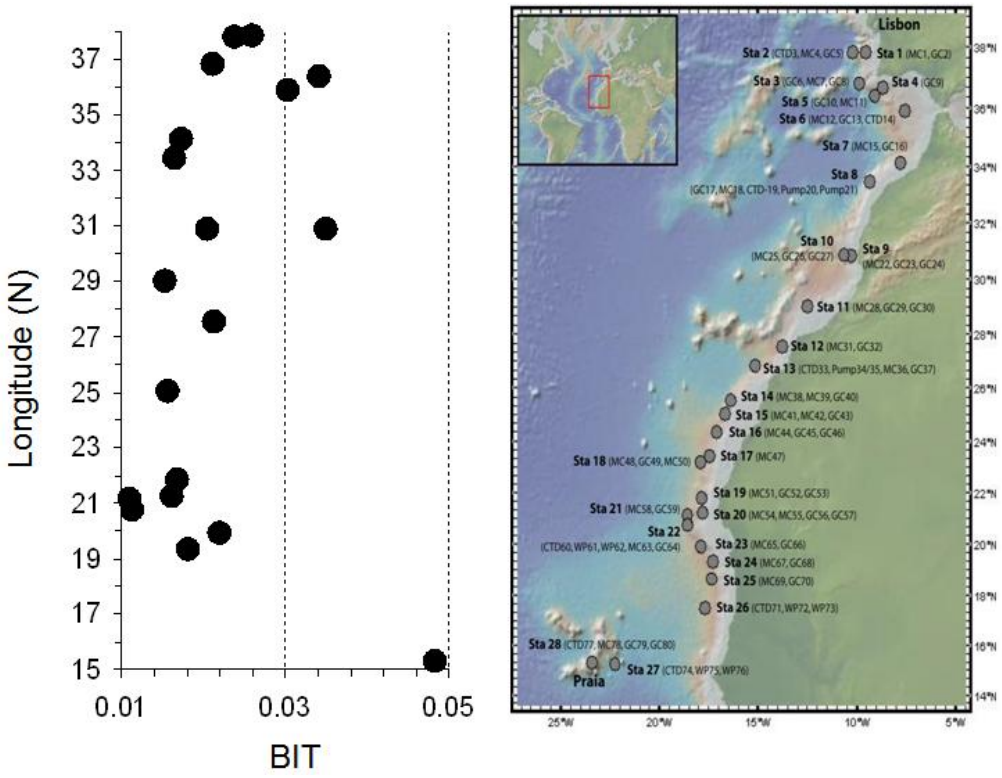

Figure 5.7 BIT index determined from surface sediments from the NW African margin

Up to seven different BHPs (chemical structure, Fig 5.8) are present in all of the sediments analysed from the Northwest African margin. However, consistent with the branched GDGT results, the soil-specific BHP adenosylhopane **(VIII)** (structure, Fig 5.8; mass spectra, Fig 5.9) was not detected in the surface sediments from 4 locations (Stations 11-14) between the Morocco margin and West Sahara (Fig 5.10; Table, appendix).

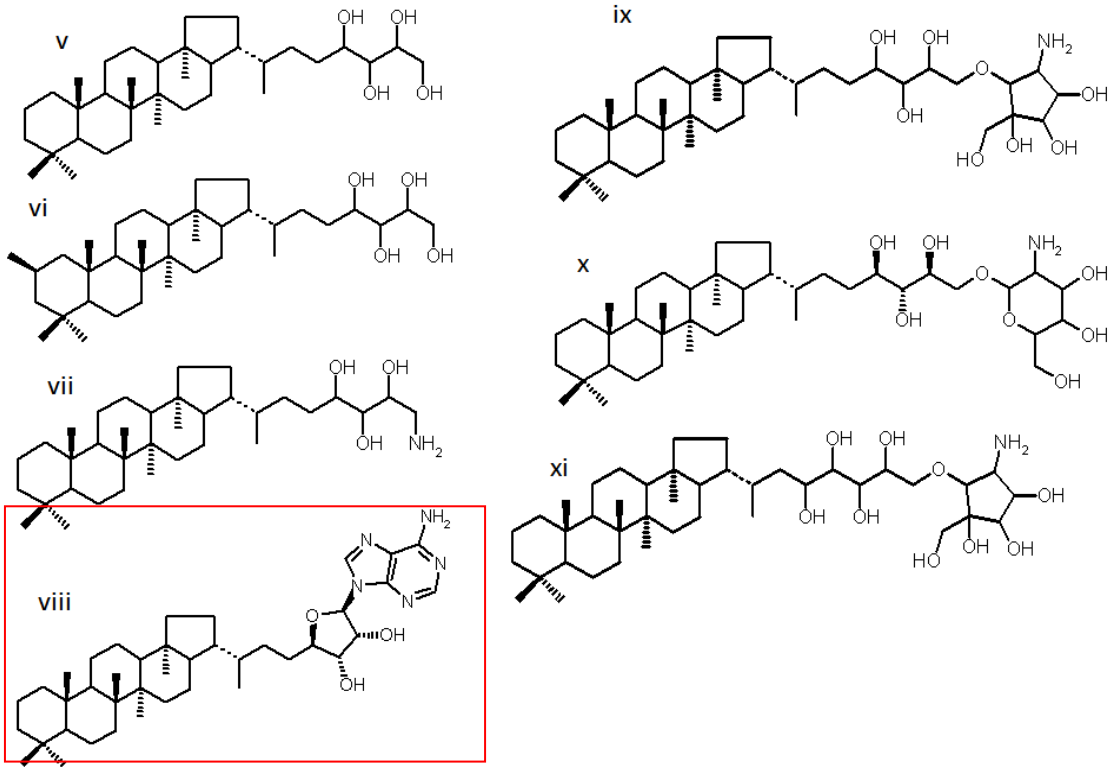

Figure 5.8 Chemical structures of the BHPs detected in surface sediments from the NW African margin.Soil marker BHPs adenosylhopane (VIII) highlighted in red.

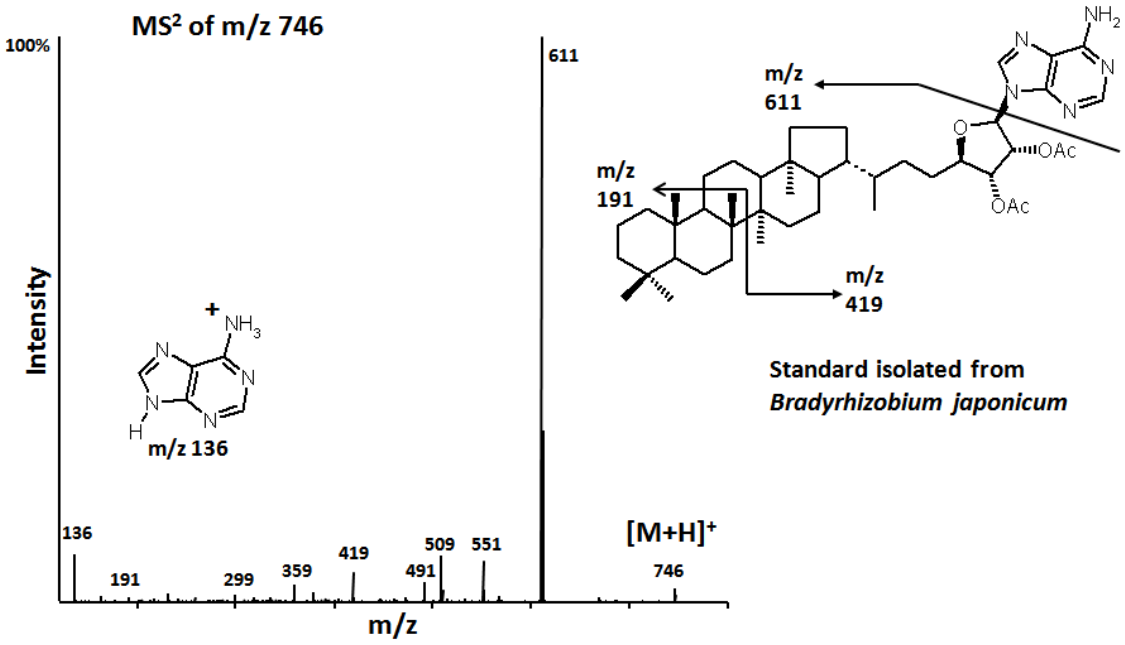

Figure 5.9 Representative APCI spectrum of adenosyl hopane diacetate detected from the NW African margin, with m/z ratio of 746

Other BHPs observed include bacteriohopanetetrol (BHT, **V**) and aminobacteriohopanetriol (**VII**) which were present in all the samples analysed and are produced by a wide variety of bacteria in a range of environments (e.g. Talbot and Farrimond, 2007; Talbot *et al.,* 2008). These two BHPs are the only ones to be regularly observed in marine sediments which are not influenced by input from large rivers (Talbot *et al.,* unpublished data). 2-Methyl BHT (**VI)** is generally considered to derive from cyanobacteria (Talbot *et al.,* 2008 and references therein). One tetrafunctionalised composite BHP (BHT cyclitol ether; **IX**) was present in all samples, has a wide range of known source organisms (Talbot *et al.,* 2008) and is frequently abundant in soils (e.g. Cooke *et al.,* 2008a) whilst the isomeric structure with a glucosamine sugar at the C-35 position (BHT glucosamine; **X**), observed in seven of the samples including Station 6 (Fig.5.6b), is less common and frequently completely absent in soils. A third composite structure, bacteriohopanepentol cyclitol (**XI**) ether, a commonly occurring but minor component in soils, was observed in 13 of the samples analysed here. The fraction of soil-marker BHP relative to total BHP range from 0 to 6% (Fig 5.10) with slightly higher soil biomarker fractions off Portugal compared to the rest of the transect (except where soil BHPs are absent) (Table 5.1). Soil BHP concentrations *(adenosylhopane*) range from 0-7 µg/g and generally match the overall trend in % soil BHP of total BHP (Table, appendix).

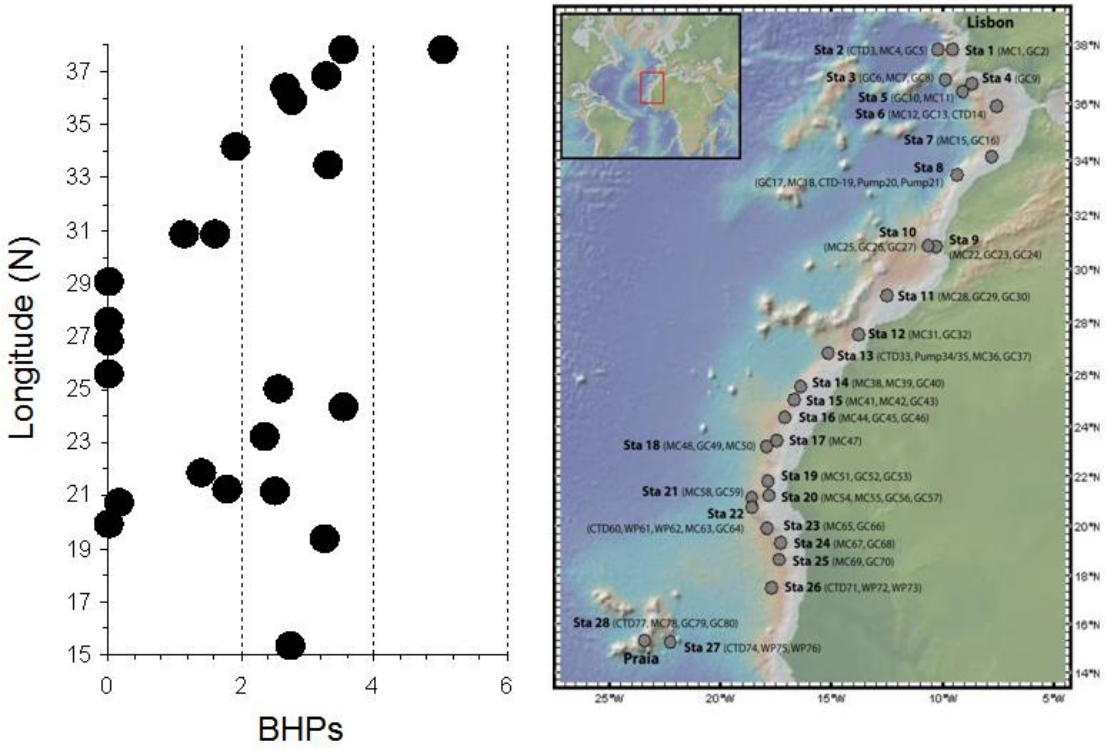

Figure 5.10 Soil marker BHPs (%) detected from sediments from the NW African margin.

5.6 ***Discussion***

Bulk organic geochemical parameters especially the TOC contents along the NW African transect identify upwelling areas of primary organic carbon burial. Although the carbonates show no clear trend along the transect, the pronounced decrease towards Cape Blanc regions indicate that the upwelling region likely reflects productivity from non carbonaceous primary producers. A comparison of the molecular records with $^{13}C_{org}$ (Fig 5.11) show that the spatial variations in surface sediments from the Portuguese - NW African margins are consistent with some supply of terrigenous OM to these open ocean sediments.

The observed $\delta^{13}C_{org}$ gradient, with an almost 4‰ overall shift, parallels the general transition from predominantly C_3 vegetation, and possibly an admixture with MOM in southern Europe and northern Morocco to C_4-dominated grassland habitats (savannah) in central and subtropical Africa. This observation is in full agreement with previous studies of dust samples and surface sediments from the NW African continental margin (Schefuβ *et al.,* 2003; Huang *et al.,* 2000; Westerhausen *et al.,* 1993). In these and other studies it is generally assumed that plant wax signals mainly originate either from direct ablation from leaf surfaces or from mobilization from the surface of soils, desiccated lake beds and dispersal by winds (Schefuβ *et al.,* 2003; Huang *et al.,* 2000). This preferential eolian transport mechanism may well predominate for NW Africa due to its overall dry climate, whereas leaf waxes may also be exported via fluvial transport in other more humid settings. Notably, although inputs of

terrestrial organic matter to the NW African margin have been previously documented, the significance of SOM in dust has not been directly addressed.

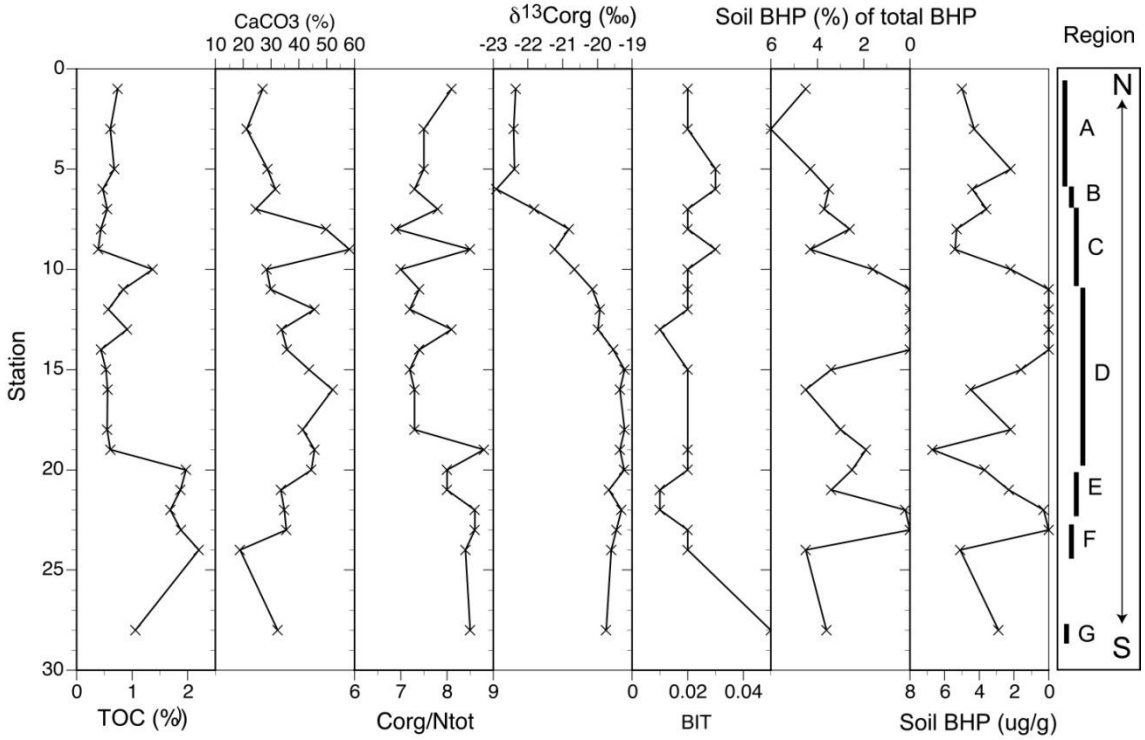

Figure 5.11 A comparison of the bulk geochemical proxies determined from surface sediments from the NW African margin

Branched GDGTs as well as soil BHPs identified in Portuguese - NW African margin surface sediments add support for SOM inputs, and reveals the potential of both compound classes to be transported to and preserved in low-TOC open marine sediments. Their fate and preservation potential within the sediments, however, is not yet known. Equally it is not known how far out into the deep North Atlantic the molecular SOM signal can be traced. The consistently low BIT index values lack any co-variation with known vegetation and export patterns along the study transect (Fig 5.11) This either argues against the use of branched GDGTs as a molecular proxy for tracing aeolian SOM in wind influenced settings, consistent with conclusions by Hopmans *et al*. (2004) or it

implies that SOM comprises a minor and relatively invariant component of the organic matter entrained on dust particles.

Low BIT values from sediments have been suggested to arise from in situ production of branched GDGTs (Tierney *et al.,* 2009; Peterse *et al.,* 2009). Significant differences in the degree of methylation and cyclisation based on the MBT/CBT index (Weijers *et al*, 2007; See chapter 2) was detected in sediments from soils and aquatic environments from Lake Towuti, Indonesia (Tierney *et al* ., 2009). Similarly, Peterse *et al* (2009) used the MBT/CBT index to reconstruct past mean annual temperature (MAT) in the lake and fjord setting in Svalbard, Norway and showed at least part of the branched GDGTs in open marine settings with low soil organic matter may be produced in situ.Despite the unavailability of the required standards to quantify branched GDGTs in this study, the chromatograms yielded values for the BIT index.

To assess in-situ production and constrain the branched GDGTs from terrestrial soil organic matter input, the calculated MAT for this region was found to vary from 0 to 14.5 °C with a non-systematic distribution across the transect (Table 5.2). Expected temperature in the region of 20°C or more is at least expected for the NW African region, but the MAT reveal values >10°C for stations 1, 7, 9, 24 and 28 north and south of the main dust corridor. The overall low MAT estimates in the surface sediments provide some evidence for in situ production of GDGTs as observed elsewhere (Peterse *et al.,* 2009; Tierney *et al.,* 2009). There is, however, no clear latitudinal temperature trend across the CHEETA transect suggesting variable mixtures of in-situ and continental GDGTs. The BIT

proxy therefore can only be used in a purely qualitative manner in this study, i.e. the BIT values cannot be directly compared to other marine settings in front of rivers, where calibration is well established (Hopmans *et al.,* 2004; Kim *et al.,* 2006, Kim *et al.,* 2007; Ménot *et al.,* 2006).

Table 5.1 MBT/CBT index showing calculated mean annual temperature (MAT) for the NW African margin

Station Numbers	MBT	cyclisation ratio	CBT	MAT
1	0.47	0.50	0.30	14
2	0.35	0.48	0.32	8
5	0.33	0.40	0.40	7
6	0.36	0.44	0.36	9
7	0.37	0.74	0.13	11
8	0.34	0.42	0.37	7
9	0.37	1.09	-0.04	13
10	0.32	0.91	0.04	9
11	0.25	0.79	0.10	6
12	0.24	1.41	-0.15	7
13	0.26	0.53	0.28	4
15	0.25	0.89	0.05	6
16	0.26	0.77	0.12	6
19	0.26	1.51	-0.18	9
21	0.26	1.62	-0.21	9
22	0.26	1.69	-0.23	9
23	0.29	1.02	-0.01	9
24	0.30	1.17	-0.07	10
25	0.14	1.24	-0.09	2
28	0.36	0.93	0.03	12

Unlike the branched GDGTs, which clearly have limitations regarding application to detecting SOM contributions to open marine sediments, soil BHPs seem more promising, at least off NW Africa. The investigation of BHP production in marine systems is currently quite limited. Although some molecular work by Blumenberg *et al* (2006) has shown that bacteria capable of BHP production are present in marine systems, few studies have linked specific BHP structures to marine sources (see Pearson *et al.,* 2009). BHP production in some species of sulphate reducing bacteria and some *planctomycetes* has

been shown but neither study demonstrated the production of adenosylhopane. Indeed, to the best of our knowledge no marine isolated bacteria have, to date, been shown to produce adenosylhopane. Therefore, lack of currently known marine source of the soil marker BHPs attributes more confidence to the proposed continental supply of adenosylhopane. This is the first observations of soil marker BHPs in this open marine setting in the NW African margin, strongly supporting its applicability in these settings and arguing for supply of organic matter derived from soils.

A recent global survey covering more than 500 samples from 34 locations, has identified a typical average value of about 28% soil-marker BHPs relative to the total BHP within soils (Cooke *et al.,* 2008a and unpublished data). Relative concentrations of soil-marker BHPs within the range of 4-6% of total BHP observed in some surface sediments off NW Africa thus appear to be depleted by a factor of 5-8 compared to the source signature, but similar to relative abundances measured in a surface sediment from off Gabon north of the Congo river (Cooke *et al.,* 2008b). This observation is interesting as it suggests that aeolian transport may be as efficient in exporting SOM as runoff from minor distributaries and/or lateral advection of SOM initially exported via large rivers. More research is necessary to establish whether this interpretation is valid.

It is also possible that the BHPs and the branched GDGTs exhibit different distributions because of their spatial or vertical provenance within soils. Previous investigations have identified the Sahara and the Sahel as the main

source area of eolian transported material over the Equatorial and subtropical North Atlantic (Schütz, 1980; Prospero, 1981; Ratmeyer *et al.,* 1999; Schefuβ *et al.,* 2003).

Although I can only speculate, it seems possible, for example, that these molecular signals originate from different depths within soils, with the BHPs originating from the upper (oxic) horizons, and the branched GDGTs derived from the lower (anoxic) part of the soil profile. Such a difference could explain the relative extent to which these biomarkers can be mobilized from soils and hence their different distribution in marine sediments. Unlike fluvial erosion which cuts through the whole soil profile eroding all layers of the column almost simultaneously, wind would preferentially erode and export the uppermost oxic soil layer, whereas deeper layers would remain undisturbed over longer time periods. Particularly intense or sustained winds or storm events may be capable of mobilizing the more deeply buried branched GDGT signal. Further studies are required to elucidate the relative propensity of soil BHP and branched GDGTs to be entrained in dust emitted from the continents.

5.7 *Conclusions*

Surface sediments collected along a transect extending from the Portuguese margin to the NW African margin (40-15°N) contain low but detectable concentrations of soil-specific biomarkers (BHPs), arguing for some supply and deposition of organic matter derived from soils. Comparable concentrations in soil-marker BHPs off NW Africa and off Gabon suggest that aeolian transport may be as efficient as some rivers in transporting SOM to the ocean but further research is required to substantiate this conclusion. The depth habitat of microbes producing the target marker compounds within the soil column may determine the signal eroded and exported to the ocean. Specifically, deeper anoxic layers where branched GDGTs are produced may be more protected against wind erosion and thus generate a weaker molecular signature in marine sediments compared to the soil-marker BHPs, which may originate from shallow (oxic) soil layers. Further studies of soil marker distributions in both marine and continental environments are required to verify and quantify the proposed relationships.

6 Chapter Six

6.1 *The last glacial to Holocene climate transition (~35 kyrs)*

One of the major goals of the CHEETA program is to utilize multiple proxies, including elemental data and the abundance and isotopic composition of bulk organic matter and higher plant leafwax alkanes, to constrain regional variations in continental climate and terrigenous supply across the deglacial-Holocene time period. The meridional array of gravity cores recovered at 28 stations along a transect from 40°N-15°N paralleling the continental slope cover different climate and vegetation zones in the SW Mediterranean and NW Africa.

Here, terrigenous signals are transmitted to the adjacent continental margin, providing a rare opportunity to assess the sensitivity of these different proxies to continental supply, climate, and vegetation during past glacial-interglacial climate conditions. A particular objective of this study is to identify the timing and regional extent of the AHP, a period of enhanced monsoonal activity over NW Africa between about 9-6 ka.

6.1.1 *Key objectives:*

1. To develop an integrated chronological framework from measured AMS radiocarbon dating (kindly provided by Prof. Peter DeMenocal from the Lamont-Doherty Earth Observatory of Columbia University as part of a larger research collaboration between Newcastle, Lamont Doherty and EHT-Zurich) and high resolution $\delta^{13}C_{org}$ records to enable accurate correlation of cores and discussion of climate variabilty along the transect since the last glacial (35 ka).

2. To generate bulk organic geochemical and isotopic time series, including: linear sedimentation rates (LSR); bulk accumulation rates (BAR) and TOC accumulation rates (ARTOC); Total organic carbon content (TOC) and carbon isotopic records $\delta^{13}C_{org}$ to explore principle trends in organic carbon supply and preservation.
3. As a pilot, to test the application of organic biomarkers and their stable carbon isotopic signatures in the relatively TOC poor sediments from the CHEETA transect as proxies for terrestrial supply using odd numbered long chain *n*-alkanes concentrations,distributions (ACL, CPI and A.I) and $\delta^{13}C$ values.

6.2 *Location of site and sample strategy*

In July, 2007 a sampling cruise aboard R/V Oceanus (OC 437-7) was conducted off the Portuguese and NW African margins. The CHEETA project coring strategy targets areas with high sediment accumulation rates, as known from the literature (inserts in Fig. 6.1), to produce high resolution proxy information on a decadal scale resolution in order to reconstruct paleoclimate parameters. The coring strategy consists of a North-south coring transect along the NW African continental margin (30-4°N) and one equatorial east-west coring transect which targets the eastern tropical Atlantic sites off the Central African continental margin and where two main rivers (Niger and Congo) are located.

The core sites within the north-south coring transect (Sites A-G) have shown high rates of deposition that exceed 20cm/ka due to the influences of coastal upwelling and African dust deposition. Although previous studies had identified individual cores along this transect with high accumulation rates, the CHEETA project is the first time a transect study has been carried out all the way along the Portuguese-NW African margin to constrain regional climate variability, terrestrial vegetation and changes in sediment accumulation.

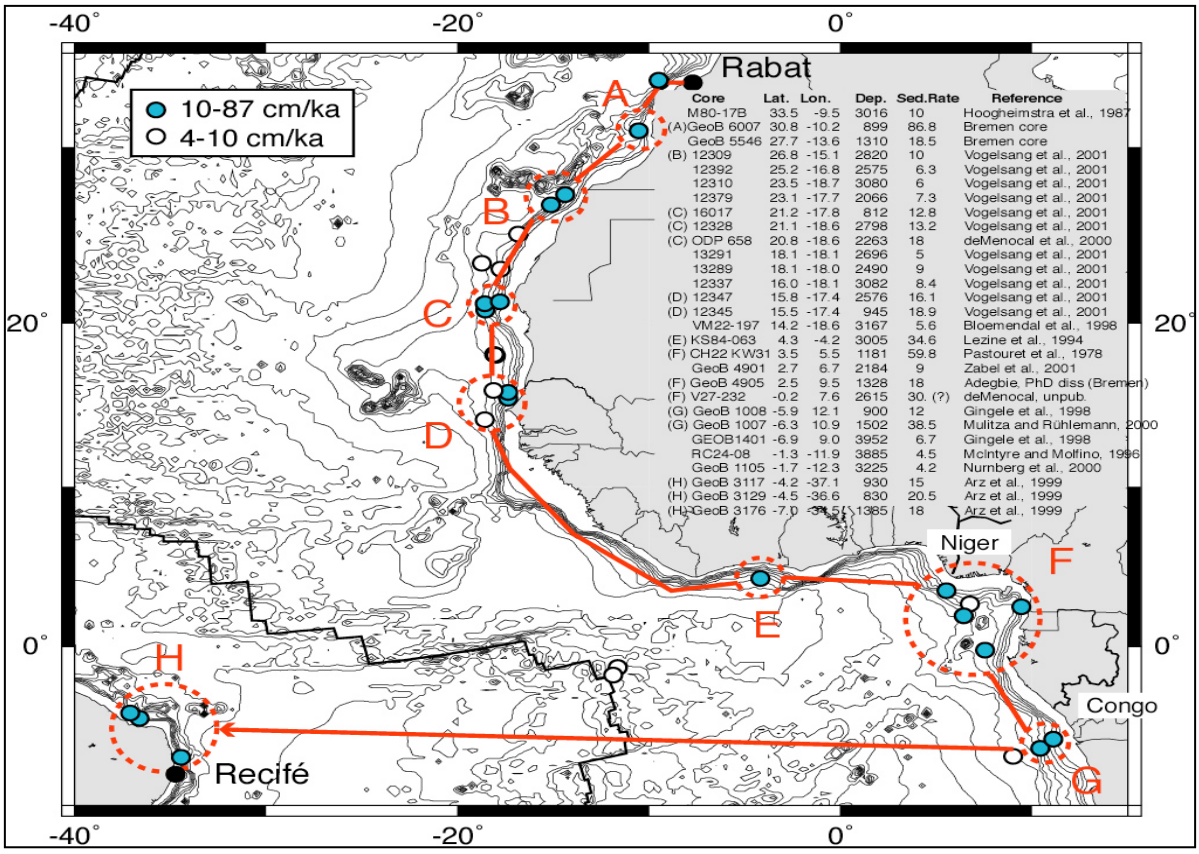

Figure 6.1 Map of the larger CHEETA project showing the cruise transects and proposed coring locations consisting of two transects A-E and F-H. Literature inserts; represent previously identified sites of high accumulation rates.

As part of the CHEETA project, this study presents the first complementary and high resolution bulk geochemistry sediment records from 16 gravity cores (GC) (out of 28 stations in total) recovered along the NW African transect from 40°N-15°N paralleling the continental slope (Fig 6.2). Station list, depth and stratigraphic data for the North West African transect are in Appendix. B and C

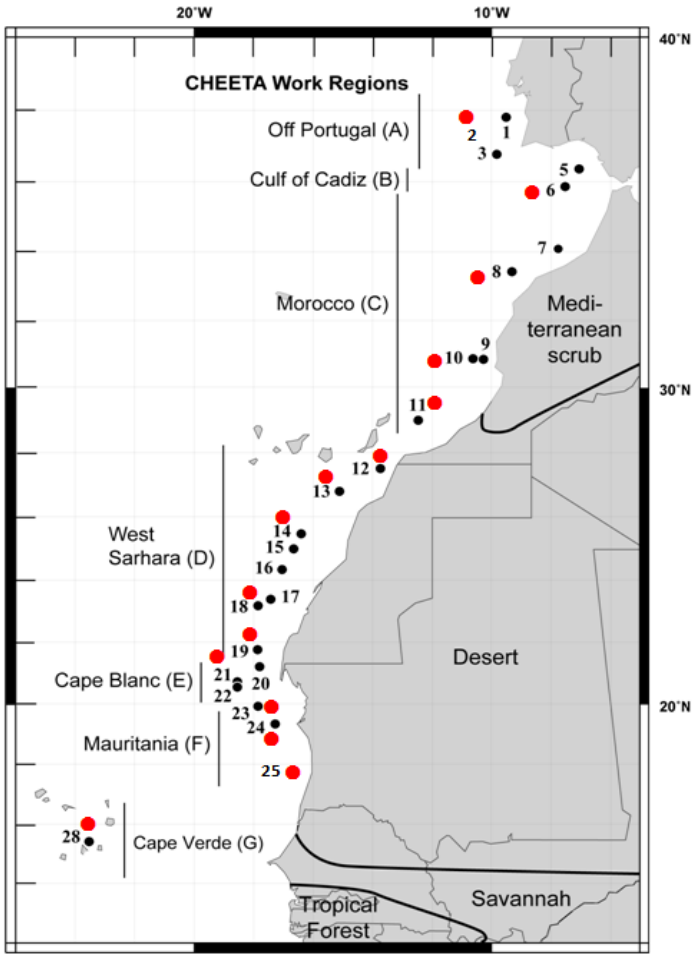

Figure 6.2 CHEETA work regions (A-G) including gravity cores for this study (red dots) and vegetation zones (annotated) from the tropical to Medditerenean region 40-15°. Station list corresponding to regions and respective cores are listed in Appendix B.

6.3 *Chronological framework for the NW African transect*

Radiocarbon dating (^{14}C) of picked monospecific samples of the planktonic foraminifer *Globigerinoides bulloides for* the 13 cores out of the 16 available cores were determined by accelerator mass spectrometer (AMS) (de Menocal *et al.,* in prep). For the remaining cores and depth intervals for which ^{14}C AMS is still pending a preliminary working age model is established to assign ages and to build a consistent chronological framework as described below.

GC 49 was used as a reference core because, at the time of writing this thesis, it had the most ^{14}C AMS dates of all CHEETA cores and showed distinct patterns in both TOC and $\delta^{13}C_{org}$, defining additional tie points for correlation (Fig 6.3). First, linear sedimentation rates (LSR cm/ka) and corresponding ages were calculated between ^{14}C AMS age tie points (Table 6.1). Below the oldest AMS age in GC 49 (17.64 ka), it is assumed that LSR remains constant at 9.65 cm/ka to the base of the core. It is clear that this is a simplification but the age control will be improved as more ^{14}C AMS dates for this core become available. In a second step, distinct turning points in the $\delta^{13}C_{org}$ profile of GC 49 were identified and corresponding ages defined as additional age tie points for correlation of $\delta^{13}C_{org}$ profiles from the other cores (Fig 6.3; Table 6.2). ^{14}C AMS data were always prioritized in all cores and $\delta^{13}C_{org}$ tie points only used where no other startigraphic information was available. At the time of writing this thesis 63 ^{14}C AMS ages for 13 cores plus $\delta^{13}C_{org}$ tiepoints was available to develop the integrated age working model.

Table 6.1 Depth profile records for GC 49 showing corrected ^{14}C age in Ka (DeMenocal et al. in prep) and $\delta^{13}C_{org}$ tie points and calculated individual ages from LSR (cm/ka) used as a reference and for correlation for the working age model.

Core	Top	Bottom	^{14}C age tiepoints (Ka)	δ^{13}Corg tiepoints (Ka)
GC-49	4.5	5.5	1.42	
GC-49	20.0	21.0	4.52	
GC-49	30.0	31.0	6.28	
GC-49	40.0	41.0	8.35	
GC-49	54.5	55.5	9.99	
GC-49	64.5	65.5		10.57
GC-49	86.0	87.0	11.84	
GC-49	104.5	105.5		13.75
GC-49	140.0	145.0	17.64	
GC-49	204.5	205.5		24.12
GC-49	284.5	285.5		32.41
GC-49	314.5	315.5		35.52

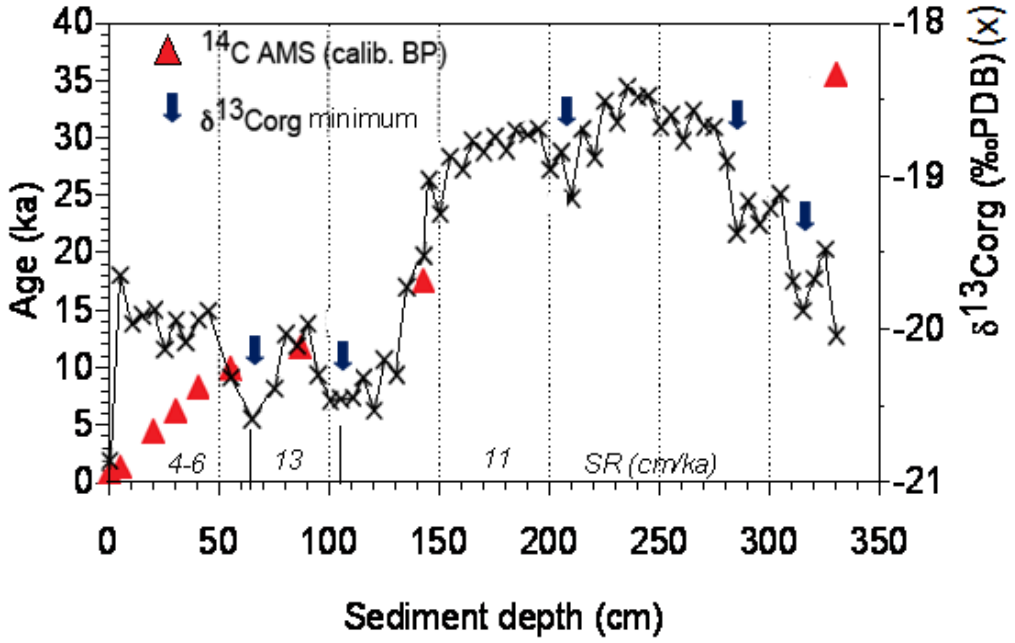

Figure 6.3 The chronological framework of reference core GC 49 is based on radiocarbon (14C) AMS datings of Globigerinoides bulloides (red triangles, calibrated ages in BP, DeMenocal et al, in prep) and additional tiepoints marking δ13Corg minima (black triangles). $\delta^{13}C_{org}$ tiepoints were used for correlation with the other cores where no ^{14}C AMS data were available.

In a second step all other cores for which $\delta^{13}C_{org}$ and or ^{14}C AMS data are available were correlated with reference to core GC 49. All age /depth relationships and data for this corelation are detailed in Table 6.2. Despite uncertainties, this initial correlation provides a first robust framework to identify and discuss changes in environmental conditions along the transect.

Table 6.2 Age/Depth assignment for all cores from the NW African margin

Core	Top(cm)	Bottom(cm)	^{14}C Age tiepoints(Ka)	$\delta^{13}C_{org}$ tiepoints(Ka)	LSR (cm/Ka)
GC-05	10	11		2.00	16.34
GC-05	150	151		10.57	20.00
GC-05	210	211		13.57	9.46
GC-05	300	301		23.08	9.46
GC-13	30	31		10.57	13.33
GC-13	70	71		13.57	12.62
GC-13	190	191		23.08	12.62
GC-13	270	271		31.38	12.62
GC-17	130	131	6.83		27.94
GC-17	235	236		10.57	27.94
GC-27	0	1	0.49		3.08
GC-27	5	6	1.79		5.89
GC-27	60	61	11.30		9.14
GC-27	90	91	14.80		9.14
GC-29	165	166		6.52	35.40
GC-32	80	81	6.71		4.37
GC-32	110	111		13.57	31.49
GC-32	190	191		23.08	41.02
GC-32	270	271		31.38	41.02
GC-37	4	5	1.91		5.36
GC-37	14	15	4.10		4.57
GC-37	18	19	4.98		5.88
GC-37	46	47	9.74		7.63
GC-37	80	81	14.46		11.37
GC-37	180	181		23.08	7.23
GC-37	240	241		31.38	16.13
GC-37	290	291		34.48	16.13
GC-40	4	5	3.48		2.71
GC-40	24	25	9.76		-3.09
GC-40	30	31	7.82		5.54
GC-40	90	91	18.66		5.54
GC-49	5	6	1.42		4.99
GC-49	20	21	4.52		5.70

GC-49	30	31	6.28		4.82
GC-49	40	41	8.35		8.87
GC-49	55	56	9.99		17.03
GC-49	65	66		10.57	17.03
GC-49	86	87	11.84		9.65
GC-49	105	106		13.75	9.65
GC-49	140	145	17.64		9.65
GC-49	205	206		24.12	9.65
GC-49	285	286		32.41	9.65
GC-53	0	1	2.17		5.39
GC-53	21	22	6.26		21.67
GC-53	44	45	7.27		12.87
GC-53	70	71	9.29		6.20
GC-53	110	111	15.74		30.25
GC-53	200	201	18.72		11.10
GC-53	260	261		24.12	11.10
GC-59	4	5	1.23		6.28
GC-59	30	31	5.37		10.68
GC-59	40	41	7.06		10.39
GC-59	60	61	8.21		17.04
GC-59	150	151		13.73	9.08
GC-59	180	181	16.59		12.33
GC-59	260	261		23.08	7.95
GC-59	330	331	31.88		7.95
GC-66	0	1	1.57		2.57
GC-66	10	11	4.69		2.57
GC-66	90	91	6.26		38.26
GC-66	100	101	6.99		11.03
GC-66	130	131	8.95		17.30
GC-66	250	251	11.80		42.11
GC-68	4	5	2.67		6.93
GC-68	18	19	4.69		7.37
GC-68	40	41	7.67		23.66
GC-68	62	63	8.60		7.53
GC-68	90	91	12.32		16.17
GC-68	120	121	12.47		16.17
GC-68	150	151	16.03		16.17
GC-70	11	12	0.94		20.47
GC-70	55	56	3.09		15.38
GC-70	96	97	5.82		7.51
GC-70	110	111	7.68		24.21
GC-70	176	177	10.41		27.84
GC-70	310	311	15.22		27.84
GC-80	10	11	1.25		14.81
GC-80	140	141	10.03		14.81

6.4 ***Results***

This section presents the high resolution geochemical results from the selection of cores available for this thesis. All raw data from the CHEETA cores are presented in Appendix D. From the 28 cores recovered from the CHEETA cruise, 16 were available for bulk organic carbon records including carbon isotopic records ($\delta^{13}C_{org}$), TOC and carbonates and organic carbon content (TOC_{cf}). Of these, 11 cores had dry bulk densities (DBD) (DeMenocal et al., in prep) that were used to calculate Bulk and TOC Accumulation rates. As a pilot study, preliminary molecular records (leaf wax content and their distribution proxies) are tested from 3 cores (GC 17, 27 and 49) as well as preliminary compound specific stable carbon isotopic data for GC 49.

6.4.1 *Dry Bulk densities*

This chapter presents results from the NW African cores for which Dry Bulk densities (DBD) (g/cm^3) data were kindly provided by Professor P. DeMenocal, Lamont–Doherty Earth Observatory, Columbia University. The dry bulk density of sediments from the North West African transect vary from 0.3 to 1.3g/cm^3, as presented in Fig 6.4. DBD in sediments from GC 05 to GC 13 in the north remain relatively constant at 1g/cm^3 to the base of the core. Towards the south, in sediments from GC 32 to GC 49, slight variations from ~0.5-1g/cm^3 are observed with minimum values of 0.4 g/cm^3 recorded in GC 49 in the glacial part of the core. Further south of the transect, from GC 53, DBD shows a generally decreasing trend from the glacial to towards the Holocene.

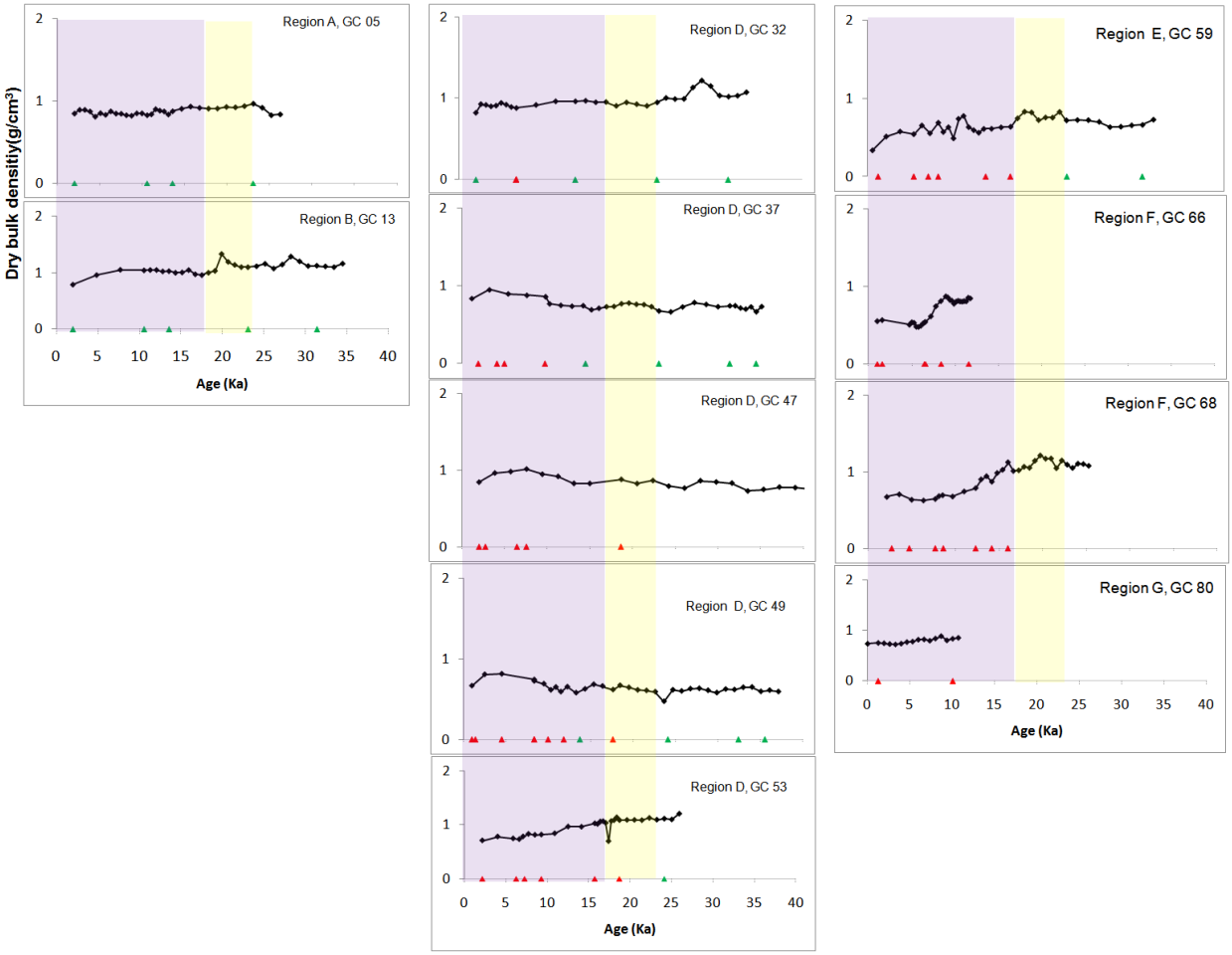

Figure 6.4 Dry bulk density data (gcm^3) from the CHEETA cores separated by Regions. In the North, Regions, A, Portuguese margin; B, Gulf of Cadiz; C, Morrocco margin; In the South regions, D, West Sahara; E, Cape Blanc; F, Mauritania; G, Cape Verde. Red triangles, ^{14}CAMS tie points, green triangles, $^{13}C_{org}$ tie points; yellow band, LGM, purple band, Holocene.

6.4.2 *LSR and Bulk Accumulation Rates*

Based on the first integrated chronological framework, linear sedimentation rates (LSR) (Table 6.2) range from ~42cm/ka in the south at GC 32 to ~3.5cm/ka at GC 13. Maximum LSR are reported for the glacial sections in the cores studied. Two maxima in accumulation rates with different regional expressions and variations are evident from the CHEETA cores (Fig 6.5). During glacial periods, pronounced BAR maxima of up to 40 g/cm^2ka^{-1} are recorded in the south of the transect, in cores GC 32, 53, and 66. In the Holocene sections, BARs of about 20 g/cm^2ka^{-1} are reported at GC 05 and 13 in the North as well as GC 53, 66 and 68 in the south. Elevated BARs approaching 20 g/cm^2ka^{-1} at GC 40; 49; 53; 59; 68 are also prominent between 15-5ka covering the AHP, with a period of lower BARs centered at around 10ka.

6.4.3 *Organic Carbon Records –TOC; TOCcf and TOCAR*

Total organic carbon content (TOC) is presented for 15 cores while TOC on a carbonate free basis (TOCcf) and the corresponding accumulation rates (TOCAR) are only presented for 11 cores for which DBD data were available.

The TOC records are presented in Fig 6.6. The values vary from 0.1 to 3% with a clear maximum occurring in the south at GC 49. Elevated glacial TOC levels > 1% with high amplitude cyclic variations are observed in the south at GC 32; 37; 40 49; 59 and 68 which tend to decrease towards the Holocene. In contrast, in the north at GC05; GC13; GC17 and GC27 TOC values remain relatively stable during the Holocene and glacial periods around ~1% or below. Two pronounced peaks in TOC are recognized at GC 29 in the Holocene section, between 6 and

4 ka, suggesting a direct response to the AHP. Although generally decreasing trends in TOC are observed in the cores from the south, they also show high amplitude cyclic patterns that may be related to changes in productivity during the glacial in the south and Holocene in the north. These potentially productivity-driven TOC cycles are evident between 15-10 ka and 10-5 ka, and become more prominent at GC 49, GC53, GC59 but with varying responses at GC37 and GC66.

The TOC_{cf} records for CHEETA cores vary from 0.5 to 5 % (Fig 6.7). These records show similarities to the TOC content suggesting minor influence for carbonate dissolution. Accordingly, TOCcf are higher with cyclic patterns evident during glacial periods from the south of the transect from GC 32; 37 40 and 49, with a clear maximum in the records at GC 49. Other cores in the south, GC 53-80, show contrasting patterns with lower values recorded during the glacial and higher records during the Holocene instead. In particular, sediments from GC 53 show a strong response to the AHP. In the northern part of the transect, TOC_{cf} values of about 1% occur\ during the Holocene at GC 05 and below that at GC 13. These overall observations in TOCcf clearly separate the north from the south of the transect albeit with regional influences and varying responses of organic carbon burial and productivity to the changing climatic conditions in this study.

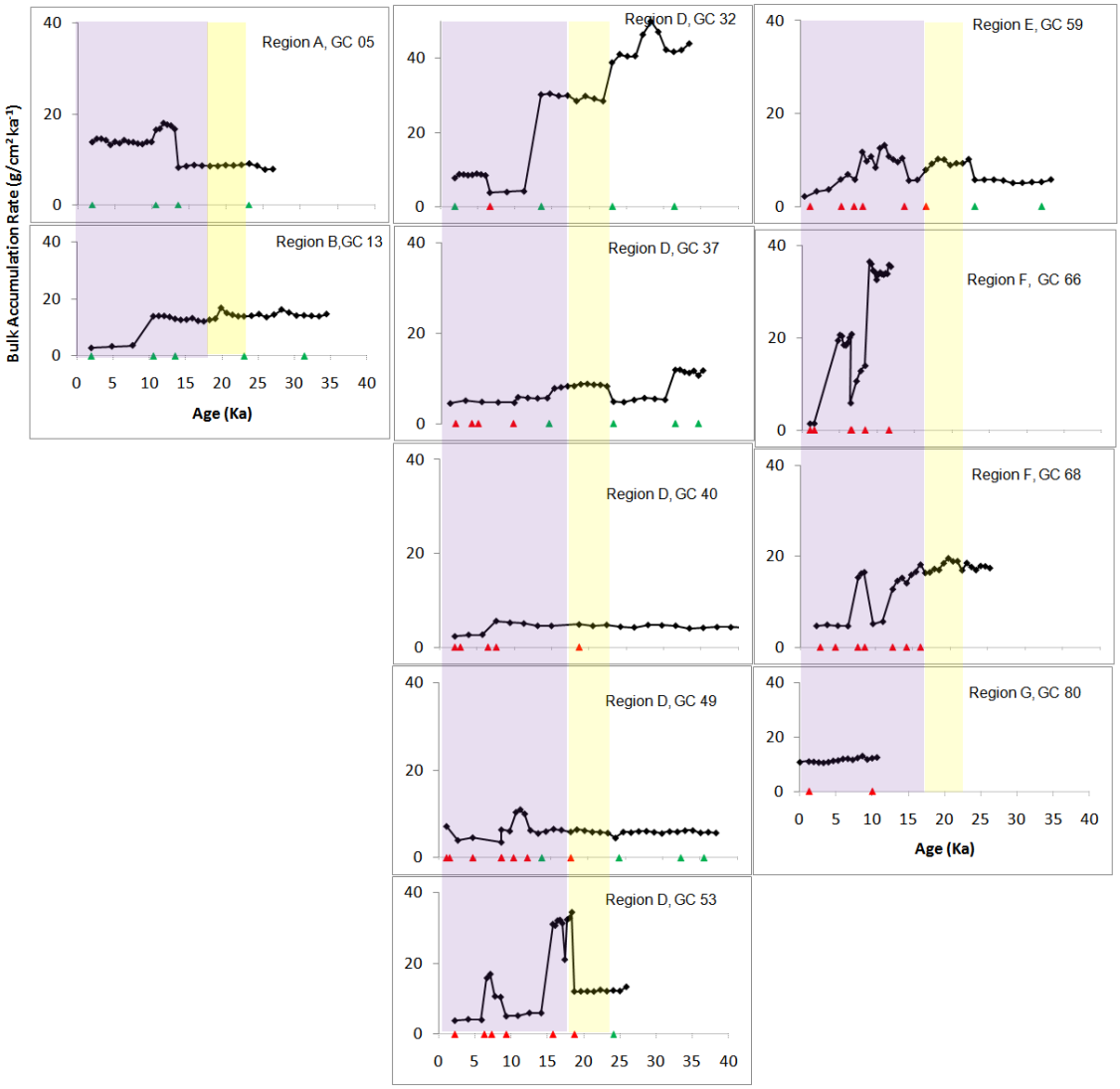

Figure 6.5 Bulk accumulation rates (g/cm^2 ka^{-1}). from the CHEETA cores separated by Regions. In the North, Regions, A, Portuguese margin; B, Gulf of Cadiz; C, Morrocco margin; In the South regions, D, West Sahara; E, Cape Blanc; F, Mauritania; G, Cape Verde. Red triangles, ^{14}CAMS tie points, green triangles, $^{13}C_{org}$ tie points; yellow band, LGM, purple band, Holocene.

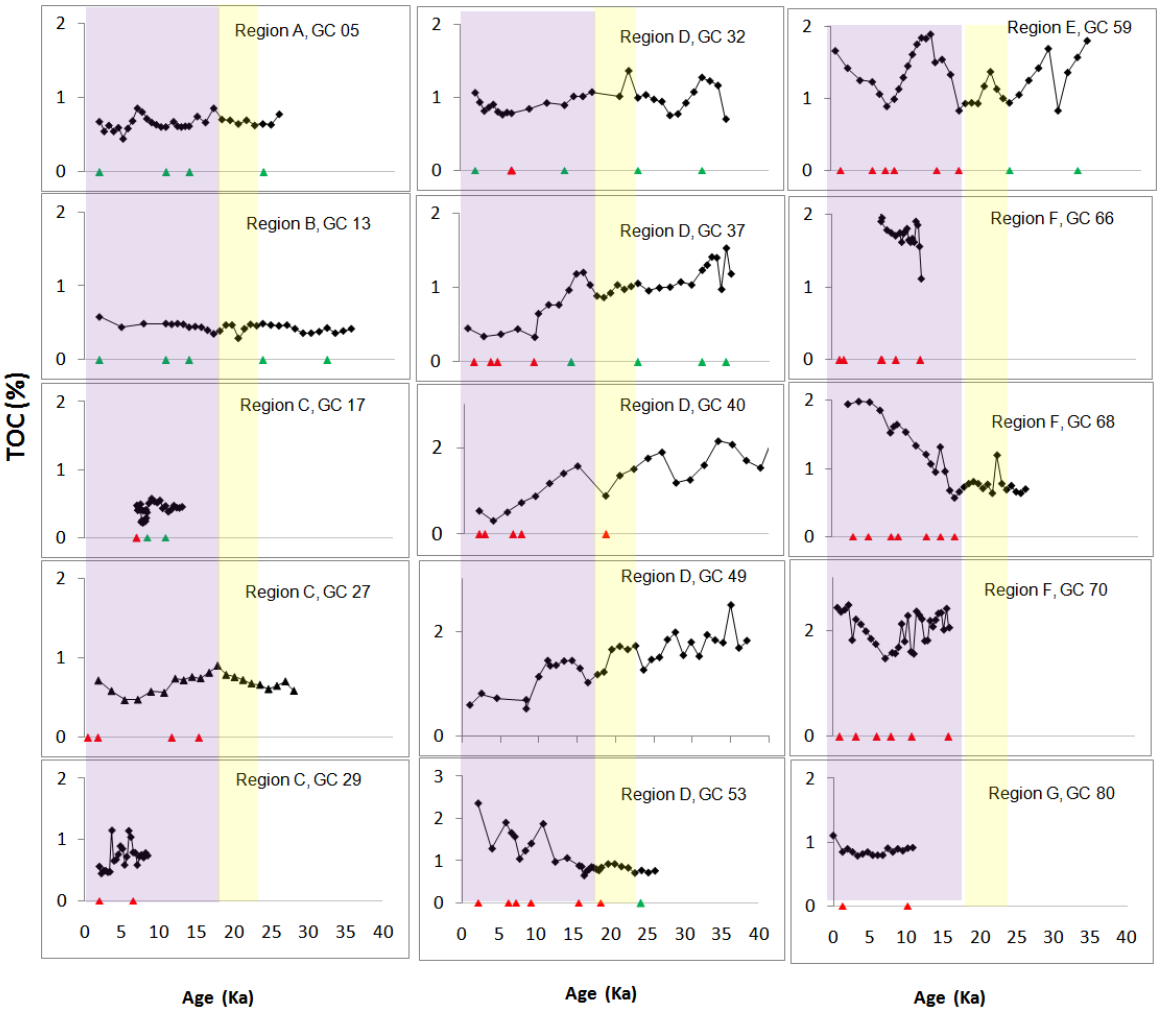

Figure 6.6 TOC records from the CHEETA cores separated by Regions. In the North, Regions, A, Portuguese margin; B, Gulf of Cadiz; C, Morrocco margin; In the South regions, D, West Sahara; E, Cape Blanc; F, Mauritania; G, Cape Verde. Red triangles, ^{14}CAMS tie points, green triangles, $^{13}C_{org}$ tie points; yellow band, LGM, purple band, Holocene

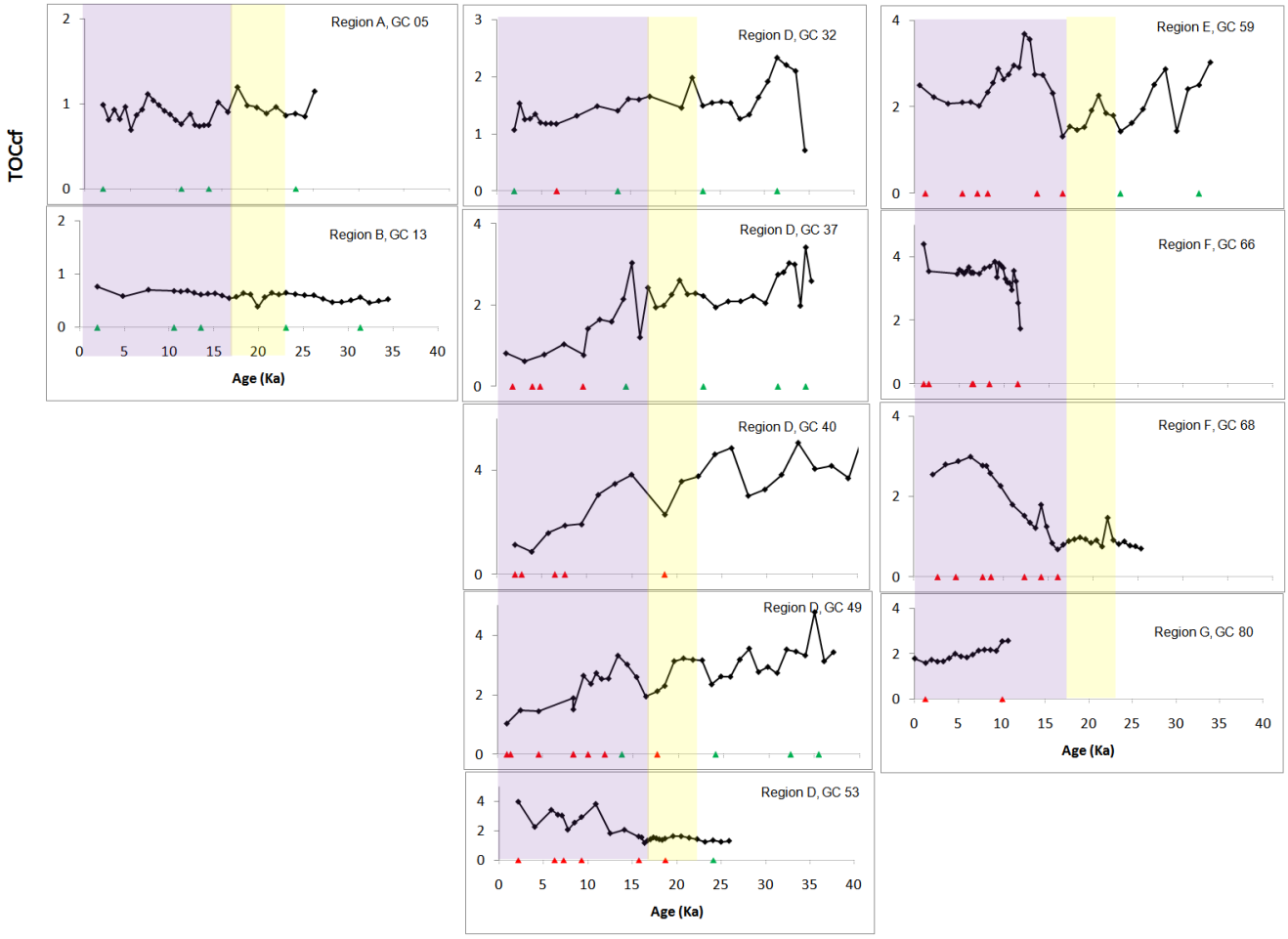

Figure 6.7 TOCcf from the CHEETA cores separated by Regions. In the North, Regions, A, Portuguese margin; B, Gulf of Cadiz; C, Morrocco margin; In the South regions, D, West Sahara; E, Cape Blanc; F, Mauritania; G, Cape Verde. Red triangles, ^{14}CAMS tie points, green triangles, $^{13}C_{org}$ tie points; yellow band, LGM, purple band, Holocene.

6.4.4 *Accumulation rates of organic carbon (TOC AR)*

The organic carbon AR records (Fig 6.8) show closely related patterns to the Bulk AR, with TOC AR varying from close to 0 to 0.8 g/cm^2/ka. In the Holocene parts of the records, two distinct peaks of elevated TOC AR indicate enhanced organic carbon burial between 15-10Ka and 10-5Ka, the AHP, although this response differs considerably spatially and temporally across the transect.

During glacial periods, TOC AR is low and stable in the north at GC 05 and 13 with a minimum during the LGM at GC 13. In constrast, variable patterns in TOC AR on millennial scales occur in the south at GC32, GC37; GC40; and GC49 where they tend to decrease gradually into the Holocene apart from GC 49, where elevated levels persist into the Holocene. Further, contrasting patterns emerge in sediments from the other cores in the south. GC 53 shows minimum TOC AR in the glacial between 30-20 ka; two maxima peaks covering the LGM and deglacial periods between 18 ka and 16 ka. From here, a decrease for about 5 ka occurs which then increases to a maximum between 10-5 ka. At GC 59 and 68, in the south, lower values with cyclic patterns in the glacial tend to increase towards the Holocene reaching maximum values at GC 59 between 15 and 10 ka and between 10-5ka at GC 68. The nature of these variations in marine productivity and upwelling depending in response to the evolving climatic conditions along NW Africa.

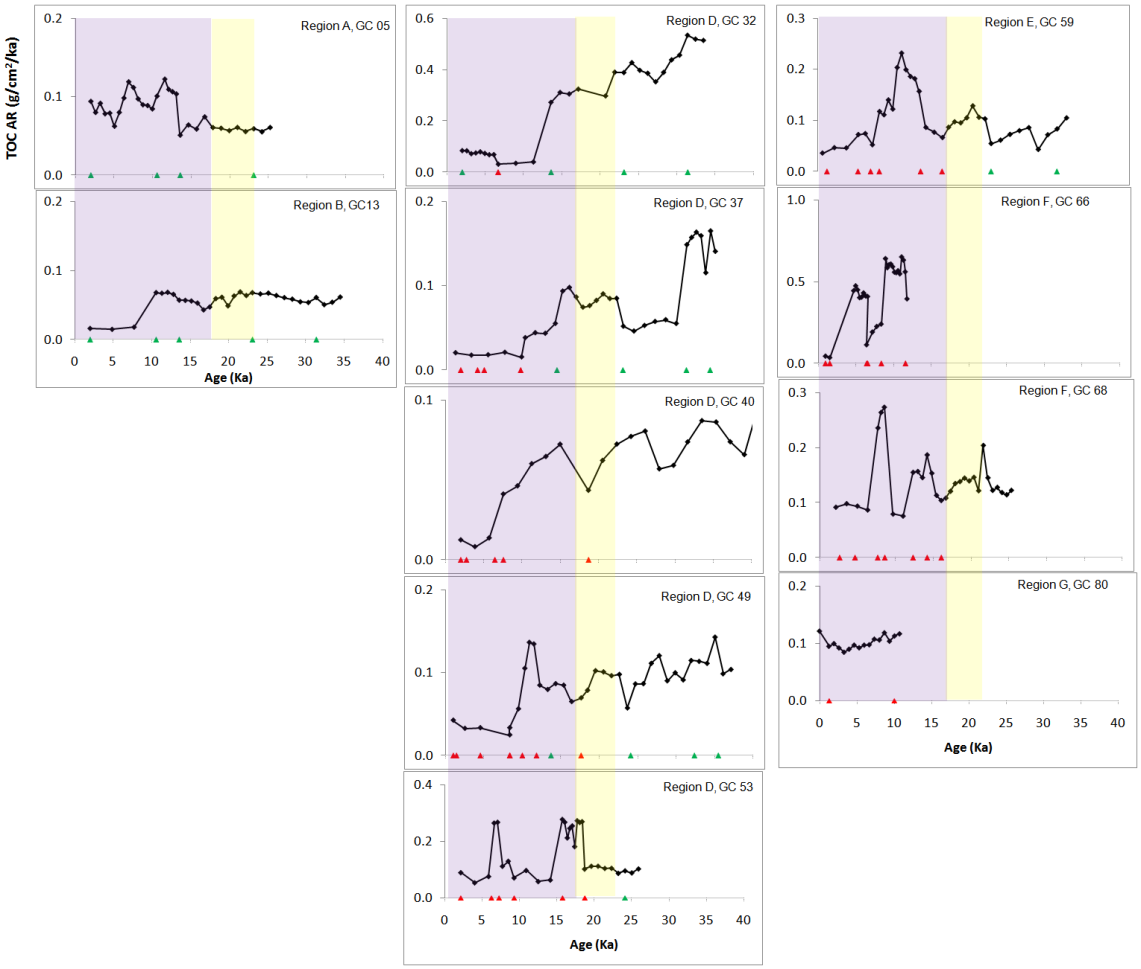

Figure 6.8 TOC accumulation rates (g/cm^2/ka) from the CHEETA cores separated by Regions. In the North, Regions, A, Portuguese margin; B, Gulf of Cadiz; C, Morrocco margin; In the South regions, D, West Sahara; E, Cape Blanc; F, Mauritania; G, Cape Verde. Red triangles, ^{14}CAMS tie points, green triangles, $^{13}C_{org}$ tie points; yellow band, LGM, purple band, Holocene.

6.5 *Organic matter composition and $\delta^{13}C_{org}$ values*

The $\delta^{13}C_{org}$ records for sediments from the CHEETA transect are presented in figure 6.9. Overall, $\delta^{13}C_{org}$ values range from -18 to -24 ‰ for the last 35 kyr.

In the north, sediments from GC 05 to 29 show isotope values that range from -20 to -24‰ typical of a mixture of marine organic matter (MOM) and C_3 type vegetation. In the south, organic matter is less depleted with $\delta^{13}C_{org}$ values ranging from -18 to -20.5‰ reflecting typical marine isotope signatures possibly with minor admixture of organic matter from C_4 type vegetation.

Distinct variations pronounced in the glacial sections between 30-25ka and 20-15ka, similar to patterns observed from the TOC records are observed in sediments from GC 32 to 59. These variations, however, differ significantly on a temporal and spatial scale. Sediments from GC 37, GC 69 and GC 49 show large isotope shifts of 1.2 to 1.5‰ between 22-18 ka and 18-15 ka, respectively. Further south, sediments from GC 66-80 also show minimal variations of up to 1‰, prominent in GC 66 and GC70. Half the variation in the adjacent cores of up to 0.5 ‰, however, occurs at GC 80. This observation suggest that the admixture of organic matter from C_4 type vegetation increases further south of the transect.

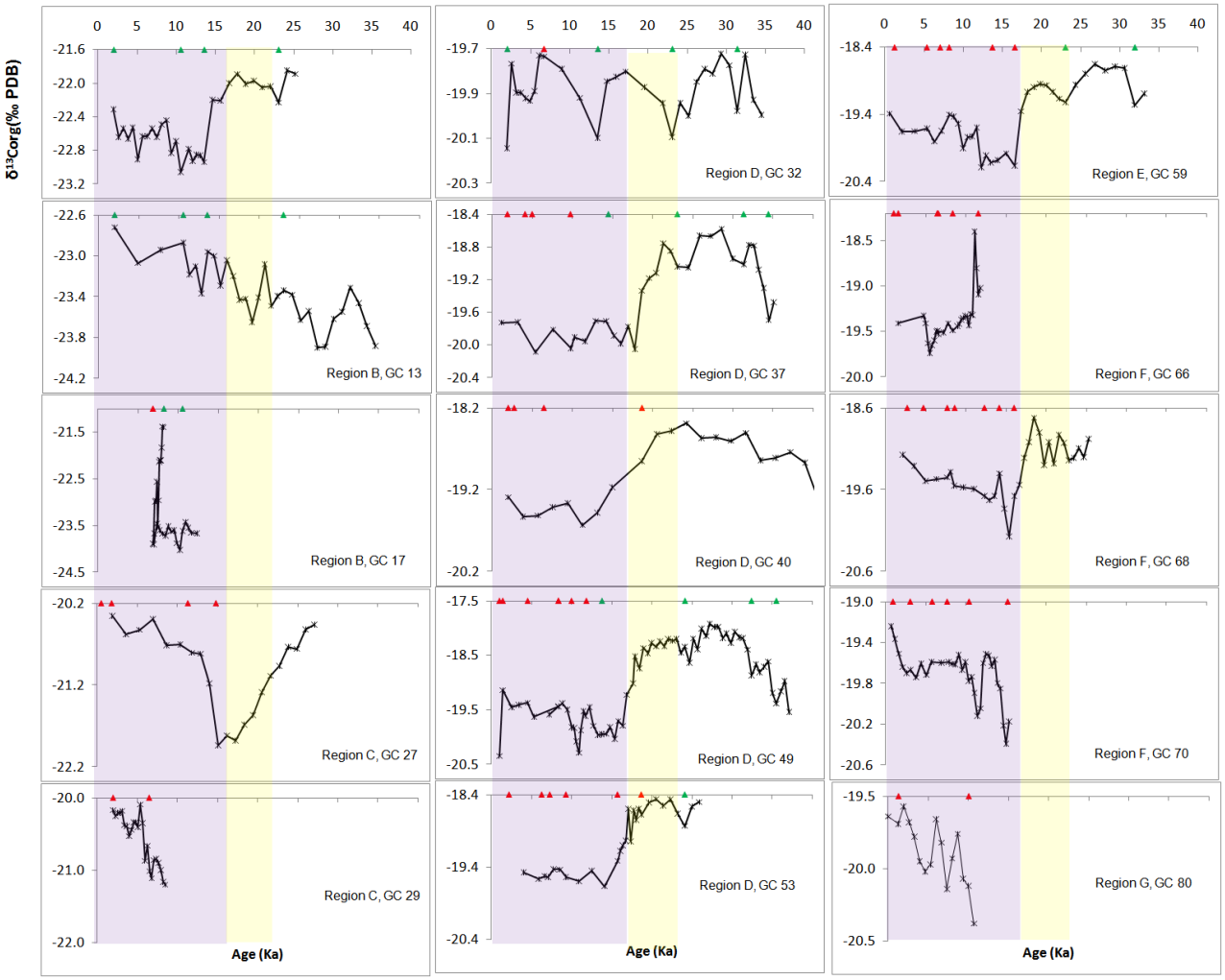

Figure 6.9 The $\delta^{13}C_{org}$ values from the CHEETA transect, separated by Regions. In the North, Regions, A, Portuguese margin; B, Gulf of Cadiz; C, Morrocco margin; In the South regions, D, West Sahara; E, Cape Blanc; F, Mauritania; G, Cape Verde. Red triangles, ^{14}CAMS tie points, green triangles, $^{13}C_{org}$ tie points; yellow band, LGM, purple band, Holocene

6.5.1 *Molecular records*

To further investigate the factors responsible for the variations in organic carbon burial and supply, biomarker distributuions were used.to examine of sedimentary organic matter. At the time of writing this thesis, preliminary biomarker data from GC 17, 27, 49 were available and the results are presented here. The cores were selected because they were the only available after specific resampling for molecular work in December 2008. In this regard, this thesis recognises that this is the initial step in gathering molecular data for the CHEETA transect and that future work is necessary to take the initial observations from this thesis forward. Despite limited molecular data, the first results from GC 49 at least offer preliminary insight into the type plant material (C_3 and $C_{4)}$ plants preserved in the sediments. Analytical methods for determination of these proxies have been detailed in the Methods chapter (Chapter 3).

6.5.1.1 *Long chain n-alkanes and $\delta^{13}C$*

Representative GC chromatograms for sediments from GC 49 (Fig 6.10) show typical higher molecular weight long chain *n*-alkanes with a predominance of odd over even carbon predominance of $C_{27\ to}\ C_{33}$, indicative of epicuticular leaf waxes from vascular plants (Eglinton and Hamilton, 1967).

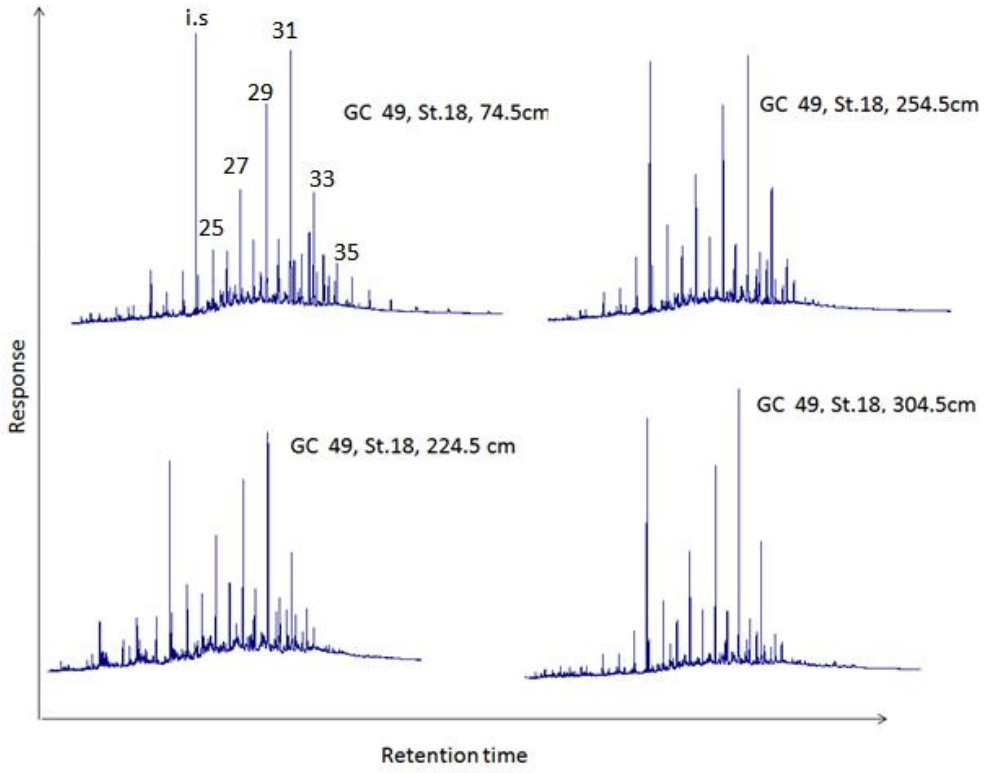

Figure 6.10 Representative gas chromatograms from the aliphatic fraction of marine sediments from GC 49 in the North West African margin showing leaf wax lipids as predominant in the extracts ($nC_{27\text{-}33}$) Individual depths for the extracts are annotated. Whole numbers represent long chain n-alkane carbon numbers and the patterns of odd over even carbon numbers are the same for each chromatogram.

6.5.2 *Concentrations of the n-alkanes*

The leaf wax lipid concentrations are shown in Fig 6.11. They range from 2 to 7 µg/TOC in GC 27 and GC 49, and from 4 to 12µg/TOC in the GC 17. Different scales have been used to present the results for easier correlation with each core and corresponding distribution proxies. Higher leaf wax lipid concentrations of ~7µg/TOC are observed in the glacial sediments from GC 27 in the north which tends to decrease towards the Holocene. In the south, at GC 49, concentrations remain at 6µg/TOC over the profile studied; with about half the supply before 30Ka and during two short periods during the deglacial centered around 19 and 16 ka. The *n*-alkane distribution proxies (Fig 6.11) generally correspond with the *n*–alkane concentration records. Overall, CPI values range from about 1 to 4 with maximum values recorded in the south at GC 49 during glacial times and minimum values recorded in GC 17 and 27 in the north during the Holocene.

ACL and A.I. values correspond closely with the patterns in CPI recording differences in vegetation sources. ACL varies between the cores studied, with values around ~23 at GC 17 and significantly longer chain lengths, between 28-30, calculated for GC 27 in the north and GC 49 in the south. A.I above 0.5 has been associated with vegetation from grasses and savannahs. The results show that GC 49 received stronger input from grass vegetation while sediments in the North carry stronger signatures typical for Mediterreanean shrubs and forests.

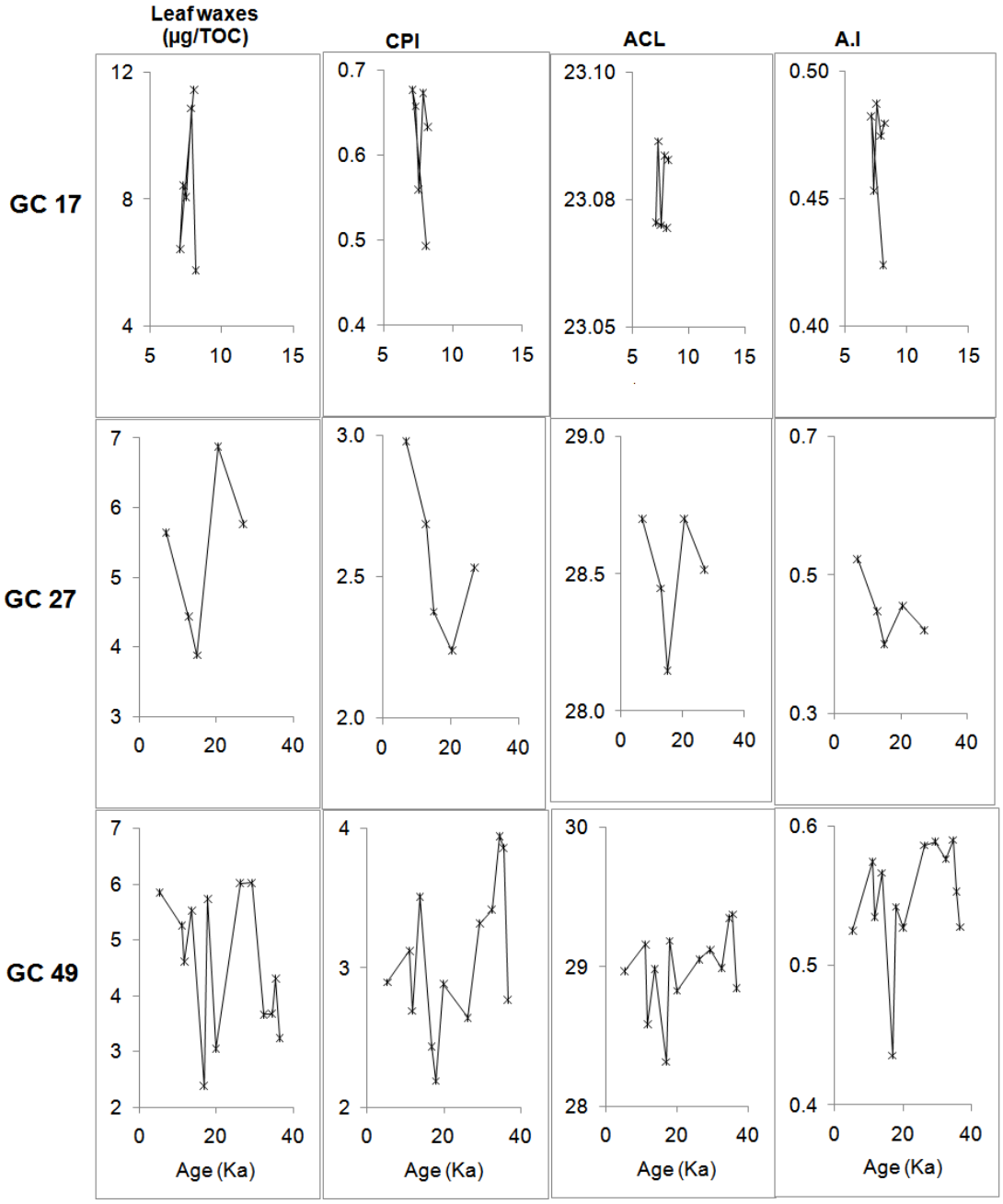

Figure 6.11 Pilot molecular data for the studied CHEETA cores showing concentration of leaf waxes lipids (n-C_{27-33}) CPI; ACL and A.I Note different scales used.

6.5.2.1 *$\delta^{13}C$ of n -alkanes*

The preliminary compound specific results for GC 49 are shown in Fig 6.12. The $\delta^{13}C$ record for *n*-alkanes from GC 49 range from -25 to -28‰ and indicates a ~3‰ negative shift between 12-14 ka. These initial results however require confirmation and closer spacing of the isotope record to support the observed initial trends.

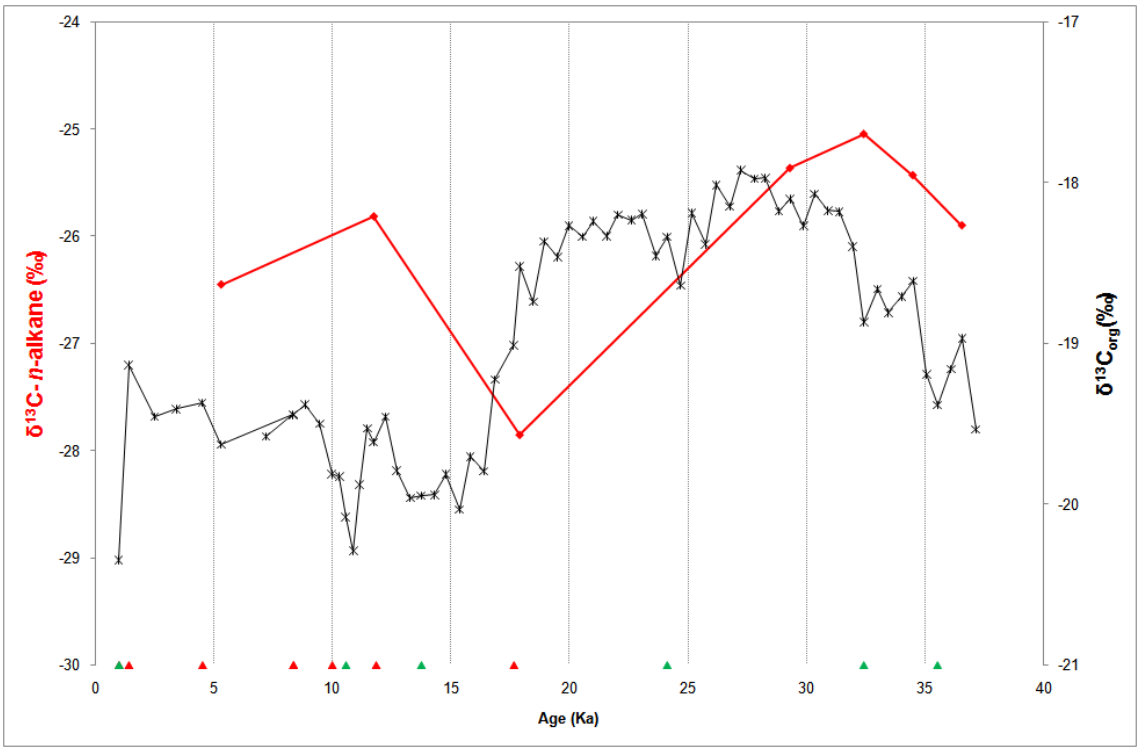

Figure 6.12 compound specific carbon isotopic records ($\delta^{13}C$) of the weighted mean average of n alknes C_{29} and C_{31} from GC 49 in the NW African margin compared with δ^{13} C_{org} as a reference.

6.6 ***Discussion***

The records from the CHEETA cores along the NW African margin between 40-15°N suggest strong regional and temporal variations in organic matter supply and burial related to millennial and longer time scale fluctuations in marine upwelling and associated productivity and African climate.

6.6.1 *Upwelling and marine productivity*

The higher linear sedimenation rates, TOC contents and AR during glacial periods, observed in most records along the transect, argue for enhanced dust input and stimulated marine primary productivity linked to upwelling, and good organic carbon preservation most strongly developed along the West Sahara margin. The TOCcf records suggest no significant dilution effect of the original organic signal by carbonate components. High TOC concentrations (Fig 6.6) are often interpreted as an indicator for enhanced upwelling and primary producitivity (Muller and Suess, 1979). It has been suggested that stronger trade wind intensity over NW Africa was responsible for elevated upwelling intensity during colder and drier conditions including the LGM (Sarnthein *et al.,* 1982; Hooghiemstra *et al.,* 1987; Romero *et al.,* 2008).

Interestingly, large variations of the TOCAR during the Holocene, between 15-5 Ka also identify a period of increased organic carbon burial across large parts of the transect, particularly the along the W Sahara and the Mauritania margin, suggesting at least a close response of organic carbon supply and burial to the AHP. This implies that more humid conditions and consequently increased precipitation did have similar effects on organic carbon burial as compared to

past arid conditions. This response to humid conditions became more prominent further south in the Cape Blanc and Mauritania upwelling regions indicating enhanced productivity.

Glacial productivity although not prominent in the organic carbon records from the North, Portugal to the Morrocco margin, responded to Holocene climate variability in the south, with enhanced organic carbon burial. . The carbon and isotope records suggests that variations in Holocene climate in these regions would have been influenced by the productivity patterns associated with changes in wind stress, local hydrographic differences and periodic increases of upwelling. This interpretation is consistent with previous TOC records from the Morrocco and Portuguese margin which also found high TOC concentrations that were related to periods of enhanced productivity (Bozzano *et al.,* 2009).

Numerous marine sedimentation records from off NW Africa have been linked to past climate variations (Sarnthein *et al.,* 1981; Wefer *et al.,* 1991; Abrantes, 2000; Romero *et al.,* 2008; Bozzanno *et al.,* 2009; Zarriess *et al.,* 2010) on orbital and millennial scales (Holzwarth *et al.,* 2010). However these studies have been to a certain extent contradictory with regards to glacial upwelling (e.g Sarnthein *et al.,* 1982; Sarnthein *et al.,* 1988) or interglacial upwelling (e.g Bertrand *et al.,* 1996; Martinex *et al.,* 1999) off NW Africa.

The new results from this study combine both aspects as they support both upwelling during glacial conditions, in particular off Western Sahara, but also a

response to humid conditions during the Holocene. The Holocene response however is stronger in the south, off Cape Blanc and Mauritania because of more persistent upwelling in the region. Northern Africa has been shown to have fluctuated between arid to hyper arid conditions, such as the late Holocene to LGM, and much wetter conditions during the AHP (Cole *et al.,* 2009). Previous studies have provided climatic and productivity evidence of Holocene variations in the southern regions off Sahara (e.g Nave *et al.,* 2003; Romero *et al.,* 2008; Itambi *et al.,* 2009) consistent with the observations from this transect study. Itambi *et al.* (2009) showed that marine productivity was strongly enhanced in marine sediments offshore Senegal during the AHP while off Mauriatania, upwelling inferred from diatom and other geochemical records increased during glacial times (Romero et al, 2008). This is in contrast to what was found in this study, i.e. we found no evidence for glacial upwelling in the north. It is possible that the complex atmospheric and hydrographic setting of the Mauritania transect as described by Romero et al (2008) may be responsible for such discrepancies.

6.6.2 *Organic matter input $\delta^{13}C_{org}$*

To confirm the inferred marine productivity cycles along the NW African margin and/or to establish variations in supply from terrigenous organic components, bulk $\delta^{13}C_{org}$ is used as a proxy in combination with the leaf wax lipid data. The observed variations in $\delta^{13}C_{org}$ along the North West African margin reveal regional and temporal differences in the supply of organic matter from different sources.

In the northern part of the transect, off Portugal and northern Morocco, the carbon isotopic records reflect mainly a combination of C_3 type and MOM while the southern part spanning West Sahara and Mauritania suggest stronger admixture of C_4 type vegetation in particular during glacial periods. Further south off W Sahara, admixture of C_4 type vegetation is suggested to be higher. These trends suggest temporal and geographical differences in vegetation composition, and a large variability in the organic matter composition along the SW Portuguese to NW Africa.The pronounced shift of up to 1.5‰ observed in the deglacial periods from W Sahara implies a transition from C_4 to C_3 type vegetation consistent with an expansion of C_3 type vegetation with progressive warmer and more humid African conditions. Further south off W Sahara, this isotope shift is much smaller, only up to 0.5‰, suggesting less pronounced fluctuations in African vegetation, i.e. a less clearly developed transition zone between C_4 and C_3 type vegetation.

Previous studies have shown that organic matter from C_4 type plants became widespread in central and North Africa during the last glacial maximum (Street-Perrott *et al.,* 1990). These arid condition linked to African climate resulted in increased wind speeds, transporting terrestrial material from dust source areas over the African continent (de Menocal, 1995; Schefuß *et al.,* 2003). Thus, variations in the organic matter input from C_4 type plants, especially along W Sahara through time, may be interpreted to be related to wind intensity consistent with dust input during cold and arid conditions. As conditions and regional differences changed, towards warmer and humid conditions, and towards Cape Blanc and Mauritania, the transition to C_3 type plants may have been fostered possibly by riverine input and upwelling conditions.

In the north, off Portugal, the CHEETA records suggest that enhanced organic matter supply is dominated by Holocene variations of MOM and C_3 type vegetation (wood land and forest) when conditions were humid and wet (Gasse *et al.,* 2000). Humid conditions in the north of the Gulf of Guinea have been documented to result in an increase in Mangrove and rainforest pollen groups (Fredoux, 1994). Independent pollen records from NW Africa also suggested that vegetation in central Africa experienced major changes throughout the glacial/interglacial cycle (Hooghiemstra, 1998). The relative distribution of the $\delta^{13}C_{org}$ indicative of admixture of C_4 type vegetation along the W Sahara sector supports the conclusion that this region expanded in both north and south directions during the LGM in response to an intensification of the NE trade winds and the Saharan air layer that transported pollen and dust in both

directions (Hooghiemstra 1998). Climate conditions in central Africa changed significantly towards the middle Holocene. Geomorphic and biostratigraphic evidence suggested that NW Africa was already extensively vegetated during the middle Holocene, prior to the AHP, with lakes and grasslands evident in the Sahara (Joussaume *et al.,* 1999; de Menocal *et al.,* 2000).

6.6.3 *Molecular records- leaf wax lipids and $\delta^{13}C$ values*

Higher plant leaf waxes (Eglinton and Hamilton, 1967; Simoneit *et al.,* 1977; Gagosian *et al.,* 1981; Huang *et al.,* 2000) have been linked to dust transport into the North and Equatorial Atlantic (Zhao *et al.,* 2000), traced in dust samples (Eglinton *et al.,* 2002; Schefuß *et al.,* 2003) and surface sediments (Wagner and Dupont, 1999; Huang *et al.,* 2000). It is crucial to determine the source of organic matter input using additional molecular techniques as it provides diagnostic evidence for vegetation changes along the North West African margin.

The first biomarker data reflect good preservation of leaf wax lipids in the CHEETA sediments. Although the resolution of the molecular records from the cores studied is still very limited the variations in chain length are consistent with general differences between arid and humid vegetation sources. The distribution of the CPI suggests preferential marine derived organic matter, although petroleum contamination in the Moroccan sediments cannot be excluded given the low CPI values. CPI values > 2 off the W Saharan sector, recorded in glacial sediments, reflect stronger terrestrial organic matter supply,

consistent with arid conditions. ACL values support regional variations in the type of terrestrial organic matter supplied, with low chain lengths in the north (GC 17) and longer chain lengths in the south (GC 27). The low ACL observed in the north may be due to contamination or marine components. In contrast,, the longer ACL values observed off West Sahara and northern Morroco (31°N) argue for stronger supply from higher plants growing under arid conditions (grasses). Previous studies on the Moroccan regions have reported dominant aeolian activity after the mid Holocene (Ait Hassain and Bridgland, 2009) but to confirm such comparisons, more data from this region are necessary. The A.I indices recorded in the CHEETA sediments are consistent with the vegetation distribution across the study region, with savannah type vegetation in West Sahara resulting in elevated A.I. values and Mediterranean shrub being reflected by low A.I records.

6.6.4 *The $\delta^{13}C$ values of leaf wax n-alkanes*

Few compound specific isotope analyses of leaf wax lipids exist from the NW African margin and even fewer studies have been carried out on dust to identify vegetation from SAL and NETW dust source regions. $\delta^{13}C$ records from aerosol dust over the eastern Atlantic showed C_4 type vegetation (-25 to 33‰) in the Sahara and Sahel regions (Schefuß *et al.,* 2003) dependent on the intensity of the SAL. Mapping studies of marine surface sediments over a wide region off North West Africa from Portugal to the Gulf of Guinea, have shown the main track of the NETW had more negative $\delta^{13}C$ values (-32‰), indicating C_3 type

vegetation than areas below the SAL with more positive $\delta^{13}C$ values (-26.2‰) (Huang *et al.,* 1993; 2000).

Further, the *n*-alkane $\delta^{13}C$ records from aerosols collected from northern Nigeria under Harmattan conditions had values of between -26.6 to 30.1‰ sourced from vegetation of sub montane savannah, shrubs and forests proposed to be transported by the NETW towards equatorial East Atlantic and Gulf of Guinea (Simoneit *et al.,* 1997). For the NW African margin, it is recognized that more molecular data are needed to accurately reconstruct the source and wind systems that control the export of C_3 vs. C_4 type vegetation markers to the marine sediments.

The preliminary $\delta^{13}C$ values of *n*-alkanes from GC 49 suggest that an isotopic distinction between different types of leaf waxes is at least preserved in the sediments. The ~3‰ negative shift observed between 14-12 ka may suggest a transition from C_4 to C_3 consistent with Holocene C_3 type vegetation expansion. Unfortunately, the limited data from this core and other cores limits the interpretation, and it is recognised that more research need to be done in this regard. Previous studies from NW Africa at least have shown similar $\delta^{13}C$ values of leaf waxes from dust samples along North West African coast (Schefuß *et al.,* 2003), and sediments from Site 658 off North West Africa which suggested higher $\delta^{13}C$ records during glacial periods (Zhao *et al.,* 2000). This new $\delta^{13}C$ data do not show a similar magnitude of the shift which is 8‰ at ODP Site 658 for the same time period.

6.7 *Conclusion*

For the CHEETA transect spanning the SW Portuguese and NW African region, bulk organic geochemical records ($\delta^{13}C_{org}$) and ^{14}C AMS data are used to develop an integrated chronological framework for the last 35 kyrs in order to correlate all cores across the transect and assess the geochemical proxies with regard to their potential to reconstruct the palaeoenvironmental conditions since the last glaciation.

The geochemical proxy records (TOC; TOCcf TOCAR; and $\delta^{13}C_{org}$) show:

- Millennial scale variations in organic carbon burial and marine productivity during glacial periods in the south, consistent with arid conditions in central Africa.
- The Holocene sections also broadly show enhanced organic carbon burial between 15-5Ka, reflecting a response to the African Humid Period, interrupted by a reduction in organic carbon accumulation centered around 10ka.
- The $\delta^{13}C_{org}$ records broadly delineate the sources of organic carbon supply from C_3 and C_4 type vegetation including regional admixture of MOM. The records show that C_3 type vegetation and MOM dominated the northern part of the transect, off the Portuguese to Moroccan margin, while C_4 type vegetation off SW Sahara was enhanced during glacial periods followed by a transitioned to more MOM and possibly C_3 type supply towards the Holocene.

- First molecular data provide evidence from higher plant leaf waxes showing that CPI, ACL and A.I *n*-alkane distribution patterns respond to variations in African climate and continental vegetation supply.
- $\delta_{13}C$ of leaf waxes suggest C_4 vegetation that show a transition to C_3 vegetation in the Holocene only in the W Sahara region where available records are presented.

7 Chapter Seven

7.1 *Conclusions and future work*

The overall aim of the research presented in this thesis has been to increase knowledge and understanding of tropical African climate and marine sedimentation during two major climate transitions - the late Miocene to early Pliocene time period and the glacial - Holocene transition. To investigate this, a particularly climate sensitive region in the tropical eastern equatorial Atlantic (ODP Site 959) has been identified and a transect study was conducted from the North West African margin spanning SW Europe and the NW African regions (CHEETA Cruise transect). From these locations, a large number of sediment samples from ODP Site 959 (136); CHEETA surface sediments (23) and CHEETA Core sediments (467 sediments from 15 cores) were analysed using organic bulk and molecular geochemical techniques. Methods used include GC –FID; Elemental analyses, GC-irms-MS and the HPLC LC MS techniques.

All sediments studied yielded results which were used to reconstruct the paleoclimatic evolution in the eastern equatorial Atlantic and the North West African margin. Further, spectral analyses were performed on the geochemical records from ODP Site 959 to explore the influence of orbital forcing on marine sedimentation and continental climate during the late Miocene to early Pliocene transition. The integrated findings from this study provided an improved understanding of the processes and feedback mechanisms that drove central

African climate in the past. The main conclusions of each study in this thesis are summarized in the following discussion.

7.1.1 *The late Miocene to early Pliocene climate transition – ODP Site 959 off Equatorial West Africa*

Although the late Miocene to early Pliocene (7-5 Ma) has been shown to be a relatively stable period in the last 65 Myrs transition, (Zachos *et al.,* 2001) this transition can not be ignored, as long term cooling have been proposed at this time which forced a principal change in terrestrial vegetation in the low latitudes with a general shift from C_3 to C_4 type terrestrial vegetation (Cerling *et al.,* 1993; Cerling *et al.,* 1997). The core of this study coupled detailed organic carbon with sea surface temperature and plant leafwaxes from ODP Site 959 off West Africa in the equatorial Atlantic with frequency analyses in order to reconstruct tropical African vegetation change and surface ocean response for the time interval of about 7-5 Ma and to explore high latitude climate forcing. Sediment from ODP Site 959 were well preserved and recovered at high resolution which made it possible to explore the complex relationships between marine sedimentation and African climate and their development over time.

The key finding is a notable influence of high latitude climate processes on the tropics influencing tropical African conditions and marine sedimentation as expressed by high amplitude fluctuations in TOC, SST and leaf wax lipids. Despite low TOC (<0.5%) but high carbonate (>40%) concentrations molecular

climate signals were preserved in the sediments providing robust and consistent proxy records.

The alkenones and *n*-alkanes detected in ODP Site 959 sediments enabled the reconstruction of SST using the unsaturation index $U^{k'}_{37}$ of alkenones ($C_{37:3}$ and $C_{37:2}$) (Prahl *et al.,* 1988) and examination of the distribution and transport patterns of higher plant leaf waxes. The alkenone based SST records confirm for the first time pronounced warming/cooling cycles of a magnitude of 4°C which intensified around 5.6 Ma. In this thesis, SSTs are of a larger magnitude and range from 24.8 to 29°C. Elevated leaf waxlipids concentrations corresponded with cooler temperatures and were intimately coupled given the consistent similarities in the cycles derived from time series analyses. It is proposed that these relationships have been directly linked to the coupled atmospheric and oceanic circulation during the late Miocene to early Pliocene interval.

The combination of these proxies supports the conclusion that upwelling and atmospheric circulation patterns were linked to the position of the ITCZ during the late Miocene to early Pliocene climate transition. The new SST records from this thesis argue that variations must have been linked to much larger and cyclic shifts in SST in the equatorial Atlantic and it is proposed that this would have influenced the position of the ITCZ and thermocline structure much earlier than proposed in previous studies (Billups *et al.,* 1999; Norris, 1998)

The leaf wax lipids records from ODP 959 favor dust transport reflecting arid conditions in the dust source areas. This suggests that trade wind strength and continental aridity was ultimately linked to the position of the ITCZ that determined and controlled marine conditions in tropical Atlantic ocean. Future research will be necessary to analyse for carbon and hydrogen isotopic signatures e.g. from the leaf wax lipids to accurately delineate the source type and composition of the vegetation from these sediments.

Frequency analyses showed that the distinct cyclic patterns related strongly to orbital forcing, with a dominance of obliquity frequencies (41 kyr). This observation strongly argues for a direct influence of high latitude climate on tropical conditions and processes. An additional 100 kyr-frequency is confirmed for the TOC record suggesting a control of deep water circulation on preservation of organic matter in the sediments. Interestingly, a 75 kyr frequency was identified for the leaf wax lipids and SST records, which may indicate a strong coupling of both records in response to (initial) small scale variations in continental ice volume associated with the Miocene to Pliocene climate. More evolutionary spectral investigations, comparative studies of the SST records for example with oxygen isotope records at this time interval from the North Atlantic may be useful to validate these initial suggestions. A lead/lag relationship confirmed in the records suggests that the African continent was preconditioned for aridity before upwelling processes and cooling of surface water occured.

There are still some remaining gaps in this study of the Miocene-Pliocene transition such as confirming the nature of the frequency cycles in the biomarker records as well as the reconstruction of vegetation and precipitation patterns which can determine ambient conditions across this climate transition. Despite this, the findings of this research have revealed better understanding the complex processes and mechanisms associated with the tropical African climate.

7.1.2 *Future work: the late Miocene to early Pliocene climate*

1. *Obtaining compound specific $\delta^{13}C$ and δD isotopic values from leafwaxes.*

   During this PhD, attempts to obtain $\delta^{13}C$ values proved challenging given the amount of sample required for analyses, low TOC contents of the sediments and time constraints. Despite this, retrieving such information from the ODP Site 959 sediments in the tropical eastern equatorial Atlantic is necessary because these proxies can provide key information on paleovegetation patterns and climate of the tropical eastern equatorial Atlantic during the late Miocene to early Pliocene (7-5Ma). The $\delta^{13}C$ values will distinguish different types of vegetation, identify vegetation source and provide information on the utilization of CO_2 by C_3 or C_4 plants. C_3 and C_4 plants have been suggested to have different conditions such as high temperatures and low pCO_2 that favour growth (See Cerling et al., 1993; 1997 and Ehleringer et al., 1997). In particular, Cerling et al (1997) attributed global expansion of C_4 plants in the Miocene to a decrease in atmospheric pCO2. However, alkenone based pCO_2 estimates for the late Miocene

showed increase in pCO_2 which Pagani et al (1999) attributed to enhanced low –latidue aridity or changes in seasonal precipitation patterns. It would be interesting to combine $\delta^{13}C$ records with δD to take this research further. The hydrogen isotopic composition δD of plant leafwaxes are largely determined by ambient conditions i.e. enhanced evapo transpiration results in a loss of moisture and deuterium enrichment in plants (Chikaraishi *et al.,* 2004a). Therefore obtaining the δD of plant leafwaxes of plantwaxes will provide information for precipitation which is a relatively new area of research. Recent advancement in this regard e.g Schefuß et al., 2005; Sauer et al., 2004; Sachse et al., 2004) have been compelling support for this proxy. It is believed that with the analytical expertise and instrumentation at Newcastle University, contributions to the the developments in this area can be an achievable goal.

2. Obtaining marine productivity proxies

Variations in marine productivity, linked to atmospheric CO_2 could be a key mechanism in exploring climate conditions during the late Miocene to early Plicoene climate. Apart from TOC and SST obtained in this thesis, it is recognized that past ocean productivity patterns can be reconstructed using proxies for marine productivity such as excess Ba and Al in combination with high resolution nannofossil biota and ^{15}N of bulk sediments. Although with limitations, due to inaccuracies in timescales, taxonomic discrepancies, and poor geographic and temporal spread of data (Gibbs et al., 2005) previous studies in obtaining nannofossil biota from the Miocene (Gartner, 1992) and

the Pliocene (Gibbs et al., 2005) have proved useful to address past ocean productivity.

3. *Combining inorganic geochemical analyses with organic geochemical and proxy records at ODP Site 959*

Previous studies have shown that modern and past African climate variability and mineral export can be deduced from element to element ratios (See Zabel et al., 2001; Hofman et al., 2003). High relative contents of heavy metals such as Ti and K associated wtith enhanced transport energy and arid conditions, and Al indicatative of tropical weathering under humid conditions can provide insight into the contribution of terrestrial organic matter to the sediments at ODP Site 959. The well established GC/GCMS techniques and inorganic geochemical analyses using the inductively coupled plasma mass spectrometry (ICP/MS) will be an appropriate approach to use in taking this research further.

7.1.3 *The glacial to Holocene transect –The CHEETA programme*

This thesis contributes to some of the aims of the larger, multi-institutional CHEETA project involving ETH, Lamont Doherty University, and Newcastle University which is to develop high-resolution records of terrestrial climate and surface ocean variability for the eastern Atlantic from the mid-latitudes to the subtropics. This thesis, conducted at Newcastle University contributed to some of the aims of the program by carrying out two independent studies on the CHEETA transect

1. Using a paired biomarker approach, in addition to other geochemical proxies (TOC; $CaCO_3$; $Corg/N_{tot}$; $\delta^{13}C_{org}$) from surface sediments were used to trace soil organic matter in marine sediments and constrain regional variations in continental supply.
2. From the CHEETA core transect, a paleo-study using a host of new high resolution geochemical records was carried out by developing a new integrated chronological framework to correlate all glacial to Holocene records along the latitudinal transect and to better understand regional and spatial variations and the response of the tropical African climate to these changes.

1. CHEETA – Testing the applicability of novel soil biomarkers on surface sediments

The main aim of this study was to trace the transport of soil organic matter (SOM) in surface sediments recovered along the Portuguese and NW African margin. One key finding of this study was that organic carbon concentrations and $\delta^{13}C_{org}$ gradients off Portugal to W Africa identified areas of upwelling off Cape Blanc and the transition from C_3 to C_4 vegetation habitats in Northern Africa. In addition two soil-specific biomarkers, the BIT index based on branched GDGTs and soil-specific BHPs, were detected in this region of almost exclusive aeolian export. Such compounds have usually been associated with fluvial transport of soil derived organic matter (see Hopmans *et al.,* 2004) rather than aeolian transport, thus the detection of such compounds yields interesting explanations for the terrestrial organic matter transport and SOM. However,

concentrations of these biomarkers (GDGTs) in the CHEETA surface sediments were low. Despite this, there seems to be greater input of soil marker BHPs in the sediments than the GDGTs which may be related to the initial location of the respective microbial communities in the soil column.

2. CHEETA (Gravity core sediments)

To assess the sensitivity of proxies and processes related with transmitting terrigenous signals to the adjacent continental margin, gravity core and multicore pairs were recovered at 28 stations along the CHEETA cruise transect from 40°N-15°N paralleling the continental slope. In this study multiple organic proxies, including bulk elemental data of organic carbon records, abundance and isotopic composition of bulk organic matter and molecular records, were determined to constrain regional variations in African continental climate and terrigenous supply and marine sedimentation. The compilation of the geochemical data from a selection of cores within a newly integrated chronological framework revealed regional patterns that fluctuated with the transition from glacial to Holocene climate conditions. Organic carbon records showed millennial scale variability off the West Sahara to the Mauritania region during glacial conditions reflecting repetitive fluctuations in upwelling and marine productivity. The Holocene sections also show a period of maximum organic carbon burial reflecting a close response to humid conditions associated with the AHP.

Analysis of detailed $\delta^{13}C_{org}$ records from the southern West Sahara region show values typical of enhanced C_4 plant supply during the glacial and C_3 plant and

MOM in the Holocene sections in the North. For preliminary molecular work three cores (GC 17; GC27 and GC 49) were available at the time of writing this thesis. The results show that *n*-alkanes from higher plant leaf wax lipids were present in sediments from off W Sahara, while more marine and or petroleum components dominated the Moroccan margin sediments. CPIs reflect this general pattern with low values (<1) in the north and elevated values (2- 4) in the south. ACL which range from 23 -29.5 are consistent with the CPI values and supporting arid conditions in the W Sahara and more humid conditions in Morocco. Finally, the A.I index reflects *n*-alkane distributions indicative for savannah vegetation off West Sahara and Mediterranean shrub signatures off the Moroccan coastline. The $\delta^{13}C$ values of leaf waxes lipids for the W Sahara range from -25 to -28‰ with a marked 3‰ negative shift observed between 14-12 ka which may suggest dominance of C_3 plants at least consistent with more humid conditions and expansion of C_3 vegetation at that time .

7.1.4 *Future work for the CHEETA project:*

1 One of the future goals of the CHEETA project is to integrate this thesis with work from the different groups' inorder to understand past subtropical and tropical SST changes and vegetation change.

2 It is believed that with time, the integrated chronological framework using ^{14}C AMS data will be completed for all remaining cores to constrain regional patterns from glacial to the Holocene climate.

3 More surface samples are needed to confirm and quantify the branched GDGTs and BHPs which will further assess and evaluate in

situ production of GDGTs. The low BIT index and MAT temperature do not provide any latitudinal trend across the CHEETA transect suggesting variable mixtures of insitu and continental GDGTs. Unfortunately dust samples for the CHEETA transect were not available at the writing of this thesis which may accurately evaluate the extent of insitu production.

4 For future research, foraminiferal Mg/Ca and stable isotopes can provide information on the temperature for the tropics and subtropics (e.g Lea et al., 1999; Nurnberg et al., 1996; Elderfield and Ganssen, 2000). This method has proven useful for measuring surface dwelling species from warmer tropical temperatures *(e.g G.sacculifer, G.ruber)* where Mg contents are high and readily measurable and analytical error is small (Lea et al., 1999). Analytical approach will include the use of the ICP-OES.

5 In addition to the biomarkers and organic geochemical proxies used in this thesis for the CHEETA surface and core sediments, another future research goal is employ a host of other biomarkers which will ultimately provide an integrated view on the tropical climate dynamics from the Medditerenean to the tropics. To this end, more $\delta^{13}C$ values from the remaining CHEETA cores will be assessed. It has been established from the pilot study that leafwax lipids were preserved in the cores studied. Leafwax lipids have shown to be a useful marker in low latitude Atlantic. Long chain *n*-alkanes exhibiting an odd-carbon number predominance are synthesized exclusively by vascular plants

as epicuticular leafwaxea (Eglinton and Hamilton, 1967; Kolattukudy, 1976). Obtaining leafwaxes from other cores along the NW African margin, as well as its $\delta^{13}C$ values, will be invaluable for evaluating vegetation change or patterns of atmospheric circulation (Rieley et al., 1991; Ohkouchi et al., 1997; Huang et al., 1997).

8 References

Abrantes, F., (2000) 200 000 yr diatom records from Atlantic upwelling sites reveal maximum productivity during LGM and a shift in phytoplankton community structure at 185 000 yr. *Earth and Planetary Science Letters*, **176**(1), 7-16.

Adegbie, A.T., Schneider, R.R., Röhl, U., Wefer, G. (2003) Glacial millennial-scale fluctuations in central African precipitation recorded in terrigenous sediment supply and freshwater signals offshore Cameroon. *Palaeogeograhpy,Palaeoclimatology,Palaeoecology*, **197**, 323-333.

Ait Hssaine, A., Bridgland, D., (2009) Pliocene-Quaternary fluvial and aeolian records in the Souss Basin, southwest Morocco: A geomorphological model. *Global and Planetary Change*, **68**(4), 288-296.

Alexandre, A., Meunier, J.D., LÃzine, A.M., Vincens, A., Schwartz, D. (1997) Phytoliths: Indicators of grassland dynamics during the late Holocene in intertropical Africa. *Palaeogeography, Palaeoclimatology, Palaeoecology*, 136(1-4), 213-229.

Alley, R.B., Meese, D.A., Shuman, C.A., Gow, A.J., Taylor, K.C., Grootes, P.M., White, J.W.C., Ram, M., Waddington, E.D., Mayewski, P.A., Zielinski, G.A. (1993) Abrupt increase in Greenland snow accumulation at the end of the Younger Dryas event. *Nature*, **362**, 527-529.

Bakun, A., 1978: Guinea Current Upwelling. *Nature*, **271**, 147-150.

Basile, C., Mascle, J., Sage, F., Lamarche, G., Pontoise, B. (1996) Pre-cruise and site-surveys: a synthesis of marine geological and geophysical data on the Côte d'Ivoire-Ghana Transform Margin. In: J. Mascle, G.P. Lohmann, P.D. Clift (Eds.), Proceedings of the Ocean Drilling Program, Initial Reports Leg 159 (Ed. by J. Mascle, G.P. Lohmann, P.D. Clift), pp. 47-60. Ocean Drilling Program, College Station, TX (Ocean Drilling Program).

Batjes, N.H. 1996. Total Carbon and nitrogen in the soils of the world. *European Journal of Soil Science* **47**, 151-163.

Bechtel, A., Smittenberg, R.H., Bernasconi, S.M., Schubert, C.J. (2010) Distribution of branched and isoprenoid tetraether lipids in an oligotrophic and a eutrophic Swiss lake: Insights into sources and GDGT-based proxies. *Organic Geochemistry*, **41**, 822-832.

Bentaleb, I., Grimalt, J.O., Vidussi, F., Marty, J.C. Martin, V., Denis, M., Hatté, C., Fontugne, M., (1999) The C37 alkenone record of seawater

temperature during seasonal thermocline stratification. *Marine Chemistry*, **64**(4), 301-313.

Berger, W.H., G.Wefer, C.Richter., and the Shipboard Scientific party (1998) Colour cycles in Quaternary sediments from the Congo fan region (Site 1075); A statistical analysis, *Proceedings .Ocean Drilling Programme Initial Reports,* **175**, 561-567.

Berger, W.H., Wefer G. (1996) Expeditions into the past: paleoceanographic studies in the South Atlantic. In: G. Wefer, W.H. Berger, G. Siedler, D. Webb (Eds.), *The South Atlantic: Present and Past Circulation* (Ed. by G. Wefer, W.H. Berger, G. Siedler, D. Webb), pp. 363-410, Springer, Berlin.

Bertrand, P., Shimmield, G., Martinez, P., Grousset, F., Jorissen, F., Paterne, M., Pujol, C., Bouloubassi, I., Buat Menard, P., Peypouquet, J.-P., Beaufort, L., Sicre, M.A., Lallier-Verges, E., Foster, J.m., Ternois, Y., (1996) The glacial ocean productivity hypothesis: the importance of regional temporal and spatial studies. *Marine Geology*, **130**, 1-9.

Bi, X., Sheng, G., Liu, X., Li, C., Fu, J. (2005) Molecular and carbon and hydrogen isotopic composition of *n*-alkanes in plant leaf waxes. *Organic Geochemistry,* **36** , 1405–1417.

Bijma, J., Altabet, M., Conte, M., Kinkel, H., Versteegh, G.J.M., Volkman, J.K., Wakeham, S.G., Weaver, P.P. (2001) Primary signal: Ecological and environmental factors; Report from Working Group 2. *Geochemistry. Geophysics. Geosystems* **2**(1).

Billups, K. (2002) Late Miocene through early Pliocene deep water circulation and climate change viewed from the sub-Antarctic South Atlantic. *Palaeogeography, Palaeoclimatology, Palaeoecology*, **185,** 287-307.

Billups, K., Ravello, A.C., Zachos, J.C., Norris, R.D., (1999) Link between oceanic heat transport, thermohaline circulation, and the Intertropical Convergence Zone in the early Pliocene Atlantic. *Geology*, **27,** 319-322.

Billups, K., Ravelo, A.C., Zachos, J. (1998). Early Pliocene climate: A perspective from the western tropical Atlantic warm pool. Paleoceanography **13**, 459-470.

Binet, D., 1997: Climate and pelagic fisheries in the Canary and Guinea currents 1964-1993: The role of Trade Winds and the Southern Oscillation. *Oceanologia Acta*, **20**, 177-190.

Bird, M.I., Summons, R.E., Gagan, M.K., Roksandic, Z., Dowling, L., Head, J., Keith Fifield, L., Cresswell, R.G., Johnson, D.P.(1995) Terrestrial vegetation change inferred from *n*-alkane [sigma]13C analysis in the marine environment. *Geochimica et Cosmochimica Acta*, **59,** 2853-2857.

Blaga, C., Reichart, G.-J., Heiri, O., Sinninghe Damsté, J. (2009) Tetraether membrane lipid distributions in water-column particulate matter and sediments: a study of 47 European lakes along a north–south transect. *Journal of Paleolimnology*, **41,** 523-540.

Bloomfield, P. (1976). *Fourier Analysis of Time series: an Introduction*. Wiley. London

Blumenberg, M., Krüger, M., Nauhaus, K., Talbot, H.M., Oppermann, B.I., Seifert, R., Pape, T., and Michaelis, W. (2006). Biosynthesis of hopanoids by sulfate-reducing bacteria (genus *Desulfovibrio*). *Environmental Microbiology,* **8**, 1220-1227.

Bond, G., Kromer, B., Beer, J., Muscheler, R., Evans, M.N., Showers, W., Hoffmann, S., Lotti-Bond, R., Hajdas, I., Bonani, G. (2001) Persistent Solar Influence on North Atlantic Climate During the Holocene. *Science*, **294,** 2130-2136.

Bond, G., Showers, W., Cheseby, M., Lotti, R., Almasi, P., deMenocal, P., Priore, P., Cullen, H., Hajdas, I., Bonani, G.(1997) A Pervasive Millennial-Scale Cycle in North Atlantic Holocene and Glacial Climates. *Science*, **278**, 1257-1266.

Bonifay, D., Giresse, P. (1992) Middle to late Quaternary sediment flux and post-depositional processes between the continental slope off Gabon and the Mid-Guinean margin. *Marine Geology*, **106**, 107-129.

Boon,J.J., Van deer Meer,F.W., Schuyl, J .W. (1978). Organic Geochemical Analysis of core samples from Site 362. *Initial reports of the Deep Sea Drilling Project*, **40**, 627-637.

Boot, C.S., Ettwein, V.J., Maslin, M.A., Weyhenmeyer, C.E., Pancost, R.D. (2006) A 35,000 year record of terrigenous and marine lipids in Amazon Fan sediments. *Organic Geochemistry*, **37,**208-219.

Boyle, E.A., Keigwin, L.D. (1982) Deep Circulation of the North Atlantic over the Last 200,000 Years: Geochemical Evidence. *Science*, **218**, 784-787.

Bozzano, G., Alonso, B., (2009) Transfer of organic carbon on the Moroccan Atlantic continental margin (NW Africa): Productivity and lateral advection. *Geo-Marine Letters*, 29(5), 277-289.

Bradley, R.S. (1999) *Paleoclimatology - Reconstructing Climates of the Quaternary*. Academic Press, San Diego.

Brassel, S.C., Eglinton, G., Marlowe, I.T., Pflaumann, U., Sarntheim, M. (1986) Molecular stratigraphy: a new tool for climatic assessment. *Nature*, **320,** 129-132.

Brassell, S.C., Dumitrescu, M. (2004) Recognition of alkenones in a lower Aptian porcellanite from the west-central Pacific. *Organic Geochemistry*, **35,** 181-188.

Bray, E.E., Evans, E.D. (1961) Distribution of n-paraffins as a clue to recognition of source beds. *Geochimica et Cosmochimica Acta*, **22**, 2-15.

Brewster, N.A. (1980) Cenozoic biogenic silica sedimentation in the Antarctic Ocean based on two Deep Sea Drilling Project sites. *Geol. Soc. Am. Bull.* **91,** 337–347.

Burdige, D.J. (2005) Burial of terrestrial organic matter in marine sediments: A re-assessment. *Global Biogeochemical Cycles* **19**, doi: 10.1029/2004GB002368.

Calvert, S.E., Pedersen, T.F. (1992) Organic carbon accumulation and preservation in marine sediments: how important is anoxia? In: J.K. Whelan, J.W. Farrington (Eds.), *Organic Matter: Productivity, Accumulation, and Preservation in Recent and Ancient Sediments* (Ed. by J.K. Whelan, J.W. Farrington), pp. 231-263. Columbia University Press, New York.

Calvo, E., Pelejero, C., Herguera, J. (2001) Insolation dependence of the southern eastern subtropical pacific sea temperature over the last 400 kyrs.Geophysical research letters, **28**, 2481-2844.

Cane, M.A. (1998) A Role for the Tropical Pacific. *Science*, **282,** 59-61.

Carlson, T.N., Prospero, J.M. (1972) The Large-Scale Movement of Saharan Air Outbreaks over the Northern Equatorial Atlantic. *Journal of Applied Meteorology*, **11**, 283-297.

Castañeda, I.S., Schefuß, E., Pätzold, J., Sinninghe Damsté, J.S., Weldeab, S., Schouten, S. (2010) Millennial-scale sea surface temperature changes in the eastern Mediterranean (Nile River Delta region) over the last 27,000 years. *Paleoceanography*, **25**, 1208.

Cerling, T.C., Harris, J.M., MacFadden, B.J., Leakey, M.G., Quade, J., Eisenmann, V., Ehleringer, J.R. (1997) Global vegetation change through the Miocene/Pliocene boundary. *Nature*, **389**, 153-158.

Cerling, T.C., Wang, Y., Quade, J. (1993) Expansion of C_4 _ecosystem as an indicator of global ecological change in the late Miocene. *Nature*, **361**, 344-345.

Chaisson W.P. and. Ravelo, A.C. (2000) Pliocene development of the east–west hydrographic gradient in the equatorial Pacific. *Paleoceanography* **15**, 497–505.

Chaisson, W.P. (1995) Planktonic foraminiferal assemblages and paleoceanographic change in the trans-tropical Pacific Ocean: A comparison of west (Leg 130) and east (Leg 138), latest Miocene to Pleistocene, *Proceedings of the Ocean Drilling Program, Scientific results*, **138**, 555–597

Chappell, J., Shackleton, N.J. (1986) Oxygen isotopes and sea level. *Nature*, **324,** 137-140.

Chiang, J., Bitz, C., (2005) Influence of high latitude ice cover on the marine Intertropical Convergence Zone. *Climate Dynamics*, **25**(5), 477-496.

Chiang, J.C.H. (2009) The tropics in paleoclimate. *Annual Review of Earth and Planetary Sciences,* **37**, 263 -297

Chiapello, I., Bergametti, G., Chatenet, B., Bousquet, P., Dulac, F., Soares, E.S., (1997) Origins of African dust transported over the northeastern tropical Atlantic. J*ournal Geophysical Research*, **102**, 13701-13709.

Chiapello, I., Bergametti, G., Gomes, L., Chatenet, B., Dulac, F., Pimenta, J., Suares, E.S. (1995) An additional low layer transport of Sahelian and Saharan dust over the north;eastern Tropical Atlantic. *Geophysical. Research. Letters,* **22,** 3191-3194.

Chikaraishi, Y., Naraoka, H. (2003) Compound-specific [delta]D-[delta]13C analyses of *n*-alkanes extracted from terrestrial and aquatic plants. *Phytochemistry*, **63**, 361-371.

Chikaraishi, Y., Naraoka, H., Poulson, S.R. (2004a) Hydrogen and carbon isotopic fractionations of lipid biosynthesis among terrestrial (C3, C4 and CAM) and aquatic plants. *Phytochemistry*, **65**, 1369-1381.

Chikaraishi, Y., Suzuki, Y., Naraoka, H. (2004b) Hydrogen isotopic fractionations during desaturation and elongation associated with polyunsaturated fatty acid biosynthesis in marine macroalgae. *Phytochemistry*, **65,** 2293-2300.

Chikaraishi, Y., Yamada, Y., Naraoka, H. (2005) Carbon and Hydrogen Isotopic Compositions of Sterols from Riverine and Marine Sediments. *Limnology and Oceanography*, **50**, 1763-1770.

Chu, G., Sun, Q., Li, S., Zheng, M., Jia, X., Lu, C., Liu, J., Liu, T. (2005) Long-chain alkenone distributions and temperature dependence in lacustrine surface sediments from China. *Geochimica et Cosmochimica Acta*, **69**, 4985-5003.

Ciesielski, P.F., Ledbetter, M.T., Ellwood, B.B. (1982) The development of antarctic glaciation and the Neogene paleoenvironment of the Maurice Ewing Bank. *Marine Geology*, **46,** 1-51.

Cita, M.B., McKenzie, J.A. (1986) The terminal Miocene event. In: K.J. Hsu (Ed.), *Mesozoic and Cenozoic Oceans* (Ed. by K.J. Hsu), pp. 123-140. American Geophysical Union, Geodynamics Series 15, Washington DC.

Clark, P.U., Dyke, A.S., Shakun, J.D., Carlson, A.E., Clark, J., Wohlfarth, B., Mitrovica, J.X., Hostetler, S.W., McCabe, A.M., (2009) The Last Glacial Maximum. *Science*, **325**, 710-714.

Claussen, M., Kubatzki, C., Brovkin, V., Ganopolski, A., Hoelzmann, P., Hans-Joachim,P. (1999).Simulation of an abrupt change in Saharan vegetation in the mid-Holocene. *Geophysical. Research. Letters.* **26**, 2037–2040

Coates, A.G., Jackson, J.B.C., Collins, L.S., Cronin, T.M., Dowsett, H.J., Bybell, L.M., Jung, P., Obando, J.A. (1992) Closure of the Isthmus of Panama: The near-shore marine record of Costa Rica and western Panama. *Geological Society of America Bulletin*, **104**, 814-828.

Cole, J.M., Goldstein, S.L., deMenocal, P.B., Hemming, S.R., Grousset, F.E. (2009) Contrasting compositions of Saharan dust in the eastern Atlantic Ocean during the last deglaciation and African Humid Period. *Earth and Planetary Science Letters*, **278**, 257-266.

Collatz, G., Berry, J.A., Clark, J.S. (1998) Effects of climate and atmospheric CO_2 partial pressure on the global distribution of C4 grasses: present, past, and future. *Oecologia*, **114**, 441-454.

Collister, J.W., Rieley, G., Stern, B., Eglinton, G., Fry, B. (1994) Compound-specific δ^{13} C analyses of leaf lipids from plants with differing carbon dioxide metabolisms. *Organic Geochemistry*, **21,** 619-627.

Conte, M.H., Sicre, M.-A., Rühlemann, C., Weber, J.C., Schulte, S., Schulz-Bull, D., Blanz, T. (2006) Global temperature calibration of the alkenone unsaturation index in surface waters and comparison with surface sediments. *Geochemistry Geophysics Geosystems,* **7,** Q02005.

Conte, M.H., Thompson, A., Eglinton, G. (1994) Primary production of lipid biomarker compounds by Emiliania Huxleyi: Results from an experimental mesocosm study in fjords of southwestern Norway. *Sarsia*, **79**, 319-331.

Cooke, M.P., Talbot, H.M., Farrimond, P. (2008b) Bacterial populations recorded in bacteriohopanepolyol distributions in soils from Northern England. *Organic Geochemistry*, **39**, 1347–1358.

Cooke, M.P., Talbot, H.M., Wagner, T. (2008a) Tracking soil organic carbon transport to continental margin sediments using soil-specific hopanoid biomarkers: a case study from the Congo fan area. *Organic Geochemistry*, **39**, 965-971.

Cooke, M.P., van Dongen, B.E., Talbot, H.M., Semiletov, I., Shakhova, N., Guo, L., Gustafson, Ö. (2009) Transport of terrestrial organic matter to the Arctic Ocean via the great Arctic rivers. *Organic Geochemistry in press*, doi: 10.1016.

Cooper, J.E., Bray, E.E. (1963) A postulated role of fatty acids in petroleum formation. *Geochimica et Cosmochimica Acta*, **27,** 1113-1127.

Cranwell, P. (1981) Diagenesis of free and bound lipids in terrestrial detritus deposited in a lacustrine sediment. *Organic Geochemistry*, **3**, 79-89.

Crossman, Z.M., McNamara, N., Parekh, N., Ineson, P., Evershed, R.P. (2001) A new method for identifying the origins of simple and complex hopanoids in sedimentary materials using stable isotope labelling with 13CH4 and compound specific stable isotope analyses. *Organic Geochemistry*, **32**, 359-364.

Crowley, T. J. & Burke, K. C (1998). *Tectonic Boundary Conditions for Climate Reconstructions*. Oxford Monographs on Geology and Geophysics Series no. 39 pp. 285. New York, Oxford: Oxford University Press.

Dahl-Jensen, D., Mosegaard, K., Gundestrup, N., Clow, G.D., Johnsen, S.J., Hansen, A.W., Balling, N. (1998) Past Temperatures Directly from the Greenland Ice Sheet. *Science*, **282**, 268-271.

D'Andrea, W.J., Huang, Y. (2005) Long chain alkenones in Greenland lake sediments: Low $\delta^{13}C$ values and exceptional abundance. *Organic Geochemistry*, **36**, 1234-1241.

Dansgard, W., Johnsen, S.J., Clausen, H.B., Dahl-Jensen, D., Gundestrup, N.S., Hammer, C.U., Hvidberg, C.S., Steffersen, J.P., Sveinbjörnsdottir, A.E., Jouzel, J.(1993) Evidence for general instability of past climate from a 250-kyr ice-core record. *Nature*, **364**, 218-220.

de Leeuw , J.W., Largeau, C. (1993) *A review of macromolecular organic compounds that comprise living organisms and their role in kerogen, coal and petroleum formation.* In: Engel, M.H., Macko, S.A. (Eds.), Organic Geochemistry. Plenum Press, New York, pp. 23-72.

de Leeuw J.W., Versteegh G.J.M., Van Bergen P.F. Biomacromolecules of algae and plants and their fossil analogues. *Plant Ecology* **182**, 209-233.

de Leeuw, J.W., Van de Meer, F.W., Rijpstra, W.I.C., Schenck, P.A., (1980) On the occurrence and structural identification of long chain unsaturated ketones and hydrocarbons in sediments. *Advances in Organic Geochemistry,* **1979**, 211-217.

de Menocal, P., Ortiz, J., Guilderson, T., Adkins, J., Sarthnthein, M., Baker, L., Yarusinsky, M. (2000a) Abrupt onset and termination of the African humid period: rapid climate responses to gradual insolation forcing. *Quaternary Science Reviews*, **19,** 347-361.

de Menocal, P., Ortiz, J., Guilderson, T., Sarnthein, M. (2000b) Coherent high- and low latitude climate variability during the Holocene warm period. *Science*, **288**,2198-2202.

de Menocal, P.B. (1995) Plio-Pleistocene African climate. *Science*, **270**, 53-59.

de Menocal, P.B., Ruddiman, W.F., Pokras, E.M. (1993) Influences of high- and low-latidude processes on African terrestrial climate: Pleistocene eolian records from equatorial Atlantic Ocean Drilling Program site 663. *Paleoceanography*, **8**, 209-242.

de Vernal, A., Hillaire-Marcel, C., Turon, J.L., Matthiessen, J. (2000) Reconstruction of sea-surface temperature, salinity, and sea-ice cover in the northern North Atlantic during the last glacial maximum based on dinocyst assemblages. *Canadian Journal of Earth Sciences*, **37,** 725-750.

Diester-Haass, L., Billups, K., Emeis, K.C. (2005) In search of the late Miocene–early Pliocene ‘‘biogenic bloom’’ in the Atlantic Ocean (Ocean Drilling Program Sites 982, 925, and 1088).*Paleoceanography*, **20**, PA4001, doi: 10.1029/2005PA001139.

Dowsett, H. J. Chandler, M. A. Cronin, T. M. and Dwyer G. S. (2005), Middle Pliocene sea surface temperature variability, *Paleoceanography*, **20**, PA2014, doi:10.1029/2005PA001133.

Dowsett, H., Barron, J., Poore, R., (1996) Middle Pliocene sea surface temperatures: a global reconstruction. *Marine Micropaleontology*, **27**, 13-25.

Dowsett, H.J., Cronin, T.M., Poore, R.Z., Thompson, R.S., Whatley, R.C., Wood, A.M. (1992) Micropaleontological Evidence for Increased Meridional Heat Transport in the North Atlantic Ocean During the Pliocene. *Science*, **258**, 1133-1135.

Dupont, L.M., 1989. Palynology of the last 680,000 years of ODP site 658 (off NW-Africa): fluctuations in paleowind systems. In: Leinen,M.,Sarnthein,M. (Eds.),Paleoclimatology and Paleometeorology:

Modern and Past Patterns of Global Atmospheric Transport (NATO ASI Series 282). Kluwer Academic,London, pp. 779–794.

Eglinton, G., Calvin, M. (1967) Certain rocks as much as three billion years old have been found to contain organic compounds. What these compounds are and how they have originated in living matter is under active study. *Scientific American*, **26,** 32-43.

Eglinton, G., Hamilton, R.J. (1963) *The distribution of n-alkanes*. In Swain, T.(Ed.), Chemical plant taxonomy Academic press London, pp. 187-208.

Eglinton, G., Hamilton, R.J., (1967) Leaf epicuticular waxes. *Science*, **156**, 1322-1335.

Eglinton, T. I., Conte, M. H. Eglinton, G. and Hayes J. M. (2001), Proceedings of a workshop on alkenone- based paleoceanographic indicators, *Geochemistry Geophysics. Geosystems*, **2**, 1031, doi:10.1029/2000GC000122.

Eglinton, T., Conte, M., Eglinton, G., Hayes, J. (2000) Alkenone biomarkers gain recognition as molecular paleoceanographic proxies. *Eos*, **81**, 253-260.

Eglinton, T.I., Benitez-Nelson, B.C., Pearson, A., McNichol, A.P., Bauer, J.E., Druffel, E.R.M. (1997) Variability in radiocarbon ages of individual organic compounds from marine sediments. *Science*, **277**, 796-799.

Eglinton, T.I., Eglinton, G., (2008) Molecular proxies for paleoclimatology. *Earth and Planetary Science Letters*, **275**, 1-16.

Eglinton, T.I., Eglinton, G., Dupont, L., Sholkovitz, E.R., Montluçon, D., Reddy, C.M. (2002) Composition, Age and Provenance of Organic Matter in NW African Dust over the Atlantic Ocean. *Geochemistry Geophysics Geosystems* **3**, doi: 10.1029/2001GC000269.

Eglinton, T.I., Reperta, D.J. (2003) Organic Matter in the Contemporary Ocean. In: K. Turekian, H. Holland (Eds.), *Treatise on Geochemistry*, *Vol. 6: The Oceans and Marine Geochemistry* (Ed. by K. Turekian, H. Holland), pp. 145-180. Elsevier, London.

Ehleringer, J.R., Cerling, T.E., Helliker, B.R., (1997) C_4 photosynthesis, atmospheric CO_2, and climate. *Oecologia*, **112**, 285-299.

Emiliani, C. (1955). "Pleistocene Temperatures." *Journal Geology* **63**: 538-78.

Farquhar, G.D., Ehleringer, J.R., Hubick, K.T. (1989) Carbon isotope discrimination and photosynthesis. In: W.R. Briggs, R.L. Jones, V. Walbot (Eds.), *Annual Review of Plant Physiology and Plant Molecular*

Biology. vol 40 (Ed. by W.R. Briggs, R.L. Jones, V. Walbot), pp. 503-537. Annual Reviews Inc., Palo Alto.

Farrimond, P., Eglinton, G., Brassell, S.C. (1986) Alkenones in Cretaceous black shales, Blake-Bahama Basin, western North Atlantic. *Organic Geochemistry*, **10**, 897-903.

Farrimond, P., Fox, P.A., Innes, H.E., Miskin, I.P., Head, I.M. (1998) Bacterial Sources of Hopanoids in Recent Sediments: Improving our Understanding of Ancient Hopane Biomarkers. *Ancient Biomolecules*, **2**, 147-166.

Farrington, J.W., Davis, A.C., Sulanowski, J., McCaffrey, M.A., McCarthy, M., Clifford, C.H., Dickinson, P., Volkman, J.K. (1988) Biogeochemistry of lipids in surface sediments of the Peru upwelling area at 15°C. *Organic Geochemistry*, **13**, 607-617.

Fisher, E., Oldfield, F., Wake, R., Boyle, J., Appleby, P., Wolff,G.A., 2003. Molecular marker records of land use change.Organic Geochemistry **34**, 105–119.

Frédoux, A., (1994) Pollen analysis of a deep- sea core in the Gulf of Guinea: vegetation and climatic changes during the last 225,000 years B.P. *Palaeogeography, Palaeoclimatology, Palaeoecology*, 109, 317-330.

Fry, B., Sherr, E.B. (1984) $\delta^{13}C_{org}$ measurements as indicators of carbon flow in marine and freshwater ecosystems. *Contributions to Marine Science*, **27**, 13-47.

Gagosian, R.B., Peltzer, E.T. (1986) The importance of atmospheric input of terrestrial organic material to deep sea sediments. *Organic Geochemistry*, **10**, 661-669.

Gagosian, R.B., Peltzer, E.T., Zafiriou, O.C. (1981) Atmospheric transport of continentally derived lipids to the tropical North Pacific. *Nature*, **291**, 312-314.

Gartner, S., (1992) Miocene nannofossil chronology in the North Atlantic, DSDP Site 608. *Marine Micropaleontology*, **18**(4), 307-313, 317-331.

Gasse, F. (2000) Hydrological changes in the African tropics since the Last Glacial Maximum. *Quaternary Science Reviews*, **19**, 189 - 211.

Gasse, F., Tehet, R., Durand, A., Gibert, E., Fontes, J.-C., (1990) The arid to humid transition in the Sahara and the Sahel during the last deglaciation. *Nature*, **346** (6280), 141-146.

Gasse, F., van Campo, E. (1994) Abrupt post-glacial climate events in West Asia and North Africa monsoon domains. *Earth and Planetary Science Letters*, **126**, 435-456.

Gibbs, S.J., Young, J.R., Bralower, T.J., Shackleton, N.J., (2005) Nannofossil evolutionary events in the mid-Pliocene: an assessment of the degree of synchrony in the extinctions of Reticulofenestra pseudoumbilicus and Sphenolithus abies. *Palaeogeography, Palaeoclimatology, Palaeoecology*, **217**(1-2), 155-172.

Gillespie, R., Street-Perrott, F.A., Switsur, R. (1983) Post-glacial arid episodes in Ethiopia have implications for climate prediction. *Nature*, **306**, 680-683.

Giresse, P., Gadel, F., Serve, L., Barusseau, J.P., (1998) Indicators of climate- and sediment source-variations at Site 959: implications for the reconstruction of paleoenvironments in the Gulf of Guinea trough Pleistocene times. In: J. Mascle, G.P. Lohman, M. Moullard (Eds.), *Ocean Drilling Program Scientific Results Volume, Leg 159* (Ed. by J. Mascle, G.P. Lohman, M. Moullard), pp. 585-604. College Station, TX (Ocean Drilling Program), USA.

Giresse, P., Maley, J., Brenac, P. (1994) Late Quaternary palaeoenvironments in the Lake Barombi Mbo (West Cameroon) deduced from pollen and carbon isotopes of organic matter. *Palaeogeography,Paleoclimatology, Palaeoecology*, **107**, 65-78.

Goñi, M.A., Ruttenberg, K.C., Eglinton, T.I. (1998) A reassessment of the sources and importance of land-derived organic matter in surface sediments from the Gulf of Mexico. *Geochimica et Cosmochimica Acta* **62**, 3055-3075.

Gough, M.A., Fauzi, R., Mantoura, C., Preston, M. (1993) Terrestrial plant biopolymers in marine sediments. *Geochimica et Cosmochimica Acta*, **57**, 945-964.

Griffin, D.L. (2002) Aridity and humidity: two aspects of the late Miocene climate of North Africa and the Mediterranean. *Palaeogeography, Palaeoclimatology, Palaeoecology*, **182**, 65-91

Grimalt, J.O., Calvo, E., Pelejero, C., (2001) Sea Surface Paleotemperature Errors in UK37 Estimation Due to Alkenone Measurements Near the Limit of Detection. *Paleoceanography*, **16**, 226-232.

Haug, G.H., Ganopolski, A., Sigman, D.M., Rosell-Mele, A., Swann, G.E.A., Tiedemann, R., Jaccard, S.L., Bollmann, J., Maslin, M.A., Leng, M.J., Eglinton, G. (2005) North Pacific seasonality and the glaciation of North America 2.7million years ago. *Nature*, **433**, 821-825.

Haug, G.H., Highen, K.A., Sigman, D.M., Peterson, L.C., Röhl, U. (2001) Southward migration of the Intertropical Convergence Zone through the Holocene. *Science*, **293**, 1304-1307.

Hay, W.W., Brock, J.C. (1992) Temporal variation in intensity of upwelling off Soutwest Africa. In: C.P. Summerhayes, W.L. Prell, K.C. Emeis (Eds.), *Upwelling Systems: Evolution Since the Early Miocene*, *64* (Ed. by C.P. Summerhayes, W.L. Prell, K.C. Emeis), pp. 463-448. Geological Society Special Publication.

Hays, J.D., Imbrie, J., Shackleton, N.J. (1976) Variations in the Earth's Orbit: Pacemaker of the Ice Ages. *Science*, **194**, 1121-1132

Hedges, J. I., Keil, R.G. (1995) Sedimentary organic matter preservation: an assessment and speculative synthesis. *Marine Chemistry* **49**, 137-139.

Hedges, J.I., Keil, R.G., Benner, R. (1997) What happens to terrestrial organic matter in the ocean? *Organic Geochemistry* **27**, 195-212.

Hedges, J.I., Oades, J.M. (1997) Comparative organic geochemistries of soils and marine sediments. *Organic Geochemistry*, **27**(7/8), 319-361.

Herbert, T.D, (2001) Review of alkenone calibrations (culture, water column, and sediments. *Geochemistry, Geophysics, Geosystems, **2,** doi.10.1029*/2000GC000055.

Herbert, T.D., and Schuffert, J.D. (1998) Alkenone unsaturation estimates of late Miocene through late Pliocene sea-surface temperatures at Site 958. *In* Firth, J.V. (Ed.), *Proc. ODP, Sci. Results,* 159T: College Station, TX (Ocean Drilling Program), 17–21. doi:10.2973/odp.proc.sr.159t.063.1998

Herbert, T.D., Schuffert, J.D., Thomas, D., Lange, C., Weinheimer, A., Peleo-Alampay, A., Herguera, J.C., (1998) Depth and Seasonality of Alkenone Production along the California Margin Inferred from a Core Top Transect. *Paleoceanography*, 13 (3), 263-271.

Hilgen, F.J. (1991) Astronomical calibration of Gauss to Matuyama sapropels in the Mediterranean and implication for the Geomagnetic Polarity Time Scale. *Earth and Planetary Science Letters*, **104**, 226-244.

Hilgen, F.J., Krijgsman, W., Langereis, C.G., Lourens, L.J., Santarelli, A., Zachariasse, W.J., (1995) Extending the astronomical (polarity) time scale into the Miocene. *Earth and Planetary Science Letters*, **136,** 495-510.

Hinrichs, K.-U., 1998. Late quaternary paleoenvironmental conditions indicated by marine and terrestrial molecularbiomarkers in sediments from the Santa Barbara Basin. In:Wilson, R.C., Tharp, V.L. (Eds.), Proceedings of

the Fourteenth Annual Pacific Climate (PACLIM) Workshop, April 6–9, 1997. Interagency Ecological Program, Technical Report 57, California Department of Water Resources, pp. 125–133.

Hodell, D.A., Elmstrom, K.M., Kennett, J.P. (1986) Late Miocene benthic d18O changes, global ice volume, sea level, and the "Messinian salinity crisis". *Nature*, **320**, 411-414.

Hofmann, P., Beckmann, B., Wagner, T., (2003) A millenial- to centennial-scale record of African climate variability and organic carbon accumulation in the Coniacian-Santonian eastern tropical Atlantic (ODP Site 959, off Ivory Coast/Ghana). *Geology*, **31**(2), 135-138.

Höll, C., Kemle-von Mücke, S. (2000) Late Quaternary Upwelling Variations in the Eastern Equatorial Atlantic Ocean as Inferred from Dinoflagellate Cysts, Planktonic Foraminifera, and Organic Carbon Content. *Quaternary Research*, **54,** 58-67.

Holtvoeth, J., Wagner, T., Schubert, C., Horsfield, B., Mann, U. (2001) Late Quaternary supply of terrigenous organic matter to the Congo Deep Sea Fan (ODP Site 1075): Implications for equatorial African paleoclimate. *Geo-Marine Letters*, **21**, 23-33.

Holz, C., Stuut, J.-B.W., Henrich, R., Meggers, H., (2007) Variability in terrigenous sedimentation processes off northwest Africa and its relation to climate changes: Inferences from grain-size distributions of a Holocene marine sediment record. *Sedimentary Geology*, 202(3), 499-508.

Holzwarth, U., Meggers, H., Esper, O., Kuhlmann, H., Freudenthal, T., Hensen, C., Zonneveld, K.A.F., (2010) NW African climate variations during the last 47,000 years: Evidence from organic-walled dinoflagellate cysts. *Palaeogeography, Palaeoclimatology, Palaeoecology*, **291**(3-4), 443-455.

Hooghiemstra, H. (1998) Variations of the NW African trade wind regime during the last 140,000 years: changes in pollen flux evidenced by marine sediment records. In: M. Leinen, M. Sarnthein (Eds.), *Paleoclimatology and Paleometeorology: modern and past patterns of global atmospheric transport*, *ASI Series C 282* (Ed. by M. Leinen, M. Sarnthein), pp. 733-770. NATO, ASI Series C 282.

Hooghiemstra, H., A. Bechler, and H.- J. Beug (1987), Isopollen maps for 18,000 years B.P. of the Atlantic offshore of northwest Africa: Evidence for paleowind circulation, Paleoceanography, **2**(6), 561-582.

Hopmans, E.C., Weijers, J.W.H., Schefuß, E., Herfort, L., Damsté, J.S.S., Schouten, S. (2004) A novel proxy for terrestrial organic matter in

sediments based on branched and isoprenoid tetraether lipids. *Earth and Planetary Science Letters*, **224**, 107 - 116.

Hovan, S.A., (1995) Late Cenozoic atmospheric circulation intensity and climatic history recorded by eolian deposition in the eastern Equatorial Pacific Ocean, Leg 138. In: N.G. Pisias, L.A. Mayer, T.R. Janecek, e. al. (Eds.), *Ocean Drilling Program Scientific Results Volume, Leg 138* (Ed. by N.G. Pisias, L.A. Mayer, T.R. Janecek, e. al.), pp. 615-625. College Station, TX (Ocean Drilling Program), USA.

Huang, Y., Clemens, S.C., Liu, W., Wang, Y., Prell, and W.L. (2007) Large-scale hydrological change drove the late Miocene C4 plant expansion in the Himalayan foreland and Arabian Peninsula. *Geology*, **35**, 531-534.

Huang, Y., Dupont, L., Sarnthein, M., Hayes, J.M., Eglinton, G. (2000) Mapping of C4 plant input from North West Africa into North East Atlantic sediments. *Geochimica et Cosmochimica Acta*, **64,** 3505-3513.

Huang, Y., Freemen, K.H., Eglinton, T.I., Street-Perrott, F.A., (1999) d13C analyses of individual lignin phenols in Quatenary lake sediments: a novel proxy for deciphering past terrestrial vegetation changes. *Geology*, **27**(5), 471-474.

Huang,Y., Collister,J.W.,Chester, J., Eglinton, G. (1993) Molecular and d13C mapping of aeolian input of organic compounds into marine sediments in the Northeastern Atlantic. In: Øygard, K. (Ed.), *Organic Geochemistry*. Falch Hurtigtrykk,Oslo,pp. 523–528.

Imbrie, J., Hays, J.D., Martinson, D.G., McIntyre, A., Mix, A.C., Morley, J.J., Pisaias, N.G., Prell, W.L., Shackleton, N.J. (1984) The orbital theory of Pleistocene climate: support from a revised chronology of marine $\delta^{18}O$ record. In: A.L. Berger, J. Imbrie, J.D. Hays, J. Kulka, J. Saltzman (Eds.), *Milankovitch and Climate (Part 1)* (Ed. by A.L. Berger, J. Imbrie, J.D. Hays, J. Kulka, J. Saltzman), pp. 269-305. Reidel, Hingham, Massechussets.

Ingham, M.C., 1970: Coastal upwelling in the northwestern gulf of Guinea. *Bulletin of Marine Science*, **20**, 1-34.

Ishiwatari, R., Yamada, K., Matsumoto, K., Houtatsu, M., Naraoka, H. (1999) Organic molecular and carbon isotopic records of the Japan Sea over the past 30 kyr. *Palaeoceanography*, **14**, 260-270.

Itambi, A.C., von Dobeneck, T., Adegbie, A.T., (2009) Millennial-scale precipitation changes over central Africa during the late quaternary and Holocene: Evidence in sediments from the Gulf of Guinea. *Journal of Quaternary Science*, **25**(3), 267-279.

Jeng, W.-L. (2006) Higher plant *n*-alkane average chain length as an indicator of petrogenic hydrocarbon contamination in marine sediments. *Marine Chemistry*, **102,** 242-251.

Jennings, A., Knudsen, K., Hald, M., Hansen, C. and Andrews, J. (2002) A mid-Holocene shift in Arctic sea-ice variability on the East Greenland Shelf. *The Holocene* **12**, 49–58

Jiménez-Moreno, G., Fauquette, S., Suc, J.-P., Miocene to Pliocene vegetation reconstruction and climate estimates in the Iberian Peninsula from pollen data. *Review of Palaeobotany and Palynology*, **162**(3), 403-415.

Johnsen, S.J., Clausen, H.B., Dansgaard, W., Fuhrer, K., Gundestrup, N., Hammer, C.U., Iversen, P., Jouzel, J., Stauffer, B., steffensen, J.P. (1992) Irregular glacial interstadials recorded in a new Greenland ice core. *Nature*, **359,** 311-313.

Joussaume, S. and 35 co-authors, 1999. Monsoon changes for 6000 years ago: results of 18 simulations from the Paleoclimate Modeling Intercomparison Project (PMIP). *Geophysical Research Letters,* **26**, 859-862.

Jung, S.J.A., Davies, G.R., Ganssen, G.M., Kroon, D. (2004) Stepwise Holocene aridification in NE Africa deduced from dust-borne radiogenic isotope records. *Earth and Planetary Science Letters*, **221,** 27-37.

Kannenberg, E.L., Poralla, K. (1999) Hopanoid Biosynthesis and Function in Bacteria. *Naturwissenschaften*, **86**, 168-176.

Karner, M.B., DeLong, E.F., Karl, D.M. (2001) Archaeal dominance in the mesopelagic zone of the Pacific Ocean. *Nature, **437***, 543–546.

Kennett, J.P. (1982) *Marine Geology*. Prentice Hall, Englewood Cliffs, N. J.

Keough, B.P., Schmidt, T.M., Hicks, R.E. (2003) Archaeal nucleic acids in picoplankton from great lakes on three continents. *Microbial Ecology* **46**, 238–248.

Kienast, M., Kienast, S.S., Calvert, S.E., Eglinton, T.I., Mollenhauer, G., Francois, R., Mix, A.C. (2006) Eastern Pacific cooling and Atlantic overturning circulation during the last deglaciation. *Nature*, **443**, 846-849.

Kim, J.H., Ludwig, W., Schouten, S., Kerhervé, P., Herfort, L., Bonnin, J., Sinninghe Damsté, J.S. (2007) Impact of flood events on the transport of terrestrial organic matter to the ocean: A study of the Têt River (SW France) using the BIT index. *Organic Geochemistry*, **38**, 1593-1606.

Kim, J.H., Schouten, S., Buscali, R., Ludwig, W., Bonnin, J., Sinninghe Damsté, J.S. (2006) Origin and distribution of terrestrial organic matter in the NW Mediterranean (Gulf of Lion): application of the newly developed BIT index. *Geochemistry Geophysics Geosystems,* **7**, Q11017 doi: 10.1029/2006GC001306.

Kirst, G.J., Schneider, R.R., Müller, P.J., von Storch, I., Wefer, G. (1999) Late Quaternary Temperature Variability in the Benguela Current System Derived from Alkenones. *Quaternary Research*, **52**, 92-103.

Kollatukudy, P.E. (1976) *Chemistry and Biochemistry of Natural Waxes*. Elsevier, Amsterdam.

Korte, C., Kozur, H.W., Veizer, J. (2005) [delta]13C and [delta]18O values of Triassic brachiopods and carbonate rocks as proxies for coeval seawater and palaeotemperature. *Palaeogeography, Palaeoclimatology, Palaeoecology*, **226**, 287-306.

Krijgsman, W., Hilgen, F.J., Langereis, C.G., Santarelli, A., Zachariasse, W.J. (1995) Late Miocene magnetostratigraphy, biostratigraphy and cyclostratigraphy in the Mediterranean. *Earth and Planetary Science Letters*, **136**, 475-494.

Krijgsman, W., Langereis, C.G., Daams, R., van der Meulen, A.J. (1994) Magnetostratigraphic dating of the middle Miocene climate change in the continental deposits of the Aragonian type area in the Calatayud-Teruel basin (Central Spain). *Earth and Planetary Science Letters*, **128,** 513-526.

Krom M.D. and Berner R.A. (1983) A rapid method for the determination of organic and carbonate method in geological samples. *Journal of Sedimentary Petrology*, **53**, 660-663

Kuhlmann, H., Freudenthal, T., Helmke, P., Meggers, H. (2004) Reconstruction of paleoceanography off NW Africa during the last 40,000 years: influence of local and regional factors on sediment accumulation. *Marine Geology*, **207,** 209-224.

Kutzbach, J.E. (1981) Monsoon Climate of the Early Holocene: Climate Experiment with the Earth's Orbital Parameters for 9000 Years Ago. *Science*, **214**, 59-61.

Kutzbach, J.E., Liu, Z. (1997) Response of the African monsoon to orbital forcing and ocean feedbacks in the middle Holocene. *Science*, **278**, 440-443.

Kutzbach, J.E., Prell, W.L., Ruddiman, W.F. (1993) Sensitivity of Eurasian Climate to Surface Uplift of the Tibetan Plateau. *The Journal of Geology*, **101**, 177-190.

Kuypers, M.M.M., Pancost, R., Shinninghe Damsté, J.S. (1999) A large and abrupt fall in atmospheric CO_2 concentration during Cretaceous times. *Nature*, **399**, 342-345.

Lamb, H.F., Gasse, F., Benaddour, A., El Hamouti, N., van der Kaars, S., Perkins, W.T., Pearce, N.J., Roberts, C.N. (1995) Relation between century-scale Holocene arid intervals in tropical and temperate zones. *Nature*, **373**, 134-137.

Laskar, J., Joutel, F., and Boudin, F. (1993) Orbital, precessional, and insolation quantities for the Earth from −20 Myr to +10 Myr', *Astron. Astroph.* **270**, 522–533.

Lawrence K.T, Herbert T.D, Dekens P.S, Ravelo A.C (2007) The application of the alkenone organic proxy to the study of Plio-Pleistocene climate. In *Deep time perspectives on climate change: marrying the signal from computer models & biological proxies* Williams M, Haywood A.M, Gregory J, Schmidt D pp. 539–562. Eds. London, UK:Geological Society of London and The Micropalaeontological Society.

Lawrence, K.T., Herbert, T.D., Brown, C.M., Raymo, M.E., Haywood, A.M. (2009) High-amplitude variations in North Atlantic sea surface temperature during the early Pliocene warm period. *Paleoceanography*, **24**, PA2218.

Lawrence, K.T., Liu, Z., Herbert, T.D. (2006) Evolution of the Eastern Tropical Pacific Through Plio-Pleistocene Glaciation. *Science*, **312**, 79-83.

Lea, D.W., Mashiotta, T.A., Spero, H.J. (1999) Controls on magnesium and strontium uptake in planktonic foraminifera determined by live culturing. *Geochimica et Cosmochimica Acta*, **63**, 2369-2379.

Lea, D.W., Pak, D.K., Peterson, L.C., Hughen, K.A. (2003) Synchroneity of Tropical and High-Latitude Atlantic Temperatures over the Last Glacial Termination. *Science*, **301**, 1361-1364.

Lézine, A.-M. (1991) West African paleoclimates during the last climatic cycle inferred from an Atlantic deep- sea pollen record. *Quaternary Research*, **35**, 456-463.

Lichtfouse, É., Derenne, S., Mariotti, A., Largeau, C. (1994) Possible algal origin of long chain odd *n*-alkanes in immature sediments as revealed by distributions and carbon isotope ratios. *Organic Geochemistry*, **22**, 1023-1027.

Longhurst, A.R., 1962: A review of the Oceanography of the Gulf of Guinea. *Bull. Inst. Afr. Noire*, **24**, 633-663.

Lyle, M.W., Prahl, F.G., Sparrow, M.A. (1992) Upwelling and productivity changes inferred from a temperature record in the central equatorial Pacific. *Nature*, **355**, 812-815.

Madureira, L.S., van Krefeld, S.A., Eglinton, G., Conte, M.H., Ganssen, G., van Hinte, J.A., Ottens, J.J. (1997) Late Quaternary high-resolution biomarker and other sedimentary climate proxies in a northeast Atlantic core. *Paleoceanography*, **12,** 255-269.

Marlowe, I.T., Brassell, S.C., Eglinton, G., Green, J.C. (1984) Long chain unsaturated ketones and esters in living algae and marine sediments. *Organic Geochemistry*, **6**, 135-141.

Marlowe, I.T., Brassell, S.C., Eglinton, G., Green, J.C. (1990) Long-chain alkenones and alkyl alkenoates and the fossil coccolith record of marine sediments. *Chemical Geology*, **88**, 349-375.

Marret, F., Scourse, J., Versteegh, G., Jansen, J.H.F., Schneider. (2001) Integrated marine and terrestrial evidence for abrupt Congo River palaeodischarge fluctuations during the last deglaciation. *Journal of Quaternary Science* **16**, 761–766.

Martinez, P., Bertrand, P., Shimmield, G.B., Karen, C., Jorissen, F.J., Foster, J., Dignan, M., (1999) Upwelling intensity and ocean productivity changes off Cape Blanc (northwest Africa) during the last 70,000 years: geochemical and micropalaeontological evidence. *Marine Geology*, **158** (1-4), 57-74.

Martrat, B., Grimalt, J.O., Lopez-Martinez, C., Cacho, I., Sierro, F.J., Flores, J.A., Zahn, R., Canals, M., Curtis, J.H., Hodell, D.A. (2004) Abrupt Temperature Changes in the Western Mediterranean over the Past 250,000 Years. *Science*, **306 ,**1762-1765.

Martrat, B., Grimalt, J.O., Shackleton, N.J., de Abreu, L., Hutterli, M.A., Stocker, T.F. (2007) Four Climate Cycles of Recurring Deep and Surface Water Destabilizations on the Iberian Margin. *Science*, **317,** 502-507.

Marty, J.C., Saliot, A. (1982) Aerosols in equatorial Atlantic air: *n*-alkanes as a function of particle size. *Nature*, **298**, 144-147.

Marzi, R., Torkelson, B.E., Olson, R.K. (1993) A revised carbon preference index. *Organic Geochemistry*, **20**, 1303-1306.

Mascle, J., Lohmann, G.P., Clift, P.D.,(1996) Proceedings of the Ocean Drilling Program, Initial Reports, 159, College Station, TX (Ocean Drilling Program).

Maslin, M.A., Christensen, B. (2007) Tectonics, orbital forcing, global climate change, and human evolution in Africa: introduction to the African paleoclimate special volume. *Journal of Human Evolution*, **53,** 443-464.

Maslin, M.A., Li, X.S., Loutre, M.F., Berger, A. (1998) The contribution of orbital forcing to the progressive intensification of northern hemisphere glaciation. *Quaternary Science Reviews*, **17**, 411-426.

Mazurek, M.A. and Simoneit, B.R.T. (1984). Characterization of biogenic and petroleum-derived organic matter in aerosols over remote, rural and urban areas. In: *Identification and Analysis of Organic Pollutants in Air*, ACS Symp., L.H. Keith (ed.), Ann Arbor Science Butterworth Publishers, Woburn, MA, pp. **353-370.**

McCaffrey, M.A., Farrington, J.W., Repeta, D.J. (1990) The organic geochemistry of Peru margin surface sediments: I. A comparison of the C37 alkenone and historical El Niño records. *Geochimica et Cosmochimica Acta*, **54,** 1671-1682.

McClymont, E.L., Rosell-Mele, A. (2005) Links between the onset of modern Walker circulation and the mid-Pleistocene climate transition. *Geology*, **33**, 389-392.

McIntosh, S.K., McIntosh, R.J. (1983) Current Directions in West African Prehistory. *Annual Review of Anthropology*, **12**, 215-258.

McIntyre, A., (1970) Gephyrocapsa protohuxleyi sp. n. a possible phyletic link and index fossil for the Pleistocene. *Deep Sea Research and Oceanographic Abstracts*, 17(1), 187-188, IN21-IN22, 189-190.

McIntyre, A., Molfino, B. (1996) Forcing of Atlantic equatorial and subpolar millennial cycles by precession. *Science*, **274**, 1867-1870.

McIntyre, A., W. F. Ruddiman, K., Mix., A.C. (1989) Surface water response of the equatorial Atlantic Ocean to orbital forcing, *Paleoceanography,* **4,** 19-55.

Ménot, G., Bard, E., Rostek, F., Weijers, J.W.H., Hopmans E.C., Schouten, S., Sinninghe Damsté, J.S. (2006). Early reactivation of European rivers during the last deglaciation. *Science* **313**, 1623-1625.

Meyers, P.A., (1997) Organic geochemical proxies of paleoceanographic, paleolimnologic, and paleoclimatic processes. *Organic Geochemistry*, **27**, 213-250.

Mikolajewicz, U., Maier-Reimer, E., Crowley, T.J., Kim, K.-Y., (1993) Effect of Drake and Panamanian Gateways on the Circulation of an Ocean Model. *Paleoceanography*, **8**, 409-426.

Milankovitch, M. (1930). Mathematische Klimalehre und astronomische Theorie der Klimaschwankungen. *In* "Handbuch der Klimatologie, **1."** (W. Köppen, and R.

Mittelstaedt, E. (1991) The ocean boundary along the northwest African coast: Circulation and oceanographic properties at the sea surface. *Progress In Oceanography*, **26**, 307-355.

Mix, A.C., Morey, A.E. (1996) Climate feetback and Pleistocene variations in the Atlantic South Equatorial Current. In: G. Wefer, W.H. Berger, G. Siedler, D. Webb (Eds.), *The South Atlantic: Present and Past Circulation* (Ed. by G. Wefer, W.H. Berger, G. Siedler, D. Webb), pp. 503-525, Springer, Berlin.

Molfino, B., McIntyre, A. (1990) Precessional forcing of nutricline dynamics in the Equatorial Atlantic. *Science*, **249**, 766-769.

Molnar, P., England, P., Martinod, J. (1993) Mantle Dynamics, Uplift of the Tibetan Plateau, and the Indian Monsoon. *Review Geophysics,* **31**, 357-396.

Mudelsee, M., Schulz, M. (1997) The Mid-Pleistocene climate transition: onset of 100 ka cycle lags ice volume build-up by 280 ka. *Earth and Planetary Science Letters*, **151**, 117-123.

Mulitza, S., Rühlemann, C. (2000) African Monsoonal Precipitation Modulated by Interhemispheric Temperature Gradients. *Quaternary Research*, **53,** 270-274.

Müller, P.J., Fischer, G.(2001) A 4-year sediment trap record of alkenones from the filamentous upwelling region off Cape Blanc, NW Africa and a comparison with distributions in underlying sediments. *Deep Sea Research Part I: Oceanographic Research Papers*, **48**, 1877-1903.

Müller, P.J., Kirst, G., Ruhland, G., von Storch, I., Rosell-Melé, A. (1998) Calibration of the alkenone paleotemperature index UK37' based on core-tops from the eastern South Atlantic and the global ocean (60°N-60°S). *Geochimica et Cosmochimica Acta*, **62,** 1757-1772.

Müller, P.J., Suess, E. (1979) Productivity, sedimentation rate, and sedimentary organic matter in the oceans--I. Organic carbon preservation. *Deep Sea Research Part A. Oceanographic Research Papers*, **26**, 1347-1362.

Nave, S., Salgueiro, E., Abrantes, F., (2003) Siliceous sedimentary record of the last 280 kyr in the Canary basin (NW Africa). *Marine Geology*, 196(1-2), 21-35.

Niebler, H.-S., Arz, H.W., Donner, B., Mulitza, S., Pätzold, J.., Wefer, G.(2003) Sea surface temperatures in the equatorialand South Atlantic Ocean during the Last Glacial Maximum (23–19 ka). *Paleoceanography*, **18**(3): 1069.

Niedermeyer, E.M., SchefuÃŸ, E., Sessions, A.L., Mulitza, S., Mollenhauer, G., Schulz, M., Wefer, G., Orbital- and millennial-scale changes in the hydrologic cycle and vegetation in the western African Sahel: Insights from individual plant wax Î´D and Î´¹³C. *Quaternary Science Reviews*, **29** (23-24), 2996-3005.

Nikolaev, S.D., Oskina, N.S., Blyum, N.S., Bubenshchikova, N.V. (1998) Neogene-Quaternary variations of the Pole-Equator temperature gradient of the surface oceanic waters in the North Atlantic and North Pacific. *Global and Planetary Change*, **18,** 85-111.

Norris, R.D. (1998) Miocene-Pliocene surface water hydrography of the eastern Equatorial Atlantic. In: J. Mascle, G.P. Lohman, M. Moullard (Eds.), *Ocean Drilling Program Scientific Results Volume, Leg 159* (Ed. by J. Mascle, G.P. Lohman, M. Moullard), pp. 539-555. College Station, TX (Ocean Drilling Program), USA.

Nürnberg, D., Bijma, J., Hemleben, C. (1996) Assessing the reliability of magnesium in foraminiferal calcite as a proxy for water mass temperatures. *Geochimica et Cosmochimica Acta*, **60**, 803-814.

Nürnberg, D., Müller, A. and Schneider, R.R. (2000) Paleo-seasurface temperature calculations in the equatorial east Atlantic from Mg/Ca ratios in planktic foraminifera: A comparison to sea surface temperature estimates from, oxygen isotopes,and foraminiferal transfer functions. *Paleoceanography*, **15**(1): 124–134.

Nürnberg, D., Müller, A., Schneider, R.R., (2000) Paleo-Sea Surface Temperature Calculations in the Equatorial East Atlantic from Mg/Ca Ratios in Planktic Foraminifera: A Comparison to Sea Surface Temperature Estimates from U37K′, Oxygen Isotopes, and Foraminiferal Transfer Function. *Paleoceanography*, **15**(1), 124-134.

O'Brien, S.R., Mayewski, P.A., Meeker, L.D., Meese, D.A., Twickler, M.S., Whitlow, S.I. (1995) Complexity of Holocene Climate as Reconstructed from a Greenland Ice Core. *Science*, **270,** 1962-1964.

Ohkouchi, N., Kawamura, K., Kawahata, H., Okada, H. (1999) Depth ranges of alkenone production in the central Pacific Ocean. *Global Biogeochemical Cycles*, **13**, 695-704.

Ohkouchi, N., Kawamura, K., Taira, A. (1997) Molecular paleoclimatology: reconstruction of climate variabilities in the late Quaternary. *Organic Geochemistry*, **27**(3/4), 173-183.

Okada, H., Honjo, S., (1973) Distribution of oceanic coccolithophorids in th Pacific. *Deep Sea Res*, **20**(4), 355-374.

Okada, H., McIntyre, A., (1977) Modern Coccolithophores of the Pacific and North Atlantic Oceans. *Micropaleontology*, **23**(1), 1-55.

O'Leary, M.H. (1981) Carbon isotope fractionation in plants. *Phytochemistry*, **20,** 553-567.

Oros, D.R., Standley, L.J., Chen, X., Simoneit, B.R.T. (1999) Epicuticular wax compositions of predominant conifers of western North America. *Zeitschrift für Naturforschung* **54C**, 17–24.

Ourisson, G., Albrecht, P. (1992). 1. Geohopanoids: The most abundant natural products on earth, *Hopanoids* **25**, 398-402.

Pagani, M., Arthur, M.A., Freeman, K.H. (1999) Miocene evolution of atmospheric carbon dioxide. *Palaeoceanography*, **14**, 273-292.

Pancost, R.D., Boot, C.S., (2004) The palaeoclimatic utility of terrestrial biomarkers in marine sediments. *Marine Chemistry***, 92**(1-4 SPEC. ISS.), 239-261.

Parkin, D.W., Shackleton, N.J. (1973) Trade Wind and Temperature Correlations down a Deep-sea Core off the Saharan Coast. *Nature*, **245**, 455-457.

Partridge, T.C., Demenocal, P.B., Lorentz, S.A., Paiker, M.J., Vogel, J.C. (1997) Orbital forcing of climate over South Africa: A 200,000-year rainfall record from the Pretoria saltpan. *Quaternary Science Reviews*, **16,** 1125-1133.

Pastouret, L., chamley, H., Delibrias, G., Duplessy, J.C., Thiede, J. (1978) Late Quaternary climatic changes in the western tropical Africa deduced from deep-sea sedimentation off the Niger delta. *Oceanologica Acta*, **1,** 217-232.

Pearson, A., Leavitt, W.D., Sáenz, J.P., Summons, R.E., Tam, M.C.-M., Close, H.G. (2009). Diversity of hopanoids and squalene-hopene cyclises across a tropical land-sea gradient. *Environmental Microbiology***, 11**, 1208-1223.

Pelejero, C., Calvo, E. (2003) The upper end of the UK37' temperature calibration revisited. *Geochemistry Geophysics Geosystems,* **4**, 1014.

Percival, D.B. and Walden, A.T. (1993) Spectral Analysis for Physical Applications. Cambridge University Press, pp 1-583.

Peterse, F., Kim, J.-H., Schouten, S., Kristensen, D.K., Koç, N., Sinninghe Damsté, J.S. (2009) Constraints on the application of the MBT/CBT palaeothermometer at high latitude environments (Svalbard, Norway). *Organic Geochemistry*, **40,** 692-699.

Peterson, R.G., Stramma, L. (1991) Upper-level circulation in the South Atlantic Ocean. *Progress in Oceanography*, **26**, 1-73.

Philander, S., Pacanowski, R. (1986), The Mass and Heat Budget in a Model of the Tropical Atlantic Ocean. *Journal of Geophysical Research,* **91**, 14212-14220.

Pisias, N.G., Mayer, L.A., Mix, A.C. (1995) Paleoceanography of the eastern Equatorial Pacific during the Neogene: synthesis of Leg 138 drilling results. In: N.G. Pisias, L.A. Mayer, T.R. Janecek, e. al. (Eds.), *Ocean Drilling Program Scientific Results Volume, Leg 138* (Ed. by N.G. Pisias, L.A. Mayer, T.R. Janecek, e. al.), pp. 5-21. College Station, TX (Ocean Drilling Program), USA.

Pokras, E.M., Mix, A.C. (1985) Eolian evidence for spatial variability of Late Quaternary climates in tropical Africa. *Quaternary Research*, **24**, 137-149.

Powers, L.A., Johnson, T.C., Werne, J.P., Castaňeda, I.S., Hopmans, E.C., Sinninghe Damsté J.S., Schouten, S. (2004) Crenarchaeotal membrane lipids in lake sediments: A new paleotemperature proxy for continental paleoclimate reconstruction *Geology,* **32**, 613-616.

Powers, L.A., Werne, J.P., Johnson, T.C., Hopmans, E.C., Damste, J.S.S., Schouten, S. (2004) Crenarchaeotal membrane lipids in lake sediments: A new paleotemperature proxy for continental paleoclimate reconstruction. *Geological Society of America*, **32**, 613-616.

Poynter, J.G., Eglinton, G. (1991) A biomarker concept - strengths and weaknesses. *Fresenius Journal of Analytical Chemistry*, **339**, 725-731.

Poynter, J.G., Farrimond, P., Brassell, S.C.,Eglinton,G.(1989a). Molecular stratigraphic study of sediments from Holes 658A and 660A, Leg 108. In: Ruddimann, W., Sarnthein,M. et al. (Eds.), *Proceedings of the Ocean Drilling Program. Scientific Results* **108**, 387–394.

Poynter, J.G., Farrimond, P., Robinson, N., Eglinton, G. (1989b) Aeolian-derived higher plant lipids in the marine sedimentary record: links with Paleoclimate. In: M. Leinen, M. Sarnthein (Eds.), *Paleoclimatology and Paleometeorology: Modern and past patterns of global atmospheric*

transport (Ed. by M. Leinen, M. Sarnthein), pp. 435-462. Kluwer Academic Publishers.

Prahl, F.G., Collier, R.B., Dymond, J., Lyle, M., Sparrow, M.A. (1993) A biomarker perspective on prymnesiophyte productivity in the northeast Pacific Ocean. *Deep Sea Research Part I: Oceanographic Research Papers*, **40**, 2061-2076.

Prahl, F.G., Dymond, J., Sparrow, M.A., (2000) Annual biomarker record for export production in the central Arabian Sea. *Deep Sea Research II*, **47**, 1581-1604.

Prahl, F.G., Muehlhausen, L.A., Zahnle, D.B. (1988) Further evaluation of long-chain alkenones as indicators of paleoceanographic conditions. *Geochimica et Cosmochimica Acta*, **52**, 2303-2310.

Prahl, F.G., Wakeham, S.G. (1987) Calibration of unsaturation patterns in long-chain ketone compositions for palaeotemperature assessment. *Nature*, **330**, 367-369.

Prell, W.L., Kutzbach, J.E. (1987) Monsoon variability over the past 150,000 years. *Journal of Geophysical Research*, **92**, 8411-8425.

Prell, W.L., Kutzbach, J.E. (1992) Sensitivity of the Indian monsoon to forcing parameters and implications for its evolution. *Nature*, **360**, 647-652.

Priestley, M.B. (1988) *Non linear and Non stationary Time Series analysis*. Academic Press, London pp.1-237.

Prospero, J.M. (1981) Arid regions as sources of mineral aerosols in the marine environment. In: Pewe, T.L. (Eds.), *Desert Dust: Origins, Characteristics and Effects on man.* Geological Society of America **186**, 71-86.

Prospero, J.M., Ginoux, P., Torres, O., Nicholson, S.E., Gill, T.E. (2002) Environmental characterization of global sources of atmospheric soil dust identified with the NIMBUS 7 Total Ozone Mapping Spectrometer (TOMS) absorbing aerosol product. *Rev. Geophys.*, **40**, 1002.

Prospero, J.M., Lamb, P.J. (2003) African Droughts and Dust Transport to the Caribbean: Climate Change Implications. *Science*, **302**, 1024-1027.

Quade, J., Cerling, T.E. (1995) Expansion of C4 grasses in the Late Miocene of Northern Pakistan: evidence from stable isotopes in paleosols. *Palaeogeography, Palaeoclimatology, Palaeoecology*, **115**, 91-116.

Ratmeyer, V., Balzer,W., Bergametti, G., Chiapello, I., Fischer, G., Wyputtaet U. (1999) Seasonal impact of mineral dust on deep-ocean particle flux in the eastern subtropical Atlantic Ocean. *Marine Geology,* **159**, 241-252.

Ravelo, A.C., Andreasen, D. 2000. Enhanced circulation duringa warm period. Geophys. Res. Lett. **27**, 1001-1004.

Raymo, M.E., Grant, B., Horowitz, M., Rau, G.H. (1996) Mid-Pliocene warmth: stronger greenhouse and stronger conveyer. *Marine Micropaleontology*, **27**, 313-326.

Raymo, M.E., Hodell, D., Jansen, E. (1992) Response of Deep Ocean Circulation to Initiation of Northern Hemisphere Glaciation (3-2 Ma). *Paleoceanography*, **7,** 645-672.

Raymo, M.E., Ruddiman, W.F. (1992) Tectonic forcing of late Cenozoic climate. *Nature*, **359 ,**117-122.

Raymo, M.E., W.F. Ruddiman, N.J. Shackleton, and D. Oppo, 1990, Evolution of Atlantic-Pacific d13C gradients over the last 2.5 m.y., *Earth and Planetary Science Letters*, **97**, 353-368.

Rea, D.K. (1994) The paleoclimatic record provided by eolian deposition in the deep-sea: the geologic history of wind. *Review Geophysics,* **32**,159–195.

Rechka, J.A., Maxwell, J.R. (1988) Unusual long chain ketones of algal origin. *Tetrahedron Letters*, **29,** 2599-2600.

Redshaw, C., Cooke, M., Talbot, H., McGrath, S., Rowland, S. (2008) Low biodegradability of fluoxetine HCl, diazepam and their human metabolites in sewage sludge-amended soil. *Journal of Soils and Sediments*, **8,** 217-230.

Retallack, G.J., Tanaka, S., Tate, T. (2002) Late Miocene advent of tall grassland paleosols in Oregon. *Palaeogeography Palaeoclimatology Palaeoecol*ogy **183**, 329– 354.

Richardson, P., Philander, S. (1987) The Seasonal Variations of Surface Currents in the Tropical Atlantic Ocean: A Comparison of Ship Drift Data With Results From a General Circulation Model, *Journal Geophysics* Research, **92**, 715-724.

Richardson, P.L., McKee, T.K. (1984) Average Seasonal Variation of the Atlantic Equatorial Currents from Historical Ship Drifts. *Journal of Physical Oceanography*, **14**, 1226-1238.

Rieley, G., Collier, R.J., Jones, D.M., Eglinton, G. (1991) The biogeochemistry of Ellesmere Lake, U.K.-I: source correlation of leaf wax inputs to the sedimentary lipid record. *Organic Geochemistry*, **17**, 901-912.

Rieley, G., Collister, J.W., Stern, B., Eglinton, G.(1993) Gas chromatography/isotope ratio mass spectrometry of leaf wax *n*-alkanes

from plants of differing carbon dioxide metabolisms. *Rapid Communications in Mass Spectrometry*, **7**, 488-491.

Ries-Kautt, M., Albrecht, P. (1989) Hopane-derived triterpenoids in soils. *Chemical Geology*, **76**, 143-151.

Rinna, J., Guntner, U., Hinrichs, K.-U., Mangelsdorf, K., van derSmissen, J.H., Rullkotter, J., 1999. Temperature-related molecular proxies: degree of alkenone unsaturation andaverage chain length of *n*-alkanes. In: Wilson, R.C., Tharp, V.L. (Eds.),Proceedings of the Sixteenth Annual Pacific Climate(PACLIM).

Ritchie, J.C., Eyles, C.H., Haynes, C.V. (1985) Sediment and pollen evidence for an early to mid-Holocene humid period in the eastern Sahara. *Nature*, **314**, 6009), 352-355.

Roberts, N., 1998. In: *The Holocene,* Oxford, Blackwell, pp 1-316.

Rohmer, M (1993) The biosynthesis of the triterpenoids of the hopane series in eubacteria: a mine of new enzyme reactions. *Pure and Applied Chemistry,* **65**, 1293-1298.

Rohmer, M., Bouviernave, P., Ourisson, G. (1984) Distribution of hopanoid triterpenes in Prokaryotes. *Journal of General Microbiology*, **130**, 1137-1150.

Romankevich, E.A., (1984) *Geochemistry of Organic Matter in the Ocean*. Springer-Verlag, Berlin, Heidelberg, New York, Tokyo.

Romero, O. E., J.H. Kim, and B. Donner (2008), Submillennial- to- millennial variability of diatom production off Mauritania, NW Africa, during the last glacial cycle, *Paleoceanography*, **23**, PA3218, doi:10.1029/2008PA001601.

Rommerskirchen, F., Eglinton, G., Dupont, L., Günter, U., Wenzel, C., Rullkötter, J. (2003) A north to south transect of Holocene southeast Atlantic continental margin sediments: Relationship between aerosol transport and compound-specific land plant biomarker and pollen records. *Geochemistry Geophysics Geosystems*, **4**, doi: 10.1029/2003GC000541.

Rosell-Melé, A., Eglinton, G., Pflauman, U., Sarnthein, M. (1995) Atlantic core-top calibration of the $U^{K}37'$ index as a sea-surface palaeotemperature indicator. *Geochimica et Cosmochimica Acta*, **59**, 3099-3107.

Rosenthal, Y., Boyle, E.A., Slowey, N. (1997) Temperature control on the incorporation of magnesium, strontium, fluorine, and cadmium into benthic foraminiferal shells from Little Bahama Bank: Prospects for

thermocline paleoceanography. *Geochimica et Cosmochimica Acta*, **61**, 3633-3643.

Rosenthal, Y., Lohmann, G.P., Lohmann, K.C., Sherrell, R.M. (2000) Incorporation and Preservation of Mg in Globigerinoides sacculifer: Implications for Reconstructing the Temperature and 18O/16O of Seawater. *Paleoceanography*, **15**, 135-145.

Ruddiman, W.F., Janecek, T.R. (1989) Pliocene- Pleistocene biogenic and terrigenous fluxes at equatorial Atlantic Sites 662, 663 and 664. In: W.F. Ruddimann, M. Sarnthein, e. al. (Eds.), *Proceedings of the ODP, Scientific Results*, *108* (Ed. by W.F. Ruddimann, M. Sarnthein, e. al.), pp. 211-240. Ocean Drilling Program, College Station, Texas.

Ruddiman, W.F., McIntyre, A. (1984) Ice-age thermal response and climatic role of the surface Atlantic Ocean, 40Â°N to 63Â°N. *Geological Society of America Bulletin*, **95**, 381-396.

Rueda, G., Rosell-Melé, A., Escala, M., Gyllencreutz, R., Backman, J. (2009) Comparison of instrumental and GDGT-based estimates of sea surface and air temperatures from the Skagerrak. *Organic Geochemistry*, **40**, 287-291.

Sachs, J.P., Anderson, R.F. (2005) Increased productivity in the subantarctic ocean during Heinrich events. *Nature*, **434,** 1118-1121.

Sachs, J.P., Anderson, R.F., Lehman, S.J. (2001) Glacial Surface Temperatures of the Southeast Atlantic Ocean. *Science*, **293**, 2077-2079.

Sachse, D., Radke, J., Gaupp, R., Schwark, L., Lüniger, G., Gleixner, G., (2004) Reconstruction of palaeohydrological conditions in a lagoon during the 2nd Zechstein cycle through simultaneous use of δD values of individual *n*-alkanes and δ^{18}O an δ^{13} values of carbonates. *Int Journ Earth Sciences*, **93**, 554-564.

Sarnthein, M., Pflaumann, U., Ross, R., Tiedemann, R., Winn, K., (1992) Transfer functions to reconstruct ocean paleoproductivity: a comparison. In: C.P. Summerhayes, Prell, W.L. & Emeis, K.C. (Ed.), *Upwelling Systems: Evolution Since the Early Miocene*, *64* (Ed. by C.P. Summerhayes, Prell, W.L. & Emeis, K.C.), pp. 411- 427. Geological Society Special Publication.

Sarnthein, M., Tetzlaf, G., Koopmann, B., Wolter, K., Pflau-mann, U. (1981) Glacial and interglacial wind regimes over the eastern subtropical Atlantic and North-West Africa. *Nature*, **293**, 193-196.

Sarnthein, M., Thiede, J., Pflaumann, U., Erlenkeuser, H., Fütterer, D., Koopmann, B., Lange, H., Seibold, E. (1982) Atmospheric and oceanic circulation patterns off Northwest Africa during the past 25 million years. In: U. von Rad, K. Hinz, e. al. (Eds.), *Geology of the Northwest African Continental Margin* (Ed. by U. von Rad, K. Hinz, e. al.), pp. 545-604. Springer- Verlag, Berlin.

Sarnthein, M., Winn, K., Jung, S.J.A., Duplessy, J.-C., Labeyrie, L., Erlenkeuser, H., Ganssen, G. (1994) Changes in east Atlantic deepwater circulation over the last 30,000 years: eight time slice reconstructions. *Paleoceanography*, **9**, 209-267.

Sauer, P.E., Eglinton, T.I., Hayes, J.M., Schimmelmann, A., Sessions, A.L., (2001) Compound-specific D/H ratios of lipid biomarkers from sediments as a proxy for environmental and climatic conditions. *Geochimica et Cosmochimica Acta*, **65** (2), 213-222.

Schefuß, E., Ratmeyer, V., Stuut, J.-B., Jansen, H.F., Sinninghe Damsté, J.S. (2003) Carbon isotope analysis of *n*-alkanes in dust from the lower atmosphere over the central eastern Atlantic. *Geochimica et Cosmochimica Acta*, **67**, 1757-1767.

Schefuß, E., Schouten, S., Jansen, J. H. F. & Sinninghe Damste, J. S. (2003) African vegetation controlled bytropical sea surface temperatures in the mid-Pleistocene period. *Nature* **422**, 418–421

Schefuß, E., Schouten, S., Schneider, R.R. (2005) Climatic controls on central African hydrology during the past 20,000 years. *Nature*, **437**, 1003-1006.

Schefuß, E., Sinninghe Damsté, J.S., Jansen, J.H.F. (2004) Forcing of tropical Atlantic sea surface temperatures during the mid-Pleistocene transition. *Paleoceanography*, **19,** PA4029.

Schlünz, B., Schneider, R.R. (2000) Transport of terrestrial organic carbon to the oceans by rivers: re-estimating flux- and burial-rates. *International Journal of Earth Sciences*, **88**, 599-606.

Schmittner, A., Clement, A.C. (2002) Sensitivity of the thermohaline circulation to tropical and high latitude freshwater forcing during the last glacial-interglacial cycle. *Paleoceanography*, **17,** 1017.

Schneider, R.R., Müller, P.J., Ruhland, G., Meinecke, G., Schmidt, H., Wefer, G., (1996) Late Quaternary surface temperatures and productivity in the East-Equatorial South Atlantic: Response to changes in trade/monsoon wind forcing and surface water advection. In: G. Wefer, W.H. Berger, G. Siedler, D. Webb (Eds.), *The South Atlantic: Present and Past Circulation* (Ed. by G. Wefer, W.H. Berger, G. Siedler, D. Webb), pp. 527-551, Springer, Berlin

Schouten, S., Hopmans, E.C., Forster, A., van Breugel, Y., Kuypers, M.M.M., Damsté, J.S.S. (2003) Extremly high sea-surface temperatures at low latitudes during the middle Cretaceous as revealed by archaeal membrane lipids. *Geology*, **31**, 1069-1072.

Schouten, S., Hopmans, E.C., Pancost, R.D., Sinninghe Damsté, J.S. (2000) Widespread occurrence of structurally diverse tetraether membrane lipids: Evidence for the ubiquitous presence of low-temperature relatives of hyperthermophiles. *Proceedings of the National Academy of Sciences USA*, **97**, 14421-14426.

Schouten, S., Hopmans, E.C., Schefuß, E., Damste, J.S.S. (2002) Distributional variations in marine crenarchaeotal membrane lipids: a new tool for reconstructing ancient sea water temperatures? *Earth and Planetary Science Letters*, **204**, 265-274.

Schulz, M., Stattegger, K. (1997) Spectrum: spectral analysis of unevenly spaced paleoclimatic time series. *Computers & Geosciences*, **23**, 929-945.

Schütz, L. (1980) Long range transport of desert dust with special emphasis on the Sahara. In: T.J. Kneip, P.J. Lioy (Eds.), *Annals of the New York Academy of Sciences, Vol. 338* (Ed. by T.J. Kneip, P.J. Lioy), pp. 515-532. The New York Academy of Sciences, New York.

Schwark, L. Zink K., and Lechterbeck J. (2002) Reconstruction of postglacial to early Holocene vegetation history in terrestrial Central Europe via cuticular lipid biomarkers and pollen records from lake sediments. *Geology*, **30**, 463-466.

Seki, O., Ishiwatari, R., Matsumoto, K. (2002) Millennial climate oscillations in NE Pacific surface waters over the last 82 kyr, New evidence from alkenones. *Geophysical Research Letters,* **29,** 2144.

Severinghaus, J.P., Brook, E.J. (1999) Abrupt Climate Change at the End of the Last Glacial Period Inferred from Trapped Air in Polar Ice. *Science*, **286** (5441), 9

Shackleton, N.J., Imbrie, J., Pisias, N.G., Rose, J., (1988) The Evolution of Oceanic Oxygen-Isotope Variability in the North Atlantic Over the Past Three Million Years [and Discussion]. *Philosophical Transactions of the Royal Society of London. B, Biological Sciences*, **318** (1191), 679-688.

Shackleton, N.J., Kennett, J.P. (1975a) Late Cenozoic oxygen and carbon isotope changes at DSDP Sites 284: Implications for glacial history of the northern hemisphere and Antarctica. Initial *reports of the Deep Sea Drilling Project*, ***29****, 801-807*. *29* (Ed. by J.P. Kennett) U.S. Government Printing Office, Washington, D.C.

Shackleton, N.J., Kennett, J.P. (1975b) Paleotemperature history of the Cenozoic and the initiation of Antarctic glaciation: Oxygen and carbon isotope analyses in DSDP Sites 277, 279, and 281. In: J.P. Kennett, e. al. (Eds.), *Initial reports of the Deep Sea Drilling Project*, *29* (Ed. by J.P. Kennett)U.S. Government Printing Office, Washington, D.C.

Shackleton, N.J., Opdyke, N.D. (1973) Oxygen isotope and palaeomagnetic stratigraphy of Equatorial Pacific core V28-238: Oxygen isotope temperatures and ice volumes on a 105 year and 106 year scale. *Quaternary Research*, **3**, 39-55.

Shunthirasingham, C., Simpson, M.J. (2006) Investigation of bacterial hopanoid inputs to soils from Western Canada. *Applied Geochemistry*, **21**, 964-976.

Simoneit, B.R.T., (1997) Compound-specific carbon isotope analyses of individual long-chain alkanes and alkanoic acids in Harmattan aerosols. *Atmospheric Environment*, **31**(15), 2225-2233.

Sinninghe Damsté, J.S., Hopmans, E.C., Pancost, R.D., Schouten, S., Geenevasen, J. (2000) Newly discovered non-isoprenoid dialkyl diglycerol tetraether lipids in sediments. *Journal of Chemical Society, Chem. Comm.*, 1683-1684.

Sinninghe Damsté, J.S., Rijpstra W.I.C., Hopmans, E.C., Prahl , F., Wakeham , S.G., Schouten,S.(2002a) Distribution of membrane lipids of planktonic Crenarchaeota in the Arabian Sea. *Applied and Environmental Microbiology* **68**, 2997-3002.

Sinninghe Damsté, J.S., Rijpstra, I.C., Reichart, G.J. (2002) The influence of oxic degradation on the sedimentary biomarker record II: evidence from Arabian Sea sediments. *Geochimica et Cosmochimica Acta*, **66**, 2719-2735.

Sonzogni, C., Bard, E., Rostek, F., Dollfus, D., Rosell-Melé, A., Eglinton, G.(1997) Temperature and Salinity Effects on Alkenone Ratios Measured in Surface Sediments from the Indian Ocean. *Quaternary Research*, **47**, 344-355.

Spicer, R.A (1989) Physiological characteristics of land plants in relation to environment through time. *Earth-Science*, **80**, 321-329.

Srinivasan, M.S., Sinha, D.K. (1998) Early Pliocene closing of the Indonesian Seaway: evidence from north-east Indian Ocean and Tropical Pacific deep sea cores. *Journal of Asian Earth Sciences*, **16**, 29-44.

Steinke, S., Kienast, M., Pflaumann, U., Weinelt, M., Stattegger, K. (2001) A High-Resolution Sea-Surface Temperature Record from the Tropical

South China Sea (16,500-3000 yr B.P.). *Quaternary Research*, **55**, 352-362.

Stocker, T.F. (1998) Palaeoclimatology: A glimpse of the glacial. *Nature*, **391**, 338-339.

Street, F.A., Grove, A.T. (1976) Environmental and climatic implications of late Quaternary lake-level fluctuations in Africa. *Nature*, **261,** 385-390

Street, F.A., Grove, A.T. (1979) Global maps of lake-level fluctuations since 30,000 yr B.P. *Quaternary Research* **12**, 83–118.

Street-Perrott, F.A., Perrott, R.A. (1990) Abrupt climate fluctuations in the tropics: the influence of Atlantic Ocean circulation. *Nature*, **343**, 607-612.

Stromberg, C.A.E. (2005) Decoupled taxonomic radiation and ecological expansion of open-habitat grasses in the Cenozoic of North America. *Proceedings of the National Academy of Sciences of the United States of America*, **102**, 11980-11984.

Sun, Q., Chu, G., Li, S., Lü, C., Zheng, M. (2004) Long-chain alkenones in sulfate lakes and its paleoclimatic implications. *Chinese Science Bulletin*, **49,** 2082-2086.

Swezey, C. (2001) Eolian sediment responses to late Quaternary climate changes: temporal and spatial patterns in the Sahara. *Palaeogeography, Palaeoclimatology, Palaeoecology*, **167**, 119-155.

Talbot, H.M., Farrimond, P. (2007) Bacterial populations recorded in diverse sedimentary biohopanoid distributions. *Organic Geochemistry*, **38,** 1212-1225.

Talbot, H.M., Squire, A.H., Keely, B.J., Farrimond, P. (2003) Atmospheric pressure chemical ionisation reversed-phase liquid chromatography/ion trap mass spectrometry of intact bacteriohopanepolyols. *Rapid Communications in Mass Spectrometry*, **17**, 728-737.

Talbot, H.M., Summons, R.E., Jahnke, L.L., Cockell, C.S., Rohmer, M., Farrimond, P. (2008) Cyanobacterial bacteriohopanepolyol signatures from cultures and natural environmental settings. *Organic Geochemistry*, **39,** 232-263.

Ternois, Y., Sicre, M.A., Boireau, A., Conte, M.H., E, G. (1997) Evaluation of long-chain alkenones as paleo-temperature indicators in the Mediterranean Sea. *Deep Sea Research Part I: Oceanographic Research Papers*, **44,** 271-286.

Tetzlaf, G., Wolter, W. (1980). Meteorological patterns and the transport of mineral dust from the North African continent. *Paleoecology Africa*, **12**, 31-42.

Thompson, R.S., Fleming, R.F. (1996) Middle Pliocene vegetation: reconstructions, paleoclimatic inferences, and boundary conditions for climate modeling. *Marine Micropaleontology*, **27**, 27-49.

Tiedemann, R. and Franz, S.O. (1997). Deep water circulation ,chemistry ,and terrigenous sediment supply in the equatorial Atlantic during the Pliocene , 3.3-2.6 Ma and 5-4.5 Ma. *Proceedings Ocean Drilling Programme. Science Results* .**154**: 299-318.

Tiedemann, R., Sarnthein, M., Shackleton, N.J., (1994) Astronomic timescale for the Pliocene Atlantic δ^{18}O and dust flux records of Ocean Drilling Program Site 659. *Paleoceanography*, **9** (4), 619-638.

Tierney, J.E., Russell, J.M. (2009) Distributions of branched GDGTs in a tropical lake system: Implications for lacustrine application of the MBT/CBT paleoproxy. *Organic Geochemistry*, **40**, 1032-1036.

Tipple, B.J., Pagani, M. (2007) The early origins of terrestrial C-4 photosynthesis. *Annual Review of Earth and Planetary Sciences*, **35**, 435-461.

Tipple, B.J., Pagani, M.A. (2010) A 35 Myr North American leaf-wax compound-specific carbon and hydrogen isotope record: Implications for C4 grasslands and hydrologic cycle dynamics. *Earth and Planetary Science Letters*, **299,** 250-262.

Tjallingii, R., Claussen, M., Stuut, J.-B.W., Fohlmeister, J., Jahn, A., Bickert, T., Lamy, F., Röhl, U. (2008). Coherent high- and low-latitude control of the Northwest African hydrological balance. *Nature Geosciences* **1**, 670–675. doi:10.1038/ngeo289.

Tyson, R.V. (1995) *Sedimentary organic matter: organic facies and palynofacies*. Chapman & Hall, London.

van Leeuwen, R.J.W. (1989) Sea-floor distribution and Late Quaternary faunal patterns of planktonic and benthic foraminifers in the Angola Basin. *Utrecht Micropaleontology Bulletin.* **38**, 1-287.

VanderBurgh, J., Visscher, H., Dilcher, D.L., Kreschner, W.M. (1993) Paleoatmospheric signatures in neogene fossil leaves. *Science*, **260**, 1788-1790.

Vellinga, M., Wood, R.A. (2002) Global climatic impacts of a collapse of the Atlantic thermohaline circulation. *Climate Change*, **54**, 251–267.

Versteegh, G.J.M., Riegman, R., deLeeuw, J.W., Jansen, J.H.F. (2001) U37K' values for Isochrysis galbana as a function of culture temperature, light intensity and nutrient concentrations. *Organic Geochemistry*, **32**, 785-794.

Verstraete, J.M. (1992) The seasonal upwellings in the Gulf of Guinea. *Progress in Oceanography*, **29**, 1-60

Villanueva, J., Grimalt, J.O. (1996) Pitfalls in the chromatographic determination of the alkenone UK37' index for paleotemperature estimation. *Journal of Chromatography, **A***, 723, 285-291.

Voituriez, B., Herbland, A. (1982) Comparison des systèmes productifs de l`Atlantique Tropical est: dômes thermiqies, upwellings côtier et upwelling équatorial. *Rapp. P.- v. Réun. Cons. int. Explor. Mer*, **180**, 114-130.

Volkman, J.K., Barrett, S.M., Blackburn, S.I., Sikes, E.L. (1995) Alkenones in _Gephyrocapsa oceanica_: Implications for studies of paleoclimate. *Geochimica et Cosmochimica Acta*, **59**, 513-520.

Volkman, J.K., Eglinton, G., Corner, E.D.S. (1980). Long chain alkenes and alkenones in the marine coccolithophorid *Emiliana huxleyi Phytochemistry,* **19**, 2619-2622.

Wagner, T. (1998) Pliocene-Pleistocene carbonate and organic carbon fluxes off Ivory Coast/Ghana (ODP Site 959): Paleoenvironmental implications for the eastern Equatorial Atlantic. In: J. Mascle, G.P. Lohman, M. Moullard (Eds.), *Ocean Drilling Program Scientific Results Volume, Leg 159* (Ed. by J. Mascle, G.P. Lohman, M. Moullard), pp. 557-574. College Station, TX (Ocean Drilling Program), USA.

Wagner*, T.*, (2000) Control of organic carbon accumulation in the late Quaternary Equatorial Atlantic (ODP Sites 664, 663): productivity versus terrigenous supply. *Paleoceanography*, **15**(2), 181-199.

Wagner, T., Dupont, L., Holtvoeth, J., Schubert, C.J. (2004) Terrigenous signals in sediments of the low latitude Atlantic: implications for environmental variations during the Late Quaternary, Part I: Organic carbon. In Wefer, G., Mulitza, S., Ratmeyer, V., (Eds*.), the South Atlantic in the Late Quaternary: reconstruction of material budgets and current systems*: Heidelberg, Springer, pp. 295-322.

Wagner, T., Dupont, L.M. (1999) Terrestrial organic matter in marine sediments: analytical approaches and eolian-marine records from the central Equatorial Atlantic. In: G. Fischer, G. Wefer (Eds.), *The Use of Proxies in Paleoceanography: Examples from the South Atlantic* (Ed. by G. Fischer, G. Wefer), pp. 547-574. Springer, Heidelberg.

Wara, M.W., Ravelo, A.C., Delaney, M.L. (2005) Permanent El Nino-Like Conditions During the Pliocene Warm Period. *Science*, **309**, 758-761.

Webb, R.S., Rind, D.H., Lehman, S.J., Healy, R.J. and Sigman, D.,(1997) Influence of ocean heat transport on the climate of the Last Glacial Maximum. *Nature*, **385**, 695–699.

Weedon, G.P. (2003) *Time series analysis and cyclosratigraphy; Examining stratigraphic records of environmental cycles.* Cambridge University Press pp.1-243.

Wefer, G., Berger, W.H., Richter, C. (1998) Proceedings of the Ocean Drilling Program, Initial Reports. *Initial Reports, College Station, Texas: Ocean Drilling Program: 175*

Weijers, J.W.H., Schouten, S., Schefuß, E., Schneider, R.R., Sinninghe Damsté, J.S., (2009) Disentangling marine, soil and plant organic carbon contributions to continental margin sediments: A multi-proxy approach in a 20,000 year sediment record from the Congo deep-sea fan. *Geochimica et Cosmochimica Acta*, **73**, 119-132.

Weijers, J.W.H., Schouten, S., Spaargaren, O.C., Sinninghe Damsté, J.S. (2006) Occurrence and distribution of tetraether membrane lipids in soils: Implications for the use of the TEX86 proxy and the BIT index. *Organic Geochemistry*, **37**, 1680-1693.

Weijers, J.W.H., Schouten, S., van den Donker, J.C., Hopmans, E.C., Sinninghe Damsté, J.S. (2007a) Environmental controls on bacterial tetraether membrane lipid distribution in soils. *Geochimica et Cosmochimica Acta,* **71**, 703-713.

Weijers, J.W.H., Schouten, S., van der Linden, M., Van Geel, B., Damsté, J.S. (2004) Water table related variations in the abundance of intact archaeal membrane lipids in a Swedish peat bog. *FEMS Microbiology Letters*, **239**, 51-56.

Weijers, J.W.H.,Schefuß, E., Schouten, S., Damsté, J.S. (2007b) Coupled Thermal and Hydrological Evolution of Tropical Africa over the Last Deglaciation. *Science*, **315**, 1701-1704.

Weldeab, S., Lea, D.W., Schneider, R. R. & Andersen, N. (2007)155,000 Years of West African Monsoon and Ocean thermal evolution. *Science* **316**, 1303–1307

Westerhausen, L., Poynter, J., Eglinton, G., Erlenkeuser, H., Sarnthein, M. (1993) Marine and terrigenous origin of organic matter in modern sediments of the equatorial East Atlantic: the □13C and molecular record. *Deep-Sea Research, Part 1*, **40,** 1087-1121.

Winkler, A., Haumaier, L., Zech, W. (2001) Variation in hopanoid composition and abundance in forest soils during litter decomposition and humification. *Organic Geochemistry*, **32**, 1375-1385.

Winter, K, Smith, J.A.C. (1996) Crassulacean acid metabolism: biochemistry , ecophysiology and evolution. Ecological Studies, 114, Springer, Verlag, Berling, Heidelberg.

Wuchter, C., Schouten, S., Coolen, M.J.L., Sinninghe Damsté, J.S. (2004) Temperature dependant variation in the distribution of tetraether membrane lipids of marine crenarchaota: Implication for TEX_{86} paleothermometry. *Paleoceanography*, **19**, doi: 10.1029/2004PA001041.

Xie, S., Chen, F., Wang, Z., Wang, H., Gu, Y., Huang, Y. (2003) Lipid distributions in loess-paleosol sequences from northwest China. *Organic Geochemistry*, **34**, 1071-1079.

Xie, S., Wang, Z., Wang, H., Chen, F., An, C. (2002) The occurrence of a grassy vegetation over the Chinese Loess Plateau since the last interglacier: the molecular fossil record. *Science in China Series D: Earth Sciences*, **45**, 53-62.

Xu, Y., Cooke, M.P., Talbot, H.M., Simpson, M.J. (2009) Bacteriohopanepolyol signatures of bacterial populations in Western Canadian soils. *Organic Geochemistry*, **40**, 79-86.

Zabel, M., Bickert, T., Dittert, L., Haese, R.R. (1999) The significance of sedimentary Al/Ti ratio as indicator for reconstructions of the terrestrial input to the Equatorial Atlantic. *Paleoceanography*, **14**, 789-799.

Zabel, M., DeMenocal, P., Wagner, T. (2004) Terrigenous signals in sediments of the low latitude Atlantic – implications to environmental variations during the late Quaternary: Part I: lithogenic matter. In: G. Wefer, S. Mulitza, V. Rathmeyer (Eds.), *The South Atlantic in the Late Quaternary: Reconstruction of material budgets and current systems* (Ed. by G. Wefer, S. Mulitza, V. Rathmeyer), pp. in press. Springer, Heidelberg.

Zabel, M., Schneider, R.R., Wagner, T., deVries, U., Kolonic, S.(2001) Documentation of Late Quaternary Climate Changes in Central Africa by Variations of Terrigenous Input to the Niger Fan. *Quaternary Research*, **56**, 1-11.

Zachos, J., Pagani, M., Sloan, E., Thomas, E., Billups, K. (2006) Trends, Rhythms, and Aberrations in Global Climate 65 Ma to Present. *Science*, **292**, 686-693.

Zachos, J.C., Shackleton, N.J., Revenaugh, J.S., Palike, H., Flower, B.P. (2001) Climate Response to Orbital Forcing Across the Oligocene-Miocene Boundary. *Science*, **292**, 274-278.

Zafiriou, O.C., Gagosian, R.B., Peltzer, E.T., Alford, J.B., Loder, T. (1985) Air-to-sea fluxes of lipids at Enewetak Atoll. *J. Geophysical Research.* **90,** 2409-2423.

Zarriess, M., Mackensen, A., The tropical rainbelt and productivity changes off northwest Africa: A 31,000-year high-resolution record. *Marine Micropaleontology*, **76**(3-4), 76-91.

Zhang, C., Wang, Y., Deng, T., Wang, X., Biasatti, D., Xu, Y., Li, Q. (2009) C4 expansion in the central Inner Mongolia during the latest Miocene and early Pliocene. *Earth and Planetary Science Letters*, **287,** 311-319.

Zhang, J., Scott, D.B. (1996) Messinian Deep-Water Turbidites and Glacioeustatic Sea-Level Changes in the North Atlantic: Linkage to the Mediterranean Salinity Crisis. *Paleoceanography*, **11**, 277-297.

Zhang, Z., Zhao, M., Eglinton, G., Lu, H., Huang, C.-Y. (2006) Leaf wax lipids as paleovegetational and paleoenvironmental proxies for the Chinese Loess Plateau over the last 170 kyr. *Quaternary Science Reviews*, **25**, 575-594.

Zhang, Z., Zhao, M., Lu, H., Faiia, A.M. (2003) Lower temperature as the main cause of C4 plant declines during the glacial periods on the Chinese Loess Plateau. *Earth and Planetary Science Letters*, **214**, 467-481.

Zhao, M., Dupont, L.M., Eglinton, G., Teece, M. (2003) n-Alkane and pollen reconstruction of terrestrial climate and vegetation for N.W. Africa over the last 160 kyr. *Organic Geochemistry*, **34**, 131-143

Zhao, M., Eglinton, G., Haslett, S.K., Jordan, R.W., Sartnhein, M., Zhang, Z. (2000) Marine and terrestrial biomarker records of the last 35,000 years at ODP Site 658C off NW Africa. *Organic Geochemistry*, **31**, 919-930.

Zhao, M., Mercer, J.L., Eglinton, G., Higginson, M.J., Huang, C.-Y. (2006) Comparative molecular biomarker assessment of phytoplankton paleoproductivity for the last 160 kyr off Cap Blanc, NW Africa. *Organic Geochemistry*, **37**, 72-97.

Zhisheng, A., Kutzbach, J.E., Prell, W.L., Porter, S.C. (2001) Evolution of Asian monsoons and phased uplift of the Himalaya-Tibetan plateau since Late Miocene times. *Nature*, **411**(6833), 62-66.

LEG	SITE	H	Core	T	Depth (mbsf)	Age (Ma)	LSR(cm/ka)	CaCO3 (%)	TOC (bulk)	TOCcf(%)	Sum of Alkenones (µg/TOC)	SST (°C)	n-alkane / alkenone index	Leaf wax lipids (µg/TOC)	CPI	ACL	A.I.
159	959	C	10	H	78.84	5.10	1.93	44.49	0.22	0.39	11.01	27.16	0.29	7.88	4.26	29.89	0.46
159	959	C	10	H	78.94	5.10	1.93	41.17	0.31	0.52	54.57	27.76	0.11	14.96	9.98	29.81	0.38
159	959	C	10	H	79.04	5.11	1.93	44.91	0.32	0.58	16.22	27.69	0.09	2.78	2.46	29.79	0.49
159	959	C	10	H	79.14	5.11	1.93	46.48	0.29	0.54	5.92	27.91	0.36	5.78	4.36	29.75	0.51
159	959	C	10	H	79.54	5.13	1.93	48.90	0.20	0.39	67.18	27.96	0.04	5.11	3.87	29.90	0.53
159	959	C	10	H	79.94	5.15	1.93	41.32	0.34	0.58	6.71	25.81	0.27	4.60	6.25	30.36	0.58
159	959	C	10	H	80.14	5.17	1.93	34.07	0.40	0.61	58.73	27.44	0.06	7.06	5.15	30.10	0.56
159	959	C	10	H	80.24	5.17	1.93	32.82	0.60	0.89	1.12	26.50	0.77	6.91	6.84	30.27	0.54
159	959	C	10	H	81.34	5.24	1.23	36.26	0.30	0.47	1.40	25.14	0.42	1.55	1.02	29.21	0.45
159	959	C	10	H	81.44	5.25	1.23	43.86	0.43	0.77	6.25	27.75	0.11	1.36	1.86	29.70	0.53
159	959	C	10	H	81.54	5.26	1.23	37.59	0.35	0.56	1.91	25.70	0.43	2.64	1.97	29.80	0.48
159	959	C	10	H	81.64	5.27	1.23	34.07	0.26	0.39	1.01	26.64	0.49	1.87	1.96	30.06	0.51
159	959	C	10	H	81.74	5.28	1.23	35.72	0.55	0.86	2.71	26.24	0.30	2.17	3.01	29.99	0.50
159	959	C	10	H	81.84	5.28	1.23	38.57	0.46	0.75	13.56	26.88	0.28	10.26	13.19	30.41	0.56
159	959	C	10	H	81.94	5.29	1.23	41.82	0.40	0.69	12.47	26.04	0.12	3.07	2.16	29.79	0.53
159	959	C	10	H	82.04	5.30	1.23	39.82	0.33	0.55	2.45	26.51	0.37	2.58	1.93	29.70	0.45
159	959	C	10	H	82.14	5.31	1.23	39.65	0.37	0.61	10.24	27.30	0.26	5.72	3.53	29.96	0.60
159	959	C	10	H	83.04	5.38	1.23	37.49	0.30	0.48	58.53	26.12	0.01	1.49	1.77	29.58	0.49
159	959	C	10	H	83.14	5.39	1.23	34.70	0.38	0.59	19.53	26.62	0.03	1.21	1.31	29.60	0.53
159	959	C	10	H	83.24	5.40	1.23	30.07	0.30	0.43	4.83	26.40	0.06	0.56	1.64	30.06	0.59
159	959	C	10	H	83.34	5.41	1.23	29.42	0.44	0.62	3.27	25.90	0.30	2.48	2.59	29.85	0.49
159	959	C	10	H	83.44	5.41	1.23	29.72	0.37	0.53	3.25	26.17	0.17	1.20	2.23	29.86	0.48
159	959	C	10	H	83.54	5.42	1.23	32.74	0.39	0.58	3.94	25.01	0.32	2.90	2.14	29.67	0.54
159	959	C	10	H	83.74	5.44	1.23	34.19	0.32	0.48	0.29	27.32	0.85	2.84	3.12	29.91	0.54
159	959	C	10	H	83.94	5.45	1.23	29.75	0.40	0.57	1.05	26.42	0.68	4.03	3.97	29.96	0.52
159	959	C	10	H	84.04	5.46	1.23	25.07	0.45	0.60	6.84	27.05	0.47	11.80	12.22	30.35	0.55
159	959	C	10	H	84.14	5.47	1.23	32.58	0.41	0.61	2.54	25.60	0.47	3.99	3.43	29.92	0.51
159	959	C	10	H	84.34	5.49	1.23	32.90	0.30	0.45	13.77	27.77	0.01	0.26	1.21	29.81	0.48
159	959	C	10	H	84.44	5.49	1.23	33.53	0.40	0.59	6.81	28.00	0.28	4.71	3.85	29.81	0.51
159	959	C	10	H	84.54	5.50	1.23	40.84	0.43	0.72	5.75	28.97	0.53	10.95	9.84	30.16	0.52

159	959	C	10	H	84.64	5.51	1.23	37.83	0.44	0.71	15.05	27.50	0.12	3.54	3.02	29.93	0.50
159	959	C	10	H	84.74	5.52	1.23	44.57	0.31	0.56	29.25	26.59	0.25	17.84	13.57	30.16	0.56
159	959	C	10	H	84.84	5.53	1.23	31.82	0.45	0.66	0.75	27.80	0.71	3.28	4.73	30.06	0.53
159	959	C	10	H	85.04	5.54	1.23	41.90	0.35	0.60	0.36	25.83	0.76	2.06	2.58	30.05	0.53
159	959	C	10	H	85.14	5.55	1.23	48.65	0.20	0.39	3.13	25.59	0.55	6.98	2.82	29.95	0.53
159	959	C	10	H	85.24	5.56	1.23	45.93	0.26	0.47	21.25	28.21	0.56	19.73	9.37	29.35	0.51
159	959	C	10	H	85.34	5.57	1.23	43.19	0.28	0.48	4.46	27.12	0.51	8.40	4.62	29.74	0.47
159	959	C	10	H	85.44	5.58	1.23	44.44	0.32	0.57	1.49	25.59	0.56	3.52	3.08	30.05	0.50
159	959	C	10	H	85.54	5.58	1.23	48.06	0.20	0.39	3.74	26.22	0.20	1.70	1.63	29.54	0.44
159	959	C	10	H	85.64	5.59	1.04	45.77	0.46	0.86	27.50	27.42	0.04	2.02	2.57	29.97	0.49
159	959	C	10	H	85.74	5.60	1.04	38.91	0.46	0.75	78.46	27.48	0.03	4.37	3.73	29.90	0.54
159	959	C	10	H	85.84	5.61	1.04	42.57	0.40	0.70	6.37	27.20	0.14	1.87	1.72	29.90	0.69
159	959	C	10	H	85.94	5.62	1.04	42.53	0.42	0.74	0.66	26.54	0.57	1.54	1.62	29.88	0.50
159	959	C	10	H	86.04	5.63	1.04	37.13	0.30	0.48	2.85	25.65	0.06	0.32	0.88	29.60	0.57
159	959	C	10	H	86.14	5.64	1.04	40.92	0.37	0.62	2.90	24.80	0.31	2.27	2.15	29.67	0.45
159	959	C	10	H	86.24	5.65	1.04	42.16	0.28	0.48	235.05	26.66	0.01	2.74	1.95	29.69	0.52
159	959	C	10	H	86.34	5.66	1.04	36.82	0.34	0.54	69.67	25.84	0.21	34.89	15.54	30.26	0.58
159	959	C	10	H	86.54	5.68	1.04	45.65	0.27	0.50	30.07	26.48	0.02	1.24	1.05	29.66	0.52
159	959	C	10	H	86.64	5.69	1.04	45.86	0.26	0.49	6.65	27.25	0.31	5.20	3.57	29.86	0.53
159	959	C	10	H	86.74	5.70	1.04	39.40	0.31	0.51	5.60	27.35	0.47	9.24	7.57	30.09	0.55
159	959	C	10	H	86.84	5.71	1.04	41.40	0.32	0.55	1.78	25.94	0.41	2.31	2.03	30.05	0.50
159	959	C	10	H	86.94	5.72	1.04	47.66	0.25	0.47	4.17	28.10	0.48	7.66	4.26	30.00	0.46
159	959	C	10	H	87.04	5.73	1.04	47.01	0.22	0.41	5.88	26.13	0.40	7.37	4.15	30.37	0.53
159	959	C	10	H	87.14	5.74	1.04	45.01	0.24	0.43	6.28	27.45	0.41	7.77	3.51	29.81	0.50
159	959	C	10	H	87.34	5.76	1.04	50.56	0.30	0.61	9.84	25.53	0.12	2.34	1.70	29.95	0.56
159	959	C	10	H	87.44	5.77	1.04	50.93	0.35	0.70	11.77	27.26	0.31	9.76	6.93	30.21	0.54
159	959	C	10	H	87.54	5.78	1.04	41.71	0.56	0.97	3.48	27.97	0.51	6.92	7.41	30.15	0.53
159	959	C	10	H	87.64	5.79	1.04	42.32	0.44	0.76	1.33	27.80	0.71	5.65	5.50	29.96	0.53
159	959	C	10	H	87.84	5.80	1.04	46.40	0.26	0.49	7.44	27.71	0.26	4.62	3.30	29.80	0.53
159	959	C	10	H	87.94	5.81	1.04	43.82	0.32	0.57	2.23	25.68	0.40	2.72	1.97	30.04	0.52
159	959	C	11	H	88.04	5.82	1.04	41.73	0.36	0.62	34.18	26.48	0.23	18.27	12.06	30.00	0.51
159	959	C	11	H	88.24	5.84	1.04	52.31	0.20	0.42	2.63	26.35	0.44	3.67	2.28	30.02	0.55
159	959	C	11	H	88.34	5.85	1.04	54.05	0.34	0.74	27.84	26.68	0.14	8.23	5.18	29.99	0.56

159	959	C	11	H	88.44	5.86	1.04	58.64	0.18	0.44	85.67	25.06	0.15	26.08	7.24	29.83	0.53
159	959	C	11	H	88.54	5.87	1.04	58.06	0.22	0.52	31.30	25.42	0.21	13.85	5.12	29.57	0.50
159	959	C	11	H	88.64	5.88	1.04	57.98	0.17	0.40	18.56	26.39	0.29	14.00	8.62	30.25	0.58
159	959	C	11	H	88.74	5.89	1.04	52.40	0.20	0.42	17.91	27.41	0.28	13.07	9.48	30.18	0.63
159	959	C	11	H	88.84	5.90	1.04	50.75	0.17	0.34	0.71	26.08	0.80	5.22	2.15	29.81	0.50
159	959	C	11	H	88.94	5.91	1.04	51.73	0.17	0.35	2.95	25.99	0.63	8.67	3.03	29.74	0.51
159	959	C	11	H	89.04	5.92	1.04	60.83	0.22	0.56	2.13	26.43	0.60	5.82	2.77	29.98	0.54
159	959	C	11	H	89.14	5.94	1.04	60.73	0.14	0.36	6.62	27.87	0.53	13.36	3.50	29.70	0.49
159	959	C	11	H	89.24	5.95	1.04	51.83	0.14	0.29	4.48	27.05	0.72	21.75	5.50	30.05	0.57
159	959	C	11	H	89.34	5.95	1.04	47.91	0.44	0.84	2.14	25.71	0.59	5.54	4.42	29.87	0.50
159	959	C	11	H	89.54	5.97	1.04	54.48	0.35	0.77	16.03	27.15	0.08	2.73	2.21	29.88	0.48
159	959	C	11	H	89.64	5.98	1.04	50.01	0.22	0.43	4.62	26.15	0.48	7.30	3.14	29.64	0.51
159	959	C	11	H	89.74	5.99	1.04	45.65	0.14	0.26	15.87	26.62	0.48	26.92	6.39	30.07	0.55
159	959	C	11	H	89.84	6.00	1.04	49.90	0.27	0.54	7.72	27.45	0.52	14.98	6.83	30.00	0.51
159	959	C	11	H	89.94	6.01	1.04	55.06	0.30	0.67	5.75	25.14	0.18	4.22	2.26	29.94	0.50
159	959	C	11	H	90.04	6.02	1.04	56.31	0.18	0.41	30.38	26.53	0.20	13.13	4.45	29.84	0.54
159	959	C	11	H	90.14	6.03	1.04	54.89	0.26	0.58	3.77	26.92	0.20	1.56	1.09	29.68	0.55
159	959	C	11	H	90.24	6.04	1.04	46.98	0.29	0.55	1.57	25.89	0.68	6.24	5.69	30.16	0.53
159	959	C	11	H	90.44	6.06	1.04	56.06	0.21	0.48	3.11	26.33	0.37	3.21	2.12	29.74	0.50
159	959	C	11	H	90.54	6.06	1.04	52.31	0.18	0.38	8.10	27.20	0.32	6.71	2.81	29.94	0.54
159	959	C	11	H	90.64	6.07	1.04	47.56	0.16	0.31	6.92	26.81	0.57	18.07	6.40	30.28	0.57
159	959	C	11	H	90.74	6.08	1.04	47.15	0.15	0.28	16.37	27.01	0.44	24.51	7.36	30.25	0.57
159	959	C	11	H	90.84	6.09	1.04	46.40	0.21	0.39	13.58	27.02	0.41	18.20	6.72	30.22	0.59
159	959	C	11	H	90.94	6.10	1.04	42.09	0.41	0.70	17.31	26.64	0.22	8.69	6.48	30.03	0.55
159	959	C	11	H	91.04	6.11	1.04	46.35	0.34	0.63	10.63	25.58	0.29	7.72	4.79	29.94	0.53
159	959	C	11	H	91.24	6.13	1.04	40.15	0.20	0.33	8.14	27.71	0.31	6.86	6.93	30.18	0.59
159	959	C	11	H	91.44	6.15	1.04	46.69	0.33	0.61	7.61	27.10	0.34	10.13	6.27	30.04	0.52
159	959	C	11	H	91.64	6.17	1.04	45.01	0.25	0.45	8.37	26.10	0.44	12.01	5.71	30.11	0.55
159	959	C	11	H	91.74	6.18	1.04	40.09	0.25	0.41	6.56	26.86	0.61	19.33	8.67	30.11	0.54
159	959	C	11	H	91.84	6.19	1.04	41.05	0.38	0.65	13.37	26.93	0.51	26.13	15.14	30.15	0.52
159	959	C	11	H	91.94	6.20	1.04	42.23	0.35	0.61	38.24	26.76	0.06	4.47	4.21	29.99	0.49
159	959	C	11	H	92.04	6.21	1.04	47.73	0.29	0.55	22.63	25.39	0.29	16.91	9.58	29.87	0.47
159	959	C	11	H	92.24	6.23	1.04	44.23	0.21	0.38	10.56	26.33	0.55	23.72	8.15	30.12	0.52

159	959	C	11	H	92.44	6.25	1.03	48.40	0.22	0.43	17.33	26.00	0.24	9.81	4.08	29.86	0.52
159	959	C	11	H	92.54	6.26	1.04	49.98	0.20	0.40	28.77	26.29	0.21	13.33	5.00	29.88	0.53
159	959	C	11	H	92.64	6.27	1.04	47.81	0.19	0.36	9.88	26.90	0.50	18.91	6.92	30.21	0.59
159	959	C	11	H	92.74	6.28	1.04	53.81	0.23	0.50	10.84	27.46	0.56	26.70	10.14	30.34	0.56
159	959	C	11	H	92.84	6.29	1.04	58.89	0.34	0.83	15.67	27.07	0.13	4.19	3.88	29.89	0.51
159	959	C	11	H	92.94	6.30	1.04	56.29	0.30	0.69	2.99	25.42	0.36	2.84	1.97	29.55	0.42
159	959	C	11	H	93.14	6.32	1.04	47.16	0.29	0.55	6.16	26.56	0.61	18.22	9.64	30.26	0.55
159	959	C	11	H	93.34	6.33	1.04	43.68	0.22	0.38	4.64	27.28	0.58	11.90	4.32	30.29	0.56
159	959	C	11	H	93.44	6.34	1.04	44.15	0.18	0.32	4.80	25.98	0.55	10.05	7.35	29.47	0.52
159	959	C	11	H	93.54	6.35	1.04	42.88	0.77	1.35	2.12	26.96	0.52	4.37	8.04	30.24	0.53
159	959	C	11	H	93.64	6.36	1.04	53.85	0.25	0.53	6.99	27.23	0.44	10.53	7.89	30.28	0.56
159	959	C	11	H	93.74	6.37	1.04	48.73	0.24	0.47	5.86	26.61	0.45	8.66	7.86	30.13	0.53
159	959	C	11	H	93.84	6.38	1.04	51.56	0.33	0.68	17.73	27.19	0.07	2.40	2.04	29.56	0.39
159	959	C	11	H	93.94	6.39	1.04	49.73	0.21	0.42	38.07	26.03	0.05	3.57	2.00	29.63	0.47
159	959	C	11	H	94.64	6.43	1.96	48.23	0.25	0.48	9.21	27.48	0.40	11.10	8.19	30.09	0.53
159	959	C	11	H	94.74	6.44	1.96	50.40	0.21	0.42	9.38	26.23	0.31	7.55	3.24	30.00	0.53
159	959	C	11	H	94.84	6.44	1.96	47.98	0.19	0.37	4.31	27.74	0.44	6.05	2.33	30.09	0.57
159	959	C	11	H	94.94	6.45	1.96	43.52	0.23	0.40	9.03	27.22	0.49	16.34	6.36	30.11	0.54
159	959	C	11	H	95.04	6.45	1.96	46.42	0.35	0.65	7.07	26.40	0.24	4.04	2.82	30.01	0.54
159	959	C	11	H	95.24	6.46	1.96	51.48	0.30	0.62	3.20	25.82	0.34	3.02	2.64	30.02	0.57
159	959	C	11	H	95.34	6.47	1.96	52.48	0.30	0.63	4.49	25.90	0.32	3.60	2.12	29.46	0.46
159	959	C	11	H	95.54	6.48	1.96	53.90	0.29	0.63	20.38	26.46	0.25	11.91	6.32	29.91	0.51
159	959	C	11	H	95.74	6.49	1.96	48.31	0.22	0.43	25.21	26.17	0.06	2.82	1.81	29.71	0.52
159	959	C	11	H	95.84	6.49	1.96	45.76	0.22	0.40	10.79	26.88	0.32	9.21	3.96	29.99	0.50
159	959	C	11	H	95.94	6.50	1.96	46.65	0.28	0.52	14.80	27.14	0.31	11.19	4.55	29.61	0.49
159	959	C	11	H	96.04	6.50	1.96	47.39	0.25	0.48	3.63	27.55	0.47	5.76	3.03	29.79	0.52
159	959	C	11	H	96.14	6.51	1.96	53.48	0.16	0.34	2.31	26.58	0.44	3.25	2.91	30.12	0.56
159	959	C	11	H	96.24	6.51	1.96	49.92	0.28	0.55	10.03	27.13	0.41	13.08	6.87	30.18	0.55
159	959	C	11	H	96.44	6.52	1.96	45.48	0.40	0.73	18.02	25.36	0.42	21.94	12.86	29.45	0.40
159	959	C	11	H	96.64	6.53	1.96	51.74	0.29	0.60	20.43	27.21	0.17	7.29	4.34	29.84	0.50
159	959	C	11	H	96.74	6.54	1.96	46.72	0.35	0.66	15.26	26.58	0.16	5.56	3.99	30.15	0.55
159	959	C	11	H	96.84	6.54	1.96	46.65	0.20	0.37	5.30	25.87	0.35	5.40	3.17	30.16	0.55
159	959	C	11	H	96.94	6.55	1.96	47.72	0.17	0.33	8.28	26.83	0.28	5.83	2.45	29.96	0.52

159	959	C	11	H	97.04	6.55	1.96	48.65	0.28	0.55	16.74	26.12	0.29	12.23	7.69	29.98	0.52
159	959	C	11	H	97.14	6.56	1.96	49.31	0.27	0.53	8.05	27.36	0.12	1.75	1.14	29.34	0.40
159	959	C	11	H	97.24	6.56	1.96	50.48	0.33	0.67	11.06	27.84	0.19	4.50	2.99	29.61	0.49
159	959	C	11	H	97.44	6.57	1.96	45.32	0.22	0.40	64.57	26.78	0.06	6.75	5.36	29.69	0.51
159	959	C	11	H	97.64	6.57	1.96		0.20	0.20	0.91	26.05	0.78	6.02	3.02	30.03	0.55

APPENDIX B CHEETA CRUISE (OC-437-7) Surface sediment records from the North West African margin

Cruise	Station	Event (core)	Longitude (N)	Latitude (W)	Water depth (m)	Region	C_{org}/N_{tot}	$CaCO_3$%	TOC (%)	δ^{13}Corg(‰ PDB)	BIT Index	Adenosylhopane (µg/g)	Soil BHPs (%) of total BHPs
OC437-7	1	MC01 (E)	37°49.67	9°30.77	1123	(A) Portugal Margin	8.1	26.99	0.74	-22.35	0.02	5	4.5
OC437-7	3	MC07 (E)	36°46.33	9°52.03	2735	(A) Portugal Margin	7.5	21.24	0.61	-22.41	0.02	4.3	6
OC437-7	5	MC11 (E)	36°23.41	7°3.92	577	(A) Portugal Margin	7.5	28.74	0.68	-22.39	0.03	2.2	4.3
OC437-7	6	MC12 (E)	35°53.42	7°31.89	1184	(B) Gulf of Cadiz	7.3	31.57	0.47	-22.91	0.03	4.4	3.5
OC437-7	7	MC15 (H)	34°6.71	7°45.50	366	(C) N Morocco	7.8	24.57	0.55	-21.82	0.02	3.6	3.7
OC437-7	8	MC18 (F)	33°26.91	9°18.89	835	(C) Mid Morocco	6.9	49.81	0.44	-20.82	0.02	5.3	2.6
OC437-7	9	MC22 (G)	30°51.70	10°16.97	835	(C) S Morocco	8.5	58.23	0.39	-21.23	0.03	5.4	4.3
OC437-7	10	MC25 (D)	30°53.29	10°37.97	1244	(C) S Morocco	7.0	28.41	1.37	-20.66	0.02	2.2	1.6
OC437-7	11	MC28 (C)	29°01.08	12°28.02	776	(C) S Morocco	7.4	29.9	0.84	-20.14	0.02	0	0
OC437-7	12	MC31 (G)	27°32.23	13°44.45	1090	(D) W Sahara	7.2	45.65	0.57	-19.93	0.02	0	0
OC437-7	13	MC36 (D)	26°49.64	15°7.21	2812	(D) W Sahara	8.1	33.82	0.91	-19.98	0.01	0	0
OC437-7	14	MC38 (B)	25°30.11	16°24.42	1774	(D) W Sahara	7.4	35.74	0.44	-19.54	0	0	0
OC437-7	15	MC42 (C)	25°00.70	16°39.62	1425	(D) W Sahara	7.2	43.73	0.53	-19.22	0.02	1.6	3.4
OC437-7	16	MC44 (E)	24°21.62	17°3.10	1646	(D) W Sahara	7.3	52.23	0.56	-19.35	0	4.5	4.5
OC437-7	18	MC 50 (B)	23°12.43	17°51.25	1659	(D) W Sahara	7.3	41.4	0.55	-19.22	0	2.2	3
OC437-7	19	MC51 (D)	21°47.82	17°52.25	1276	(D) W Sahara	8.8	45.65	0.61	-19.35	0.02	6.7	1.9
OC437-7	20	MC55 (A)	21°14.36	17°48.17	798	(E) Cape Blanc	8.0	44.48	1.97	-19.23	0.02	3.7	2.5
OC437-7	21	MC58 (D)	21°7.96	18°35.54	2784	(E) Cape Blanc	8.0	33.57	1.87	-19.67	0.01	2.3	3.4
OC437-7	22	MC63 (G)	20°44.78	18°33.07	2106	(E) Cape Blanc	8.6	34.74	1.69	-19.31	0.01	0.3	0.2
OC437-7	23	MC65 (A)	19°7.56.60	17°51.64	1455	(F) Mauritania	8.6	35.49	1.88	-19.45	0.02	0	0
OC437-7	24	MC67 (A)	19°21.73	17°17.01	1400	(F) S Mauritania	8.4	18.83	2.2	-19.6	0.02	5.1	4.5
OC437-7	28	MC78 (B)	15°18.60	17°24.79	944	(G) Cape Verdes	8.5	32.4	1.06	-19.75	0.05	2.9	3.6

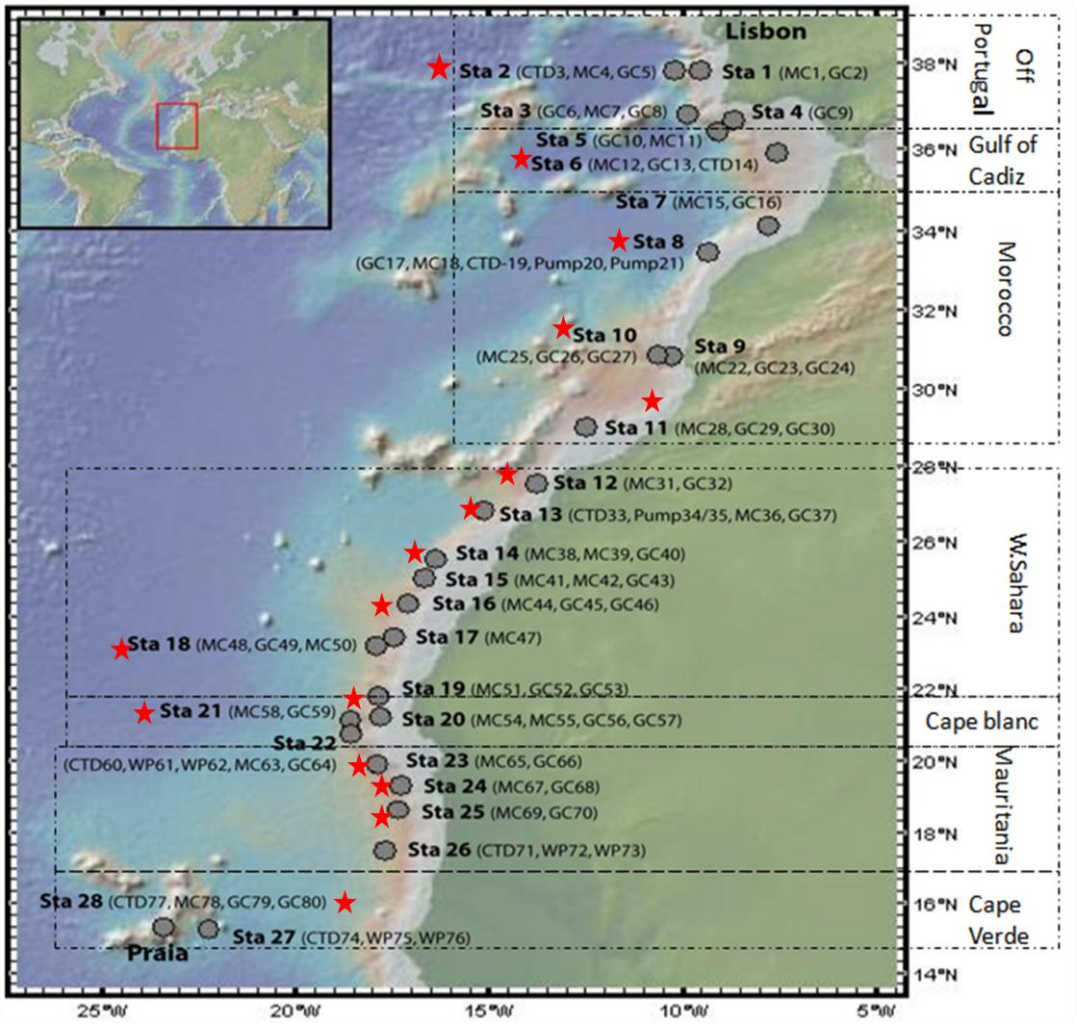

Figure Appendix 1 1 Overview map of North West Africa. Shown are the gravity core ID numbers and the corresponding stations IDs. On the right, latitudinal positions of the corresponding regions. The red star indicates the cores that were investigated in this thesis.

APPENDIX D GLACIAL TO HOLOCENE TRANSECT (CHEETA CORE DATA)

Core	$CaCO_3$ (%)	DBB (g/cm^3)	BAR (g/cm^2ka^{-1})	TOC bulk (%)	TOCcf	TOC AR ($g/cm^2/ka$)	$\delta^{13}C_{org}$ (‰)
GC-05	31.38	0.85	13.82	0.68	0.99	0.09	-22.31
GC-05	32.61	0.89	14.55	0.55	0.82	0.08	-22.64
GC-05	32.60	0.89	14.54	0.63	0.93	0.09	-22.54
GC-05	33.27	0.87	14.23	0.55	0.82	0.08	-22.66
GC-05	37.99	0.81	13.20	0.60	0.97	0.08	-22.53
GC-05	35.63	0.85	13.89	0.45	0.70	0.06	-22.91
GC-05	32.30	0.83	13.56	0.59	0.87	0.08	-22.63
GC-05	26.32	0.87	14.24	0.69	0.94	0.10	-22.63
GC-05	22.99	0.85	13.82	0.86	1.12	0.12	-22.54
GC-05	22.30	0.84	13.78	0.81	1.04	0.11	-22.64
GC-05	27.16	0.83	13.49	0.72	0.99	0.10	-22.49
GC-05	27.28	0.82	13.39	0.67	0.92	0.09	-22.44
GC-05	27.32	0.85	13.86	0.64	0.88	0.09	-22.83
GC-05	25.03	0.85	13.85	0.61	0.81	0.08	-22.69
GC-05	20.34	0.83	16.51	0.61	0.77	0.10	-23.06
GC-05	23.23	0.90	17.97	0.68	0.89	0.12	-22.78
GC-05	18.07	0.88	17.61	0.62	0.76	0.11	-22.93
GC-05	17.77	0.87	17.42	0.61	0.74	0.11	-22.85
GC-05	17.63	0.83	16.68	0.62	0.75	0.10	-22.86
GC-05	18.07	0.87	8.26	0.62	0.76	0.05	-22.94
GC-05	26.48	0.90	8.55	0.75	1.02	0.06	-22.20
GC-05	26.14	0.93	8.80	0.67	0.91	0.06	-22.21
GC-05	28.20	0.91	8.65	0.86	1.20	0.07	-22.00
GC-05	27.81	0.91	8.57	0.71	0.98	0.06	-21.89
GC-05	27.11	0.91	8.58	0.70	0.96	0.06	-22.01
GC-05	27.00	0.93	8.76	0.65	0.89	0.06	-21.97
GC-05	27.57	0.92	8.71	0.70	0.97	0.06	-22.05
GC-05	27.24	0.94	8.85	0.63	0.87	0.06	-22.04
GC-05	26.79	0.96	9.13	0.65	0.89	0.06	-22.23
GC-05	25.08	0.92	8.67	0.64	0.85	0.06	-21.85
GC-05	32.16	0.83	7.81	0.78	1.15	0.06	-21.89
GC-13	23.89	0.79	2.75	0.58	0.76	0.02	-22.72
GC-13	24.65	0.95	3.33	0.44	0.58	0.01	-23.07
GC-13	30.37	1.05	3.65	0.49	0.70	0.02	-22.94
GC-13	27.97	1.04	13.84	0.49	0.68	0.07	-22.87
GC-13	28.37	1.04	13.92	0.48	0.67	0.07	-23.18
GC-13	28.41	1.04	13.92	0.49	0.68	0.07	-23.10
GC-13	25.80	1.02	13.59	0.48	0.65	0.07	-23.37
GC-13	28.29	1.02	12.92	0.44	0.61	0.06	-22.96
GC-13	28.47	1.00	12.56	0.45	0.63	0.06	-23.00

GC-13	30.61	1.00	12.64	0.44	0.63	0.06	-23.29
GC-13	32.63	1.04	13.16	0.40	0.59	0.05	-23.04
GC-13	35.72	0.97	12.23	0.35	0.54	0.04	-23.20
GC-13	31.75	0.95	12.04	0.39	0.57	0.05	-23.43
GC-13	26.50	1.00	12.57	0.47	0.64	0.06	-23.42
GC-13	23.71	1.03	12.98	0.47	0.62	0.06	-23.65
GC-13	24.98	1.33	16.75	0.29	0.39	0.05	-23.41
GC-13	25.43	1.19	14.98	0.42	0.56	0.06	-23.08
GC-13	25.75	1.14	14.33	0.48	0.65	0.07	-23.49
GC-13	25.17	1.10	13.82	0.46	0.61	0.06	-23.39
GC-13	24.33	1.09	13.81	0.49	0.65	0.07	-23.34
GC-13	24.16	1.11	14.01	0.47	0.62	0.07	-23.38
GC-13	23.49	1.15	14.57	0.46	0.60	0.07	-23.63
GC-13	21.77	1.07	13.52	0.47	0.60	0.06	-23.54
GC-13	21.10	1.14	14.42	0.42	0.53	0.06	-23.90
GC-13	23.12	1.28	16.19	0.36	0.47	0.06	-23.89
GC-13	23.87	1.20	15.11	0.36	0.47	0.05	-23.62
GC-13	24.92	1.12	14.07	0.38	0.51	0.05	-23.55
GC-13	23.49	1.12	14.14	0.43	0.56	0.06	-23.31
GC-13	21.63	1.11	13.98	0.36	0.46	0.05	-23.46
GC-13	21.12	1.09	13.82	0.39	0.49	0.05	-23.69
GC-13	20.05	1.16	14.61	0.42	0.53	0.06	-23.88
GC-17	57.53			0.37			-21.21
GC-17	59.65			0.29			-21.40
GC-17	61.47			0.24			-21.38
GC-17	62.65			0.25			-21.83
GC-17	57.31			0.24			-22.11
GC-17	61.36			0.22			-22.11
GC-17	65.42			0.25			-22.14
GC-17	44.90			0.23			-22.96
GC-17	77.67			0.41			-23.53
GC-17	58.53			0.43			-22.57
GC-17	28.51			0.41			-22.97
GC-17	33.52			0.40			-22.99
GC-17	30.29			0.47			-23.67
GC-17	28.19			0.46			-23.89
GC-17	39.34			0.49			-23.91
GC-17	27.09			0.40			-23.46
GC-17	24.60			0.41			-23.60
GC-17	26.10			0.50			-23.68
GC-17	21.63			0.57			-23.72
GC-17	27.63			0.53			-23.52
GC-17	29.35			0.51			-23.63
GC-17	23.27			0.54			-23.60
GC-17	30.96			0.43			-23.88
GC-17	27.10			0.47			-24.02
GC-17	41.17			0.38			-23.62

GC-17	34.21	0.41	-23.42
GC-17	27.66	0.47	-23.55
GC-17	36.96	0.44	-23.66
GC-17	30.09	0.44	-23.73
GC-17	19.69	0.45	-23.67
GC-27	33.13	0.72	-20.35
GC-27	38.05	0.59	-20.58
GC-27	38.87	0.47	-20.53
GC-27	38.80	0.48	-20.39
GC-27	38.09	0.58	-20.71
GC-27	36.85	0.57	-20.70
GC-27	38.74	0.74	-20.81
GC-27	40.62	0.72	-20.82
GC-27	41.76	0.76	-21.18
GC-27	47.96	0.75	-21.94
GC-27	49.45	0.82	-21.82
GC-27	48.49	0.90	-21.88
GC-27	49.70	0.79	-21.68
GC-27	49.69	0.76	-21.57
GC-27	47.10	0.73	-21.29
GC-27	44.96	0.68	-21.09
GC-27	40.53	0.67	-20.96
GC-27	40.19	0.61	-20.74
GC-27	40.66	0.65	-20.76
GC-27	42.33	0.71	-20.52
GC-27	39.84	0.59	-20.46
GC-29	55.23	0.56	-20.17
GC-29	25.77	0.44	-20.25
GC-29	51.21	0.49	-20.21
GC-29	64.03	0.49	-20.21
GC-29	55.86	0.46	-20.18
GC-29	57.21	0.47	-20.38
GC-29	64.45	1.15	-20.39
GC-29	59.27	0.65	-20.53
GC-29	64.08	0.67	-20.44
GC-29	51.34	0.75	-20.34
GC-29	48.11	0.89	-20.33
GC-29	87.95	0.85	-20.40
GC-29	95.32	0.58	-20.09
GC-29	84.90	0.72	-20.35
GC-29	78.28	1.14	-20.87
GC-29	94.88	0.79	-21.01
GC-29	57.79	0.78	-21.11
GC-29	60.13	0.58	-20.86
GC-29	61.29	0.72	-20.84
GC-29	60.91	0.75	-20.90
GC-29	57.41	0.70	-20.99

GC-29	57.97			0.78			-21.16
GC-29	58.15			0.74			-21.20
GC-32	38.75	0.93	8.80	0.94	1.53	0.08	-19.77
GC-32	34.58	0.92	8.70	0.82	1.25	0.07	-19.90
GC-32	31.20	0.90	8.54	0.87	1.26	0.07	-19.90
GC-32	32.39	0.91	8.62	0.91	1.35	0.08	-19.92
GC-32	32.35	0.94	8.93	0.81	1.20	0.07	-19.93
GC-32	34.67	0.92	8.73	0.77	1.18	0.07	-19.89
GC-32	32.29	0.89	8.46	0.80	1.18	0.07	-19.73
GC-32	32.68	0.88	3.83	0.79	1.17	0.03	-19.73
GC-32	35.43	0.92	4.00	0.85	1.32	0.03	-19.79
GC-32	37.35	0.96	4.19	0.93	1.48	0.04	-19.92
GC-32	35.98	0.96	30.21	0.90	1.41	0.27	-20.10
GC-32	36.66	0.97	30.44	1.02	1.61	0.31	-19.84
GC-32	36.31	0.95	29.86	1.02	1.60	0.30	-19.83
GC-32	34.78	0.95	29.96	1.08	1.66	0.32	-19.80
GC-32	30.97	0.90	28.45	1.37	1.98	0.39	-19.94
GC-32	33.03	0.95	38.82	1.00	1.49	0.39	-20.10
GC-32	32.66	1.00	41.05	1.04	1.54	0.43	-19.94
GC-32	37.27	0.99	40.52	0.98	1.56	0.40	-20.00
GC-32	38.44	0.99	40.58	0.95	1.54	0.39	-19.85
GC-32	39.86	1.13	46.33	0.76	1.26	0.35	-19.79
GC-32	41.62	1.22	49.87	0.78	1.34	0.39	-19.81
GC-32	43.24	1.15	47.08	0.93	1.64	0.44	-19.72
GC-32	43.70	1.03	42.25	1.08	1.92	0.46	-19.77
GC-32	45.21	1.02	41.72	1.28	2.34	0.53	-19.98
GC-32	44.30	1.03	42.18	1.23	2.21	0.52	-19.73
GC-32	44.35	1.07	43.92	1.17	2.10	0.51	-19.93
GC-37	45.03	0.84	4.49	0.45	0.82	0.02	-19.73
GC-37	45.58	0.95	5.10	0.34	0.62	0.02	-19.72
GC-37	53.12	0.90	4.82	0.37	0.79	0.02	-20.09
GC-37	57.75	0.88	4.71	0.44	1.04	0.02	-19.81
GC-37	57.31	0.86	4.62	0.33	0.77	0.02	-20.04
GC-37	54.29	0.77	5.85	0.65	1.42	0.04	-19.91
GC-37	53.25	0.75	5.70	0.77	1.65	0.04	-19.95
GC-37	51.68	0.74	5.62	0.77	1.59	0.04	-19.71
GC-37	54.79	0.74	5.66	0.97	2.15	0.05	-19.71
GC-37	60.75	0.69	7.84	1.19	3.03	0.09	-19.88
GC-37	57.10	0.73	8.29	1.04	2.42	0.09	-19.77
GC-37	54.18	0.73	8.34	0.89	1.94	0.07	-20.05
GC-37	56.23	0.77	8.74	0.87	1.99	0.08	-19.34
GC-37	58.75	0.78	8.84	0.93	2.25	0.08	-19.18
GC-37	60.08	0.76	8.65	1.04	2.61	0.09	-19.12
GC-37	56.74	0.76	8.61	0.98	2.27	0.08	-18.76
GC-37	55.40	0.73	8.31	1.02	2.29	0.08	-18.85
GC-37	52.30	0.67	4.87	1.06	2.22	0.05	-19.04
GC-37	50.61	0.66	4.78	0.96	1.94	0.05	-19.05

GC-37	52.14	0.73	5.25	1.00	2.09	0.05	-18.66
GC-37	51.78	0.78	5.67	1.01	2.09	0.06	-18.67
GC-37	51.40	0.76	5.50	1.08	2.22	0.06	-18.58
GC-37	49.23	0.73	5.28	1.04	2.05	0.05	-18.95
GC-37	54.86	0.74	11.96	1.24	2.75	0.15	-19.01
GC-37	53.26	0.74	11.97	1.31	2.80	0.16	-18.77
GC-37	53.11	0.71	11.49	1.42	3.03	0.16	-18.78
GC-37	52.92	0.70	11.27	1.41	2.99	0.16	-19.08
GC-37	50.57	0.73	11.73	0.98	1.98	0.12	-19.30
GC-37	54.86	0.66	10.69	1.54	3.41	0.16	-19.70
GC-37	54.03	0.73	11.79	1.19	2.59	0.14	-19.48
GC-40	52.91	0.84	2.29	0.54	1.15	0.01	-19.29
GC-40	64.74	0.96	2.61	0.31	0.88	0.01	-19.53
GC-40	68.06	0.98	2.66	0.51	1.60	0.01	-19.52
GC-40	61.37	1.02	5.62	0.73	1.89	0.04	-19.42
GC-40	54.44	0.95	5.25	0.88	1.93	0.05	-19.36
GC-40	61.50	0.92	5.09	1.18	3.06	0.06	-19.63
GC-40	59.60	0.83	4.58	1.41	3.49	0.06	-19.48
GC-40	58.90	0.83	4.57	1.58	3.84	0.07	-19.17
GC-40	61.44	0.88	4.87	0.89	2.31	0.04	-18.85
GC-40	62.07	0.83	4.57	1.36	3.59	0.06	-18.52
GC-40	60.09	0.87	4.79	1.51	3.78	0.07	-18.48
GC-40	61.95	0.79	4.38	1.76	4.63	0.08	-18.39
GC-40	60.91	0.77	4.24	1.90	4.86	0.08	-18.57
GC-40	60.74	0.86	4.77	1.19	3.03	0.06	-18.56
GC-40	61.50	0.85	4.68	1.26	3.27	0.06	-18.60
GC-40	58.34	0.83	4.61	1.60	3.84	0.07	-18.50
GC-40	57.38	0.73	4.03	2.16	5.07	0.09	-18.84
GC-40	48.87	0.75	4.14	2.08	4.07	0.09	-18.81
GC-40	59.12	0.78	4.31	1.71	4.18	0.07	-18.74
GC-40	58.43	0.77	4.27	1.54	3.70	0.07	-18.87
GC-40	58.36	0.75	4.15	2.33	5.60	0.10	-19.37
GC-40	59.50	0.74	4.09	2.83	6.99	0.12	-19.75
GC-40	58.53	0.77	4.24	2.67	6.44	0.11	-19.21
GC-40	60.77	0.84	4.66	1.92	4.89	0.09	-19.20
GC-40	62.16	0.86	4.74	1.93	5.10	0.09	-19.00
GC-40	62.68	0.86	4.73	1.83	4.90	0.09	-19.01
GC-40	63.09	0.80	4.44	2.17	5.88	0.10	-19.03
GC-40	62.49	0.85	4.69	1.64	4.37	0.08	-18.95
GC-40	58.52	0.85	4.68	1.96	4.73	0.09	-19.24
GC-40	60.23	0.79	4.35	2.05	5.15	0.09	-19.27
GC-40	59.39	0.81	4.51	2.27	5.59	0.10	-19.27
GC-40	57.84	0.81	4.50	2.13	5.05	0.10	-19.57
GC-49	42.81	0.66	7.19	0.59	1.03	0.04	-20.35
GC-49	45.09	0.80	4.01	0.81	1.48	0.03	-19.46
GC-49	50.13	0.81	4.62	0.72	1.44	0.03	-19.37
GC-49	63.41	0.74	3.56	0.69	1.89	0.02	-19.44

GC-49	65.44	0.72	6.41	0.52	1.50	0.03	-19.44
GC-49	47.01	0.59	10.05	1.34	2.53	0.13	-19.53
GC-49	46.84	0.65	6.27	1.35	2.54	0.08	-19.46
GC-49	56.83	0.58	5.56	1.43	3.31	0.08	-19.96
GC-49	52.23	0.62	6.01	1.44	3.01	0.09	-19.94
GC-49	50.18	0.68	6.57	1.29	2.59	0.08	-20.03
GC-49	47.38	0.66	6.36	1.02	1.94	0.06	-19.79
GC-49	44.73	0.61	5.93	1.17	2.12	0.07	-19.01
GC-49	46.81	0.67	6.45	1.22	2.29	0.08	-18.74
GC-49	47.21	0.64	6.19	1.65	3.13	0.10	-18.46
GC-49	46.93	0.61	5.89	1.71	3.22	0.10	-18.34
GC-49	48.00	0.60	5.83	1.65	3.17	0.10	-18.33
GC-49	45.49	0.59	5.68	1.72	3.16	0.10	-18.23
GC-49	46.27	0.47	4.54	1.26	2.35	0.06	-18.46
GC-49	44.09	0.61	5.91	1.46	2.61	0.09	-18.64
GC-49	42.33	0.60	5.77	1.50	2.60	0.09	-18.38
GC-49	42.08	0.63	6.04	1.84	3.18	0.11	-18.15
GC-49	44.21	0.63	6.08	1.98	3.55	0.12	-17.98
GC-49	44.20	0.61	5.85	1.54	2.76	0.09	-18.18
GC-49	38.94	0.58	5.57	1.79	2.93	0.10	-18.27
GC-49	44.27	0.62	5.99	1.52	2.73	0.09	-18.17
GC-49	45.15	0.62	5.94	1.93	3.52	0.11	-18.40
GC-49	46.94	0.64	6.20	1.83	3.45	0.11	-18.66
GC-49	46.34	0.65	6.24	1.78	3.32	0.11	-18.71
GC-49	47.62	0.59	5.71	2.50	4.77	0.14	-19.19
GC-49	46.20	0.61	5.86	1.68	3.12	0.10	-19.16
GC-49	46.89	0.59	5.70	1.82	3.43	0.10	-19.54
GC-53	42.87	0.78	4.20	1.29	2.26	0.05	-19.47
GC-53	44.53	0.75	4.02	1.90	3.43	0.08	-19.56
GC-53	46.37	0.73	15.86	1.66	3.10	0.26	-19.52
GC-53	48.50	0.78	16.94	1.57	3.05	0.27	-19.54
GC-53	49.36	0.83	10.68	1.05	2.07	0.11	-19.43
GC-53	51.48	0.81	10.46	1.24	2.56	0.13	-19.43
GC-53	52.03	0.82	5.07	1.41	2.94	0.07	-19.54
GC-53	51.18	0.84	5.21	1.87	3.83	0.10	-19.60
GC-53	46.31	0.97	5.99	0.98	1.83	0.06	-19.45
GC-53	48.15	0.96	5.96	1.07	2.06	0.06	-19.67
GC-53	44.45	1.03	31.01	0.89	1.60	0.28	-19.31
GC-53	43.62	1.01	30.62	0.87	1.54	0.27	-19.18
GC-53	43.08	1.06	32.02	0.66	1.16	0.21	-19.10
GC-53	42.55	1.06	32.20	0.76	1.32	0.24	-19.04
GC-53	42.58	1.03	31.28	0.81	1.41	0.25	-18.59
GC-53	44.18	0.69	21.02	0.86	1.54	0.18	-19.05
GC-53	43.16	1.07	32.30	0.84	1.48	0.27	-18.62
GC-53	42.61	1.08	32.75	0.81	1.41	0.27	-18.75
GC-53	43.07	1.14	34.38	0.78	1.37	0.27	-18.59
GC-53	41.76	1.08	12.03	0.85	1.46	0.10	-18.67

GC-53	42.91	1.09	12.07	0.93	1.63	0.11	-18.51
GC-53	42.50	1.09	12.09	0.93	1.62	0.11	-18.46
GC-53	42.48	1.08	12.03	0.87	1.51	0.10	-18.55
GC-53	41.05	1.13	12.49	0.84	1.42	0.10	-18.47
GC-53	41.64	1.09	12.13	0.72	1.23	0.09	-18.67
GC-53	41.95	1.11	12.34	0.78	1.34	0.10	-18.83
GC-53	41.13	1.10	12.18	0.73	1.24	0.09	-18.56
GC-53	40.84	1.20	13.36	0.77	1.30	0.10	-18.50
GC-59	33.18	0.34	2.12	1.67	2.50	0.04	-19.39
GC-59	35.72	0.51	3.22	1.43	2.22	0.05	-19.65
GC-59	39.23	0.58	3.62	1.26	2.07	0.05	-19.65
GC-59	41.04	0.54	5.80	1.24	2.10	0.07	-19.61
GC-59	49.30	0.65	6.89	1.07	2.11	0.07	-19.80
GC-59	55.52	0.55	5.75	0.90	2.02	0.05	-19.65
GC-59	57.22	0.69	11.72	1.00	2.34	0.12	-19.40
GC-59	55.39	0.57	9.71	1.14	2.56	0.11	-19.44
GC-59	54.91	0.63	10.76	1.30	2.88	0.14	-19.54
GC-59	44.61	0.49	8.35	1.46	2.64	0.12	-19.91
GC-59	41.10	0.74	12.57	1.62	2.75	0.20	-19.74
GC-59	40.57	0.77	13.18	1.76	2.96	0.23	-19.72
GC-59	36.50	0.63	10.77	1.85	2.91	0.20	-19.60
GC-59	50.13	0.59	10.11	1.84	3.69	0.19	-20.18
GC-59	46.74	0.56	9.56	1.90	3.57	0.18	-20.01
GC-59	45.04	0.61	10.38	1.51	2.75	0.16	-20.11
GC-59	43.38	0.61	5.54	1.55	2.74	0.09	-20.08
GC-59	42.17	0.63	5.71	1.34	2.32	0.08	-19.98
GC-59	35.99	0.64	7.85	0.84	1.31	0.07	-20.16
GC-59	39.11	0.74	9.16	0.94	1.54	0.09	-19.35
GC-59	35.15	0.83	10.20	0.95	1.46	0.10	-19.07
GC-59	38.51	0.82	10.08	0.94	1.53	0.09	-19.00
GC-59	38.40	0.72	8.88	1.18	1.92	0.10	-18.95
GC-59	39.00	0.75	9.30	1.38	2.26	0.13	-18.97
GC-59	38.43	0.75	9.28	1.14	1.85	0.11	-19.07
GC-59	43.83	0.83	10.17	1.01	1.80	0.10	-19.17
GC-59	33.55	0.72	5.71	0.95	1.43	0.05	-19.22
GC-59	34.76	0.72	5.74	1.06	1.62	0.06	-18.96
GC-59	35.26	0.72	5.73	1.26	1.95	0.07	-18.79
GC-59	43.11	0.70	5.56	1.43	2.51	0.08	-18.65
GC-59	40.85	0.63	5.03	1.70	2.87	0.09	-18.75
GC-59	41.57	0.64	5.07	0.84	1.44	0.04	-18.69
GC-59	43.25	0.65	5.21	1.37	2.41	0.07	-18.71
GC-59	36.92	0.66	5.25	1.58	2.50	0.08	-19.26
GC-59	40.30	0.73	5.78	1.81	3.03	0.10	-19.09
GC-66	33.86	0.57	1.46	2.34	3.54	0.03	-19.41
GC-66	34.01	0.51	19.51	2.28	3.46	0.44	-19.33
GC-66	36.16	0.54	20.72	2.29	3.59	0.47	-19.41
GC-66	37.78	0.53	20.46	2.20	3.54	0.45	-19.63

GC-66	37.30	0.48	18.53	2.17	3.46	0.40	-19.74
GC-66	37.96	0.48	18.44	2.20	3.55	0.41	-19.65
GC-66	38.12	0.50	18.99	2.27	3.67	0.43	-19.60
GC-66	41.20	0.53	20.14	2.05	3.49	0.41	-19.50
GC-66	43.81	0.55	20.88	1.96	3.49	0.41	-19.53
GC-66	45.51	0.54	5.91	1.91	3.51	0.11	-19.49
GC-66	48.30	0.62	10.68	1.79	3.46	0.19	-19.51
GC-66	51.84	0.75	12.89	1.75	3.63	0.23	-19.41
GC-66	53.62	0.81	14.03	1.71	3.69	0.24	-19.49
GC-66	54.42	0.87	36.65	1.75	3.84	0.64	-19.44
GC-66	51.66	0.86	36.16	1.62	3.35	0.59	-19.42
GC-66	54.04	0.82	34.73	1.74	3.79	0.60	-19.37
GC-66	52.39	0.82	34.37	1.77	3.72	0.61	-19.35
GC-66	50.28	0.78	32.71	1.81	3.64	0.59	-19.33
GC-66	50.01	0.80	33.85	1.65	3.30	0.56	-19.34
GC-66	49.20	0.81	34.27	1.62	3.19	0.56	-19.43
GC-66	47.32	0.81	33.95	1.67	3.17	0.57	-19.31
GC-66	45.13	0.80	33.83	1.62	2.95	0.55	-19.32
GC-66	46.24	0.81	34.12	1.91	3.55	0.65	-18.40
GC-66	42.34	0.81	34.01	1.86	3.23	0.63	-18.80
GC-66	38.75	0.85	35.93	1.56	2.55	0.56	-19.09
GC-66	36.39	0.84	35.57	1.11	1.74	0.39	-19.02
GC-68	23.45	0.68	4.69	1.95	2.55	0.09	-19.17
GC-68	28.89	0.71	4.92	1.99	2.80	0.10	-19.31
GC-68	31.29	0.64	4.72	1.98	2.88	0.09	-19.49
GC-68	37.82	0.63	4.65	1.86	2.99	0.09	-19.47
GC-68	44.76	0.65	15.37	1.53	2.77	0.24	-19.45
GC-68	41.37	0.69	16.25	1.62	2.76	0.26	-19.38
GC-68	36.04	0.70	16.52	1.65	2.58	0.27	-19.55
GC-68	31.97	0.68	5.13	1.54	2.26	0.08	-19.57
GC-68	25.36	0.75	5.63	1.34	1.80	0.08	-19.59
GC-68	20.42	0.79	12.79	1.21	1.52	0.15	-19.68
GC-68	20.54	0.90	14.61	1.07	1.35	0.16	-19.73
GC-68	21.73	0.94	15.28	0.95	1.21	0.15	-19.68
GC-68	26.38	0.87	14.11	1.32	1.79	0.19	-19.40
GC-68	23.08	0.99	15.95	0.96	1.25	0.15	-19.83
GC-68	18.66	1.03	16.62	0.68	0.84	0.11	-20.17
GC-68	16.14	1.12	18.19	0.57	0.68	0.10	-19.68
GC-68	17.20	1.01	16.37	0.66	0.80	0.11	-19.54
GC-68	17.80	1.02	16.50	0.73	0.89	0.12	-19.21
GC-68	16.33	1.07	17.24	0.78	0.93	0.13	-19.02
GC-68	17.19	1.05	17.02	0.81	0.98	0.14	-18.72
GC-68	16.54	1.14	18.49	0.78	0.93	0.14	-18.90
GC-68	15.93	1.21	19.60	0.71	0.84	0.14	-19.30
GC-68	15.25	1.17	18.93	0.77	0.91	0.15	-19.02
GC-68	14.70	1.17	18.96	0.64	0.75	0.12	-19.28
GC-68	18.28	1.05	16.95	1.20	1.47	0.20	-18.93

GC-68	14.37	1.15	18.56	0.78	0.91	0.14	-19.03
GC-68	15.01	1.09	17.68	0.69	0.81	0.12	-19.24
GC-68	14.58	1.05	17.01	0.75	0.88	0.13	-19.21
GC-68	14.95	1.11	17.90	0.66	0.78	0.12	-19.09
GC-68	15.56	1.10	17.82	0.64	0.76	0.11	-19.20
GC-70	17.66			2.43			-19.24
GC-70	19.39			2.35			-19.37
GC-70	22.91			2.39			-19.51
GC-70	26.05			2.48			-19.64
GC-70	21.55			1.82			-19.70
GC-70	22.32			2.21			-19.67
GC-70	24.89			2.12			-19.74
GC-70	31.45			1.99			-19.61
GC-70	29.89			1.85			-19.72
GC-70	36.51			1.75			-19.59
GC-70	31.55			1.48			-19.60
GC-70	37.49			1.59			-19.59
GC-70	35.66			1.58			-19.61
GC-70	32.54			1.69			-19.62
GC-70	24.56			2.13			-19.52
GC-70	27.36			1.80			-19.67
GC-70	19.02			2.28			-19.59
GC-70	29.70			1.61			-19.78
GC-70	20.30			1.57			-19.73
GC-70	23.47			2.36			-19.89
GC-70	25.53			2.29			-20.12
GC-70	24.85			2.22			-20.05
GC-70	23.20			1.81			-19.60
GC-70	26.62			1.82			-19.51
GC-70	24.70			2.19			-19.53
GC-70	24.62			2.08			-19.63
GC-70	25.42			2.20			-19.57
GC-70	27.62			2.32			-19.80
GC-70	23.39			2.34			-19.85
GC-70	28.42			2.02			-20.21
GC-70	26.72			2.42			-20.39
GC-70	24.08			2.06			-20.17
GC-80	38.31	0.74	10.92	1.11	1.80	0.12	-19.64
GC-80	47.09	0.75	11.17	0.85	1.61	0.09	-19.69
GC-80	48.40	0.75	11.07	0.90	1.74	0.10	-19.57
GC-80	49.02	0.73	10.84	0.85	1.67	0.09	-19.68
GC-80	52.91	0.72	10.71	0.79	1.68	0.08	-19.78
GC-80	54.80	0.74	10.96	0.82	1.81	0.09	-19.95
GC-80	57.58	0.77	11.41	0.85	2.00	0.10	-20.02
GC-80	57.69	0.78	11.55	0.80	1.89	0.09	-19.97
GC-80	56.75	0.82	12.12	0.80	1.85	0.10	-19.66
GC-80	59.35	0.82	12.20	0.80	1.97	0.10	-19.82

GC-80	57.56	0.80	11.81	0.91	2.14	0.11	-20.14
GC-80	61.00	0.84	12.47	0.85	2.18	0.11	-19.93
GC-80	58.56	0.89	13.16	0.90	2.17	0.12	-19.76
GC-80	59.17	0.81	11.93	0.87	2.13	0.10	-20.07
GC-80	64.21	0.84	12.40	0.91	2.54	0.11	-20.12
GC-80	64.14	0.86	12.67	0.92	2.57	0.12	-20.38